Tribochemical interaction of newly developed organic lubricant additives with ZDDP; the influence of organic additives on tribological performance of ZDDP

Muhammad Sohail Ahmed Siddiqui

Submitted in accordance with the requirements for the degree of
Doctor of Philosophy

The University of Leeds
School of Mechanical Engineering
Leeds, UK

July, 2020

The candidate confirms that the work submitted is his own and that appropriate credit has been given where reference has been made to the work of others. The contribution of the candidate and the other authors to this work has been explicitly indicated below. The candidate confirms that appropriate credit has been given within the thesis where reference has been made to the work of others.

The papers contributing to this thesis, the candidate (first author), performed all the experiments and analyses of the data and prepared all the manuscripts. All other authors contributed by sharing their expertise to elaborate the discussions and proof read the whole manuscripts. The X-ray Photoelectron Spectroscopy (XPS) of the tribofilms were carried out at NEXUS XPS laboratory at Newcastle University. The Scanning Electron Microscopy (SEM) and EDX spectra collection in SEM were assisted by Stuart Micklelthwaite (at LEMAS facility, The University of Leeds, UK)

This copy has been supplied on the understanding that it is copyright material and that no quotation from the thesis may be published without proper acknowledgement.

© 2020 The University of Leeds and Muhammad Sohail Ahmed Siddiqui

Acknowledgements

Firstly, I would like to thanks Almighty, for His support in completion of this research project. I would like to express sincere appreciation to my academic supervisors, Professor Anne Neville and Professor Ardian Morina for their help, guidance, support and above all the endless motivation and encouragement throughout the project. They are not just mentors; actually they are far more than that.

I would like to thanks Nouryan Surface Chemistry (previously known as AkzoNobel Surface Chemistry) for sponsoring my research project. I would like to thank my industrial supervisors, Joke C. Speelman and Wendy Huffman for sharing their knowledge, technical expertise and support throughout this project. I am also obliged to NEXUS XPS facility for conducting the XPS experiments.

I would like to express gratitude to EPSRC (CDT-Integrated Tribology) for giving me an opportunity to work on this exciting project. I am also thankful to Kim Hyde (CDT- Manager), all CDT colleagues and staff for their infinite support during this difficult journey. I would like to thank all the members of iFS research group, particularly Abdel, Abdullah, Pourya, Waleed, Chun, Fiona and Judith. I am also thankful to lab engineers and technicians for their help and support during this project.

I am particularly grateful to my Mom and Dad for their love and prayers for my success.

Finally, I would like to thank my lovely Wife (Afshan) for their support and encouragement. In difficult times, her love and motivation always help me to continue my research journey. Completion of this project is not possible without you, Afshan. Last but not least, my lovely kids (Mashal and Ashhad), I appreciate your patience and affection during this period, I love you guys.

Abstract

Reduction in fuel consumption and tighter environmental restrictions on the combustion emission products are among the key challenges of automotive industry, which can be partially addressed by developing more efficient, environmentally friendly lubricant additives. Zinc dialkyldithiophosphate (ZDDP) and friction modifier (FM) are considered as the most important lubricant additives for the tribological performance under boundary lubrication condition. ZDDP is an effective anti-wear (AW), anti-oxidant (AO) and extreme pressure (EP) additive but presence of ZDDP in engine oil increases the engine friction and have negative impact on the fuel economy. Organic friction modifiers (OFMs) are environmentally friendly lubricant additives, which have the capability to reduce boundary friction and improve lubricity by reducing the friction coefficient and contributes to improve the fuel economy. However, the performance of ZDDP in reducing wear is remarkable but it is established that the AW capability of ZDDP is compromised with the addition of OFMs in the lubricant blend. Result showed that the AW behaviour of ZDDP swings significantly from substantial increase to remarkable decrease in wear factor value.

In order to explore the tribochemical interaction between OFMs and ZDDP, firstly it is necessary to understand the elemental composition, morphology and chemical structure of the tribofilm formed by ZDDP. The focus of this study is to develop understanding about tribological performance of OFMs with ZDDP and correlate modifications emerged because of interaction of both additives to tribological performance of ZDDP. The topography, elemental and chemical composition of the resultant tribofilm has been analysed during this study. Atomic force microscope (AFM) analysis of the tribofilms showed significant modification in tribofilm topography as result of interaction between OFM and ZDDP in the base oil (BO). The X-ray photoelectron spectroscopy (XPS) was also carried out during this study. The chemical composition analysis showed modification in chemical structure of the tribofilm formed by the blend of OFM and ZDDP in-comparison to the tribofilm formed by ZDDP. Etching of the tribofilm surfaces were performed in order to mitigate any contamination effect and to further analyse change in elemental concentration

across the tribofilm surfaces. Specifically designed sequential film formation tests were also conducted to explore the possible sequence of film formation with single additive system. Results showed that amine FMs have capability to form a film on top of the pre-formed zinc phosphate film but ZDDP's capability to form AW film on top of a film formed by amine FMs is slightly compromised. The depth-profiling analysis of the tribofilm formed by interaction of amine FM on top of the pre-formed ZDDP tribofilm showed that the modification in elemental composition of the tribofilm was not as significant as observed with the addition of amine FM with ZDDP in the BO. The nitrogen (N) found more incorporated in BO interaction (continuous test) in-comparison to sequential film formation tests, which appears to be a major difference in both tribological interaction systems.

On the basis of the tribological and surface analysis results amine interaction mechanisms with ZDDP are also proposed in the end of this study, which suggested that one mechanism is not solely representing the complete film formation mechanism but possibly more than one mechanisms worked together to form a resultant tribofilm.

Table of Contents

List of Tables

List of Figures

Abbreviations

ZDDP	Zinc dialkyldithiophosphate
FM	Friction Modifier
AW	Anti-Wear additive
AO	Anti-Oxidant additive
EP	Extreme Pressure additive
OFMs	Organic Friction Modifiers
BO	Base Oil
PMAs	Polymethacrylates
PMA-N	Dimethylaminomethacrylate
DMODA	Dimethyoctadecylamine
DTP	Dithiophosphates
Wt. %	Weight Percentage
At. %	Atomic Percentage
MoDTP	Molybdenum dialkyldithiophosphate
MoDTC	Molybdenum dialkyldithiocarbamate
TBPi	Tributylphosphite
TMPi	Trimethylphosphite
VM	Viscosity Modifier
VI	Viscosity Index Improver
HFFR	High Frequency Friction Rig
OM	Optical Microscope
AFM	Atomic Force Microscope
IFM	Interfacial Force Microscope
SAPS	Sulphated Ash, Sulphur and Phosphorous
SFA	Surface Force Apparatus
SEM	Scanning Electron Microscope
TEM	Transmission Electron Microscope
EDX	Energy Dispersive X-ray
FIB	Focussed Ion Beam
XPS	X-ray Photoelectron Spectroscopy
MTM	Mini Traction Machine
SLIM	Space Layer Image Mapping

AES	Auger Electron Spectroscopy
XANES	X-ray Absorption Near Edge Spectroscopy
XAS	X-ray Absorption Spectroscopy
XRD	X-ray Powder Diffraction
XRF	X-ray Fluorescence
BE	Binding Energy
BO	Bridging Oxygen
NBO	Non-Bridging Oxygen
R_q	Root mean square surface roughness
R_{max}	Maximum peak to valley height
XPEEM	X-ray Photoelectron Emission Microscopy
LPL	Liquid Phase Lubrication
GPL	Gas Phase Lubrication
QCM	Quartz Crystal Microbalance
IRRAS	Infrared Reflection Absorption Spectroscopy
EPMA	Electron Probe Micro Analysis
P-NMR	Phosphorous Nuclear Magnetic Resonance

To my Family

Chapter 1
Thesis at a glance

1.1 Background

The role of friction, wear and lubrication between interacting surfaces while they are in relative motion has major impact on the efficiency and durability of engines/machines. Friction is the major cause of wear, which ultimately results in the form of efficiency loss and material failure. It is estimated that by reducing friction between interacting surfaces potentially one third of the global energy resources can be saved [1]. In 1966 a government committee chaired by H. Peter Jost concluded in a report (also known as Jost report) that the UK industry could make a potential saving of £515 million approximately (at 1965 currency value) by implementing the advanced proactive tribological techniques [2]. The other developed countries also conducted similar investigations and the outcome was very much comparable to the Jost report [3]. A technical report published by the Department of Energy in the United States in 1999 affirmed that the losses in transportation including maintenance, replacement, energy and time cost up to $20 billion per annum to the U.S economy [4].

The global energy supply available for consumption in 2011 was equivalent to 373 EJ and of this energy crude oil provided 152 EJ (i.e. 41%) [5]. Oil is the main source of energy for transportation sector which consume 63% of total oil resources [5]. Road transport contributed a share of 47% in transportation sector and annually wasted an average of 21 GJ energy to overcome friction [6], [7]. Figure 1-1, shows breakdown of global energy supply and oil consumption in 2011. Mega economics related with the friction, lubrication and wear forced the industries and also the governments to initiate and support the research and development programmes in the field of tribology [3].

The UK government announced a ban on selling new petrol and diesel cars from 2035 in an attempt to achieve zero carbon emission by 2050 [8]. In the current global spectrum automotive industries have to meet the legislative requirements and government regulations but at the same time also adopting the technological changes in order to accommodate the market demands [9], [10]. Improving the fuel economy and lowering emissions level are the centre

points of government regulations [10]. The first European emissions requirement (i.e. Euro 1) introduced in 1992, which set the initial emissions targets for road transportation [11]. The emissions control requirements progressed with time to Euro 6 in 2015. The Euro 6 emissions standard remarkably reduced nitrogen oxide emission from diesel cars in an attempt to improve air quality [11]. A combined emissions target of 1.065 and 0.585 g/km has introduced in Euro 6 for gasoline and diesel engines respectively [12]. Reduction in CO_2 emission and improvement of the fuel economy primarily related to friction losses in the engine components. These challenges can be addressed by developing [4], [9],

- New materials or engineered surfaces
- Better understanding about the lubricant additives and their interaction with each other along with different surfaces

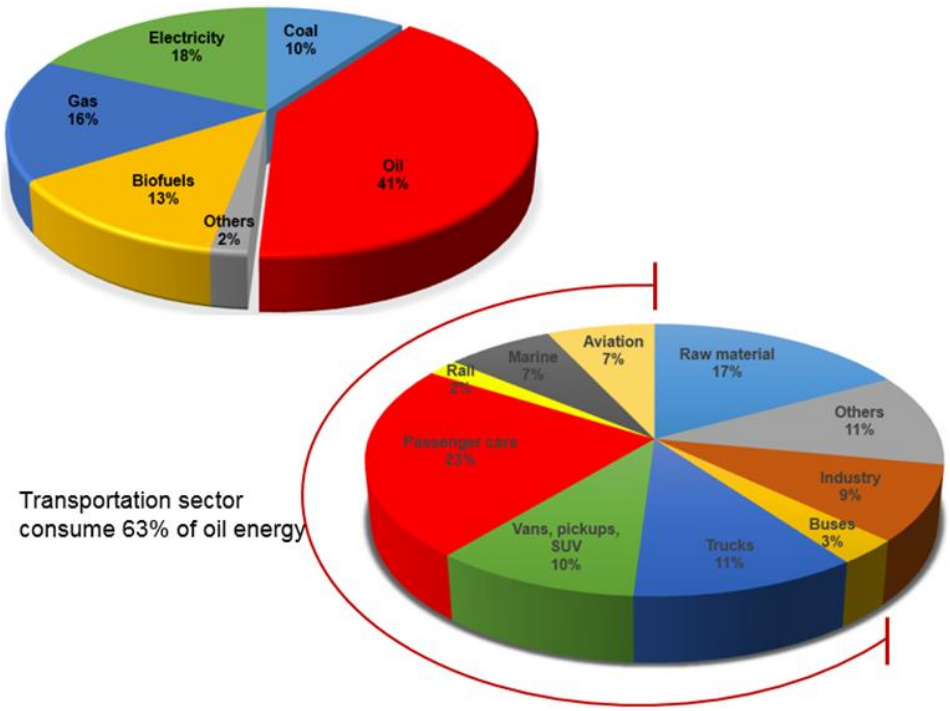

Figure 1-1. Breakdown of global energy and oil consumption in 2011 [5]

Holmberg et al. [6] in his research article mentioned that approximately 21.5% of the fuel energy is utilized to get the motion out of a passenger car and the rest of the fuel energy consumed to overcome the friction. Furthermore, they

added that 10% reduction in mechanical losses would result to a 1.5% reduction in fuel consumption. For reduction in mechanical losses, lubricants used as an anti-friction media, which reduce friction and promote continuous and gentle operation without any hindrance. Modern engine oils use friction modifiers (FMs) to reduce friction mostly in boundary and mixed lubrication regime, which are the most critical regimes in which interacting surfaces are either not separated or are partially separated by the fluid lubricant [1].

To meet the current challenges, automotive industry has been actively researching to analyse the effect of different additives in the lubricant and with the interacting surfaces. Experimental analysis of new organic additives such as amine based FMs in different concentrations along with anti-wear (AW)/extreme pressure (EP) additive such as zinc dialkyldithiophosphate (ZDDP) is part of ongoing research to overcome the current challenges.

1.2 Research motivation

Internal combustion (IC) engines are the key source of environmental pollution via exhaust emission which includes particulate matters, burned hydrocarbons, NO_x and CO_2 [13]. Environmental/emissions legislation (i.e. European emission standard), continuously lowered/tightened the limit of harmful exhaust emissions in order to reduce the IC engines contribution to environmental pollution [12]. Reduction in the fuel consumption and tighter environmental restrictions on the combustion emission products are among the key challenges of automotive industry.

One of the main additives in current engine oil formulations is ZDDP. ZDDP is an effective AW and anti-oxidant (AO) additive [14]–[18], but it is considered as non-environmentally friendly additive due to the catalyst contamination caused by phosphorous (P) and sulphur (S) present in ZDDP [19]–[21]. In addition, ZDDP show a negative impact on the friction coefficient in tribological systems lubricated in boundary and mixed regimes [15], [22], affecting the overall fuel consumption. Few engine components operate in more than one lubrication regime during a single engine cycle [23]. This situation poses a serious challenge for the tribologists to design a single component suitable for operation in all lubrication regimes along with the lubricant oil having

specification also suitable for all lubrication regimes [24]. Figure 1-2 shows the modified Stribeck curve along with different engine components operating in more than one lubrication regimes.

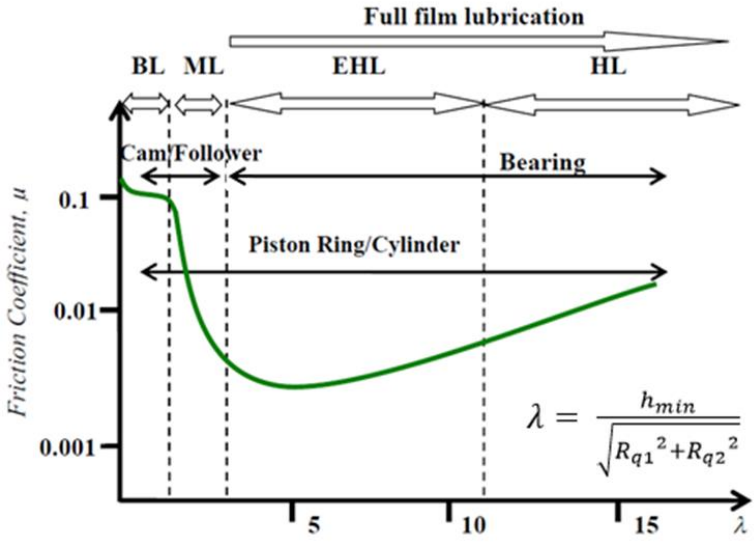

Figure 1-2. The modified Stribeck curve showing different lubrication regimes [23]

Development of low SAPS (Sulphated Ash, Phosphorus and Sulphur) engine oils with low friction and wear is essential for reducing further impact of automotive engines on the environment [19]. However, the literature shows that some research is going on in developing environmentally-friendly lubricants but still much more research is needed to gain a comprehensive and mechanistic understanding about environmentally-friendly lubricant additives, their interactions and film formation mechanisms, composition and structure of tribofilms formed as a result of tribological interaction.

1.3 Literature gaps and research objectives

Research motivation (i.e. working towards the development of environmentally friendly lubricants), was the primary driving force of this study. In the early stages of this research, it was realised that limited literature is available about organic friction modifiers (OFMs) and their interaction with ZDDP. The interaction mechanism of OFM with ZDDP and modification in tribofilm morphology did not grab substantial attention of the researchers.

Consequently, the question relating to how OFMs interact with ZDDP and why the tribofilm formed because of this interaction behave differently become important.

It is widely agreed that the decomposition of ZDDP produces reaction products and these reaction products form protective films, which minimize asperity-to-asperity contact [15], [25]–[27]. Studies [28], [29] suggested the existence of a bi-phosphate layer structure of the ZDDP tribofilm in which bulk of the film is composed of short chain phosphates and the upper most part of the film is dominated by longer chain phosphates. Ito et al. [18] with the help of focussed ion beam (FIB) and transmission electron microscope (TEM) also proposed a multi-layer structure in the ZDDP tribofilm. Round [30] mentioned that amines interact with ZDDP and end up with forming complexes in the bulk fluid. Matsui et al. [31], [32] confirmed that reduction in the tribofilm formation capability of ZDDP in the presence of nitrogen (N) containing additive is very much due to formation of complexes between them. Shiomi et al. [33] proposed that complex formation in the bulk oil and competitive adsorption of the second additive on the metal surface are the major mechanisms. In another article Matsui et al. [34] reported that N-containing additives have the capability to preferentially adsorb on steel surfaces resulting in reduced ZDDP derived tribofilm formation. The above mentioned literature indicated that limited number of researchers discussed possible interaction mechanisms between ZDDP and N-based OFMs and this area needs further research. However, discussion about modification in tribofilm chemical structure, chemical composition and furthermore effect of these changes on tribological performance did not get much attention in the past. This study is an attempt to cover these gaps and answer some open ended questions related to the interaction of OFMs with ZDDP. The key objectives of this study are,

- To understand friction and wear performance of OFMs with ZDDP
- To investigate the effect of concentration of OFMs with ZDDP and their impact on friction and wear results
- To explore the interaction between OFMs and ZDDP and analyse their impact on tribofilm morphology

- To determine the chemical composition of the tribofilm formed on interacting surfaces, more precisely the product formed as a result of the interaction between amine FMs and ZDDP
- To compare elemental composition of the tribofilm formed by adding both additives (OFMs and ZDDP), first in the bulk lubricant and then sequential film formation tests in single additive tribological system
- To understand the mechanism of interaction between amine FMs and ZDDP with the help of sequential film formation tests
- To gain insight into the interaction of amine FMs with ZDDP and their impact on tribofilm morphology and tribological performance

1.4 Thesis structure

This thesis comprises eleven chapters including the current chapter (i.e. thesis in a glance). Chapter two covers basic theory about tribology (i.e. friction, wear and lubrication), role of lubricants to minimise friction and wear in different lubrication regimes and tribological challenges specifically related to automotive application. Chapter three reviews additives in modern engine oil. This chapter includes detail literature review about ZDDP, its film formation mechanism on steel surfaces, chemical structure and tribofilm morphology. The purpose of this chapter is to get better understanding about the film formation mechanism of ZDDP. Chapter four reviews literature on FMs, classification of FMs and interaction of OFMs with ZDDP. Literature about Interaction of OFMs with ZDDP is the primary focus of this chapter, which provides basis for discussion at the end of this thesis. Chapter five is about the experimental methods and surface analysis techniques used in the current study to analyse the tribological behaviour of different lubricant blends and their impact on tribofilm morphology and composition. The fine details about the tribological tests (specifically designed to explore the interaction mechanisms of OFMs with ZDDP), are added in this chapter. Tribological

testing parameters, testing procedures and sample specimen details are also included in this chapter.

Chapter six is the first result chapter of this thesis. This chapter covers the tribological screening of seventeen OFMs with ZDDP. These OFMs blended with ZDDP in 1:1 molar ratio of FM to ZDDP. Tribological testing was performed on TE 77 (high frequency friction machine), in which pin specimen reciprocates physically against a fixed plate specimen. This chapter also covers tribological performance of five (5) shortlisted lubricant blends with two concentrations of OFMs (i.e. 0.5:1 and 1:1 molar ratio of FM to ZDDP). Concentration of ZDDP was constant in all formulations i.e. 0.55 wt. %. Chapter seven primarily focus on effect of OFM concentrations on the tribofilm morphology of ZDDP. Atomic force microscope (AFM) analysis of different tribofilms are added in this chapter to analyse the effect of OFM concentrations on ZDDP tribofilm. Chapter eight covers the surface characterisation of the tribofilm formed by the five (5) shortlisted lubricant blends with 1:1 molar ratio of FM to ZDDP (continuous two hours test). The initial section of this chapter focus on the elemental composition of the tribofilm using scanning electron microscope(SEM)-energy dispersive X-ray (EDX) analysis. The later part of this chapter present the X-ray photoelectron spectroscopy (XPS) analysis to analyse the chemical composition of the tribofilm. Depth-profiles analysis highlight the changes in elemental composition of the tribofilm from the top most layer to bottom of the tribofilm near the substrate. Chapter nine is the last result chapter in thesis. This result chapter specifically focus on the interaction sequence of amine FMs (i.e. FM 1, FM 4. FM 8 and FM 14) with ZDDP in sequential film formation tests. In these tribological tests, the tribofilm is initially formed with BO + ZDDP in the first half of the test and then in the second half of the test tribological interaction is performed on top of the pre-formed film with BO + OFM or vice versa. The first part of chapter covers friction and wear analysis of different lubricant blends. The XPS analysis of tribofilm are added in second part of chapter. Depth-profiling of the tribofilms are also included in this chapter.

Chapter 10 present a consolidated discussion by combining the key findings of this study. Chapter 11 (i.e. conclusions and future work), is the final chapter

of this thesis. The main conclusions from the study presented in light of the proposed objectives. This chapter also proposes directions and areas, which need further study in the future.

Chapter 2
Theories and challenges

2.1 Introduction

Tribology is the science of friction, wear and lubrication of interacting surfaces which are in relative motion [1]. Friction opposes the motion and arises when bodies move tangentially over one another. Friction leads to wear which is a phenomenon of physical surface damage. Wear occurs as a result of interaction of surfaces which consequently leads to material removal from interacting surfaces [35], [36]. Lubrication reduces the energy dissipation and wear by interposing low shear strength layers of solid, liquid or gas between the two interacting surfaces which improves smoothness of relative motion and reduce damage [3]. The main objective of lubrication is to minimise wear and reduce heat loss from the interacting surfaces in motion and reduce the co-efficient of friction (COF) value [37].

2.2 Friction

Friction is the opposing force which hinders the motion when bodies move tangentially over another and it is the major cause of wear and heat loss [3]. Leonardo da Vinci and Amontons presented the first two laws of dry friction which are valid for the interacting surfaces having low or no lubrication [3]. First law of dry friction (Equation 2-1), defines the COF (μ), as the ratio between the tangential force (F) and the normal applied load (W) and its value depends upon the nature of both the interacting surfaces [3]

$$\mu = F/W \qquad 2\text{-}1$$

The second law presented by Leonardo and Amontons state that dry contact friction is not dependent on apparent area of contact but on the real area of contact (i.e. peak of the asperities), just like first law, second law is also widely applicable [3]. Unwanted friction is the major source of inefficiency, wear and energy loss in engineering systems. The low COF value is desirable in

majority of engineering applications to make them efficient and reliable. The low friction between the interacting surfaces can be achieved by several methods which include using appropriate lubricant which worked as an anti-friction media by providing gentle, even and hindrance free operation and also by using engineered surfaces (i.e. surface treatment or coated surfaces) [3], [37].

2.3 Wear

The wear changes surface topography and physical properties while on the extreme side it may lead to a catastrophic failure in the long run. In the absence of protective film or tribofilm, the relative movement damages the contacting surfaces which results in material loss from a surface or both surfaces [3], [38]. Due to the severity of the losses attached with wear, it is essential to control wear in order to sustain the durability and reliability of the engine components. Wear rates change significantly and generally in the range of 10^{-4} – 10^{-18} m^3/Nm and it depends upon the operating conditions and the materials interacting with each other. Optimal design of the operating conditions and material selection including surface treatment or surface coating are the key areas to control wear [38].

There are three laws of wear, which generalize the dependence of wear mechanism. The first law of wear states that wear increases with the sliding distance and it is widely applicable over a wide range of conditions. The second law states that wear is directly proportional to the applied load, which is applicable for metal surfaces within a range of loads but not for polymers. According to third law, wear is inversely proportional with the hardness of the interacting surfaces but this statement is partially true as other material properties of the interacting surfaces are also important [3].

Wear is described as the process of material removal from the interacting surfaces and this physical separation is the result of surface micro-fracture and chemical reaction at elevated temperature between interacting surfaces [38]. It is not necessarily true that high friction always leads to high wear. Interaction of polyethylene with steel is the best example, which produce high friction but low wear [3]. The wear between interacting surfaces is result of a

wear mechanism or combination of different wear mechanisms [3]. As the tribological interaction proceeds it is possible that the wear mechanism switches from one type of wear to another in response to changes in the material properties and surface reactions of the interacting surfaces [38]. Figure 2-1 shows wear description and interrelation of different wear modes.

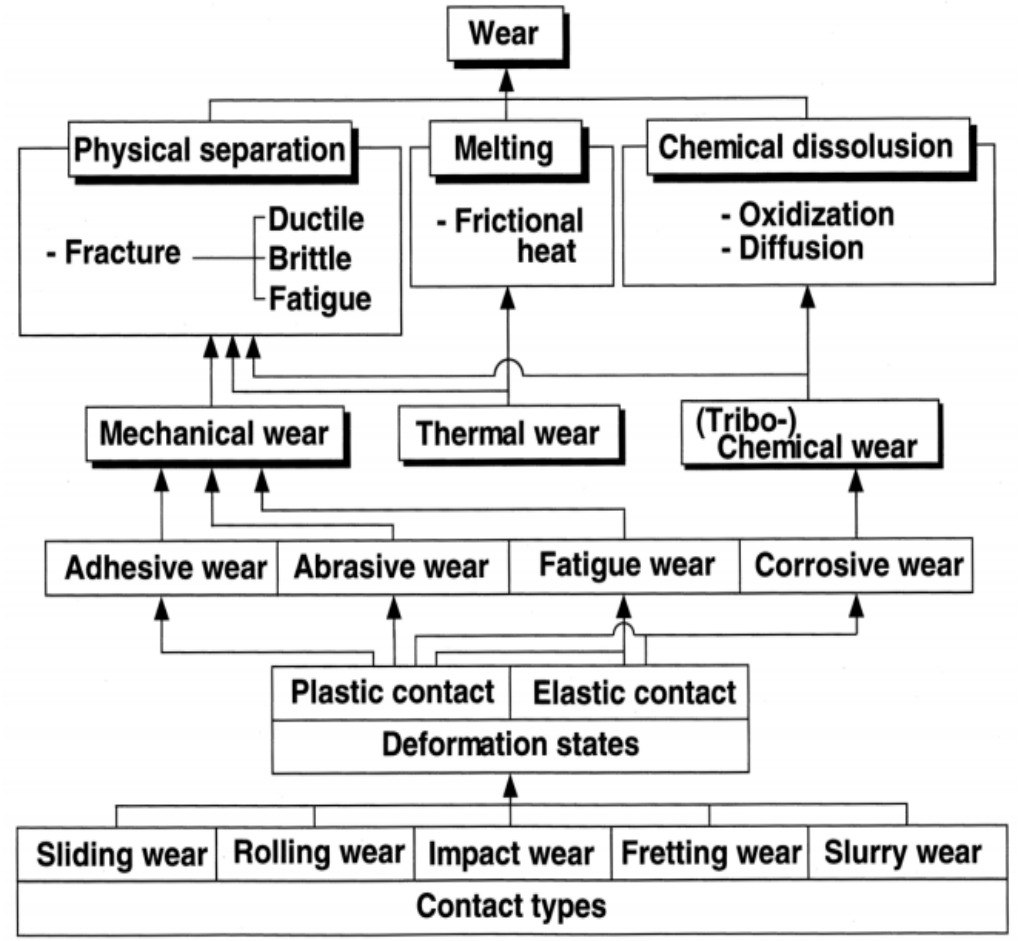

Figure 2-1. Wear description and interrelation of different wear modes [38]

Generally wear is classified into four fundamental modes and these are [38]

- Adhesive wear
- Abrasive wear
- Fatigue wear
- Tribochemical wear

2.3.1 Adhesive wear

The adhesive bonding between the asperities on the interacting surfaces has enough strength to resist the relative motion and consequently it introduce plastic deformation in the contact region. The plastic deformation initiate a crack, which move towards the contact region of the interacting surfaces. The adhesive wear, shear the relatively softer material and transfer it to harder material [38], [39]. Figure 2-2 shows the crack propagation and adhesive wear mechanism,

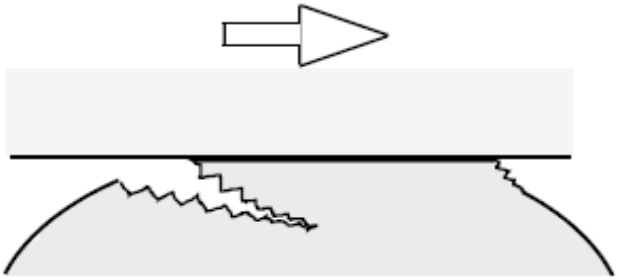

Figure 2-2. Adhesive wear mechanism showing crack propagation [38]

2.3.2 Abrasive wear

Abrasive wear occurs when the asperities of the interacting surfaces has interlocked and as a result ploughing takes place during sliding. During this wear mode hard asperities between the interacting surfaces plough grooves and penetrate inside the relatively soft surface [3], [38], [39]. Figure 2-3 shows the abrasive wear mechanism.

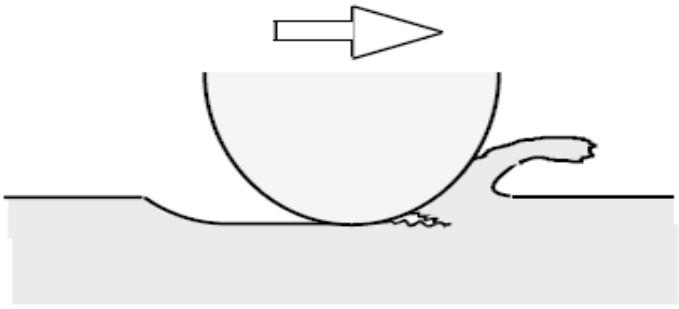

Figure 2-3. Abrasive wear mechanism showing ploughing [38]

2.3.3 Fatigue wear

Fatigue wear occur due to cyclic stresses. Conformable groove in the interacting surfaces are generated by ploughing. Repeated sliding of the interface at the same groove introduces strain in the outermost layer which develops cracks on the surface. With continuos sliding after a critical number of strain cycles the crack size increases and generate flake like debris and on severe side fatigue fracture may occur [38], [39]. Figure 2-4 shows the fatigue wear mechanism.

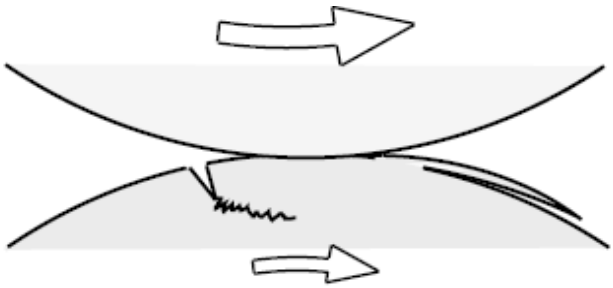

Figure 2-4. Fatigue wear mechanism showing cracks on the surface [38]

2.3.4 Tribochemical wear

Tribochemical wear occurs due to chemical interactions between the interacting surfaces and the surrounding which result in the formation of the reaction film. During tribochemical wear, material loss from the surface is due to oxidation reaction. Most common type of tribochemical wear is tribo-oxidation [39]. Figure 2-5 shows the tribochemical wear mechanism.

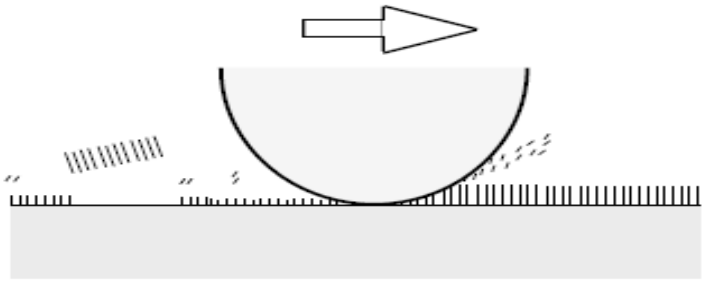

Figure 2-5. Tribochemical wear mechanism-showing chemical interaction [38]

2.3.5 Wear stages and engine components

Wear can be classified according to its stage and these stages are as follows: [3], [40]

- Break-in or running-in
- Normal wear or mild wear
- Wear-out or severe wear

Break-in or running in is the initial stage of wear mechanism in which components wear out very quickly. This high wear rate decreases rapidly as the surfaces after significant wear acquire the optimum form and surface finish and texture.

Normal wear or mild wear is relatively low wear and it continues to most of the components life cycle

Wear-out or severe wear is the last stage where interacting components almost finishes its useful life. During this stage wear rate rises steeply and results in a catastrophic failure.

Figure 2-6 shows life cycle stages of wear (also known as bathtub curve).

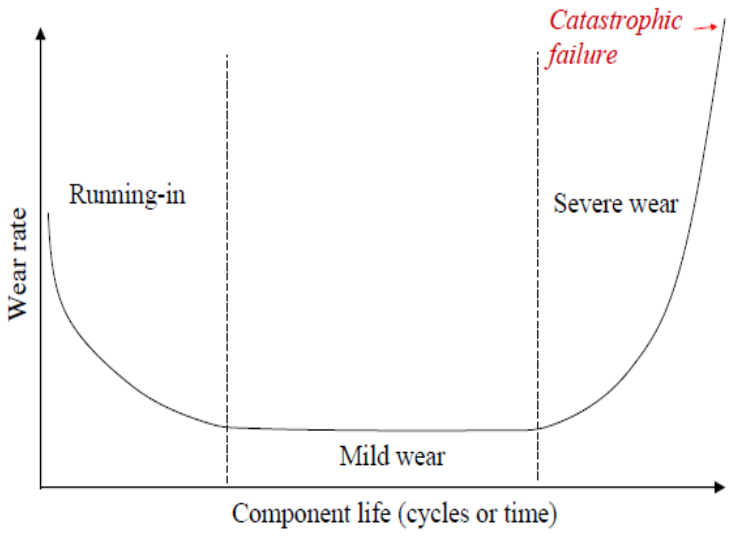

Figure 2-6. Bathtub curve showing life cycle stages of wear [40]

2.4 Lubrication regimes

Lubrication regimes are the most appropriate and the systematic way of distinguishing the form of lubrication in a tribological contact. Lubrication regimes can be identified by calculating the specific film thickness (lambda ratio, λ) which is defined in Equation 2-2 [3].

$$\lambda = \frac{h_{min}}{\sqrt{{R_{q1}}^2 + {R_{q2}}^2}} \qquad 2\text{-}2$$

Where,

λ is the specific film thickness

h_{min} is the minimum value of separation of the two interacting surfaces

R_{q1} and R_{q2} are the root mean square roughness's

h_{min}, can be calculated by using Hamrock and Dowson formula for non-conformal peizoviscous elastic contacts, as illustrated in Equation 2-3 [1]

$$\frac{h_{min}}{R'} = 3.63\,(\frac{U\eta_o}{E'R'})^{0.68}\,(\alpha E')^{0.49}\,(\frac{W}{E'R'^2})^{-0.073}(1 - e^{-0.68K}) \qquad 2\text{-}3$$

Where,

U is the entraining surface velocity [m/s]. It is average of the surface velocities of two bodies in contact [3]

η_0 is the dynamic viscosity of the lubricant [Ns/m^2]. It is measurement of fluid's internal resistance due to movement of layers over one another [41]

E' is the reduced Young's modulus [N/m^2], it is combine elastic moduli of the two solid surfaces in one comparable elastic single surface [3]

R' is the relative radius of curvature [m]. It is resultant of radius of curvature in x and y direction [3]

α is the pressure-viscosity co-efficient [m^2/N] which defines physical properties and molecular structure of the lubricant. Mathematical value of α is acquired from slope of the graph between natural log of dynamic viscosity and pressure [3]

$\boldsymbol{W}$ is the contact load [N]

$\boldsymbol{k}$ is the ellipticity parameter. $k = \frac{a}{b}$, a is the semi-axis of the contact ellipse in the transverse direction [m] and b is the semi-axis in the direction of motion [m]

$$k = 1.0339\ (\frac{R_x}{R_y})^{0.636} \qquad (k = 1 \text{ for ball}) \qquad 2\text{-}4$$

Specific film thickness (λ) values less than one show the maximum contact between the surface asperities, which is nearly similar to the contact area developed in dry contact (i.e. boundary lubrication regime), while λ value greater than 10 means that the interacting surfaces are comfortably separated by thick lubricant film (i.e. hydrodynamic lubrication regime) [3].

Stribeck, on the basis of friction experiments on bearings, demonstrated that the intensity of wear can easily be categorized by identifying different lubrication regimes in which the tribological contact is operated [3]. Stribeck discovered a relationship between the COF (μ) and dimensionless bearing number $\eta\omega/p$ (i.e. Hersey number), which shows that the COF is directly proportional to the viscosity and rotational speed and at the same time inversely proportional with the applied load on the interacting surfaces [3]. Figure 2-7 shows the modified Stribeck diagram, which elaborates the friction behaviour of the tribological interfaces in different lubrication regimes [3] and these regimes are,

- Boundary lubrication
- Hydrodynamic Lubrication
- Mixed lubrication
- Elastohydrodynamic lubrication

2.4.1 Boundary lubrication

The lubrication regime occurs when the lubricant film is unable to separate the interacting surface due to which asperity-to-asperity contact takes place. The real area of contact between the interacting asperities is comparable to the area of contact develops in the case of dry contact [3], [42]. Boundary lubrication regime is the most critical and severe in terms of friction and wear of engine components. The average film thickness in boundary lubrication regime is less than the composite surface roughness of the interacting surfaces and as a result metal-to-metal contact occur.

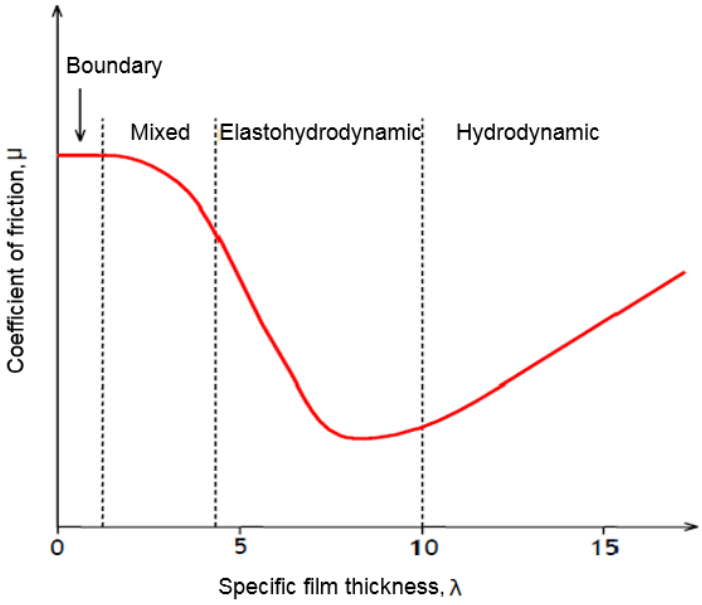

Figure 2-7. The Stribeck diagram which shows the friction behaviour of the tribological interfaces in different lubrication regimes [42]

Under boundary lubrication conditions (i.e. low speed and high load) asperities of interacting surfaces shear and expose a new metal surface. The lubricant chemically reacts with the newly exposed metal surface and forms a protective film having low friction values and wear resistance, which control friction and wear characteristics. The mechanism of lubrication is controlled by the additives in the lubricant, which modify the chemical properties of the lubricant [3]. Figure 2-8 (a) shows formation of boundary film between interacting surfaces.

In boundary lubrication, asperities of the rubbing surfaces collide with each other and as a result deformation happens elastically or plastically depending on the magnitude of applied load [42]. These collisions generate friction and heat, which upsurge the local temperature at the tip of the interacting asperities (called flash temperature) for a very short duration (i.e. for microsecond or less). High temperature and the newly exposed (nascent) surfaces initiate and proceed variety of chemical reactions which includes surface oxidation, lubricant oxidation and degradation [42].

Tribofilms formed in boundary lubrication are categorised in terms of surface action and these are [3],

- Physisorption
- Chemisorption
- Chemical reaction

Physisorption is a reversible process in which layer of lubricant attached with the surface and as a result provide moderate protection from wear. The protective layer that is usually comprise of one or more molecules attach with the surface due to intermolecular forces (i.e. van der Waal's forces). Chemisorption or chemical adsorption comprises of a degree of chemical bonding between layer of lubricant and substrate, which enables the adsorption of protective film on the interacting surfaces. The strength of chemical bond is depend on the reactivity of the metal substrate. Chemisorption is an irreversible process but in some cases, it is partially irreversible. Chemical reaction films utilize the flash temperature to produce the flexible surface layers. In this case, the lubricant chemically interact with the metal substrate and form a film, having different physical and chemical properties in comparison to substrate material. The formation of oxide layer on steel surface is a common example of chemical reaction film. Lubricant additives such as the one containing zinc (Zn) and phosphorous (P) generate effective protective films with chemical reaction and these films are even effective in extreme conditions [3], [43], [44].

2.4.2 Hydrodynamic lubrication

Hydrodynamic lubrication is the other extreme in which the surfaces are separated by the fluid lubricant and the behaviour of the surfaces are generally determined by the physical properties and more specifically by the viscosity of the lubricant. The lubricant films are usually thicker than the composite surface roughness of the interacting surfaces. Hydrodynamic lubrication is the ideal lubrication regime with no asperity-to-asperity contact [3]. Figure 2-8 (b) shows hydrodynamic lubrication between interacting surfaces.

2.4.3 Elastohydrodynamic lubrication

Elastohydrodynamic lubrication (EHL) is a sub type of hydrodynamic lubrication. In this regime, the fluid film in low conformity and in high-pressure tribological contact zone separates the interacting surfaces. The high pressure deform the shape of the interacting surfaces (i.e. elastic deformation) and significantly increase the lubricant viscosity in the contact zone. Typical example where the EHL regimes occur are gears, cams and tappets [3]. Figure 2-8 (c) shows elastohydrodynamic lubrication between interacting surfaces.

2.4.4 Mixed lubrication

Practically most of the tribological interfaces are not operated entirely in a single regime (i.e. purely boundary or hydrodynamic), but obey different lubrication mechanisms simultaneously. This additional lubrication mechanism which is a combination of several lubrication regimes is called mixed lubrication [3]. In mixed lubrication regime, there are regions in which asperities of the interacting surfaces are in contact (i.e. boundary regime), whereas the other regions in the contact are well separated by the lubricant film (i.e. hydrodynamic regime). Figure 2-8 (d) shows mixed lubrication between interacting surfaces. Surface roughness of the interacting bodies and the film thickness are very critical in order to describe the dominance behaviour of interaction as both regimes carry different characteristics. Apparently, mixed lubrication is the combination of two extreme regimes (i.e. boundary and hydrodynamic), so the chemical properties of the boundary lubricant and the physical properties of the bulk lubricant and more specifically the viscosity of the lubricant is of extreme importance in this regime [3].

2.5 Lubricants

In tribological contact lubricants are worked as anti-friction agent by providing gentle, even and hindrance free operation [37]. Lubricants reduce friction and wear, protect the engine components, keep the opposing surfaces separated by generating fluid film and ultimately reduce the risk of failure [10]. Basic function of the lubricant is to facilitate the smooth operation by reducing [37],

- Wear and heat dissipation and ultimately COF
- Oxidation and corrosion
- Water, dirt and dust ingress in tribological contact

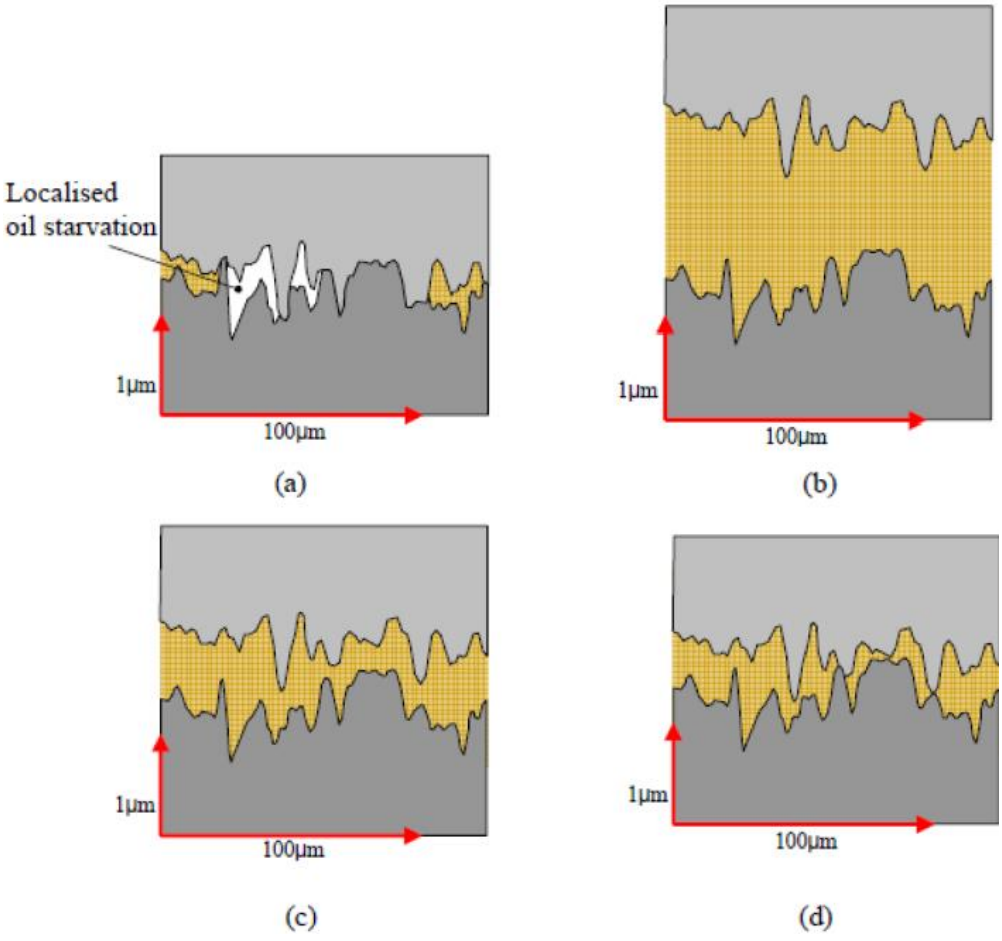

Figure 2-8. Schematic illustration of different lubrication regimes [40]

(a) boundary (b) hydrodynamic (c) elastohydrodynamic (d) mixed

In boundary lubrication regime lubricants provide lubricity by generating a protective film controlled by the additives added in the base oil (BO). These

additives improve the chemical properties of the lubricant [3]. Lubricants work as transport agent in the contact zone by transporting additives added in the BO to the regions of need and also transport waste away from the sites [10]. The formulation of modern lubricants is based on BO and chemical additives added in it to perform different functions in different operating conditions [35].

2.5.1 Base oil

Since 1852 petroleum BO has been using for lubrication, though initially it was not widely accepted due to poor performance but with time lubricant manufacturers developed understanding about crude oil composition and techniques to refine it, which improve its performance [45]. Basic function of the lubricant which contains approximately 75% - 95% of BO is to isolate the rubbing surfaces by providing fluid lubricant layer between them [3].

Table 2-1. Categories of base oil defined by API [45]

Base oil	**Description**	**Sulphur (%)**	**Saturates (%)**	**Viscosity index**
Group - I	Solvent refined oils	> 0.03%	≤90	> 80 to <120
Group - II	Mineral oils	< 0.03%	≥90	> 80 to <120
Group - III	Mineral oils	< 0.03%	≥90	> 120
Group - IV	Polyalfaolefins (PAOs)			
Group - V	All stocks not included in Groups I-IV (Pale oils and Non-PAO synthetics)			

Different type of BO are used in lubricants and these are mainly mineral oil, synthetic oil and vegetable oil. American petroleum institute (API) classified BO in five categories (mention in Table 2-1). Due to the price difference with synthetic oil, mineral oil is mostly used as BO. Mineral oil is produced by refining crude oil and the refining process consists of series of steps, which involve distillation, aromatic removal, de-waxing and finishing [45].

2.5.2 Lubricant additives

The lubricant additives are the oil soluble chemicals added in BO in order to improve the chemical properties and ultimately the performance of the lubricant in specific operating conditions [3]. The additives are added in small proportions (i.e. few weight percent 5% - 25%) in BO to get the desired level of performance, which is not possible from BO on its own. The functions of lubricant additives are [3],

- To reduce friction and wear
- To control viscosity
- To prevent corrosion and counter oxidation
- To control contamination
- To retain fluid properties in different operating conditions
- To reduce pour point and inhibit foam generation

Most of the additives are introduced between 1930 and 1940 to address the practical problem of growing auto industry, Figure 2-9 shows the development of the additives in chronological order. The most common lubricant additives used in the oil formulation include [3],

- FMs reduce friction by adsorbing on the contacting surfaces and formation of surface films. FMs reduce COF value and prevent stick slip phenomena
- AW / EP additive chemisorbs on the interacting surfaces and forms a protective surface layer which is much more stable and resistant as compared to boundary lubricant film
- Viscosity index (VI) improvers reduce the decline in viscosity with increase in temperature. High molecular weight polymers are used as VI improver as these polymers easily dissolved in BO and can change shape with the rise in temperature
- Dispersant additive precludes deposition of insoluble particles formed at lower temperature by scattering them

- Detergent additive minimizes or thwarts the insoluble deposits formed at higher temperature.
- Anti-oxidant additive reduces or delays the oxidation of BO. Oxidation of BO increases friction and wear. Oxidation gradually increases the viscosity and acidity of the base oil, which also promotes corrosion
- Anti-foam additive minimizes the foam formation capability of the lubricant
- Corrosion inhibitors protect the non-ferrous surfaces by forming a protective film against the corrosive attack by the additives having sulphur, phosphorous and halogen elements
- Rust inhibitors protect the surfaces having ferrous component by attaching the long chain anti-rust additive with the surface which minimizes the movement of water
- Pour point depressants are long chain polymers that interface with the crystallization process and preclude the wax formation at low temperature
- Tackiness additives minimize the oil loss from the surface due to gravitational force or centrifugal force

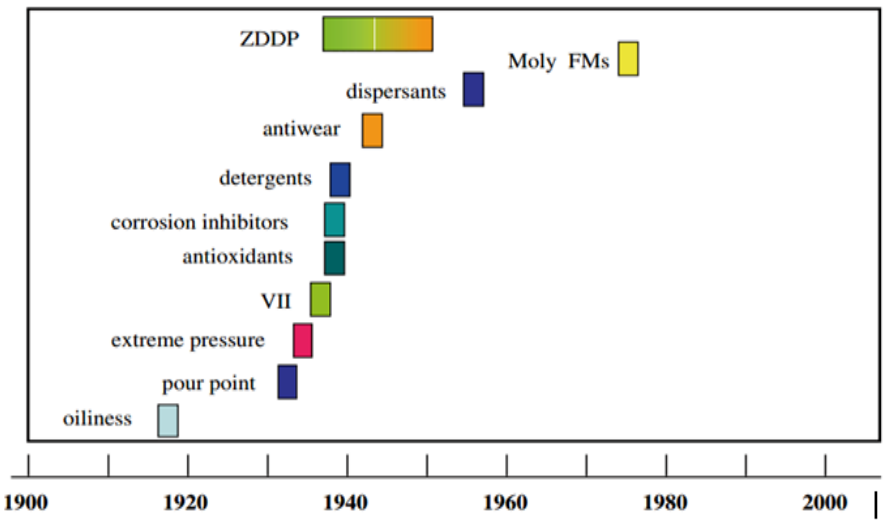

Figure 2-9. Development of lubricant additives in chronological order [15]

2.6 Engine tribology and challenges

Transportation or means of transportation utilizes approximately 20% of the energy resources consumed globally and contributes 18% in greenhouse gas emissions [5], [6]. Approximately three fourth (3/4th) of the world freight is transported by ships followed by rail and road transportation [7]. However, in terms of energy consumption situation is very interesting. Road transportation accounts 72% of the total transport energy consumption followed by ships (i.e. 10%) and rail (i.e. 3%) [7]. Light duty vehicles (motor cars, vans and SUVs) consume approximately 53% of the transport energy whereas trucks and buses both consume around 21% of the energy resources [6], [7]. Figure 2-10 shows breakdown of global transportation energy consumption. Road transportation not only consume major share of transportation energy but also contribute 80% of the greenhouse gas emissions [6], [7]. In 2009, passenger cars globally consumed 208,000 million litres of fuel to overcome friction and furthermore one passenger car consumes 310 litre of fuel per annum to overcome friction [6]. More than 32 million vehicles registered in the UK are classed as motor cars (i.e. 87.9% of the total numbers of vehicles), followed by vans, trucks and buses & coaches [46]. Majority of the vehicles in the UK are powered by petrol fuel followed by diesel, while small proportion belongs to liquid petroleum gas and other fuel groups [24], [47].

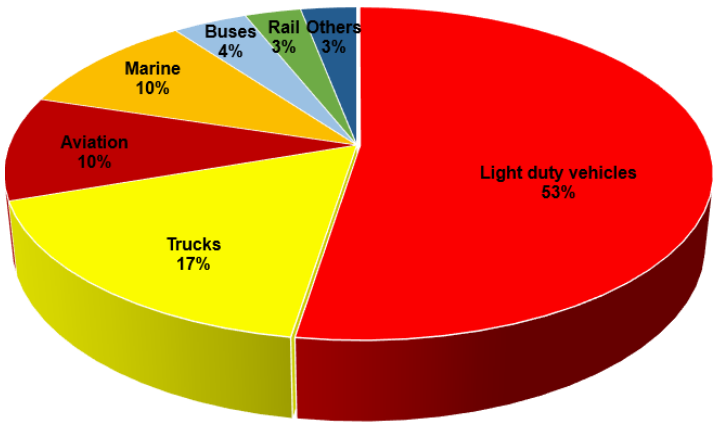

Figure 2-10. Breakdown of global transportation energy consumption [7]

2.6.1 Engine tribology

An automotive engine consists of different moving parts, which are in contact with each other under various operating conditions. During driving cycle, operating condition varies from idle running to acceleration and running at constant speed to deceleration as illustrated in Figure 2-11.

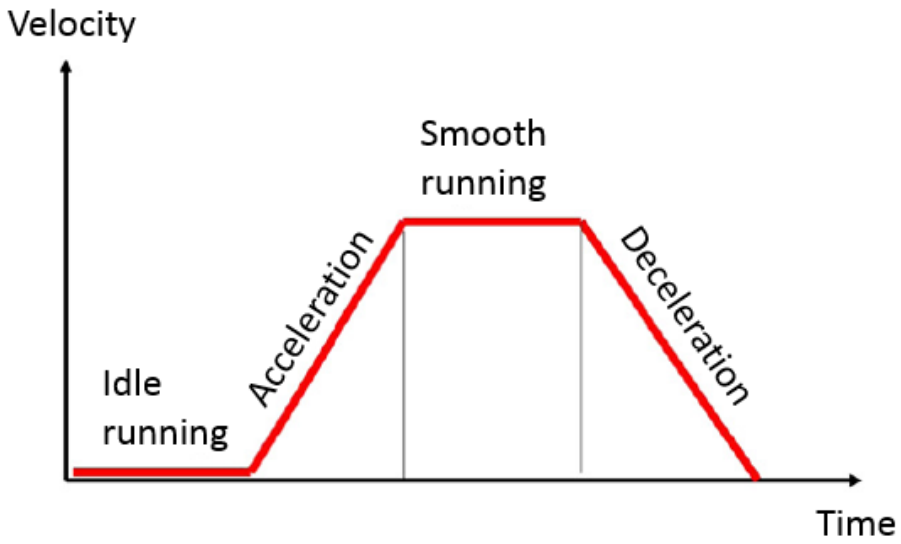

Figure 2-11. Operating conditions during driving cycle [6]

During idle running phase fuel energy is consumed to overcome engine and transmission friction losses [6]. In acceleration phase, energy is consumed in producing kinetic energy along with overcoming friction in the engine components, transmission system, tyres and air drag [6]. During smooth running phase, energy is mainly consumed in overcoming friction in engine, transmission and tyres along with air drag [6]. In deceleration phase, fuel energy is consumed mainly in overcoming friction in the engine components, transmission, tyres and brakes. It is obvious from different operating conditions that major portion of the fuel energy is consumed in overcoming friction and air drag [6].

The internal combustion (IC) engines have relatively low thermal and mechanical efficiency [24]. The IC engines dissipate major amount of fuel energy as heat from engine surface or exhaust pipe. In a typical passenger car approximately 60% of the fuel energy is dissipated as thermal losses from

engine/exhaust pipe and only quarter of the fuel energy is converted in to useful power [6], [24], [48]. Figure 2-12 shows distribution of the fuel energy in an automotive application.

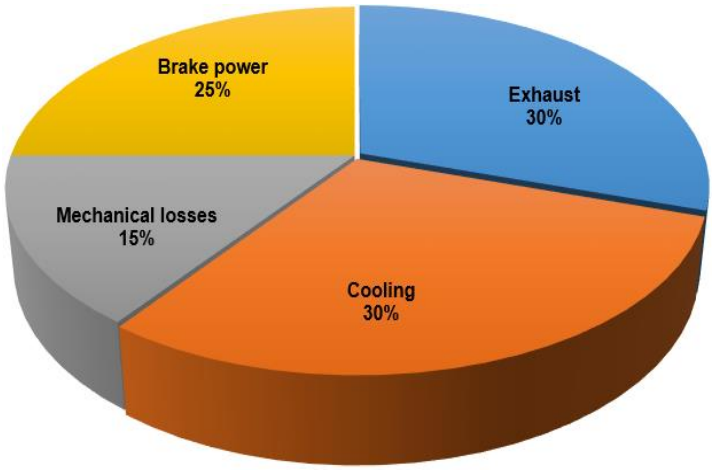

Figure 2-12. Energy distribution in an IC engine [24]

An IC engine used in passenger car converts approximately 38% of the fuel energy in to mechanical power and out of it only 21.5% power is available to move the car [6]. Mechanical interaction contributes a further 15% loss of energy, which means that around three quarter of the fuel energy is not utilized to get any output and the power is only produced by the remaining quarter of the original fuel energy [6], [7], [24], [48]. Figure 2-13 shows detail fuel distribution in passenger car. An ideal engine based on Carnot cycle produce maximum efficiency of 85% but practically it is very difficult to lowered the heat dissipation and achieve high thermal efficiency. An IC engine even with less heat dissipation received attention in the past but these engines achieved maximum brake efficiencies around 45% which is nearly half of an ideal Carnot heat engine [24].

Engine friction losses in an automotive applications can be divided in to four basic groups and these are [6], [7] ,

- Piston assembly
- Valve train system
- Bearings and seals
- Hydraulic and pumping

The piston assembly contributes the major chunk (i.e. nearly half of the total losses) followed by the losses in the bearings (i.e. one fourth of the total losses) [6], [7], [24]. Major percentage of engine losses contributed by piston skirt cylinder interaction, piston rings and bearings and the percentage of these losses are around 66% of the total engine losses, while the valve train, crankshaft, transmission and gears contributed the rest of 34% losses [10].

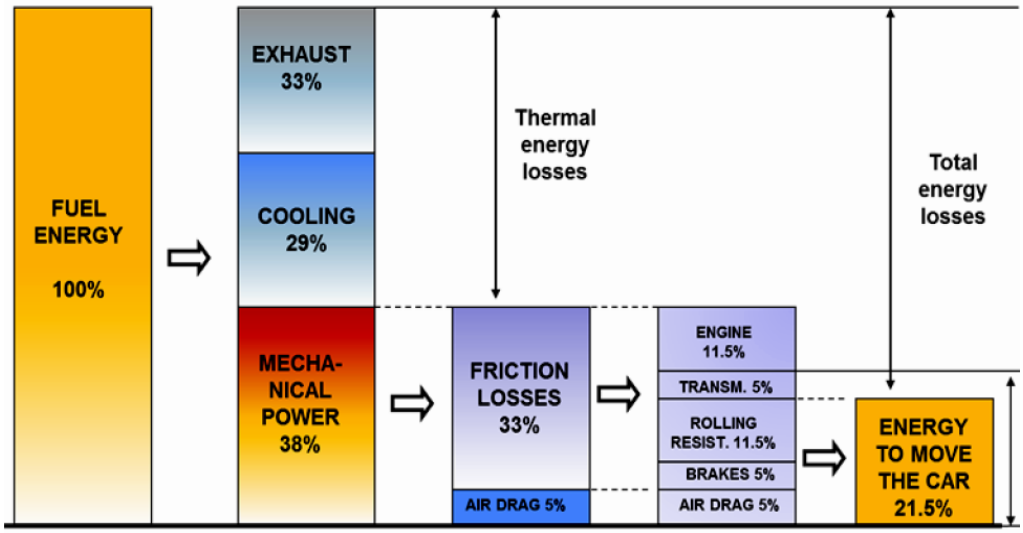

Figure 2-13. Fuel energy distribution in a typical passenger car [5], [6]

Figure 2-14, shows distribution of engine losses during urban driving cycle in a passenger car. In powertrain system major losses arise from the piston rings and piston skirt cylinder interface while the bearings (i.e. included both crankshaft and camshaft bearing) also contribute significant losses followed by pumping and the valve train losses [6], [7]. Tung et al. [10] suggested that mechanical losses distribution generally depends on several factors which include operating conditions, type of engine, engine performance and the lubricant use in an engine. Fuel consumption data, revealed that only 10% reduction in mechanical losses would lead to 1.5% potential savings in fuel usage [24].

The engine components experience different mode of lubrication in order to attain good tribological performance. A piston ring is the most complicated engine component which operates in all the four lubrication regimes during one single stroke [10], [23]. The bearings (i.e. journal or thrust bearings)

operate in hydrodynamic lubrication in which oil film separate the interacting surfaces. Lubricant viscosity is critical in hydrodynamic lubrication [10]. The cam follower operates in boundary and mixed lubrication regimes, where asperities of the interacting surfaces are in contact [23].

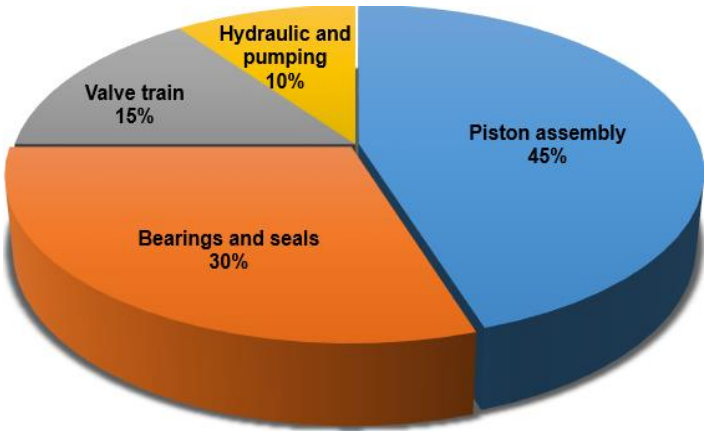

Figure 2-14. Mechanical losses in an IC engine [6], [7], [24]

The role of additives in the lubricant, chemical film and the reaction products play a crucial role in boundary and mixed lubrication regime [10]. Due to the fact that different engine components experience more than one lubrication mechanism during a single cycle, this situation poses a serious challenge for the tribologists to design a single component suitable for all lubrication regimes and also the lubricant oil having specification suitable for all lubrication regimes [24].

2.6.2 Tribological challenges

Reduction of friction and wear by effective lubrication of interacting engine components with minimal environmental impact are the desired goals of the tribologists. This job even becomes more difficult due to changing operating conditions (i.e. load, temperature and speed) of the engine. In the current global scenario with tough competition in the automotive sector and strict environmental/emissions legislation (i.e. Euro 5 or Euro 6 in Europe), the main tribological challenges are,

- Less fuel consumption
- Maximum power output

- Reduction in restricted exhaust emissions
- Reliability, durability and longer engine life
- Less maintenance

Efficiency of the internal combustion engine is the centre point of almost all the tribological challenges. Improvement in fuel economy without reducing the friction losses in the engine components is not possible. Reduction in engine weight by using lighter materials instead of conventional material, deposition of low friction coatings on engine components, surface modification (i.e. super finishing to get the smoother surface and laser surface texturing), simplifying the design of the engine components and using low viscosity lubricating oil are some of the options to meet the above mentioned challenges [6], [10], [38]. The IC engines are the key source of environmental pollution via exhaust emissions which includes particulate matters, burned hydrocarbons, NO_x and CO_2 [13]. The environmental/emissions legislation (i.e. European emission standard), continuously lowered/tightened the limit of harmful exhaust emissions in order to reduce the IC engines contribution to environmental pollution [12]. Figure 2-15 illustrates the emissions levels in previous and current standard.

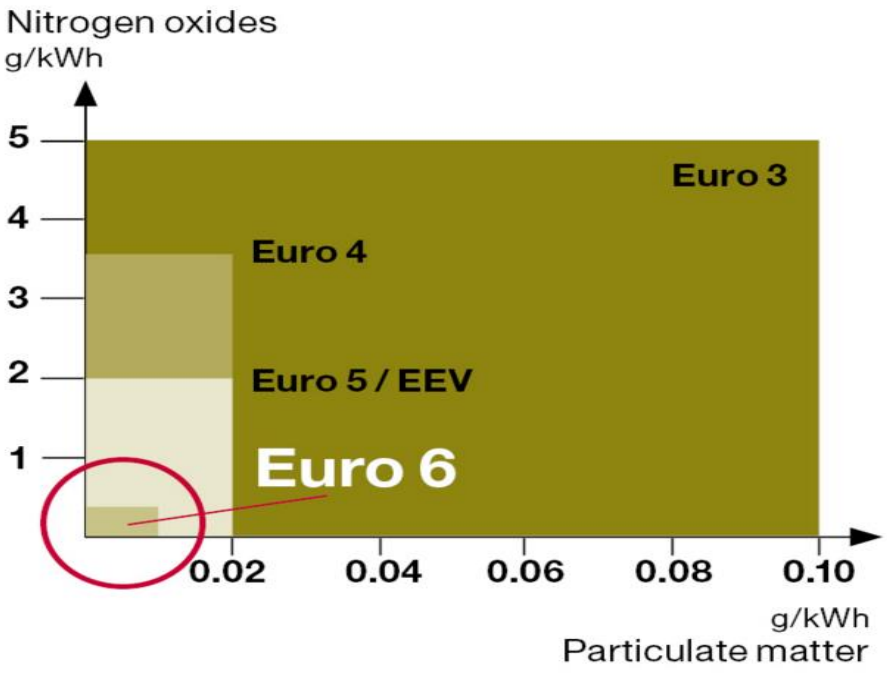

Figure 2-15. Massive reduction in exhaust emission levels [49]

One of the key challenges for the tribologists is to reduce the harmful exhaust emissions from the IC engines. AW and AO additive (i.e. zinc-dialkyldithiophosphate) in the engine oil is considered as non-environmentally friendly additive due to the catalyst contamination caused by the P and S present in ZDDP [50]. In addition, ZDDP has a negative impact on COF value in tribological systems lubricated in boundary and mixed regimes, which affect the overall fuel consumption. Development of low SAPS (Sulphated Ash, Phosphorus and Sulphur) engine oils with low friction and wear performance is essential for reducing further impact of automotive engines on environment. Among different additives in lubricant formulation, AW additive and friction modifier (FM) plays an important role.

Next chapter will discuss tribofilm structure, film formation mechanism, film morphology and mechanical properties of tribofilm formed by AW additive.

2.7 Summary

This chapter covers basic literature about tribology (i.e. friction, wear and lubrication), role of lubricants to minimise friction and wear in different lubrication regimes. Tribological challenges related to automotive application are discussed in this chapter. The friction is the opposing force, which offer hindrance to the motion when bodies move tangentially over one another and it is the major cause of wear and heat loss. The wear is process of material removal from the interacting surfaces and this physical separation is the result of surface micro fracture and chemical reaction at elevated temperature between interacting surfaces. During interaction of components, many mechanisms occur concurrently and the intensity of these mechanisms depends on several factors.

In tribological contact, lubricant worked as anti-friction media by providing gentle, even and hindrance-free operation. Lubricants reduce friction and wear, protect the automotive components, keeping the opposing surfaces separated by generating fluid film and ultimately reduce the risk of failure. Lubricant are composed of base oil (75% - 95%) and chemical additives (5% - 25%). Additives added in BO to get the desired level of performance, which is not possible from BO. Different additives added in BO for performing different functions but FM (which reduce friction) and AW additives (which reduce wear) are most important among them. Transportation sector utilizes approximately 20% of the energy resources consumed globally and light vehicles consume approximately 50% of the energy resources in transportation sector. An IC engine used in passenger car converts approximately 38% of the fuel energy in to mechanical power and out of it, only 21.5% is available to move the car. Fuel consumption data revealed that only 10% reduction in mechanical losses would lead to 1.5% potential savings in fuel usage.

Reduction of friction and wear by effective lubrication of interacting engine components with minimal environmental impact are the desired goal of the tribologists. One of the key challenges for the tribologists is to reduce the harmful exhaust emissions from the IC engines. AW and AO additive (e.g. zinc dialkyldithiophosphate) in the engine oil considered as non-environmentally friendly additive due to the catalyst contamination

caused by the P and S present in ZDDP. Development of low SAPS (Sulphated Ash, Phosphorus and Sulphur) engine oils with low friction and wear is essential for reducing further impact of automotive engines on the environment.

Chapter 3
Literature review; ZDDP tribofilm structure, morphology and film formation mechanism

3.1 Lubricants and lubrication

The automobile sector has been facing a constant challenge of reducing fuel consumption and exhaust emissions while maintaining customer satisfaction (i.e. reliability, comfort, cost and maintenance). Fuel consumption cannot be improved without reducing engine friction, which accounts approximately 48% of the energy produced by an engine [51]. Design simplification and weight reduction of the engine block/components by changing the traditional materials, surface modifications and fit for purpose lubrication on interacting surfaces are some effective ways to reduce the friction and hence the fuel consumption [51]. More specifically, there are three basic approaches to achieve an optimal tribological solution in order to reduce friction and wear in the engine components and these are often called lubrication, design and material (LUDEMA) [51]

Many additives are added in modern engine oil but the most important additives for the tribological performance of lubricant under boundary lubrication conditions are the AW additives (i.e. ZDDP) and FMs [16]. Lubricant manufacturers have been using ZDDP for more than 70 years due to its excellent performance. ZDDP was initially introduced as an AO additive but later it was discovered that as an AW and EP additive, ZDDP performed remarkable and since then ZDDP has been considered as the most effective AW additive and became an essential ingredient of lubricant formulation [16]–[18]. FMs are the lubricant additives, used for lubrication of interacting surfaces in boundary and mixed lubrication regimes. Boundary and mixed lubrication regimes are the most critical regimes due to asperity-to-asperity contacts and the control of friction and wear during these conditions are crucial. FMs reduce boundary friction and improve lubricity and thus contribute in the overall improvement of the fuel economy [22].

3.2 Zinc dialkyldithiophosphate

Zinc dialkyldithiophosphate (ZDDP) has been known as the principal AW additive since 1955 and due to its excellent performance almost all the engine oil formulations contain ZDDP [15], [52]. In reciprocating internal combustion (IC) engine, the cam follower interface is one of the highly stressed engine component, which generally operates at 1m/s speed with local pressures in the region of 1GPa. Due to the severity of operating conditions, additives like fatty acid are unable to protect the interacting surfaces from severe wear. ZDDP, as an AW additive, plays a crucial role by forming a protective film between the interacting surfaces, which minimizes wear and halts the premature failure of the engine components [53], [54]. Engineers and research scientists are continuously working to improve the fuel efficiency and these efforts ultimately demand that engine components may operate safely under even greater stress.

ZDDP is a major source of phosphorous (P) in engine oil formulation. Formation of phosphorous oxide decrease the useful life of the exhaust system by degrading the catalyst [19]–[21]. Therefore, limits on the P were introduced to address this issue and recently, limit on the amount of sulphur (S) has also been introduced. The concentration of P can be controlled by reducing the concentration of ZDDP in engine oils [19], [20], but this action has its own implications in terms of wear control [55]. The lubricant additive industry has been trying hard to replace ZDDP completely or partially with P and S free compounds and currently two options are under investigation, which are as follows [15], [56],

- Development of completely new wear control systems (e.g. nanoparticles)
- Development of new AW additives devising AW performance near enough to ZDDP but comprise of low or no P content

To proceed with the latter option, it is necessary to understand how ZDDP interacts with surfaces and other additives to perform its AW action [56]. Spikes [15] reviewed literature about ZDDP and stated that the exceptional

triple role of ZDDP as an AO, EP and AW additive is still being actively studied. He further expressed that in fully formulated oils, the blends of ZDDP with other additives show complex interactions between the additives. Therefore, it is easier to analyse the mechanism of ZDDP in a simpler solution rather in fully formulated oil.

During initial stages of surface interaction, extensive sliding of metal asperities produce a metal sulphide layer which protects against EP [20], [57]. ZDDP is decomposed in these extreme circumstances (i.e. high temperature and pressure) and forms sacrificial tribofilms comprised of thick zinc phosphate film on top of these sulphides layers [57].This protective film minimizes asperity-to-asperity contact and hence, reduces wear [20], [25], [58]. Zinc phosphate tribofilm formed by ZDDP works as a barrier between two metallic surfaces and at the same time also reacts with wear particles and digests them inside the zinc phosphate film [20], [58]. The driving force behind the formation of ZDDP AW film is still unresolved. Nicholls et al. [26] mentioned that after years of research on ZDDP, the interaction mechanism of AW film on surfaces is still not clear. They further expressed that the lubrication behaviour of ZDDP can be analysed by assessing its performance at very basic level, in the absence of other additives.

ZDDP is synthesized by the chemical interaction of phosphorus pentasulphide, alcohols and zinc salts. Chemical structure and molecular weight of alcohol used in the formation influence the behaviour and effectiveness of ZDDP [55]. Figure 3-1 shows a simple representation of ZDDP structure,

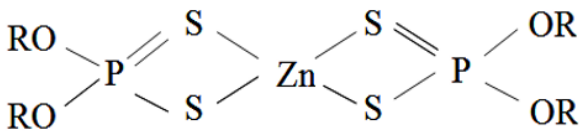

Figure 3-1. Chemical structure of ZDDP [15]

The radical group (R) in the structure shows alkyl or aryl group which basically facilitates the solubility of ZDDP in the base oil (BO) [59]. On the basis of

chemical structure, ZDDP has been categorized in different types including aryl ZDDP, primary alkyl ZDDP ($CH_3CH_2CH_2CH_2O$-) and secondary alkyl ZDDP ($CH_3CH_2CH(CH_3)O$-). The thermal decomposition temperature varies with the structure of ZDDP [25]. Barnes et al. [59] mentioned that the aryl ZDDP are more thermally stable as compared to other family members of the group. The order of thermal stability of different ZDDP structures are [25], [59],

aryl > primary alkyl> secondary alkyl

Due to their thermal stability, aryl ZDDPs are normally used in diesel engines while primary and secondary ZDDPs are used in petrol engines [60]. The AW performance of these different types of ZDDPs are believed to be inversely related to their thermal stability [15] and is ranked in the following order [15],

secondary alkyl > primary alkyl > aryl

Nicholls et al. [26] stated in a review study that the AW film form by the decomposition of alkyl and aryl ZDDP does not only differ chemically but also differs in wear performance. Protective films formed on the interactive surfaces by alkyl ZDDP are generally more effective as compared to aryl ZDDP [26]. Graham et al. [27] mentioned that the secondary alkyl ZDDP decompose very quickly to form an effective tribochemical film on the interacting surfaces while in case of the aryl ZDDP, the film formation mechanism is relatively slower. ZDDP reduces wear by forming a thick reaction film on the interacting surfaces [59]. The protective film formed by ZDDP seems like solid patches on the rubbing surfaces, which limit the metal-to-metal contact [61]. Figure 3-2 shows a typical topography of the ZDDP tribofilm from MTM tribometer. Researchers [25], [62] believe that the padded structure of the AW film is comprised of zinc metaphosphate or polyphosphate glasses most likely having zinc (Zn) as the counter cations.

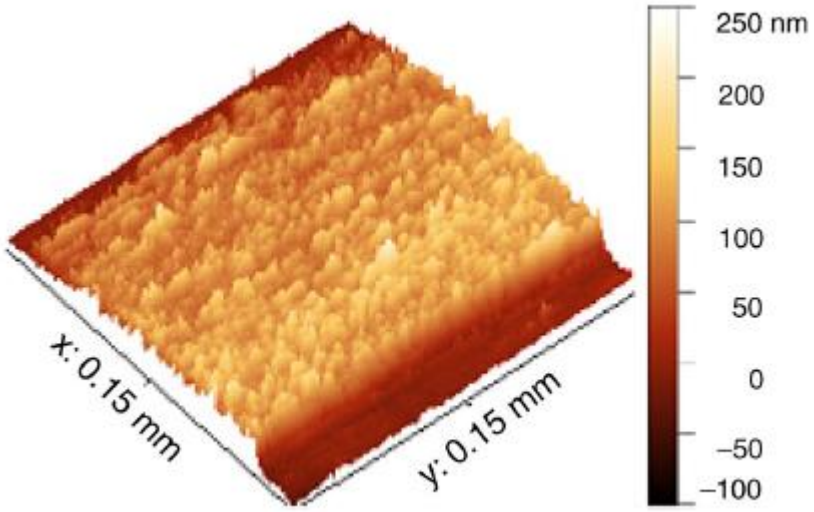

Figure 3-2. Atomic force microscope (AFM) image of a typical ZDDP tribofilm, which limit the metal-to-metal contact [61]

3.3 ZDDP anti-wear films

The decomposition of ZDDP produces reaction products which form protective films, minimizing the asperity-to-asperity contact [15], [25]–[27]. ZDDP decomposes mainly due to thermo-oxidative process at or above 100°C without any rubbing. Martin and colleagues [56], [58] mentioned that above 100°C ZDDP starts decomposing due to thermo-oxidative process in presence of molecular oxygen in the BO. The film formed as a result of this decomposition is called thermal film [15], [25], [63]. ZDDP reacts in the solution phase at even higher temperatures (i.e. 130°C - 230°C) due to thermo-oxidative degradation [15]. Spedding et al. [53] suggested that ZDDP decompose in oil due to reaction at elevated temperature. ZDDP do not chemisorb significantly on iron surfaces but it is the decomposed product of the ZDDP, which adsorbs on interacting surfaces and provides AW action. The AW film is mainly composed of Zn, P, S and O in different proportions. ZDDP can form AW films even at room temperature [20], [64], on the rubbing track whereas the protective film does not form on the surrounding of the wear track. The AW film formed due to chemisorption of the decomposed product on the wear track is called tribofilm [25], [58], [63], [64].

It is very interesting that the distinction between thermal and tribofilm was not established until the late 1970s and later it was recognised that tribofilms could even form at lower temperature on the rubbing track while thermal films formed at higher temperature (i.e. above 100°C) without rubbing. Zhang et al. [63] mentioned that difference in formation of thermal film and tribofilm significantly changes the mechanical properties of the film. Due to mechanochemical formation mechanism, tribofilms carry iron (Fe) cations originating from substrate material, which consequently alters phosphate ratio in the tribofilm and hence affects the mechanical properties of the tribofilm.

3.3.1 Thermal films

ZDDP in BO forms transparent, solid like zinc phosphate reaction film on the metal surfaces at elevated temperature [15], [25], [63]. This well-known thermal film do not need friction or rubbing of asperities and the rate of film formation increases with increase in temperature [15], [65]. Gosvami et al. [65] suggested that thermal film is formed from decomposed ZDDP products. Thermal films are weakly adsorbed films and unlike tribofilms these can easily be removed [26], [28], [65]. The thermal films have good AW properties and can resist wear up to 12 hours in base oil [15].

The composition of thermal films is similar to that of tribofilms [26]. Thermal films are comprised of short and long chain phosphates and thiophosphates deposited on the substrate surfaces [15], [66]. The thermal films are heterogeneous in structure and comprised of a mixture of iron oxides combined with zinc oxides and phosphates [26], [67]. Chemical analysis of the thermal film with X-ray absorption near edge structure (XANES) indicated a decrease in the number of O atoms surrounding Fe atoms as the temperature increased to 150 °C [26], [68]. The overall structure of the thermal film is described as a network of phosphate glasses modified by Zn and Fe cations. The protective film with this composition is good enough to protect the substrate from oxidation [26], [69]. Aktary et al. [28] stated that ZDDP deters the oxidation of the metal surface and forms phosphate sacrificial film which reduce the magnitude of wear. ZDDP AW film in general and thermal films specifically are not composed of ZDDP additive in its own but actually, ZDDP decomposed products form this film. Zinc phosphate is recognised as an important reaction product of ZDDP tribochemical reaction [56], [58], [70].

Equation 3-1 shows an over simplified global chemical reaction which shows the thermo-oxidative decomposition of ZDDP without rubbing at elevated temperatures [58],

$$Zn[(RO)_2PS_2]_2 + O_2\,(ROOH) \xrightarrow{\text{(Temp. > 100 °C solid surface film)}} Zn_{n+2}[P_nX_{3n+1}]_2 + \text{sulphur species} \qquad 3\text{-}1$$

In the above mentioned decomposition equation, X represents O atoms while some S atoms can substitute for O in the phosphate chain. Decomposed phosphate deposits on the metal surface and S species remains soluble in the lubricant phase. Martin [58] further stated that in case of the steel substrate, iron oxide and phosphate normally react and as a result, adhesion capability of the film is increased. Spikes [15] also proposed that deposition on the metal surface comes from thermal degradation of the material (ZDDP) and the possibility of chemical reaction between deposited species or film and the metal surface is considered the key reason for the tribofilm formation. It is due to this fact that Fe and other metals are Lewis acids and act as a catalyst in the thermal degradation, whereas Zn can be easily replaced with the metal ions to form dithiophosphates [15].

3.3.2 Tribofilms

ZDDP forms a thick, un-evenly distributed and primarily solid like reaction films on steel surfaces [15], [28], [29], [63], [65]. This film is mainly generated inside the rubbing track with the film roughness aligned with direction of motion [52]. ZDDP containing lubricants form tribofilm at the rubbing interfaces even in the absence of high temperature [20], [25], [63]. ZDDP tribofilm formation is dependent on various factors (e.g. flash temperature, contact pressure, surface catalysis and triboemission) [20], [63], [71], [72]. The tribofilm is composed of phosphate layers. The bottom layer (near the substrate) is comprised of short chain phosphate covered by the thin long chain phosphates, which forms the top layer (farthest from the substrate) [15], [18], [58], [70], [72]–[74]. Aktary et al. [28], [29] also supported the existence of bi-phosphate layer structure with the bulk of the film is composed of short chain phosphates while the top part of the film is dominated by longer chain

phosphates. Abdel et al. [75] analysed the decomposition of ZDDP tribofilm with synchrotron X-ray absorption spectroscopy (XAS) and demonstrated the formation of shorter and longer chain phosphates by in-situ experiments. They found that shorter chain phosphate formed first because of ZDDP decomposition and then these short chain phosphates polymerize to form longer chain phosphates. Polymerisation of shorter chain into longer chain phosphate is believed to be due to rubbing of asperities [74], [75]. On the other hand, some studies [58], [76], [77] claimed that the longer chain phosphates are formed first and then depolymerized into shorter chain phosphates due to presence of iron oxide in bulk of the tribofilm near the substrate. Long chain phosphate convert in to short chain due to extended rubbing [78] and also increase in contact pressure produce tribofilms constituted by short chain phosphate [77].

ZDDP form thick AW film on interacting surfaces, which is primarily composed of amorphous zinc phosphate [76], [79]. Digestion of iron oxide particles in ZDDP tribofilm promote amorphisation [80], [81]. However, Minfray et al. [82] observed amorphous AW film with low or no iron content in it. The X-ray powder diffraction (XRD) analysis of synthesized metaphosphate and orthophosphate suggested amorphous peak pattern in metaphosphate whereas crystalline pattern in orthophosphate [77]. The XRD results showed relationship between reduction in phosphate chain length and nano-crystallinity in structure of the tribofilm [78]. Focussed ion beam milling (FIB) and transmission electron microscopy (TEM) analysis proposed that ZDDP tribofilms possibly comprised of both amorphous and nano-crystalline structures [83]. Recently, Ueda and colleagues [78] analyse durability of ZDDP tribofilm using FIB-TEM. They observed that the tribofilm near the substrate was nano-crystalline whereas upper part was amorphous, which removed comparatively easily. Extended rubbing transformed all sections of the tribofilm into nano-crystalline structure, which subsequently increased tribofilm durability. They further claimed that reduction in phosphate chain length and thus nano-crystallinity in tribofilm structure is dependent on the availability of shear and heat in the contact zone [78].

Researchers [18], [76], [84], [85] proposed that the tribofilm is formed in two layers with top layer consist of glassy phosphate film while the bottom layer is

composed of iron sulphide and iron oxide. Figure 3-3 shows two-layer structure of the tribofilm proposed in studies [85], [86]. Rounds [87], [88] analysed the tribofilm formed on the rubbing surface with the X-ray fluorescence (XRF) spectrometer and found that tribofilm contained larger phosphorus to sulphur ratio as compared to base compound and it was '*several hundred monolayer thick'*. He further mentioned that temperature plays a central role in the growth of tribofilm and because of this reason film formed very quickly inside the rubbing track.

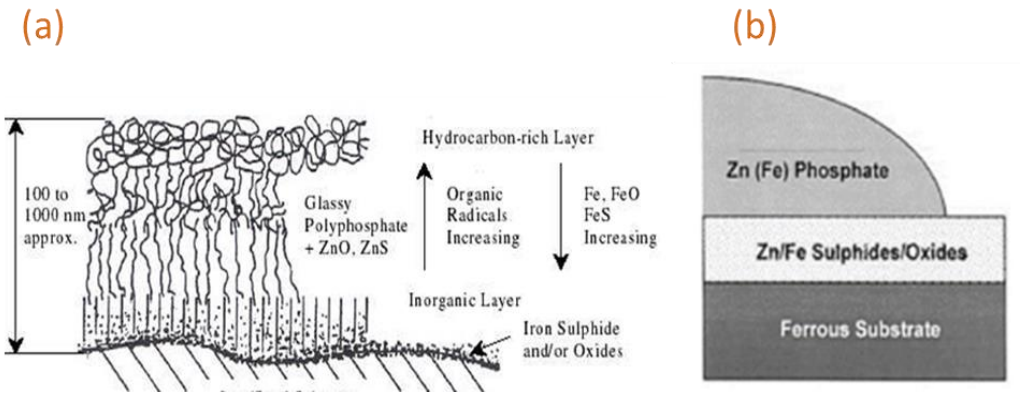

Figure 3-3. Two layer proposed structures of AW ZDDP tribofilm

(a) Bell et al. [85] (b) Smith et al. [86]

Nicholls et al. [26] stated that the tribofilm formed from neutral ZDDP is found similar to thermal films (i.e. having short and long chain phosphates). Tribofilms formed from aryl ZDDP contained only long chain phosphates while the tribofilm formed from alkyl ZDDP composed of layers of both short and long chain phosphates. The difference in tribofilm composition in aryl and alkyl ZDDP elucidates the variance in adsorption and wear performance of these two types of ZDDPs. They further claimed that physiosorption of ZDDP on Fe and iron oxide is significant up to 100 °C and chemisorption dominates at elevated temperature. S- contribute actively in the formation of two-layer structure of the tribofilm. S- is reduced to sulphide in the tribofilm and mostly exist in the depth of the tribofilm near the substrate [58], [75], [89]. The tribofilm is composed of phosphates with some traces of sulphides and these are present as zinc sulphide throughout the structure and iron sulphide mainly near the substrate [90], [91]. Tribofilm is mainly constituted by a bi-layer

structure of long and short chain phosphates with low or no ferric oxide on top surface, but the bulk of the film may contain iron oxide because of abrasive wear [58], [70].

3.4 ZDDP tribofilm formation

What drives ZDDP to form tribofilms and how this AW film form on interacting surfaces (specifically, on steel surfaces)? Rise in flash temperature promotes ZDDP tribofilm formation [72] but ZDDP also form tribofilms at low sliding speeds, when increase in flash temperature is negligible [25], [63]. Abdel et al. [92] recently performed a single asperity study to unveil the key driving force for tribofilm formation and found that rise in flash temperature along with pressure at contacting asperities play an important role in ZDDP tribofilm formation. Zhang et al. [63] on the other hand, suggested that local stress along with temperature rise in the tribological contact zone is the main driving force for tribofilm formation. ZDDP can form tribofilms even in the absence of asperity-to-asperity contacts as long as enough local shear is available (i.e. EHD lubrication) [20]. Tribofilms generated on steel surfaces are generally 50-150 nm thick [15], [25], can form in sliding as well as rolling-sliding contact conditions but due to low contact shear stress, no tribofilm is formed in pure rolling contact [63], [93]. Studies [15], [58], [65], [94] suggested that ZDDP form tribofilm due to any one of these mechanisms which include thermal, catalytic or oxidative degradation, adsorption at surfaces, oxidation and chemical reaction with iron oxide or combination of the these mechanisms. Using in-situ AFM technique, Gosvami et al. [65] monitored the evolution of ZDDP tribofilm. They observed that the ZDDP tribofilm evolve with the rubbing time (sliding cycles). Figure 3-4 shows morphological growth of ZDDP tribofilm.

In most cases ZDDP forms zinc phosphate (thermal) films on a steel surface and the film formation is the result of thermo-oxidative decomposition of ZDDP [58][28]. Rubbing between interacting asperities produce nascent surface by disturbing the thermal film. This newly expose surface chemically react with the O (already present in the lubricant) and form iron oxide (Fe_2O_3) [58], [70]. Researchers [26], [58], [70] suggested that phosphate films interact with iron oxide layer due to acid base reaction and form an inter grown layer.

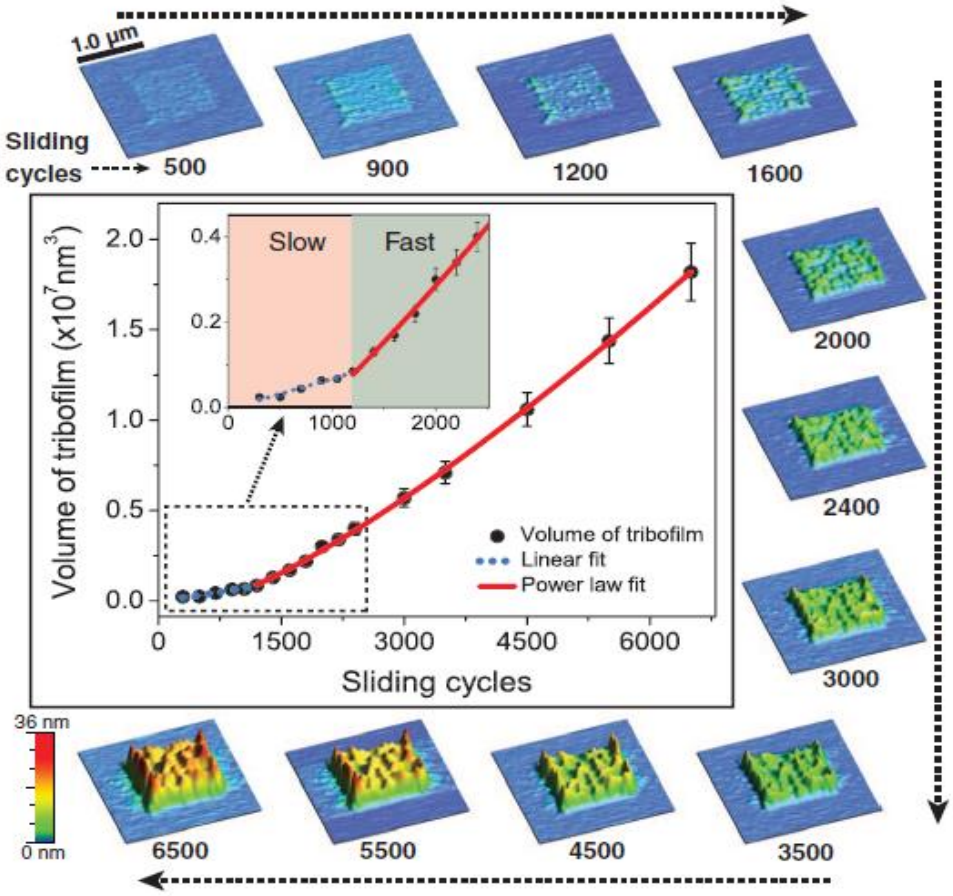

Figure 3-4. Evolution of ZDDP tribofilm with the sliding cycle [65]

Iron oxide has ability to damage the tribofilm by the mechanism of abrasive wear (i.e. due to hardness of the crystallized oxide). Abrasive wear itself produces debris due to plastic deformation and the nascent surfaces oxidise very rapidly. This mechanism of catastrophic wear can finally take the interacting components to scuffing. AW tribofilm formed by ZDDP, which is composed of phosphate glasses has capability to digest abrasive iron oxide particles with the help of tribochemical interactions. Equation 3-2 shows this tribochemical reaction to illustrate this digestion. It is based on Pearson's hard and soft acids and bases (HSAB) theory, in which zinc metaphosphate settles 1 mole of Fe_2O_3 [58], [70] ,

$$5\,Zn(PO_3)_2 + Fe_2O_3 \longrightarrow Fe_2Zn_3P_{10}O_{31} + 2\,ZnO \qquad 3\text{-}2$$

(ZnO, P_2O_5) $(Fe_2O_3, 3\,ZnO, 5\,P_2O_5)$

The Fe is a harder Lewis acid as compared to Zn and the above mentioned tribochemical reaction shows cation exchange between Fe_2O_3 and ZnO. As a result of digestion of hard acid (i.e. Fe^{3+}) in the phosphate glass, catastrophic abrasive wear which might lead to scuffing failure in engine components, is significantly reduced [58], [70]. To initiate this chemical reaction, friction or rubbing process (i.e. pressure, shear or temperature), is needed because dissolution of iron oxide in phosphate is not exothermic [15], [70]. Martin et al. [58], [70] suggested that the physical and chemical properties of the glass are not much dependent on the chemical composition of iron oxide and zinc oxide ratio, which means that the removal of abrasive wear particles is unable to modify significantly the rheological properties of the glass. As the tribochemical, reaction proceeds depolymerisation process starts and the phosphate chain length decreases. They further stated that exchange of Zn cation with Fe needs more negative charge to balance the chemical reaction, thus further negative charge is obtained by shortening the length of phosphate chains. These short chain zinc phosphates are concentrated in bulk of the tribofilm while the thermal film continuously deposited on the metal surfaces. This film formation mechanism form layer AW films, which exhibit remarkable properties.

Nicholls et al. [26] mentioned that the thermal decomposition and chemical reaction of degraded products appears more realistic. Under boundary lubrication regime at high pressure (i.e. up to 12.3 GPa) and high temperature (i.e. around 200 °C), decomposition of the ZDDP is increased. Spikes [15] on the other hand proposed that ZDDP thermally degraded in the absence of convincing level of hydro-peroxide and then reacted in solution at elevated temperature by thermo-oxidative degradation route which results in solid zinc phosphate deposits, hydrogen sulphide, alkyl sulphide and mercaptans. He further suggested that temperature of this mechanism utterly depends on the alkyl group present in ZDDP but generally it lies somewhere between 130 °C to 230 °C. Willermet et al. [14], [26], reviewed the film formation mechanism of ZDDP in detail. They presented the film formation mechanism of ZDDP on steel surfaces under mild wear conditions in four steps:

- Adsorption of ZDDP
- Reaction with surface, which produces phosphates and phosphothionic moieties, bonded with the metal surface
- Formation of phosphate film resulted from anti-oxidant reaction
- Condensation of phosphates and phosphothionic moieties, which are terminated by the compounds having zinc or other metal ions

They concluded that the phosphate film is formed by the oxidative decomposition of ZDDP, which has AW and AO properties [14]. Yin et al. [72], postulated a slightly different three step mechanism and proposed that ZDDP,

- Physically adsorbed on steel surfaces and then
- Decomposed due to thermal oxidation and produced zinc metaphosphate, zinc phosphate and little amount of zinc sulphide.

Step three was sub divided in two stages, it is due to the reaction temperature, and availability of cations and these stages are,

- Formation of pyrophosphate ($FeZnP_2O_7$).
- Formation of orthophosphates {$Fe_2Zn\ (PO_4)_2$}.

Gosvami et al. [65] on the basis of in-situ experimental work proposed that ZDDP tribofilm formation and growth kinetics is proportional with the stress and thermally activated tribochemical reaction rate. Figure 3-5 illustrates the relationship of tribofilm growth rate with the contact pressure and temperature. Their experiments specified that the formation of tribofilm is not the outcome of transformation of the product of adsorbed thermal film but is originated from molecular species as a result of tribochemical reaction [65]. They did not completely rule out the possibility of digestion of abrasive particles and cation

exchange as suggested by Martin and colleagues [58], [70], but their experimental results did not support the formation of tribofilm on the basis of entropy of mixing at contact pressure as low as 1 MPa. Mosey et al. [71] suggested that cross-linking of zinc phosphate molecule is the result of contact pressure forming chemically connected phosphate network and ultimately, the formation of phosphate tribofilm. The contact pressure is believed to be proportional to cross linking, meaning that higher contact pressure leads to greater degree of cross-linking and produce longer chain phosphate films [71], [74], [92].

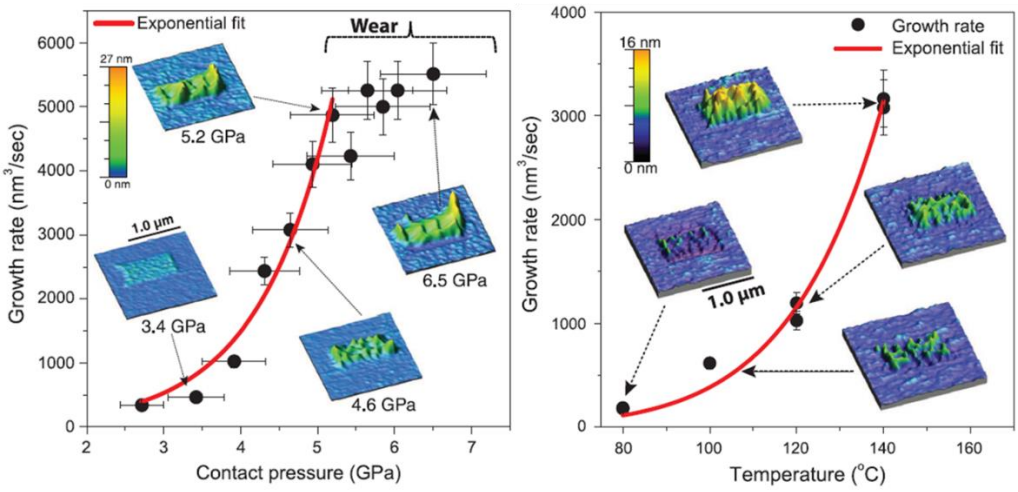

Figure 3-5. In-situ experimental work shows the dependence of tribofilm growth rate on contact pressure and temperature [65]

An increase in temperature and/or contact pressure accelerate the growth rate of the tribofilm [92]. The experimental results of Abdel and colleagues [92] are in agreement with previous studies [63], [65] suggesting that the decomposition of ZDDP is thermally and mechanically driven process which is dependent on the availability of shear and heat in the contact zone [65]. Zhang and Spikes [63] in his recent publication agreed with the concept that formation of ZDDP tribofilm is driven by mechanically applied shear stress and they called it mechanochemistry [95]. Their experimental work [63] also ruled out the possibility of ZDDP film formation due to triboemission. They further suggested that the thermal activation energy of ZDDP is reduced by almost half due to the presence of the shear stress, which accelerates the chemical

reaction and tribofilm formation process [96]. Although the in-contact shear stress seems to be the main driving force in tribofilm formation [63], [92], [95], but structure of the alkyl group also affect the tribofilm formation capability of the ZDDP [63]. Linear chain alkyl groups easily slide over one another as compared to alkyl group having branched hydrocarbons and as a result also increase film formation rate [63], [97].

Apparently, the viewpoint of researchers are slightly different about the driving force and mechanism of tribofilm formation but the shear induced tribofilm growth seems to be the most compelling argument. In recent publications [63], [65], [74], [92], [95], [96], a consensus has been evolved that tribofilm formation of ZDDP is a thermal activation phenomenon driven and accelerated by mechanical shear stress in high pressure contact zone. However, there are still disagreements regarding the exact mechanism of long and short chain phosphate formation and the sequence of tribofilm formation. Researchers [26], [28], [29], [58] are agreed that tribofilm has a two-layer structure and the film contains Zn and Fe cations at the tribofilm and the substrate interface.

3.4.1 Tribofilm morphology

AW film formed by ZDDP is heterogeneous in terms of topography and constitutes ridge and valley regions [15], [26], [27], [98]. The ridges comprise of elevated patches, commonly known as pads. These pads are solid like and closely packed phosphate glass layers, approximately 2-10 micro meter in width and generally elongated in the sliding direction [20], [25]. These AW pads are separated by deep valley regions [20], [26], [62]. The valley regions contain wear debris [62], and have low or no tribofilm [20], [62]. These glassy phosphate pads are liable to limit the asperity-to-asperity contact and also bear load between interacting asperities [25], [27], [99]. Moreover, these AW pads grow with rubbing time [25], [29], [100]. Previous studies [15], [62] suggested a film thickness of about 50-150 nm on steel surface but recently researchers [20], [63], have found that the thickness of phosphate pads levels out and attains a typical height between100-200 nm. Figure 3-6 shows topography of the ZDDP tribofilm at 100 °C and after 6 hours of rubbing on pin on plate reciprocating tribometer.

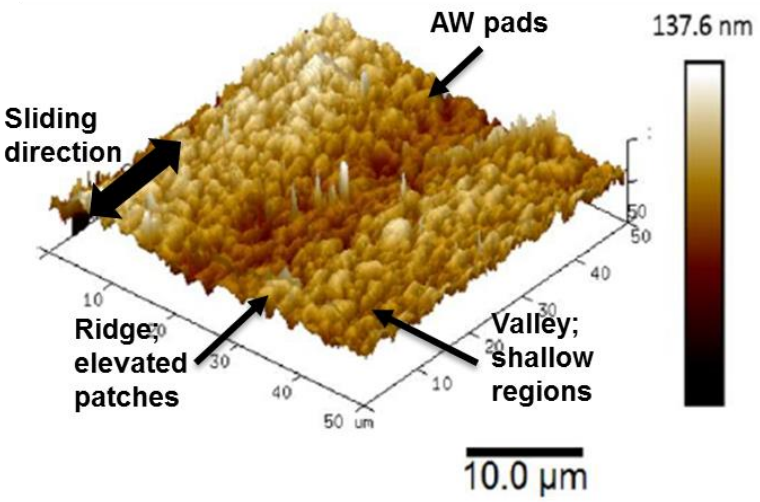

Figure 3-6. AFM image showing topography of the ZDDP tribofilm [101]

Despite of heterogeneity in the topography, tribofilm surface holds many common features, which include repetitive elevated flat/plateau regions after regular intervals. These flat/plateau regions bear the load and minimize inter-asperity contact [27]. The ridge regions are composed of phosphate glass from fully decomposed ZDDP while the valley regions are composed of glasses from partially decomposed ZDDP, AW film *intermediates* and abrasive wear debris [26], [99]. The centre of AW pads (i.e. elevated flat regions) are significantly stiffer as compared to the edges and the areas around, which supports the argument that the highest load is supported at the flat region [26]. It is also assumed that the centre of the pad may be liable to generate pressure and the temperature needed for cross-linking between polyphosphate chains [27], [99]. Figure 3-7 shows the structure of the AW pads formed by ZDDP.

The shear stress driven mechanism of tribofilm growth also describes the topography of the tribofilm. Zhang and Spikes [63] suggest that tribofilm formation starts from rubbing asperities in high pressure contact zone having highest magnitude of shear stress. Once the tribofilm formation has started at these asperities, it continues to grow at same location and develop AW pads (i.e. the ridge region), which bear the highest loads. The deep valley regions are developed because these locations have low or no shear stress, hence minimal or no tribofilm forms at these regions [63].

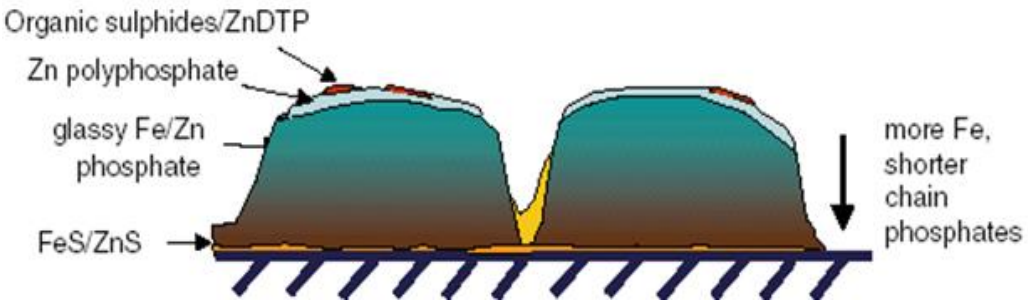

Figure 3-7. Physical structure of AW pads formed by ZDDP tribofilm [15]

3.4.1.1 Mechanical properties

The AW effectiveness of the tribofilm is shadow of the nano-mechanical properties of the film [26]. Topography of the AW pads exhibits variation in nano-mechanical properties (i.e. the geometrical centre of the pad shows elastic behaviour while corner of the pads feel softer) [29]. Using AFM and interfacial force microscopy (IFM), Warren et al. [102] analysed the thermal and tribofilms formed on steel surface. The thermal film sample produced by immersing the plate specimen in test lubricant while the tribofilm generated with a pin-on-plate reciprocating tribometer. The IFM results revealed that ridge region of the AW film showed excessive elastic capacity compared to the valley areas with the indentation modulus value of 81 and 25 GPa respectively [102]. They found that thermal films are comparatively lesser elastic than the tribofilms [102]. Spikes [15], observed that the tribofilm pads possess solid like structure at temperature up to 150 °C with elastic modulus of 90 GPa and hardness of 3.5 GPa. The film formed by ZDDP is uneven with ridges directed towards the rubbing orientation and the indentation modulus varies between 25 GPa to 80 GPa (similar to glass) and having shear strength of 2 GPa to 3GPa [52]. Morphology of the tribofilm evolve with rubbing time but nano-mechanical properties remain unaffected with this evolution process [29]. The morphology and nano-mechanical properties of the protective film vary from one geometrical position to other and this variation in morphology and nano-mechanical properties is expected to be due to the diverse contact pressures between the rubbing asperities [29].

3.4.1.2 Lubrication and friction properties

ZDDP is a well-known additive due to its versatile role as an AW, AO and corrosion inhibitor additive [15]. Thickness of the tribofilm formed by ZDDP ranges from few nano-meters up to 200 nm [20], [63] and it contains individual pad like structure with 2 um to 10 um across [15], [20], [62], [63]. The COF value of the tribofilm formed by ZDDP is quite high and ranges from 0.11 to 0.14 [22]. Presence of ZDDP have negative impact on the fuel economy and this perspective is originated from the fact that ZDDP shows high boundary friction [15] but later it was found that that ZDDP even increase friction in mixed lubrication and this friction originates from the topography of the ZDDP tribofilm [22]. Figure 3-8 shows friction behaviour of lubricant having ZDDP in formulation.

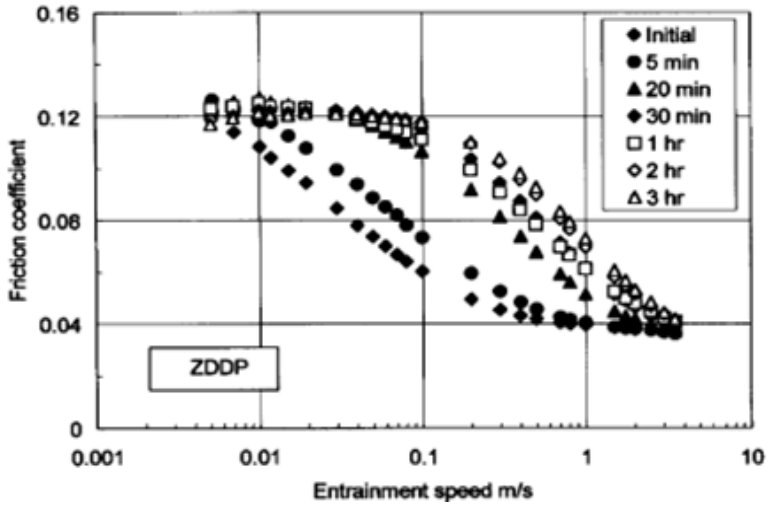

Figure 3-8. Friction coefficient analysis in lubricants with ZDDP [15]

Friction behaviour of lubricant is attributed to the tribofilm structure, which may restrict the fluid entrainment of flow inside the contact region [15]. High boundary friction may arise due to uneven topography of protective film and the inter-pad demarcation in reaction film may not only inhibit the entrainment of fluid lubricant but also drain the lubricant from the interface [22]. The lubricant may slip against the ZDDP padded structure which contain polymerized phosphate on the top layer and liquid slip in such smooth and coated surfaces is very much possible [15].

3.4.1.3 Anti-wear and extreme pressure properties

ZDDP formed protective tribofilm on the interacting surfaces under boundary lubrication regime to reduce wear but at the same time ZDDP also work as EP additive [59]. Willermet et al. [14] reported that ZDDP form two types of protective films (i.e. EP films and AW films). They further stated that EP films comprised of iron sulphides and formed due to high temperature and extreme applied load. Spikes [15] also supported this argument by an experiment in which sulphur free additives are used and it performed well as an AW additive but poorly responded as an EP additive. The bi-layer model of ZDDP film in which top phosphate glass layer is responded as an AW agent while the bottom layer which is composed of iron sulphide responded as an EP agent [15]. EP performance analysis of ZDDP by standard four ball wear test [59] revealed that majority of ZDDP had decomposed during the test but low or no effect on EP performance was observed after this major decomposition which suggested that ZDDP had EP capability as well. Optimum performance of the ZDDP as an AW/EP additive can be achieved by improving the experimental conditions which includes moderate load, minimum hardness and roughness difference, reasonable temperature and sufficient volume of lubricant to generate tribofilm [103].

Classification of FMs, types of OFM, anti-friction mechanism, film structure and interaction of OFMs with ZDDP is discussed in the next chapter.

3.5 Summary

Many additives added in modern engine oil formulation but the most important additives for the tribological performance of lubricant under boundary lubrication conditions are the AW additive (i.e. ZDDP) and friction modifiers (FMs). This chapter covers the literature about ZDDP, its film formation mechanism on steel surfaces, chemical structure and tribofilm morphology. However, the performance of ZDDP in reducing wear is remarkable but it is now established that the AW film form by ZDDP also carries high boundary friction that is one the reasons of mechanical losses in an IC engine. An important solution to overcome the high boundary friction is to design lubricants that offer low friction in engine components. FMs are the lubricants that reduce boundary friction, improve lubricity by reducing the COF value, and improve the fuel economy.

ZDDP has been considered as the most effective AW additive because it forms a protective film between the interacting asperities, which minimizes the wear and stops the pre-mature failure of the engine components. The AW film formed by ZDDP is mainly composed of Zn, P, S and O in different proportions. ZDDP starts decomposing above 100 °C due to thermo-oxidative process in presence of molecular oxygen in the BO. Decomposed product of the ZDDP adsorbs on interacting surfaces and provide AW action. Thermal films formed by ZDDP do not need rubbing of the asperities and the rate of thermal film formation is proportional with the temperature rise. These films have good AW capability and can resist up to 12 hours in BO. Thermal films are comprised of short and long chain phosphates and thiophosphates deposited on the surface.

ZDDP also forms a thick, un-evenly distributed and primarily a solid like reaction film inside the rubbing track with the roughness aligned with the direction of motion. ZDDP tribofilm is not the transformation product of adsorbed thermal film but actually tribofilm is originated from molecular species as a result of tribochemical reaction. ZDDP decomposes due to rubbing friction even at room temperature because of high contact pressure/high shear in local contact zone. Decomposition of the ZDDP is thermally and mechanically driven process, which is dependent on the

availability of shear and heat in the surface contact zone. Increase in shear stress reduce the reaction activation energy and as a result accelerate the tribochemical reaction. However, researchers disagree about the exact mechanism of short and long chain phosphate formation but in all circumstances, it is agreed that the tribofilm is formed in two layers with top layer consist of glassy phosphate film while the bottom layer is composed of iron sulphide and iron oxide..

AW film formed by ZDDP is heterogeneous in terms of topography and mechanical properties, constituted by ridge and valley regions. The ridge sections of the film are comprised of elevated patches, commonly known as pads. These closely packed solid like phosphate glassy pads are generally 5-10 μm in diameter and thickness of phosphate pads levels out and attains a typical height between100-200 nm. These glassy phosphate pads limit the asperity-to-asperity contact and bear load between the interacting asperities.

Chapter 4
Literature review; Friction modifiers and interaction of organic friction modifiers with ZDDP

4.1 Lubricant additives

The most important additives for the tribological performance of lubricant under boundary lubrication conditions are AW additive (i.e. ZDDPs) and FMs [16]. The role of ZDDP in minimizing wear, film formation mechanism, film structure and morphology is discussed in the previous chapter. FMs are the lubricant additives, used for lubrication of interacting surfaces in boundary and mixed lubrication regimes [104]. Boundary and mixed lubrication regimes are the most critical regimes in terms of friction and wear due to asperity-to-asperity contact [105]. FMs reduce boundary friction and improve lubricity by reducing the COF value and ultimately contribute to improve the fuel economy [22].

4.2 Friction modifiers

High boundary friction is one the reasons for the mechanical losses in an IC engine. In order to reduce engine losses and improve the mechanical efficiency, an important solution is to design lubricants that offer low friction in engine components [104]. In order to design better lubricants, researchers are currently working on two approaches, which are [104]–[106],

- To add efficient friction reducing additive in lubricant formulation
- To improve lubricant rheology

The first approach is to add efficient friction reducing additives in the lubricating oil, which works with other additives and reduce COF value [104], [105]. In boundary lubrication, FM reduce friction by generating a low shear strength film by adsorption or reaction with metal surfaces [22]. Improving the lubricant rheology is another approach to minimize the lubricant viscosity to a level at which lubricant still has the capability to maintain mixed film lubrication [106]. Reducing viscosity of the lubricant minimizes fluid shear, churning and

pumping losses which are usually the key losses in application where hydrodynamic lubrication regime prevails [104]. Practically both approaches need to work together. The lubricant viscosity is continually decreasing in order to reduce losses in fluid fill lubrication regime but as a result of this modification, the interactions between asperities become more severe and need to be managed using efficient FMs [104]. FMs are classified in two main categories, which are

- Organomolybdenum compounds
- Organic friction modifiers (OFMs)

Organomolybdenum compounds are further divided in three sub groups which are [105], [107].,

- S and P containing compounds (i.e. molybdenum-dialkyldithiophosphate (MoDTP))
- Compounds having S but no P (i.e. molybdenum-dithiocarbamate (MoDTC))
- Compounds without S and P (i.e. molybdate ester)

Organomolybdenum compounds reduce friction by forming a low shear strength film of MoS_2 on interacting surfaces [105]. OFMs are generally long chain surfactants having polar end groups. The head groups physically or chemically adsorbed on the rubbing asperities and form a thin monolayer or thick viscous layer. Carboxylic acid, esters, amines, amides, imide, alcohol, phosphate and borate are among the most common OFMs [16], [35], [104], [105]. Recent studies [104], [105], [108]–[112] suggested that functionalised organic polymers also have the capability to adsorb on polar metallic surfaces and form a thick film and reduce friction effectively. Polymethacrylates (PMAs) polymers already used in engine oil formulation as viscosity index (VI) improvers and dispersants. In recent investigations [104], [105], [108] it was found that functionalised PMAs are strongly adsorbed on the steel surfaces and form a thick boundary film which effectively reduce COF value and also improve the wear performance.

4.3 Organomolybdenum compounds

Organomolybdenum compounds are recognised as an effective friction reducing additives in boundary and mixed lubrication regime [104], [105]. Organomolybdenum compounds successfully reduce friction by forming a film of low shear strength molybdenum disulphide (MoS_2) on the contacting asperities and is classed as one of the most significant friction reducing additives for automotive application [22], [104], [105]. Recently, Khaemba et al. [113] proposed a two-step mechanism for formation of MoS_2. The first step involves decomposition of MoDTC and the second step is about formation of MoS_2. During the tribo-chemical reaction, MoDTC adsorbs on interacting surfaces and then due to shear stress decomposes with breaking of C-S bonds. In the second step MoS_2 is produced from MoS_x, which needs more activation energy and that energy may be supplied externally (i.e. endothermic reaction) or may be managed by increasing shear stress. Figure 4-1 shows two-step tribochemical reaction.

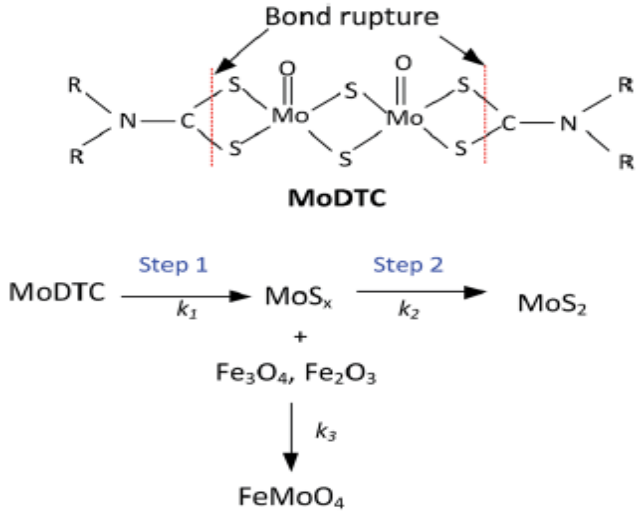

Figure 4-1. Chemical reaction showing formation of MoS_2 from MODTC [113]

Environmental-friendly S and P free molybdenum compounds (i.e. molybdate ester) are generally not as effective as other molybdenum additives. Molybdate ester cannot be used independently to reduce COF value and wear in the absence of a low shear strength MoS_2 film [105]. However, molybdate esters in combination with ZDDP performs effectively as a FM due to the

formation of MoS_2 films on the rubbing asperities [105], [114]. Yamamoto and Gondo [115] suggested that presence of both S and molybdenum (Mo) is necessary to form low friction surface layers. The S- free Mo- compounds are unable to form this protective film and are not effective in reducing friction and wear [115]. However, the S- free Mo- compounds can form MoS_2 lamellar type film along with the S- containing compounds [115].

4.4 Organic friction modifiers

Organic friction modifiers (OFMs) are alkyl chain compounds with polar end groups at one end [116]. OFMs are amphiphilic surfactants, generally consisting of at least ten carbon atoms [106], [116] and form a self-assembled ultra-thin film on rubbing asperities[116]. OFMs rapidly form films on the interacting surfaces but film formation rate is dependent on diffusion of its molecules from the lubricant oil to rubbing asperities [106], [117]. OFMs shows significant friction reducing capability with alkyl chain of more than four carbon atoms [104] and furthermore effectiveness of OFMs improves significantly as chain length increases [104], [105], [118], [119]. Jahanmir [120] suggested that optimal anti-friction performance may be achieved with maximum alkyl chain length of sixteen carbon atoms but some researchers [104] found out a levelling effect in the friction with alkyl chain length of ten or more carbon atoms. Polar end groups of the OFMs adsorb physically or chemically on interacting surfaces with the hydrogen chain extending in the lubricant oil [105], [116], [119]. The role of polar or head groups is of vital importance in the effectiveness of OFMs [104], [118]. OFMs form film in an orderly manner having closely packed molecules, attached with each other [67], [116], [121]. The alkyl chain length, polarity of the head group, degree of saturation and solubility of OFMs determine the thickness and density of the adsorbed molecules on interacting surfaces [118], [120], [122].

Amine, amide, carboxylic acid, ester, alcohol, borate and phosphate are few of the OFMs and most of them are already in commercial use [104], [105]. Many of the OFMs in commercial use are derived from natural fats or oils and due to the source of derivation it contain complex chemistry of saturated and unsaturated alkyl chains [104], [116], [123]. Recent research [104], [123] revealed that OFMs with multiple head groups promote chelation and as a

result accelerate adsorption rate on the metal surfaces. The OFMs can be classified in four basic categories on the basis of chemical structure and these are [119],

- Carboxylic acids and their derivatives (e.g. stearic acid, esters etc.)
- Nitrogen based compounds (e.g. amines, amides, imides and their derivatives)
- Phosphate compounds (e.g. phosphate esters, phosphates and amine salt etc.)
- Polymers and others

Kenbeek et al. [119] further suggested that interaction of OFMs varies significantly with types of OFMs. The saturated fatty acids, phosphoric acid and fatty acids having S- contents form layers because of chemical reaction with metal surfaces. Derivatives of carboxylic acids and nitrogen-based compounds also form film because of adsorption on the metal surfaces. Unsaturated fatty acids, methacrylates and partial complex esters form polymers on the surfaces.

Due to environmental and emissions legislation which tightens the limit of exhaust emissions, demand for environmentally friendly lubricants having additives with low or no P and S- contents has been increasing [19], [54], [117], [124]–[126]. Carboxylic acid and their derivative and nitrogen based organic additives are among those OFMs which are currently under consideration to replace chemical additives having P and S content [104], [105], [127], [128].

4.4.1 Anti-friction mechanism

An efficient lubrication in engine components, specifically during low speed operating cycles is subject to oiliness of the film formed at interacting surfaces [104], [116], [129]. Lubricity or oiliness of the lubricant inside the tribological contact is the result of a low shear strength film comprised of amphiphilic surfactants [104], [116]. OFMs form films by physical/chemical adsorption on the interacting surfaces [104], [105], [121], [130]. In physical adsorption or

physiosorption adsorbed layers and substrate interaction is due to weak van-der Walls forces whereas in chemical adsorption or chemisorption polar head groups of OFMs are covalently bonded with the substrate [67], [116], [121]. An important characteristic which is related to adsorption phenomenon of OFMs is their ability to re-form or re-heal the film in case if they remove or worn out in the rubbing zone [131], [132]. However, reformation of the film in boundary regime is dependent on the diffusion of OFM molecules from the solvent [106], [131].

Studies [104], [105] suggested two different film formation mechanisms for OFMs and these are monolayers formations and thick film formation model. OFMs reduce friction by forming an extremely thin, closely packed, vertical oriented, low shear strength and self-assembled monolayers, on the interacting surfaces [67], [104]–[106], [116], [131], [133]–[135]. Some recent studies [61], [106], [136] suggested that even loose or relatively less closely packed monolayers are also capable of reducing COF value in an effective manner. Formation of monolayers in the lubricant blends are driven by adsorption of polar head groups on metal surfaces via chemisorption or physiosorption [104], [105], [116], [131], [137]. Monolayers formed on the metal surfaces are approximately 2 nm thick but they reduce friction significantly [22], [106].

Performance of OFMs are also affected by external factors which includes temperature [106], [130], metallurgical composition of surface, applied pressure, presence of other additives in the solution and shear rate [118], [130]. Friction performance of OFMs reduces significantly above a critical temperature [106].Though other parameters also affect the film thickness but chemically adsorbed organic molecules in chemisorption and packing density of adsorbed organic molecules in physiosorption primarily affect the film thickness [116], [122]. Presence of van der Waal interactions between the adjacent alkyl groups provide rigorousness to the surface adsorbed films and at the same time it also increase internal resistance against film compression [105], [116], [131], [138]. Presence of van der Waal interactions between alkyl groups lead to more load bearing capability which also justify the friction reduction behaviour of longer chain hydrocarbons [120]. Formation of this surface adsorbed film minimises metal-to-metal contact and forms a low shear

strength plane along the sliding direction, thereby reducing COF value [67], [104], [105], [116], [131]. Figure 4-2 shows schematically the presence of monolayers between interacting surfaces. Alcohols, amines and esters adsorb on the metal surfaces and produce monolayers but the adsorption of these OFMs generally does not increase monotonically with increase in concentration [2].

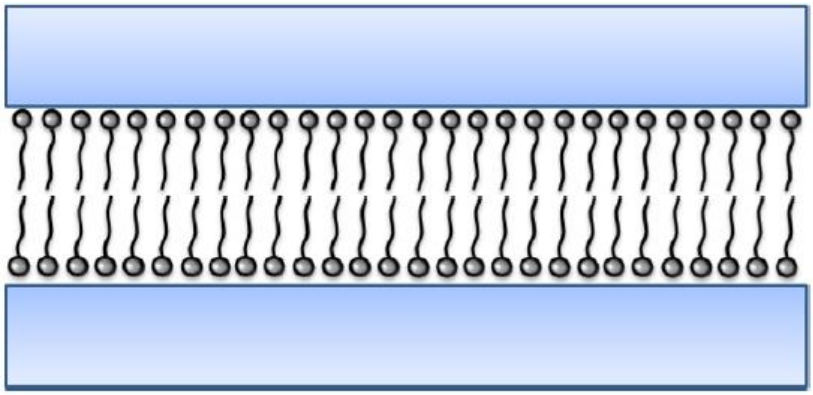

Figure 4-2. Schematic illustration of a thin molecular film [67]

OFMs may also form thick films on the metal surfaces and thickness of these films are up to hundreds of nanometres [22], [129], [139]–[141]. Studies [104], [140] proposed that OFMs may form thick film when rubbing with the metal plates in damp conditions or elevated temperature conditions. However, it is not established whether the thick films remains in the contact or are displaced under normal tribological conditions, so friction is determined by the final monolayers [104]. In full film lubrication contact when interacting surfaces are separated by thick fluid film, OFMs effectively reduce the friction by promoting fluid slip instead of following boundary/mixed lubrication film formation mechanism [104], [142], [143].

Friction reducing capability of the OFMs are directly associated with the structure of the hydrocarbon chain, alkyl chain length and functional group of the compound [67], [105], [116], [120], [131], [134]. Short chain OFMs are not as effective as long chain compounds specifically on hard surfaces having higher contact pressure [104], [120], [131]. Reduction in COF value with increase in the alkyl chain length is possibly linked with increase in cohesive forces [120], [131]. Polar head of the amphiphilic molecules anchored on the

metal surfaces with alkyl chains extends in the lubricant [119], [130]. Adsorption capability of OFMs are also affected by the presence of unsaturated bonds in the corresponding hydrocarbon chain [116]. Unsaturated alkyl chain hydrocarbons offer higher steric hindrance in comparison to saturated hydrocarbons and hence affect the adsorption performance of OFMs [131], [144]. Higher steric hindrance in unsaturated molecules are due to presence of *cis*-double bond which restrict the molecules to form closely packed monolayers and hence offer a different frictional response in comparison to saturated alkyl chain molecules [104], [131], [140]. OFMs having straight chain chemical structure, saturated bonds and small head groups usually form strong monolayers with closely packed molecules [104], [131]. Load bearing capacity of the film form by OFMs increases to maximum once the hydrocarbon chain length matches with the solvent hydrocarbon chain length [119], [131]. The tail interface of the alkyl chain of the film shear off quickly during tribological interactions which reduces COF value [119]. These shear-off layers of OFMs are instantly re-build to their original state due to existence of strong orientation forces [119].

4.5 Nitrogen based organic friction modifier (amines)

The amines belong to the family of chemical compounds having nitrogen atoms, which are sp3, hybridized, managing three single bonds with other elements. The simplest amine is named as ammonia (NH_3), having central nitrogen atom with three chemically equivalent hydrogen bonds. Replacement of hydrogen atom in ammonia with other elements (i.e. chlorine, bromine etc.) produces inorganic amines while replacement of hydrogen atom with functional groups (i.e. alkyl or aryl group) produces organic amines [145], [146]. An amine has the ability to act as a Lewis base (a nucleophile) because of its non-binding lone pair of electrons which can bond with an electrophile [145], [146]. The amines are strong bases and have capability to act as a Brønsted–Lowry base by binding with a proton (H^+) and form protonated compound [146]. Equation 4-1 and 4-2 presents chemical reactions of amine as nucleophile and as a Brønsted–Lowry base. Stabilization of ammonium ion (with respect to free amine), make an amine relatively a strong base whereas stabilization of free amine make an amine relatively weak base [146].

Presence of alkyl group increase basicity of an amine due to donation of electrons to cations which stabilize the positive charge on central nitrogen (N) atom and make them stronger base than ammonia [146].

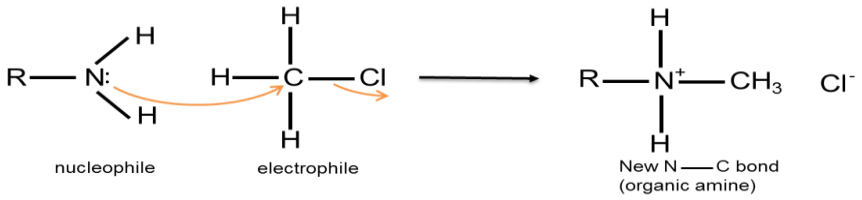

4-1

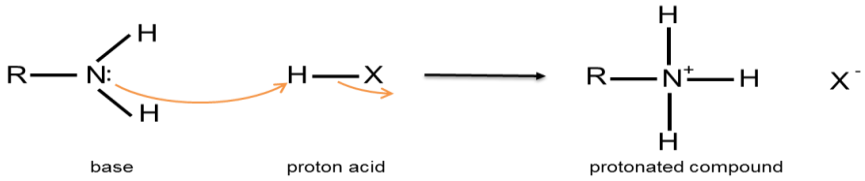

4-2

Lone pair of electrons on central nitrogen atom controls the properties of amine molecules [145]. The amines are highly polar surfactants due to large dipole moment of a lone pair of electrons in its structure [146]. Donation capability of the N atom revised in presence of functional group. Amines with sp^3 hybridization are more likely to donate pair of electron then amines with sp^2 hybridization. Sp^2 hybridized structure is dominated by the 's' character. Atomic nucleus hold the 's' orbitals more strongly than 'p' and 'd' orbitals, hence Sp^2 hybridized has low or no tendency of electron donation [145].

4.5.1 Fatty alkyl amines

Fatty alkyl amines or fatty amines (FAs) have the typical carbon chain length of 8 to 24 (i.e. C_8 – C_{24}) carbon atoms [116], [145]. Many major commercial applications such as tallow amines, coco amines, oleyl amines and soya amines derived from natural products. FAs are the mixture of saturated and un-saturated alkyl chain of different lengths [145]. Some of the FAs are designed with multiple functional groups to promote chelation and consequently adsorption [104], [116], [131]. Chemical composition of different FAs are added in Table 4-1. FAs having carbon chain length of 10 or more

show better solubility in polar and non-polar solvents. Though FAs derived from natural products but it is reported that FAs can also be produced synthetically from paraffin [145].

Table 4-1. Chemical composition of FAs [145]

Fatty alkyl amines (FAs)	**Chemical composition**
Coco amine	6% C_8 + 7% C_{10} + 51% C_{12} + 19% C_{14} + 9% C_{16} + 2% C_{18} + 6% unsaturated C_{18}
Ethoxylated hydrogenated tallow amine	4% C_{14} + 32% C_{16} + 64% C_{18}
Tallow amine	4% C_{14} + 30% C_{16} + 2% unsaturated C_{16} + 20% C_{18} + 44% unsaturated C_{18}
Ester of triethanol amine with tallow fatty acid	4% C_{13} + 30% C_{15} + 2% unsaturated C_{15} + 20% C_{17} + 44% unsaturated C_{17}
Oleyl amine	5% C_{18} + 76% unsaturated C_{18} + 19% others
Soya amine	16% C_{16} + 15% C_{18} + 50% unsaturated C_{18} + 13% doubly unsaturated C_{18} + 6% others

The amine molecular film is a combination of physical adsorption and chemical reaction with steel surface [104], [147], [148]. Fatty amine (FA) molecules quickly adsorb on metal surfaces and form thick monolayers even at low concentrations in the solvent [144]. The boundary film formed by FAs specifically on iron surfaces contains weakly adsorbed and loosely packed monolayers [131]. These weakly adsorbed monolayers can easily be damaged by applying minimal shear stress [116], [149]. Steric hindrance in the proximity of the surface plays vital role in adsorption of FA molecules [116]. Increase in concentration of FA leads to higher steric hindrance near the surface which ultimately reduces adsorption [116]. Spikes et al. [147] specified that performance of FAs is significantly disturbed if concentration of FA

molecules in solution is below the critical concentration. Presence of multiple functional groups at the head group of FAs increases adsorption masses but at the same time it also increases steric hindrance which affects the adsorption rate [116], [131]. Nalam et al. [116] compared their experimental results with previous study [144] and suggested that unsaturated FAs offer higher steric hindrance as compare to saturated and linear FAs and as a result reduce adsorbed masses on the surface.

FAs possess affinity with the iron oxide surfaces and due to this reason amines molecules quickly form chemisorb films on the iron oxide surfaces [144]. During chemisorption process N atom act as a Lewis base and donate lone pair of electrons to the surface iron (Fe) (III) ions [116], [144], [145]. As a result of this interaction, the layer adsorbed on the iron oxide surfaces may contain positive amine molecules in it [144]. Molecular adsorption model in Figure 4-3 shows that FAs form a well organised molecular layer on top of the iron oxide surface. The grey overlapping circles in the model represents surface oxygen atoms whereas relatively smaller black circles represents the upper layer of iron atoms [144]. Molecular dynamics simulation proposed that film formed by FA molecules are approximately 16-20 Å thick with molecular tilt angle somewhere between 30° and 60° with respect to the metal oxide surface [144], [150].

Campen et al. [135] studied in-situ film formation of octadecyl-amine on mica surfaces by using AFM liquid cell. They found no traces of film formation when hexadecane solution (in absence of octadecylamine) applied on the surfaces. However, non-uniform islands observed once octadecylamine solution introduced in the cell. Octadecylamine quickly adsorbs on the metal surfaces and form film in the first few minutes with a surface coverage of around 50% of the total surface area [135]. The aforementioned film comprised of scattered islands which supposedly correspond to vertical oriented (i.e. tilted) amine molecules, having mean diameter of 3 um and a thickness of around 1.5 nm [135], [151]. Island structures of the film form by octadecylamine are quite delicate [152] and even the nominal shear stress may lead to re-arrangement of the island structure [116], [149], [152]. Studies [135], [153] suggested that FAs instantly form monolayers (i.e. island structure) but these islands are not thermally stable. Consolidation of these islands to get some thermal stability

needs longer immersion time and it is supposedly due to formation of ammonium ion from amine. However, it is not known yet whether elevated temperatures desorb these islands or it is a thermal meltdown process that transforms the film into disordered liquid like structure [135], [154].

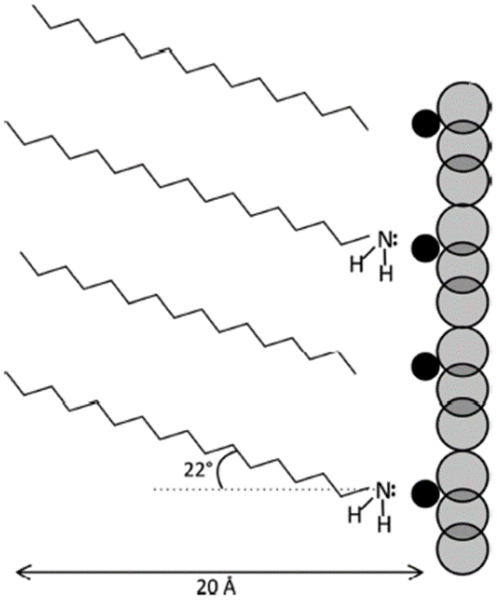

Figure 4-3. Molecular adsorption model of FAs on iron oxide surface [144]

Recently, Nalam et al. [116] investigated the adsorption behaviour of FA molecules on steel surfaces. They suggested that FA molecules randomly adsorb on the metal surfaces and form films composed of disordered amine molecules. Weak interaction forces between FA molecules and shorter equilibrium time lead to the formation of films having FA molecules lying nearly parallel to the surface. FA molecules physically and chemically adsorbed on the metal surfaces and form multilayers or in some cases form monolayers with a tilt angle around 15° [116]. FA molecules worn out during tribological interaction quickly replace with the excess amine molecules present in the solution and hence maintain a low COF value. Re-adsorbed FA molecules have limited equilibrium time in an engine set up (due to frequent piston movement), which is not enough to configure molecules in an upright position. Hence, the boundary film form by FA molecules in engines are composed of molecules that are either lying almost parallel to the surfaces or configure themselves in tilted position with respect to surface [116].

4.6 Interaction between FAs and ZDDP

Tribofilm formed by ZDDP possesses high boundary friction and this high friction is even carried to the mixed lubrication regime (i.e. at much higher speed) [22], [61]. High friction arises from uneven, rough and solid like phosphate film formed by ZDDP on interacting surfaces [61], [155]. High COF value affects the fuel economy of the engines [22], [61], [156]–[158] and to overcome this problem, FMs are added in the engine oil, which reduces the high boundary friction [22]. AW performance of ZDDP is affected by its interaction with other additives including OFMs [22], [61], [159]. FAs are mainly used as corrosion inhibitors in lubricant formulations [116], [160], [161]. Only few studies [16], [61], [133] discussed the effectiveness of FAs in reducing COF value. Miklozic et al. [22] suggested that amine and amide are effective OFMs and both reduce friction in boundary and mixed lubrication regimes. FAs can reduce friction effectively above a critical concentration [133]. Octadecyl amine works as an effective friction modifier in hexadecane which is a low viscosity fluid [104], [105]. Substitution of amino-methyl in imidazole compound significantly improves the friction performance and it works as an effective friction modifier in terms of fuel economy as compared to glycerol monooleate (GMO) [104]. Some amine FMs have capability to reduce high boundary friction of pre-formed ZDDP tribofilm [61]. Long chain primary alkyl amines has already been using as friction modifiers in limited slip rear axle lubricants and due to effective performance, FA additives have potential to be used in engine oil lubrication [162].

Studies [22], [61], [116], [163] suggested that addition of FA additives in the lubricant oil restricts the AW film formation capability of ZDDP and increases wear value significantly. Primary amines effectively reduce boundary friction but severely damage the AW film formed by ZDDP [22], [61]. On the other hand, Dawczyk et al. [61] suggested that oleyl amide reduce boundary friction without any antagonism to AW film form by ZDDP [61]. Some researchers [22], [164] claimed that dispersant additives having amino group work antagonistically with ZDDP, while some others did not observe any remarkable impact on performance of ZDDP [165]. Lundgren and Ericsson [166] investigated the tribological performance of ZDDP in the presence of different FA molecules. They concluded that FAs not only reduce boundary

friction but also disturb the film formation capability of ZDDP. Significant increase in performance of FAs was recorded when little concentration of MoDTC also added in the solution [166], [167]. Dawczyk et al. [61], studied the impact of ethoxylated amine FMs on durability and friction of the pre-formed ZDDP tribofilm and suggested that the ethoxylated amine FMs not only reduce the high boundary friction but also remove some of the ZDDP tribofilm.

AW and FM additives plays an important role in tribological performance under boundary lubrication regime and it is important to understand the interaction of FA additives with ZDDP in the lubricating oil [124], [130], [168], [169]. However, limited literature is available on the interaction of OFMs in general and specifically amine FMs with ZDDP [16], [61], [130], [170] but there are few patents which showed that some OFMs have capability to reduce higher boundary friction of the AW film formed by ZDDP [61]. Recently, some studies [91], [171] suggested that tribofilm formed as a result of interaction between some FAs and ZDDP not only reduce COF value and wear but also minimise micro-pitting to some extent.

It is not confirmed yet whether FAs restrict AW film formation capability of ZDDP by blocking the interacting surfaces or chemically interact with ZDDP or reducing the shear stress, which ZDDP molecules need to form tribofilms [61]. Few possible mechanisms have been proposed to address the question that how FAs affect the AW performance of ZDDP in normal conditions [30], [33], [64], [124], [162], [172]. These mechanisms include formation of complexes in the bulk oil [22], [30]–[33], [64], [124], [172], [173], alter ZDDP decomposition rate [22] and consequently disturb equilibrium between film formation and removal process [64], react with ZDDP decomposition products and solubilize the pre-formed zinc phosphate film [22], [164], preferential adsorption and blocking effect [22], [34], [174] are among them.

4.6.1 Effect of FAs molecular structure

Molecular structure and alkyl chain length is very crucial for the extent of ZDDP-amine interaction. Primary alkyl amines show the maximum amine interaction with ZDDP [30], [61], [124] and it is possibly due to chelation of Zn^{2+} ions from zinc phosphate film [22], [61]. Amendments in the primary amine structure by introducing branch or branches having chains, double

bonds in the structure, aromatic rings usually reduce the amine interaction significantly [30], [162], [175]. Secondary amine is less effective than the analogous primary amine and the tertiary amines are even lesser interactive with ZDDP. Difference in effectiveness of the amines in interaction with ZDDP is due to the steric factor. The order of amine effectiveness is shown below [162], [175],

primary amines > secondary amines > tertiary amines

Presence of unsaturation in alkyl chain also affects amine interaction behaviour with ZDDP [133]. Tribological performance of primary saturated stearylamine is found to be relatively better than that of primary unsaturated oleyl amine [124], [133]. Loehle et al. [117] linked these differences in tribological performance with the formation of self-assembled films and suggested that unsaturated molecules form more disordered self-assembled films than the saturated molecules. Some researchers [131], [144] have the opinion that unsaturation in the molecules promotes higher steric hindrance in-comparison to saturated hydrocarbons which affects adsorption of OFMs and hence tribological performance. Rounds [30] investigated the behaviour of FAs having different molecular structure with ZDDP. On the basis of experimental results, he concluded that primary straight chain amines with 12 or more carbon atoms demonstrated the strongest effect on performance of ZDDP followed by secondary (i.e. di-n-hexyl) and tertiary amines (i.e. tri-butyl). Alkyl chains having branches (i.e. t-octyl) and unsaturated amines having double bonds (i.e. oleyl amine) massively reduced the effect of amine. Figure 4-4 shows tribological behaviour of different amines with ZDDP. The length of alkyl chain affects AW performance of ZDDP. Amines with shorter chain length (e.g. propyl amine), reduces the AW capability of ZDDP if we compare it with the AW results in the absence of shorter chain length amines. Amines with longer chain length even adversely disturbed the AW characteristic of ZDDP. Researchers linked this decrement of AW performance of ZDDP with adsorptivity of the complex formed by ZDDP and

amines. The adsorptivity of the complex is directly related with the AW performance. Order of AW performance is shown below [33], [162],

ZDDP > Complex with short chain alkyl amine > Complex with long chain alkyl amine

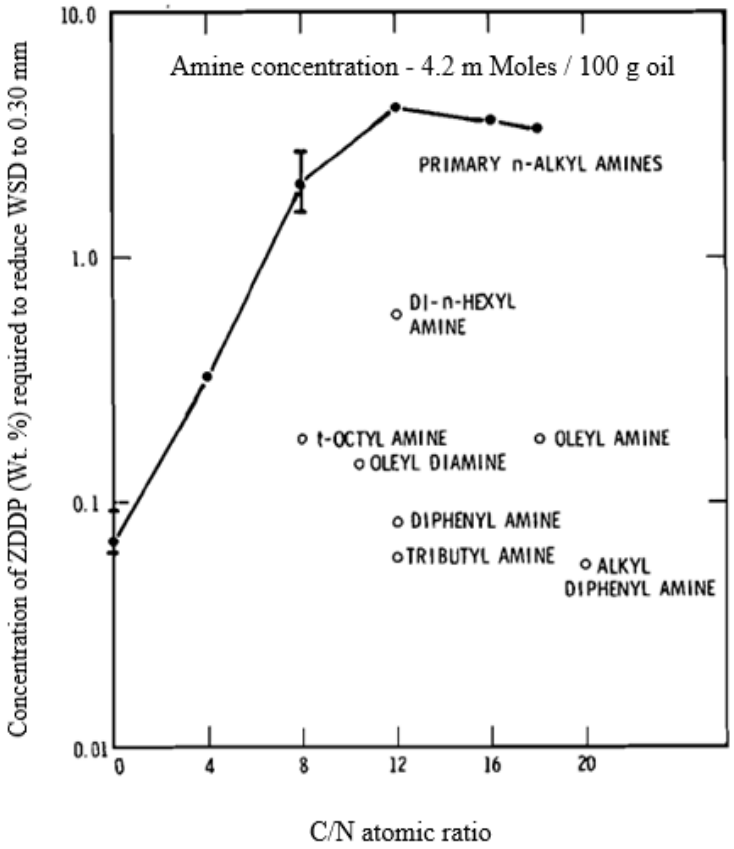

Figure 4-4. Tribological behaviour of different amines with ZDDP [30]

4.6.2 ZDDP-amine complex

ZDDP and amine interaction is very crucial to analyse the friction and wear performance in boundary and mixed lubrication regimes [30], [162]. Some studies [22], [30]–[33], [64], [124], [171]–[173] suggested that the amines and ZDDP interact in the bulk fluid and form complexes. ZDDP-amine complexes tie the ZDDP molecules and affect its AW performance. The central N atom of the amine is assumed to be co-ordinating with the zinc (Zn) atom of the ZDDP [33], which act as a Lewis acid [172]. Amine group has the capability of complex formation with Zn cation and consequently seep it out from zinc-

phosphate glass [22]. Researchers [33][172] agreed that ZDDP and amine form coordination complexes which are in equilibrium with the free molecules in the solution. ZDDP-amine complexes are in equilibrium with both the reactants and the degree of complex formation is dependent on bulkiness of the oil and basicity of the amines [33]. Tribofilm formation capability of ZDDP is compromised in complexation [31], [32] due to the formation of bigger size molecule and having large steric hindrance, which ended up with limited adsorption on the metal surface [33], [171], [176] and consequently increase the wear rate. Matsui et al. [31], [32] claimed that reduction in tribofilm formation capability of ZDDP in the presence of N containing additive is very much due to complexation between them. N-containing additives almost restricts the decomposition of ZDDP, which consequently affects its AW film formation.

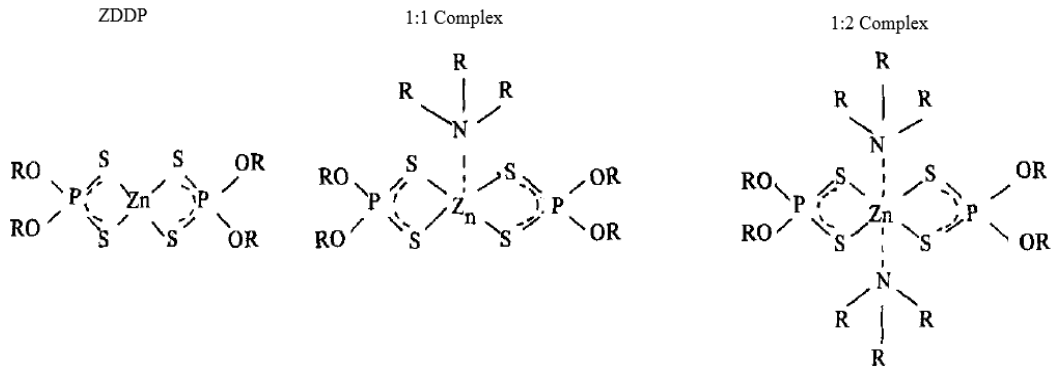

Figure 4-5. Amines complex formation with ZDDP in the bulk oil [33]

Structure of amines influences the propensity of complex formation with ZDDP. The amines having limited steric hindrance around the N atom forms 1:2 complexes with ZDDP, medium hindrance amines form 1:1 complexes while large hindrances around N atom forms no complexes. This phenomenon is due to the repulsive force between the alkyl chain of amines and ZDDP. Figure 4-5 shows the chemical structure of ZDDP, 1:1 and 1:2 complexes of ZDDP with amine.

Massoud et al. [124] discussed decomposition of ZDDP molecule in presence of FAs (i.e. octadecylamine) in the lubricant blend. They described it as two-

stage process. In first stage octadecylamine accelerate hydrolysis of the neutral ZDDP and transform it into basic ZDDP [124], [177], [178]. In second stage of the process newly formed basic ZDDP molecules decompose in to the neutral ZDDP and zinc oxide (ZnO) provided that available temperature is up and above 100 °C [124], [179]. Chemical reactions involved in both steps presented in Equation 4-3 and 4-4.

First stage

4-3

Second stage

4-4

Presence of octadecylamine and ZnO in the lubricant may lead to form ZnO-amine complexes or possibly form reverse micelles (in which FA molecules firmly attach with zinc oxide core) [124], [180]. Tribological results [124] showed synergistic wear behaviour which is not aligned with the hypothesis of complexation and competitive adsoroption (wear rate increase in both hypotheses) [16]. Massoud and co-workers [124] suggested the formation of reverse micelles due to interaction of ZnO and amine molecules. These micelles form ZnO rich tribofilm on interacting asperities, which reduces wear [124]. Recently some studies discussed AW capability of ZnO nanoparticles with surfactants [181]–[184]. However, hypothesis of formation of micelles needs further investigation [124].

4.6.3 Effect of amine concentration

The concentration of amine is very critical in terms of how it interacts with ZDDP. Tribological behaviour of ZDDP deviates with the change in amine concentration in lubricant blend [171]. Amine interacts synergistically with ZDDP until it reaches a critical concentration and above that concentration synergism turn into antagonism and consequently wear rises sharply [162].

Figure 4-6 shows effect of amine concentration and load on wear behaviour of lubricant blend having two mass percent ZDDP.

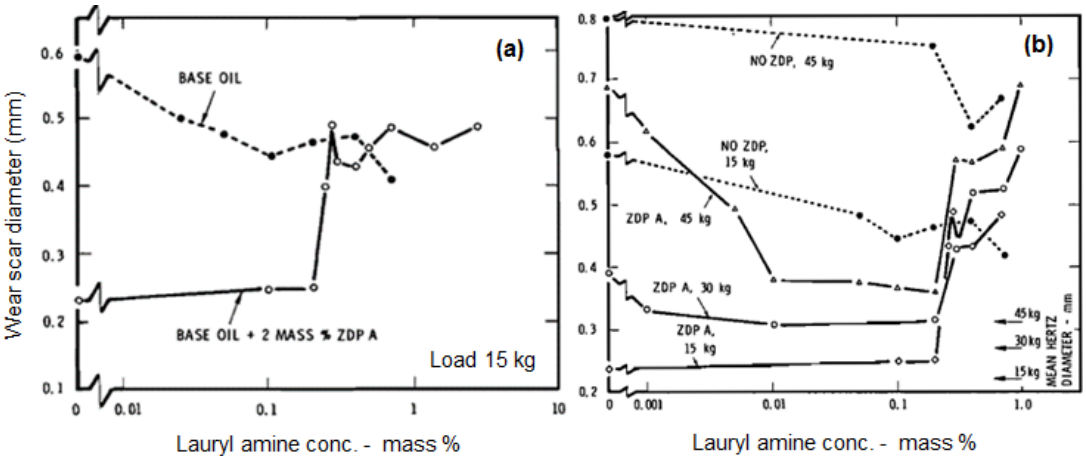

Figure 4-6. Interaction of Lauryl amine with ZDDP; temperature 93 °C [162]
(a) Effect of change in amine conc. on wear (b) Effect of load on wear

In Figure 4-6 (a), addition of lauryl amine with ZDDP reduced wear scar diameter (WSD) until critical amine concentration and beyond that, concentration WSD increased significantly. In Figure 4-6 (b), the synergistic wear effect of lauryl amine with ZDDP continued till 0.2 mass percent of amine concentration and beyond that concentration, wear increased significantly. Both 30 and 45 kg load showed decrease in WSD before critical amine concentration but 15 kg load showed no convincing change in WSD. Interestingly after critical amine concentration (i.e. 0.2 mass percent), WSD increased significantly for all three loads. Above the critical amine concentration, wear behaviour of the ZDDP-amine blend is comparable with amine alone and ZDDP has low or no input in reducing wear [162]. Critical amine concentration is independent of both load and temperature [162]. If amine concentration is below the critical concentration value, then amine interacts synergistically with ZDDP [162].

Shiomi et al. [33], presented interaction analysis of different concentrations of 2-ethylhexyl amine with fixed concentration of ZDDP in solution. N/Zn mole ratio of 1:1 produced the same level of AW performance as with only ZDDP, which means that the amount of ZDDP adsorbed on the interacting surfaces is enough for AW performance. Increasing the amine concentration increased

wear significantly and it was most probably due to reduced adsorption of ZDDP and increased formation of 1:2 complex. Further addition of amine in the blend further reduced adsorption of ZDDP on the metal surfaces due to availability of excess amine in the solution, which blocks the metal surface and as a result AW performance of the blend is significantly reduced.

Recently Massoud et al. [124] suggested that tribological behaviour of lubricant blends having FA and ZDDP depends primarily on the molar ratio of these two additives in BO. Synergistic tribological behaviour was recorded when amine/ZDDP molar ratio ≤ 0.5. Further increase in amine concentration in the blend promote formation of ZnO enriched tribofilm on rubbing asperities [124]. Once amine/ZDDP molar ratio reached about 0.8, delay in tribofilm formation was recorded and as a result wear increased [124]. At this critical concentration tribofilm formation by ZDDP and tribofilm removal by FAs work simultaneously [124].

4.6.4 Effect of amine on ZDDP adsorptivity and film formation

Presence of OFMs in the blend delay tribofilm formation of ZDDP [91], [171]. FAs affect AW film formation of ZDDP by delaying or slowing down the film formation mechanism [22], [30], [33], [164]. The rate of decomposition of ZDDP decreased in the presence of amines as it took more time to decompose [30], [162]. FAs interact with ZDDP molecule and form metal complexes in the base fluid [22], [30], [173], [31]–[33], [64], [91], [124], [171], [172] which are bulky in size and lead to higher steric hindrance and less adsorption on interacting asperities [171]. Furthermore, formation of metal complex in the solution also reduce availability of free ZDDP molecules and hence all these factors contribute to the delay in ZDDP film formation and hence affect ZDDP AW properties [91], [171], [185]. Figure 4-7 shows adsorption isotherms of ZDDP and ZDDP-ethylhexyl amine complex. Adsorption isotherm showed that ZDDP adsorption capability is far better than that of the complex and it is assumed that bulkiness or good solubility in oil might be the potential cause of low adsorption of the complex [33]. Matsui et al. [34] reported that N containing additives have the capability to preferentially adsorb on the steel surfaces and as a result reduced ZDDP derived tribofilm. Furthermore, he stated that few nitrogen containing additives increased COF

value while in case of dimethyloctadecyl amine COF value is decreased. Though both N-containing additives reduced ZDDP derived tribofilm.

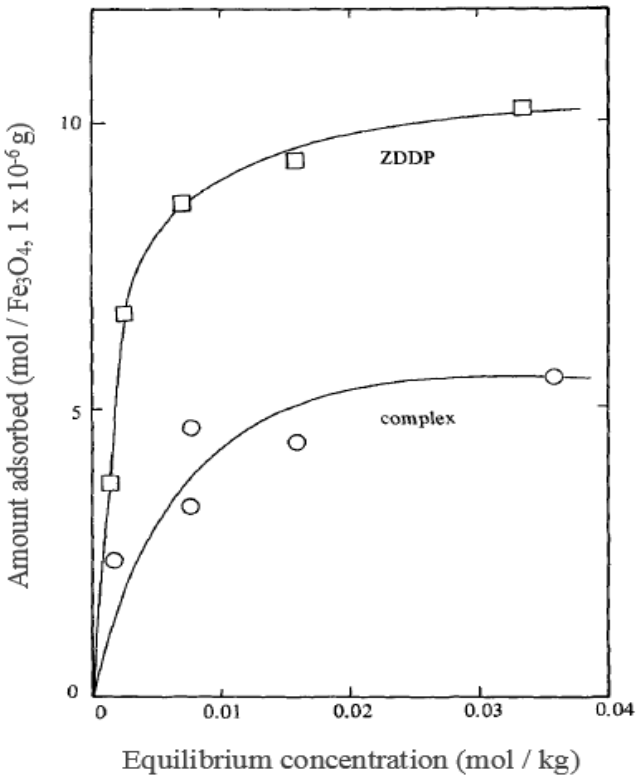

Figure 4-7. Adsorption isotherms shows less adsorption of ZDDP-amine complex on interacting surfaces [33]

4.6.5 Effect of amine on phosphate chain length

ZDDP forms tribofilm on interacting surfaces, which is heterogeneous in terms of topography and mechanical properties. AW film formed by ZDDP is characterized by a pad-like structure having ridges and valleys regions and constituted of amorphous zinc and glassy phosphates [25], [27], [99], [186]. The top layer of the tribofilm is composed of long chain phosphate while the bottom of the film is mainly composed of ortho and pyrophosphates also named as short chain phosphates [90], [186]. Previous Studies [164], [169], [174], [187] reported that composition of the tribofilm formed by ZDDP and succinimide (dispersant additive) is comprised of ammonium/zinc phosphates. Interaction between ZDDP and succinimide not only modify the chemical composition of the tribofilm but also shorten the phosphate chain length [169], [187]. Zhang et al. [164] suggested that presence of dispersant

additive do not affect the formation of phosphate film but actually it shorten the phosphate chain length. Crobu and co. workers [186] claimed that short chain phosphates show better friction and wear results but there is no evidence which supports the wear performance linkage with short or long chain phosphates.

4.7 Summary

This chapter covers the literature about basic categories and film formation mechanisms of friction modifiers (FMs). AW film formed by ZDDP carries high boundary friction, which is one of the reasons for mechanical losses in an IC engine. An important solution to overcome the high boundary friction is to design lubricants that offer low friction in engine components. FMs are the lubricant additives that reduce boundary friction, improve lubricity by reducing the friction coefficient and contribute towards improvement in fuel economy.

In boundary lubrication, FMs reduce friction by generating a low shear strength film on metal surfaces. Organic friction modifiers (OFMs) are long chain compounds with polar end groups at one end. OFMs are amphiphilic surfactant and generally consist of at least ten carbon atoms. OFMs reduce friction by forming extremely thin, closely packed, vertically oriented, low shear strength, self-assembled monolayers on interacting surfaces. Polar end groups of OFMs adsorb physically or chemically on surfaces with the hydrocarbon chain extending in the lubricant. The role of head groups is of vital importance in the effectiveness of OFMs. Carboxylic-acids and their derivatives and N-based compounds, are among those additives, which are under consideration to replace the traditional friction additives.

N-based organic friction modifiers (i.e. amines), belong to the family of chemical compounds having central N atoms, which are sp^3 hybridized managing three single bonds with other elements. Amines with alkyl chains of eight or more carbon atoms described as fatty alkyl amines (FAs). FAs as mentioned above have a typical chain length of 8 to 24 carbon atoms (i.e. C8 – C24) and are a mixture of saturated and un-saturated alkyl chains. Some of the FAs are designed with multiple functional groups to promote chelation and consequently adsorption. Fatty amine (FA) molecules quickly adsorb on metal surface and form thick monolayer even at low concentrations in the solvent. During the chemisorption, N atoms act as a Lewis base and donate the lone pair of electrons to surface iron (III) ions. Generally, FAs having carbon chain length of 10 or more show solubility in polar and non-polar solvents.

Amines reduce high boundary friction associated with the AW film formed by ZDDP. The interaction of amines with ZDDP and its impact on the AW performance of ZDDP is very critical in determining whether the result of interaction is synergistic or antagonistic. Few possible mechanisms have been proposed to address the question that how FAs affect the AW performance of ZDDP in normal conditions. Amines interact with the ZDDP and result in formation of complexes in the bulk fluid. ZDDP-amine complexes tie the ZDDP molecule and affect its AW performance. Complexes formed due to interaction between ZDDP and amines are in equilibrium with both the reactants (i.e. amines and ZDDP). Amines alter the ZDDP decomposition rate and thus disturb the AW performance. It is reported that the decomposition of ZDDP take more time in presence of amines and the decomposition rate further decreases with the increase in concentration of amines in the lubricant blend. Amines interacts synergistically with ZDDP until amine reaches a critical concentration and above that concentration synergism turns into antagonism, consequently wear increase sharply.

Chapter 5
Experimental Methods and Materials

5.1 Introduction

This chapter describes tribological testing techniques, testing conditions/parameters, testing samples and lubricant blends being used along with the surface analysis techniques employed to analyse the tribological performance of lubricants and surface interactions.

5.2 Lubricants

Initially seventeen OFMs were tribologically tested and then screened, based on friction and wear performance of lubricant blend. For screening, these OFMs were blended with ZDDP in 1:1 molar ratio of FM to ZDDP. A blend of BO + ZDDP was also tribologically tested for control purpose. Complete details of lubricant blends are given in Table 5-1. ZDDP used in the experimental work was a combination of primary and secondary ZDDP. The OFMs used in this study were derived from natural fats and oils. Fatty acid was the first OFM derived from natural fat and vegetable oils but due to high corrosive behaviour of fatty acids with metals it was later replaced with comparatively less corrosive organic additives which includes amines, amides, esters etc. [104]. OFMs used in the tribological screening belonged to different groups (i.e. amines, alcohol, esters etc.).

The shortlisted OFMs (i.e. FM 1, FM 4, FM 8, FM 10 and FM 14), were mainly fatty amines (FAs) with different structure and chain lengths, whereas one friction modifier (i.e. FM 10) was fatty alcohol. Figure 5-1 shows the chemical structure of these five OFMs along with ZDDP. These OFMs were blended with ZDDP in 0.5:1 and 1:1 molar ratio of FM to ZDDP. Some OFMs dissolved completely in BO with ZDDP whereas a couple of them partially dissolved at room temperature. Those lubricant blends were heated and stirred again just before conducting the tribological experiment. The concentration of ZDDP was constant in all formulations (i.e. 0.55 wt. %). The BO used in lubricant blends was group III mineral oil having a kinematic viscosity value of 4.4 cSt at 100 °C.

Table 5-1. Lubricant blends tribologically tested during this study

Lubricant blends	Lubricant blends
BO + FM 1 + ZDDP	BO + FM 10 + ZDDP
BO + FM 2 + ZDDP	BO + FM 11 + ZDDP
BO + FM 3 + ZDDP	BO + FM 12 + ZDDP
BO + FM 4 + ZDDP	BO + FM 13 + ZDDP
BO + ZDDP	BO + FM 14 + ZDDP
BO + FM 6 + ZDDP	BO + FM 15 + ZDDP
BO + FM 7 + ZDDP	BO + FM 16 + ZDDP
BO + FM 8 + ZDDP	BO + FM 17 + ZDDP
BO + FM 9 + ZDDP	BO + FM 18 + ZDDP

ZDDP used in tribological testing was a mixture of primary and secondary ZDDP, having alkyl group (R) C3 57% and C8 43% [15].

Zinc Dialkyldithiophosphate (ZDDP)

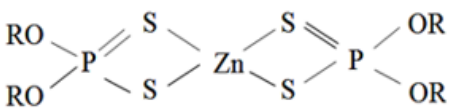

R = Alkyl group C3 57
C8 43

FM 1 (Coco amine)

$R\text{-}NH_2$ (R = coco)

C8	6
C10	7
C12	51
C14	19
C16	9
C18	2
$C18^{un\ sat.}$	6

FM 4 (Ethoxylated hydrogenated tallow amine)

R = Hydrogenated tallow

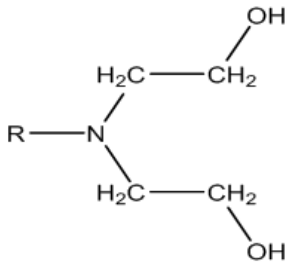

C14	4
C16	32
C18	64

FM 8 (Tallow amine)

R = Tallow

C14	4
C16	30
$C16^{un\ sat.}$	2
C18	20
$C18^{un\ sat.}$	44

FM 10 (Alcohol ethoxylate)

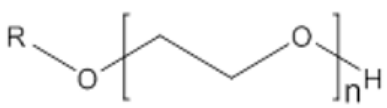

C10	100

FM 14 (Ester of triethanol amine with tallow fatty acid)

R = Tallow fatty acid

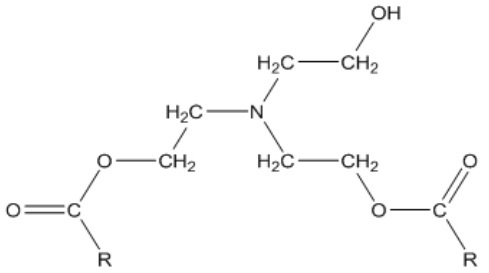

C13	4
C15	30
$C15^{un\ sat.}$	2
C17	20
$C17^{un\ sat.}$	44

Figure 5-1. Chemical composition of ZDDP and OFMs

Tribological tests with single additive systems were also conducted during this study. In these tests, shortlisted OFMs blended with BO and similarly ZDDP was also blended with BO separately. These lubricant blends then tribologically tested in a sequence and named as sequential film formation tests. AkzoNobel Surface Chemistry supplied BO, ZDDP and OFMs used in the experimental work.

5.2.1 Blending procedure

AkzoNobel Surface Chemistry provided some lubricant blends specifically for initial screening. These lubricants were blended in 1:1 molar ratio of FM to ZDDP. In later stages of the study, shortlisted OFMs were blended locally in 0.5:1 molar ratio of FM to ZDDP. For sequential tribological testing, lubricants with single additive (i.e. BO + FM and BO + ZDDP) blended separately and the amount of additive used in the blend was as per 1:1 molar ratio of FM to ZDDP. The concentration of ZDDP was constant in all formulations (i.e. 0.55 wt. %). For instance, 1:1 molar ratio of BO + FM 8 + ZDDP contains 0.825g of ZDDP (i.e. 0.55 wt. %) with 0.358g of FM 8 in 150g of BO. Therefore, 0.825g of ZDDP was added in a blend of BO + ZDDP and 0.358g of FM 8 was added in the blend of BO + FM 8. Table 5-2 describes the lubricant blending procedure of ZDDP and FM 8 in BO. Table 5-3 shows the amount of short listed OFMs along with their respective molecular weights. The specified amount of OFM and ZDDP were blended for thirty minutes while stirring at 500 RPM and 60°C.

Table 5-2. Lubricant blending procedure

Step	Procedure
Step 1	Add 0.825g of ZDDP in 50g BO (1/3 quantity) and shake
Step 2	Add 0.358g of FM 8
Step 3	Add remaining 100g of BO
Step 4	Heat at 60°c whilst stirring at 500 RPM approximately
	Lubricant blended for 30 minutes

Table 5-3. Molecular weight and amount of additives

S. No	Chemical additive	Molecular weight	Amount (g) 1:1 molar ratio	Amount (g) 0.5:1 molar ratio
1	FM 1	200	0.269	0.135
2	FM 4	351	0.472	0.236
3	ZDDP	613	0.825	0.825
4	FM 8	277	0.372	0.186
5	FM 10	312	0.419	0.209
6	FM 14	660	0.888	0.445

5.3 Tribological tests

All tribological tests were carried out by using pin on plate reciprocating tribometer. The tribofilms formed in these interactions were used to analyse the tribological performance of lubricant blends.

5.3.1 TE77 (high frequency friction machine)

Cameron Plint TE 77 reciprocating tribometer is a simple pin on plate arrangement in which moving pin specimen mounted inside a carrier and it reciprocates physically against a fixed plate. Material of fixed square plate was stainless steel (AISI 52100) having dimension (7 x 7 x 3 mm) and material of counter surface (i.e. pin) was also stainless steel (AISI 52100) with end curvature radius of 10mm. Figure 5-2 shows pin on plate interface and tribological arrangement.

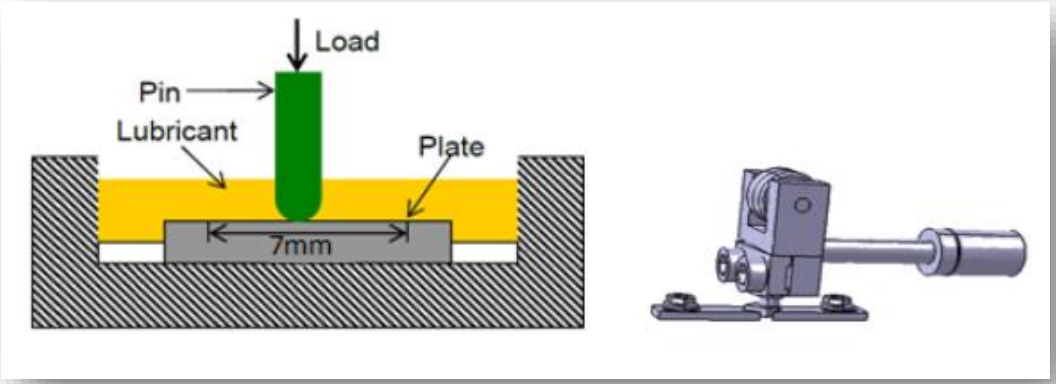

Figure 5-2. Pin on plate interface and tribological arrangement [188]

Cameron Plint TE 77 reciprocating tribometer was used to analyse the tribological performance of OFMs when blended with ZDDP and in sequential film formation tests. Friction and wear behaviour of different lubricant blends indicated that how different OFMs interact with ZDDP and how it affects the tribological performance of ZDDP? In this study, TE77 tribometer simulates piston/cylinder interaction under boundary lubrication condition in which asperity-to-asperity contact significantly increase friction and wear. In this simple reciprocating pin on plate arrangement, the pins represented the piston component whereas the plates represented the cylinder part. Tribological experiments were performed under reciprocating pure sliding conditions in which pin specimen reciprocates against a fixed plate specimen between two extreme positions. Velocity of the pin was recorded as zero at extreme position while it was maximum at middle of the wear track. As a result of this

tribological interaction a wear track is formed on the plate specimen and a wear scar diameter (WSD) on the pin specimen. Figure 5-3. shows the wear track and WSD on plate and pin specimen.

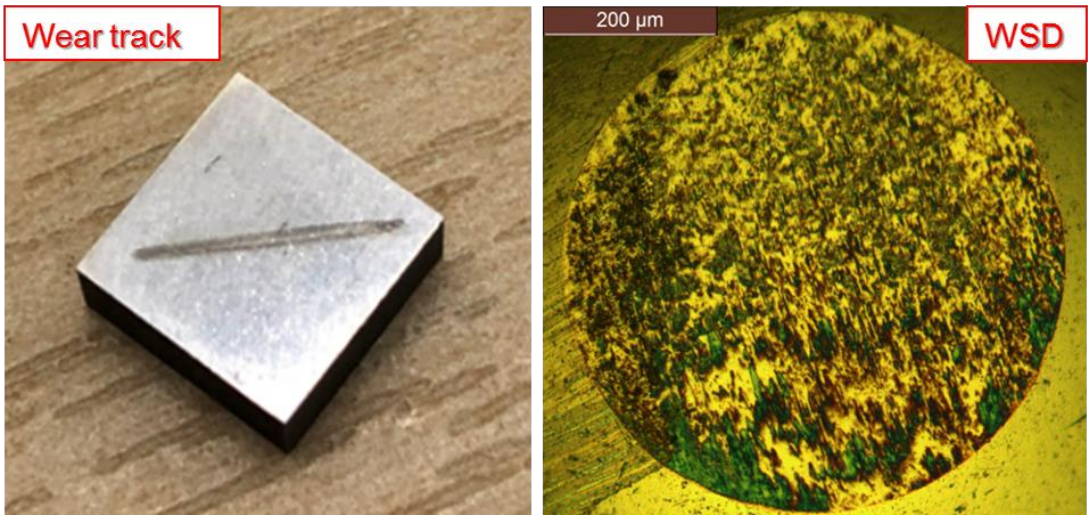

Figure 5-3. Photo of wear track and microscopic image of WSD

In pure sliding reciprocating condition speed of the pin specimen changes continuously. At start of the wear track (i.e. position 1), speed of the pin specimen is observed as zero then speed starts increasing and maximum speed is observed at middle of the wear track (i.e. position 2). Later on speed starts decreasing as the pin specimen proceeds towards the other end of the wear track and ultimately it becomes zero at the end of the wear track (i.e. position 3). During this reciprocating motion each position of the wear track experienced different speed which only matches with the same position at next half of the wear track. Output voltage curve against the time graph in Figure 5-4 shows change in speed pattern during this pure reciprocating sliding motion.

Reciprocating pin and the fixed plate interact with each other inside an oil reservoir in submerged state. Lubricant was heated inside the oil reservoir with the help of a heater plate controlled by a thermo-couple, which adjusts the temperature of the lubricant as per user's instruction. Load was applied manually and it was then converted to a digital signal by using an analogue to a digital converter. Speed was controlled by a built in speed controller and the stroke length was also adjusted manually [189], [190]. Figure 5-5 shows the

schematic of TE 77 tribometer arrangement. Data file of friction force was recorded after specific time duration (i.e. 300 seconds) but user may change it. Each data file was comprised of 1000 measurements, which was taken during the specified time.

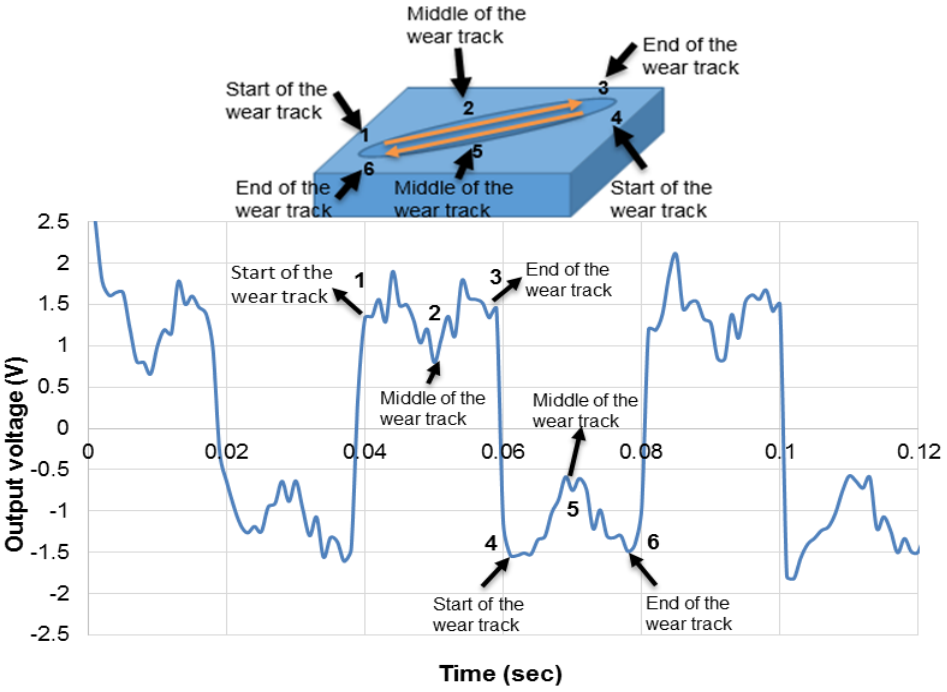

Figure 5-4. Output voltage (V) graph against time (sec) and respective positions on the wear track

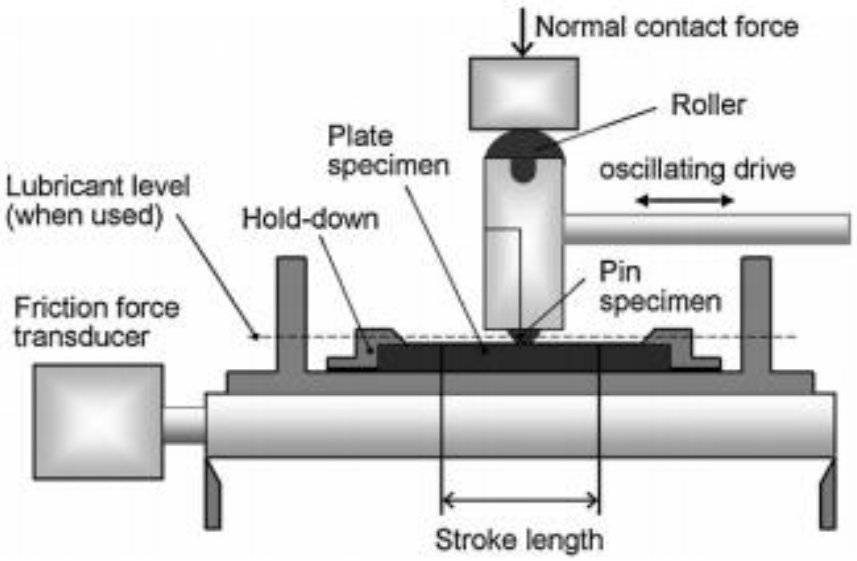

Figure 5-5. Schematic of TE 77 arrangement [190]

Transducer transmits the friction force signals from the load cell to a recorder. The gathered analogue signal was converted into digital signal and then finally processed by LabVIEW software and later on friction COF was measured from this processed data [189]. Before tribological testing mechanical components and sample specimen were cleaned with heptane and then with acetone in ultrasonic bath while after testing sample specimens were rinsed with heptane and stored in aluminium foil to avoid any environmental contamination.

5.3.2 Test methodology

In this study a blend of seventeen OFMs with ZDDP were initially tested and their tribological performance were analysed. The primary purpose of this study was to,

- Analyse the effect of OFMs on tribofilm morphology, durability, composition and film formation capability of ZDDP
- Understand tribochemical interaction between OFM (amine friction modifier) and ZDDP

To achieve above mentioned and other related objectives, tribological testing were performed in two phases (i.e. phase 1 and phase 2),

- Phase 1 was comprised of preliminary tribological screening of OFMs

In these tests, OFMs and ZDDP were blended beforehand in 1:1 molar ratio of FM to ZDDP. These tests were two hours long continuous tests. After completion of tribological screening, a few OFMs were shortlisted based on friction and wear performance for further analysis

- Phase 2 was specifically aligned with the objectives of this study and this phase was further divided in two parts

In part 1 tribological testing was performed for two hours (i.e. continuous tests) with shortlisted lubricants in which OFMs and ZDDP were blended together beforehand in 0.5:1 and 1:1 molar ratio of FM to ZDDP. Part 2 was limited to further shortlisted OFMs (i.e. amine FMs), in which film was sequentially

formed by OFM and then with ZDDP or vice versa. Complete details of sequential film formation tests are given below,

- These tests comprised of varying time durations (i.e. 30, 60 and 120 minutes)
- For a thirty minutes test, first fifteen minutes sample specimen tested with BO + OFM and then test was stopped. After replacing the lubricant with BO + ZDDP testing was resumed for another fifteen minutes

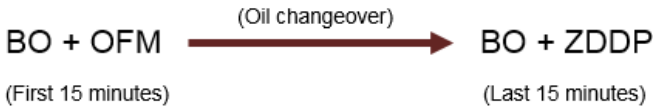

- Same test procedure applied on the test in which BO + ZDDP was tribologically tested first and then followed by BO + OFM

- Sixty and one hundred and twenty minutes tests followed the same testing protocol as mentioned above

5.3.3 Test parameters and samples

Test parameters used in TE 77 experimental work are listed in Table 5-4. The tribological tests were performed in the boundary lubrication regime. The dimensionless specific film thickness parameter '**λ**' ratio was well under the unity, which shows that the tribological interaction was in boundary lubrication regime [191]. The dimensions of the plate specimen was 7 x 7 x 3 mm and pin end curvature radius was 10 mm. Table 5-5 details properties and dimension of the sample specimen.

5.4 Post-test surface analysis

5.4.1 Wear analysis

Wear track and WSD images of the tribological pair were captured by using the optical microscope (OM). OM uses objective lenses with different magnification and with the aid of these higher magnification lenses object can be enlarged and focus to get the clearer image. Leica DM6000M optical

microscope has the capability to capture the magnified images and process it. Figure 5-6 shows image of the WSD taken from the OM.

Table 5-4. Test condition and parameters

Test condition	Parameters
Applied load	83 N
Max. Hertz. Pressure	1.2 GPa
Frequency	25 Hz (0.35 m/s)
Stroke length	7 mm
Temperature	120 °C
Test duration	120 minutes[1]
	30, 60, 90 minutes[2]
	1 Tribological testing of OFM and ZDDP blended beforehand testing
	2 Sequential film formation

Table 5-5. Specimen details and physical properties

Specimen details	
Pin radius	10 mm
Pin surface hardness	58 – 62 HRC
Pin surface roughness	0.3-0.7 µm
Plate dimension	7 x 7 x 3 mm
Plate surface hardness	58 – 62 HRC
Plate surface roughness	0.04-0.06 m

The specific wear rate or wear factor calculation presented in this study is based on the WSD of the pin specimen. This was necessary because due to extreme applied load wear debris stuck inside the wear track and as a result recorded wear depths not reflected the actual wear behaviour of the lubricant blend. Figure 5-7 shows the contact profile taken across the wear track (perpendicular to the wear track width).

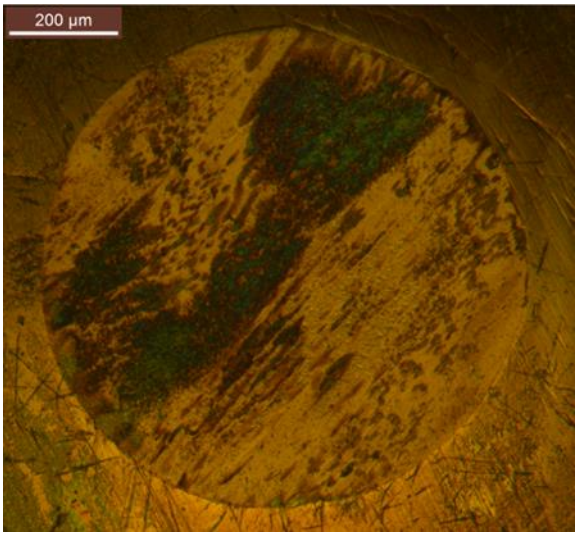

Figure 5-6. OM image of the WSD on pin specimen

Wear volume of the pins were measured using Equation 5-1 [191], [192],

$$V_{pin} = (\pi h)/6 \{3r^2 + h^2\} \quad 5\text{-}1$$

$\mathbf{V_{pin}}$ is the volume loss of the ball (mm^3), **h** is the worn height of the spherical tip of the ball/pin (mm) that can be calculated by using the formula as shown in Equation 5-2,

$$h = R - \sqrt{R^2 - r^2} \quad 5\text{-}2$$

In Equation 5.2, **R** is the tip radius of the ball (mm) before test while **r** is the wear scar radius (mm). Finally, wear factor has been calculated by using Archard's wear formula as shown in Equation 5-3,

$$V = KArL = KLW/H = kLW \quad 5\text{-}3$$

Where **k** is the wear factor or dimensionless wear co-efficient (mm^3/N mm), **L** is the sliding distance (mm), **W** is the applied load (N) and **V** is the wear volume (mm^3) [3], [9], [193].

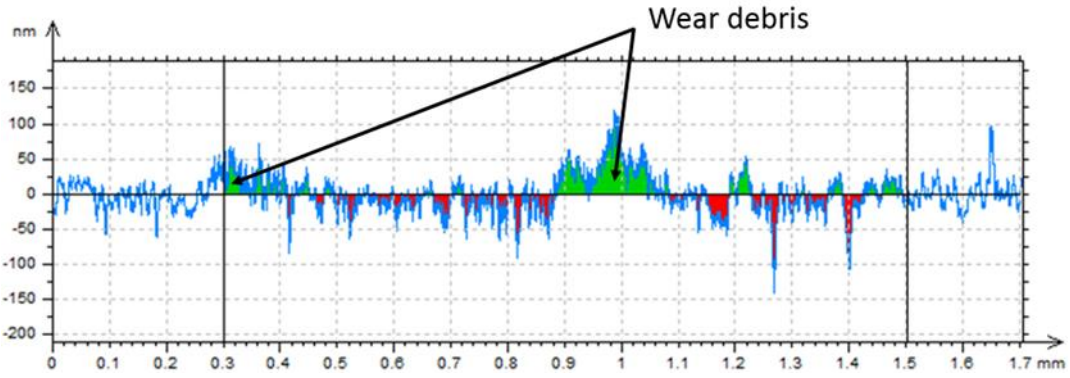

Figure 5-7. Wear track profile showing wear debris inside the wear track

5.4.2 Atomic Force Microscope

The atomic force microscope (AFM) is a high-resolution microscope with the capability to produce lateral resolution around 5 nm and vertical resolution around 0.1 nm. AFM measures force between a probe and the sample by bringing a probe and the sample in to close vicinity. Interaction between the sharp probe and the surface topography is map out by monitoring the movement of a cantilever tip with nanoscale precision. Figure 5-8 shows schematic of cantilever tip assembly and basic components.

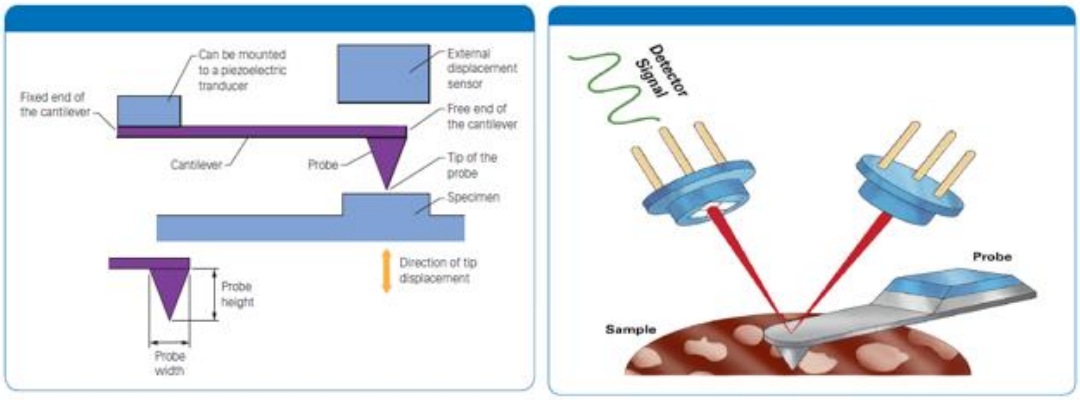

Figure 5-8. Schematic of cantilever tip assembly and basic components of AFM [194]

The AFM was used in this study to analyse the micro features of the tribofilm formed by different lubricant blends. The cantilever resonance frequency employed during AFM analysis was 0.977 Hz and spring constant was 40 N/m. An area of 30 µm x 30 µm across the wear track in different locations was scanned in peak force tapping mode, in order to get the high-resolution

(HR) topographical images with least damage to the tribofilm surface. Scanning was performed in the perpendicular direction to the long axis of cantilever in order to analyse the film morphology across the wear track [195]. AFM scans of the tribofilms formed by different lubricant blends were captured in ambient conditions.

Modification in the tribofilm topography with different lubricant blends indicated the impact of additive interaction on friction and wear behaviour. Figure 5-9 shows modification in tribofilm topography with the addition of different OFMs in the blend. Roughness parameters of the tribofilm topographies were also measured using AFM and these were;

- Root mean square roughness (R_q), which is the root mean square roughness of the profile above or below the centre line
- Maximum roughness height (R_{max}), which is the largest of the individual peak to valley height

Prior to analysis, the disc samples were cleaned with heptane to remove any oil residuals or dirt from the tribofilm.

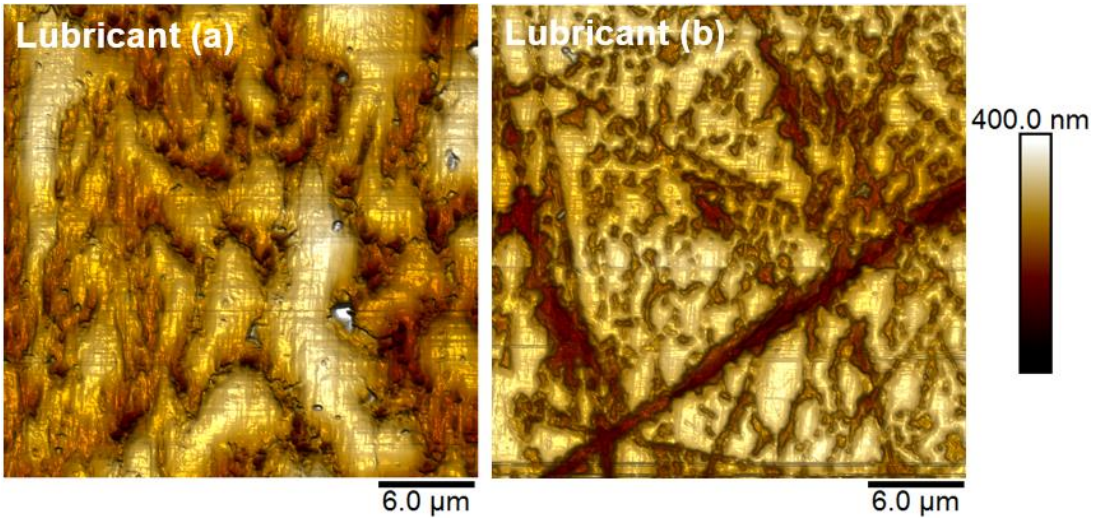

Figure 5-9. Change in tribofilm topography from one lubricant blend to another

5.4.3 Scanning Electron Microscope and Energy Dispersive X-ray

The scanning electron microscope (SEM) uses a focused beam of high energetic electrons for bombardment on the sample surface under vacuum

condition. Bombardment of electron produces variety of signals from the sample which includes secondary electrons (SE), back scattered electrons (BSE), auger electrons (AE), elastically scattered electrons, X-rays etc. Figure 5-10 shows the interaction of an electron beam on sample specimen. Out of these signals SE, BSE and X-rays are very important in terms of information and topography of the sample [196], [197]. The SE have energy below 50 eV and usually they are not much helpful in terms of elemental information however due to high spatial resolution they produce good micrographic images. The BSE are much more energetic than SE. The BSE images usually display compositional contrast which due to distribution of different atomic number elements. The energy dispersive X-ray (EDX, which is integrated with the SEM), use the energy of the X-rays signal to identify the elemental composition and their proportion in the sample [196], [197].

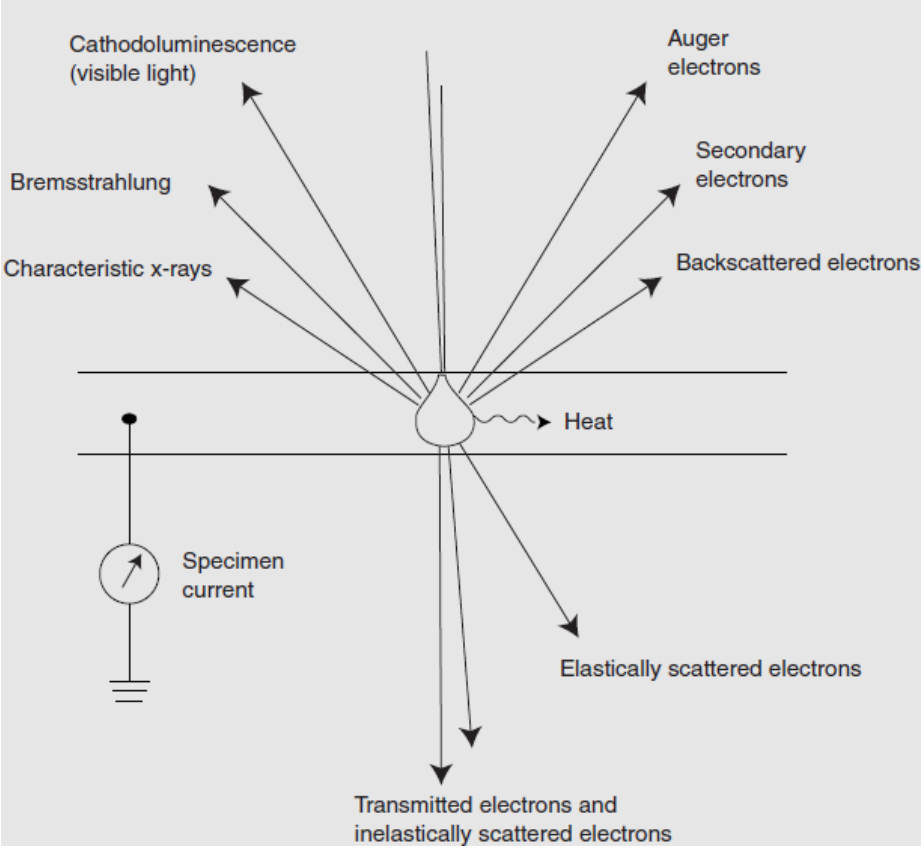

Figure 5-10. Electron bombardment illustration in the SEM [197]

The Carl Zeiss EVO MA15 SEM/EDX used in this study. EVO MA15 machine was equipped with detectors for capturing secondary and back scattered

images and also integrated with Aztec Energy EDX system for elemental mapping and line scan [198]. The EVO SEM was operated at an accelerating voltage of 10 kV and a working distance of 8.5 mm was maintained during this operation. Figure 5-11 shows the elemental mapping and EDX spectrum of the tribofilm.

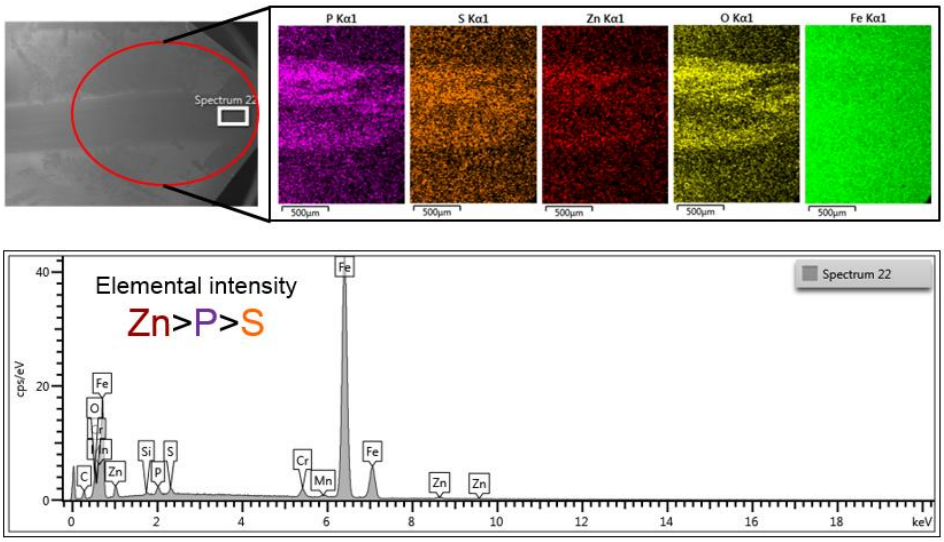

Figure 5-11. Elemental mapping and EDX spectrum of the tribofilm

5.4.4 X-ray Photoelectron Spectroscopy

The X-ray photoelectron spectroscopy (XPS) is a useful technique to examine the chemical composition of the surface. In this technique, X-rays are used to excite the electronic state of atoms below the surface of interest. Under high vacuum condition energetic electrons ejected from the surface and pass through the thin membrane. The kinetic energy (eV) of these electrons are recorded by a detector and then analysed [199], [200]. Figure 5-12 shows schematic of an XPS experiment. In this study XPS is used to analyse the chemical composition and elemental analysis of the tribofilm formed as a results of interaction between OFMs and ZDDP. The XPS used micro focused monochromatic Al K alpha source. An approximate spot size of 400 X 800 microns is analysed on the wear track on TE 77 plate specimen. The XPS analysis were conducted at the middle/centre position of the wear track. Figure 5-13 demonstrates position of the XPS analysis on a plate specimen.

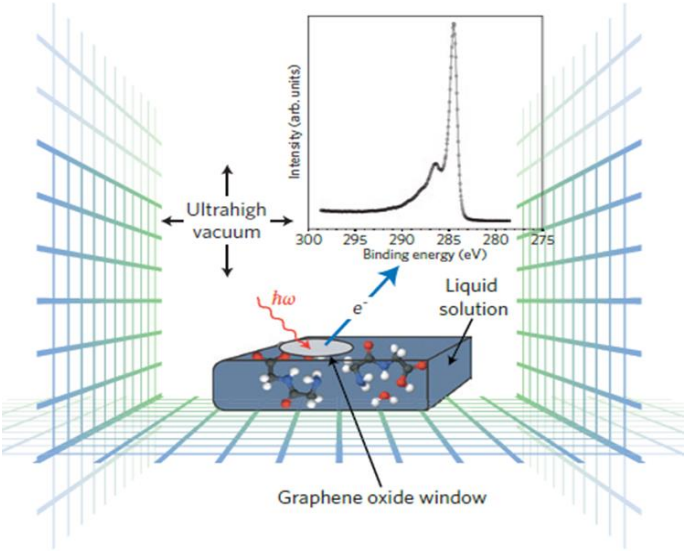

Figure 5-12. Schematic of an XPS experiment [200]

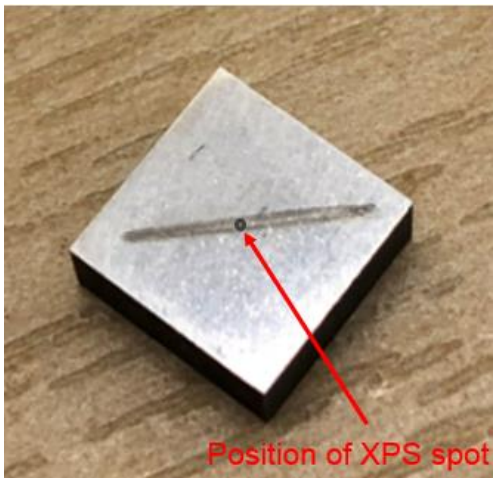

Figure 5-13. Position of the XPS spot on a plate specimen

The XPS is a surface sensitive technique which can only penetrates first few nanometres (5-8 nm) of the sample [201], [202]. The surface analysis of each sample started with a survey scan. These scans were conducted with pass energy of 150 eV, step size of 0.4eV and with dwell time of 10ms. Survey scans were carried out for initial screening of the elements in the tribofilm. This process was followed by HR scans of selected elements, which includes C1s, O1s, P 2p, S 2p, Zn 2p, Zn 3s, N 1s and Fe 2p. The HR scans were carried out with pass energy of 40 eV, step size of 0.1eV and with dwell time of 100ms.

Energy calibration of the spectra were performed with reference to adventitious aliphatic carbon binding energy (BE) at 284.8 eV.
Etching of the tribofilm surfaces were also conducted during this study. Etching profile revealed the chemical composition, quantification and elemental incorporation across the tribofilm. Etching of the tribofilm surfaces helped to mitigate any contamination effect and to further,

- Analyse change in elemental concentration across the tribofilm
- Investigate the tribochemistry of lower surfaces of the tribofilm

Tribofilm etching were performed by using 4KeV argon ion gun. Though, etching changes the chemical state of the species [82], [174] but still with this limitation comparison of XPS data from top most surface of the tribofilm with the chemical species found after few etching cycle provide a good indication about the modification in chemical structure of the tribofilm. Furthermore, depth profile data by etching of the tribofilm provided elemental quantification, changes in elemental concentration, and composition in the bulk of the tribofilm . Figure 5-14, 5-15 and 5-16 show typical survey scan, HR scan and depth profile analysed during this study.

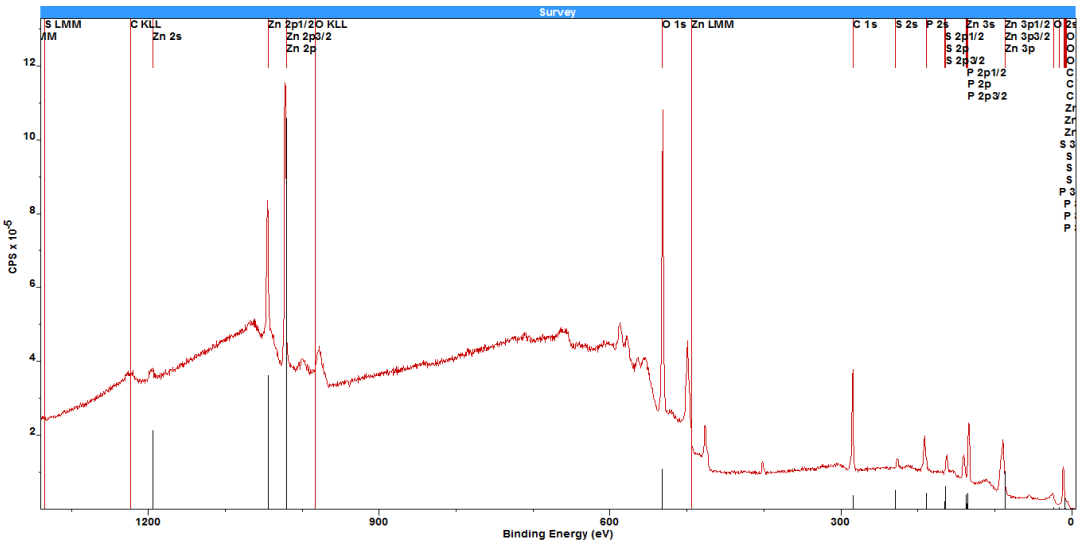

Figure 5-14. The XPS survey scan of the tribofilm

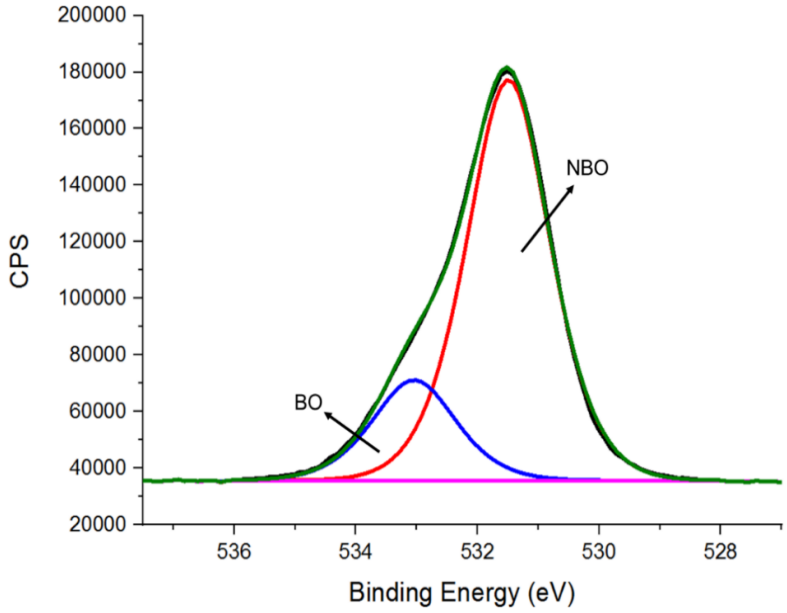

Figure 5-15. The XPS high resolution scan of an elemental signal

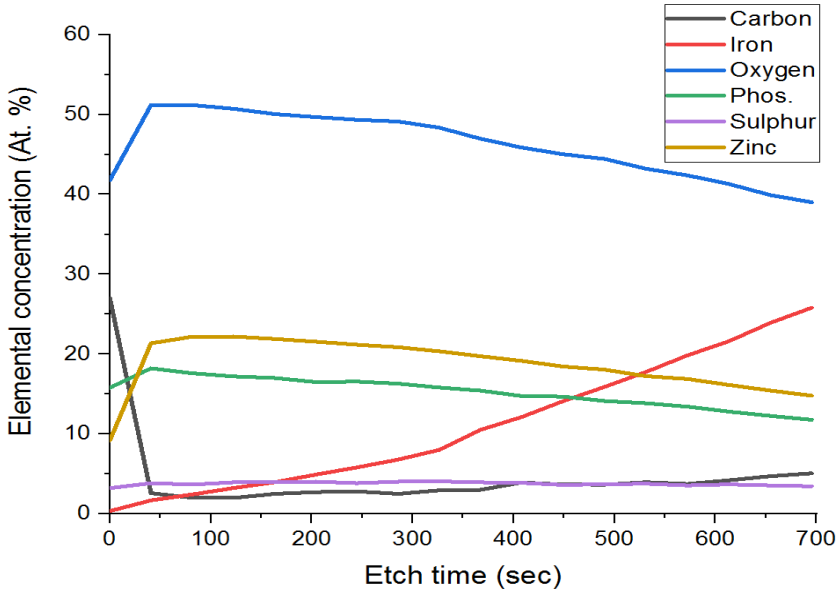

Figure 5-16. The XPS depth profile of the tribofilm showing elemental concentration across the tribofilm

The XPS spectra were processed by using Casa XPS software [186]. The Shirley-Sherwood (aka Shirley) iterative method was used for background subtraction whereas Gaussian and Lorentzian (GL) function was chosen for curve fittings [77], [186], [203], [204]. All these functions are well embedded in Casa XPS software [186]. Energy calibration of spectra were performed with

reference to adventitious aliphatic carbon binding energy (BE) at 284.8 eV [191][82]. Full width half maxima (FWHM), binding energies and sensitivity factors were gathered from the literature and then XPS data were processed with these values [77], [79], [91], [174], [186], [191], [193], [203]–[205]. Table 5-6 specifies the XPS curve fitting parameters.

Table 5-6. The XPS curve fitting parameters

Element		FWHM (eV)	Line shape	Relative Sensitivity Factor (R.S.F)
C 1s	Carbide	1.2 - 1.6	GL(60)	1.0
	Aliphatic	1.2 – 1.8		
	C-O	1.2 – 2.2		
	C=O	1.2 – 2.2		
Fe $2p_{3/2}$	Metallic	0.9 - 1.4	GL(30)	10.82
	Fe_xO_y	2.1 - 3.2		
	Fe_xS_y	2.1 - 3.2		
O 1s	Fe_xO_y/ZnO	1.2 – 1.4	GL(55)	2.93
	NBO	1.2 – 1.8		
	BO	1.2 – 1.6		
P $2p_{3/2}$	P_xO_y	1.6 – 2.0	GL(30)	1.192
S $2p_{3/2}$	Fe_xS_y/ ZnS	1.2 – 2.0	GL(20)	1.67
Zn $2p_{3/2}$	ZnO/ ZnS	1.6 – 2.0	GL(60)	18.92
Zn 3s		2.1 – 2.8	GL(30)	1.192
N 1s		1.4 – 1.6	GL(60)	1.8

Due to spin-orbit coupling the P 2p and S 2p signals were split in to respective doublets (i.e. P $2p_{3/2}$, P $2p_{1/2}$, S $2p_{3/2}$, S $2p_{1/2}$) [186], [203], [204]. The P 2p signal was deconvoluted in two components (i.e. P $2p_{3/2}$ and P $2p_{1/2}$). These components showed energy separations of 0.85 eV (i.e. lower BE is assigned to P $2p_{3/2}$) and intensity ratio of 0.5 (i.e. area of P $2p_{1/2}$ is set half as compared to P $2p_{3/2}$) [186], [203], [204], [206]. The Zn 3s peak was detected next to P 2p signal in the same BE window. The S 2p spectra was also deconvoluted in two components (i.e. S $2p_{3/2}$ and S $2p_{1/2}$). These components showed energy separations of 1.25 eV (i.e. lower BE is assigned to S $2p_{3/2}$) and intensity ratio of 0.5 (i.e. area of S $2p_{1/2}$ is set half as compared to S $2p_{3/2}$) [203], [206].

5.5 Summary

The experimental methods, lubricant formulations, specific test parameters and surface analysis techniques, which are used in this study to analyse the tribological behaviour of different lubricant blends and their impact on tribofilm morphology and composition are discussed in this chapter. The sequential film formation tests, which are designed to explore the interaction mechanism of OFMs with ZDDP, are also covered in this chapter.

Chapter 6
Tribological interaction of OFMs with ZDDP

6.1 Introduction

The efficiency of an internal combustion (IC) engine is the centre point of many tribological challenges [6], [24], [48]. Fuel economy cannot be improved without reducing the friction losses in the engine components which ingests approximately 48% of the energy developed by an engine [10]. An IC engine in passenger car converts around 38% of chemical energy in to mechanical power and after further losses around 21% of energy is available to move the car [6], [7], [24], [48]. IC engines are the key source of environmental pollution via exhaust emissions which includes particulate matters, burned hydrocarbons, NO_x (nitrogen oxides) and CO_2 [10]. Environmental/emissions legislation (i.e. European emission standards), continuously reducing the limit of harmful exhaust emissions in order to reduce environmental pollution [6]. In this emerging scenario one of the key challenges for the tribologists is to develop high energy conserving engine oils with additives having low or no SAPS content which will not only minimize the level of harmful exhaust emissions but also increase efficiency of the IC engines by an effective lubrication of interacting engine components [6], [10].

This chapter covers tribological screening of seventeen OFMs and their interaction with ZDDP. Friction and wear behaviour of these OFMs in binary additive systems are discussed in this chapter. The scope of this chapter is centred around the tribological behaviour of lubricant blends and then on the basis of friction and wear performance five OFMs are shortlisted for further study. The concentration effect of shortlisted OFMs on the tribological performance of ZDDP are also discussed in this chapter.

6.1.1 Experimental work and test parameters

In this part of the study, OFMs (having no SAPS content) blended with ZDDP (i.e. BO + OFM + ZDDP) and then tribologically tested. In these tribological experiments friction and wear performance of OFMs with ZDDP were analysed. Tribological testing was performed on TE 77 (high frequency friction machine), in which the pin specimen reciprocates physically against a fixed

plate specimen. Two-hour long continuous tests were performed at a frequency of 25 Hz with maximum Hertzian pressure of 1.2 GPa. The experimental value of the dimensionless specific film thickness parameter '**λ'** ratio was well under the unity, which shows that the tribological interaction was in boundary lubrication regime [191]. Complete detail of test parameters and specimen samples are specified in Experimental Methods and Materials chapter (i.e. Chapter 5). Same test parameters and sample specimens were used for tribological testing of shortlisted OFMs in two different concentrations (i.e. 0.5:1 and 1:1 molar ratio) of FM to ZDDP.

6.2 Friction and wear evaluation

The organic friction modifiers (OFMs) are long chain hydrocarbons having polar end groups [16], [35], [104], [105], [116]. OFMs form films by physical/chemical adsorption on the interacting surfaces [104], [105], [121], [130]. Polar end groups of OFMs adsorb physically or chemically on interacting surfaces with the hydrogen chain extending in the lubricant [105], [116], [119]. ZDDP is a remarkable AW additive which form protective films, minimizing the asperity-to-asperity contact [15]–[18], [25]–[27]. The tribofilms formed by ZDDP possess high boundary friction [15], [22], [61] which may arise due to uneven rough and solid like phosphate film [16], [22], [61], [155]. OFMs have the capability to reduce coefficient of friction (COF) in boundary and mixed lubrication regimes [16], [22], [61], [133]. The interaction of OFMs with ZDDP in binary additive systems when both additives were blended together in base oil (BO) showed some interesting tribological results. Friction and wear behaviour of different lubricant blends varies from one OFM to the other whereas the concentration of ZDDP in each blend was constant.

6.2.1 Friction analysis

Each tribological test was two-hours long and repeated twice to confirm the repeatability. COF values were calculated from the average friction values during the last thirty minutes of the test duration. Figure 6-1 shows the friction performance of blends of OFMs with ZDDP along with BO + ZDDP.

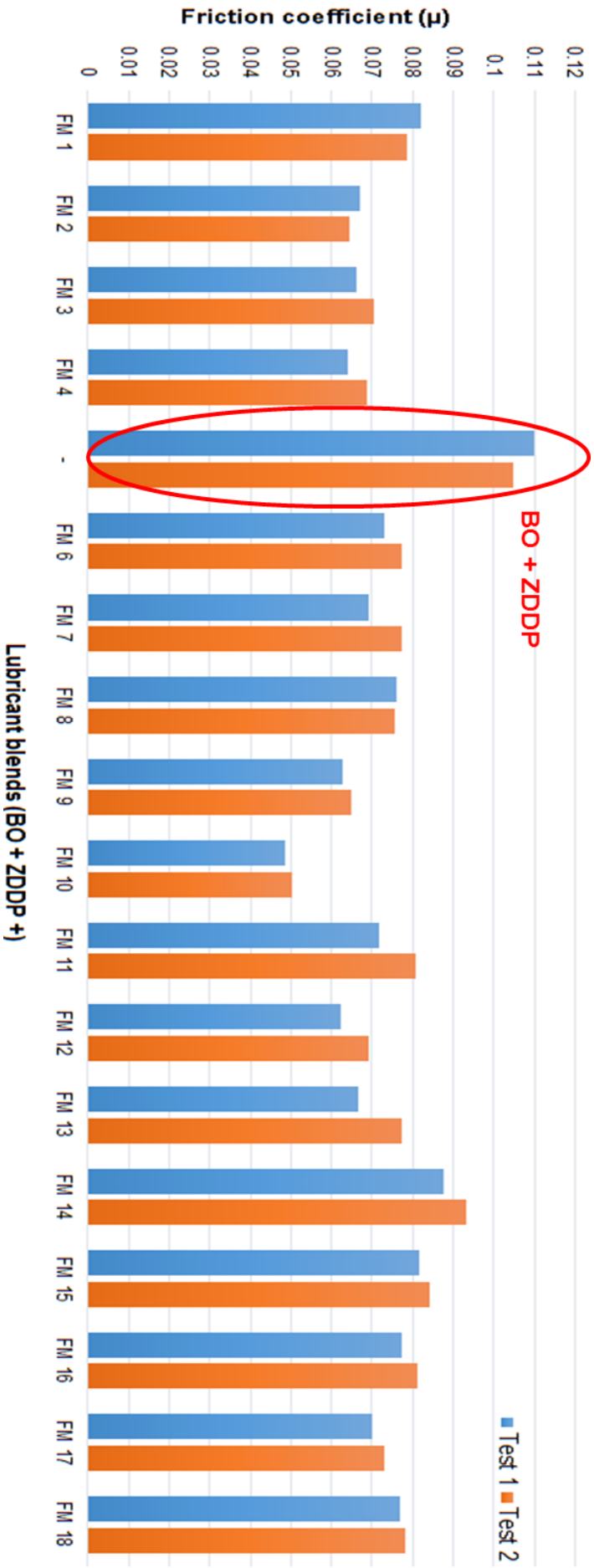

Figure 6-1. Friction behaviour of OFMs with ZDDP along with BO + ZDDP

Result revealed that BO + ZDDP showed the highest COF as expected because of uneven morphology of the tribofilm formed by ZDDP [15], [16], [22], [61], [155]. In general, all lubricant blends having OFMs performed well in reducing COF as compared to BO + ZDDP. The friction values of BO + ZDDP during the tests found around 0.11 with a standard deviation value of 0.003. Addition of FM 14 with ZDDP showed the least capability to reduce boundary friction hence showed the highest COF value. Addition of FM 10 with ZDDP remarkably reduced COF value. The friction value of FM 14 was observed to be 0.09 with a standard deviation value of 0.009, whereas average COF for the lubricant blend of FM 10 was obtained to be 0.05 with a standard deviation value of 0.001. Blend of FM 1, FM 15 and FM 16 with ZDDP showed second highest COF range. COF values of these blends were recorded 0.080, 0.083 and 0.079 with standard deviation values of 0.002, 0.002 and 0.003 respectively.

Lubricant blends of FM 6, FM 8, FM 11 and FM 18 with ZDDP showed very similar friction performance. COF values of these lubricant blends were obtained as 0.075, 0.076, 0.076 and 0.078 with standard deviation values of 0.003, 0.0004, 0.006 and 0.001 respectively. Lubricant blends of FM 7, FM 13 and FM 17 also showed similar friction behaviour. COF of these lubricant blends were found as 0.073, 0.072 and 0.072 with standard deviation values of 0.006, 0.008 and 0.002 respectively. Lubricant blends having FM 2, FM 3, FM 4, FM 9 and FM 12 with ZDDP showed effective friction performance. COF values for these lubricant blends were recorded as 0.066, 0.068, 0.066, 0.064 and 0.066 with standard deviation value of 0.002, 0.003, 0.003, 0.002 and 0.005 respectively. From friction results, it is obvious that blend of BO + ZDDP offered the highest boundary friction coefficient as expected. Addition of the OFM in the blend with ZDDP reduced COF values but the extent of that reduction is varied. Variation in the friction performance of different OFMs exposed the difference in interaction between respective OFM and ZDDP, which ultimately affects the effectiveness of that OFM.

6.2.2 Wear analysis

The balance of friction and wear is very important in all engine applications. Excessive wear in engine components results in material loss and can lead to a catastrophic failure [3][38]. Tribological testing of lubricant blends having

different OFMs and ZDDP produced some interesting wear results. The specific wear rate or wear factor calculation presented in this study is based on the WSD of the pin specimen. Wear factor has been calculated by using the Archard's wear formula. Detail about the specific wear rate is discussed in the Experimental Methods and Materials chapter (i.e. Chapter 5). Figure 6-2 shows wear behaviour of lubricant blends having OFM and ZDDP.

ZDDP is a universal AW additive and due to its remarkable performance almost all lubricant formulations have ZDDP [15], [52]. The wear results are more critical as compared to friction performance because of impact on AW performance of ZDDP. The wear result of BO + ZDDP is used as a reference for the wear analysis of the lubricant blends having OFM and ZDDP. The wear results revealed that a few OFMs worked antagonistically with ZDDP and as a result increased the wear factor value in comparison with BO + ZDDP but majority of OFMs work synergistically with ZDDP and further reduced wear factor value.

Table 6-1 shows the wear behaviour in descending order of wear factor value. Lubricant blends of FM 1 and FM 4 with ZDDP showed antagonism and as a result wear factor values increased significantly. Increase in the wear factor value indicated that addition of FM 1 and FM 4 in the lubricant blend restricted ZDDP to form AW film or the chemical composition of the tribofilm has been modified. Rest of all OFMs worked synergistically with ZDDP and decreased wear factor values significantly. Decrease in the wear factor values indicated a modification in composition of the tribofilm. Though majority of OFMs reduced the wear factor but blend of FM 8, FM 11 and FM 16 with ZDDP produced outstanding wear performance and among them FM 8 showed the best AW capability. Interaction of OFMs with ZDDP reduced COF values but this interaction mainly modified the AW performance of ZDDP.

In this situation in order to analyse the complete tribological behaviour of lubricant blends of OFMs and ZDDP, it is important to evaluate the friction and wear behaviour together.

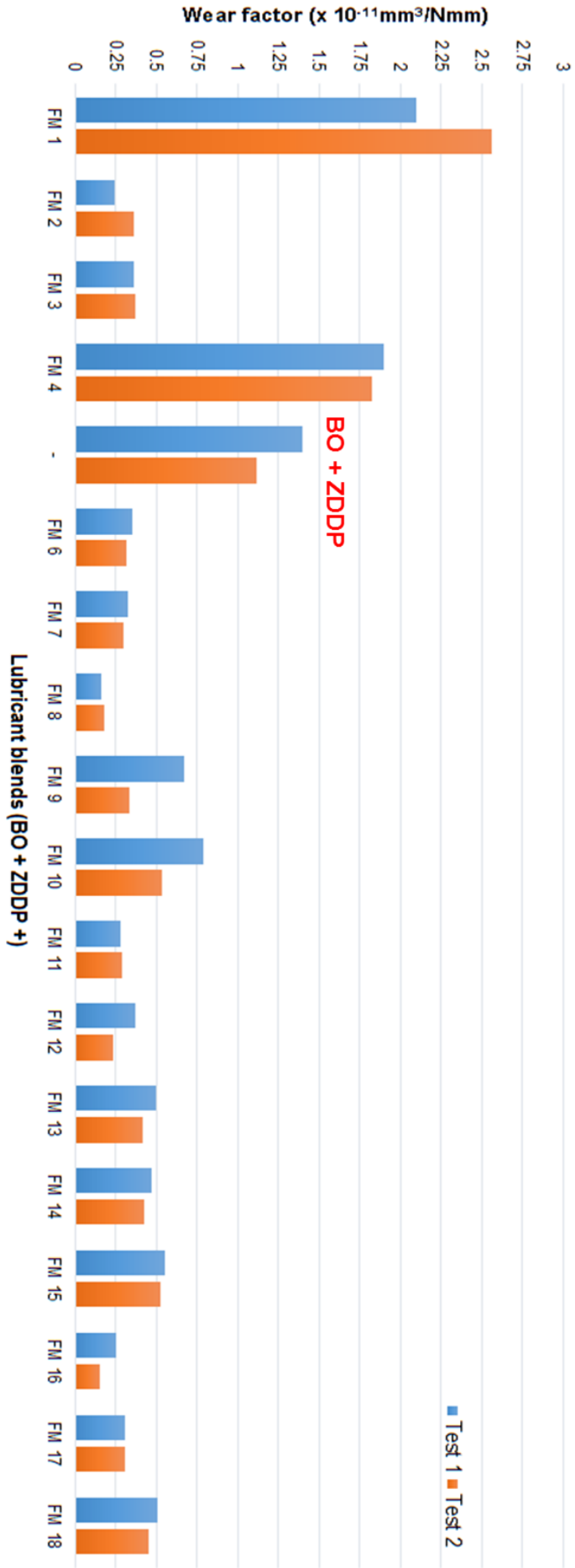

Figure 6-2. Wear behaviour of OFMs with ZDDP along with BO + ZDDP

Table 6-1. Wear factor of lubricant blends in descending order

Lubricant behaviour	Detail of lubricant blend	Wear factor value (x 10^{-11} mm^3/Nmm)
Antagonistic wear behaviour	BO + FM 1 + ZDDP	2.33
	BO + FM 4 + ZDDP	1.87
Reference lubricant blend	BO + ZDDP	1.26
Synergistic wear behaviour	BO + FM 10 + ZDDP	0.66
	BO + FM 15 + ZDDP	0.54
	BO + FM 9 + ZDDP	0.50
	BO + FM 18 + ZDDP	0.48
	BO + FM 13 + ZDDP	0.46
	BO + FM 14 + ZDDP	0.45
	BO + FM 3 + ZDDP	0.37
	BO + FM 6 + ZDDP	0.34
	BO + FM 7 + ZDDP	0.31
	BO + FM 17 + ZDDP	0.31
	BO + FM 2 + ZDDP	0.30
	BO + FM 12 + ZDDP	0.30
	BO + FM 11 + ZDDP	0.29
	BO + FM 16 + ZDDP	0.20
	BO + FM 8 + ZDDP	0.17

6.3 Friction and wear relationship

Combined friction and wear performance revealed that the highest COF was observed with the blend of BO + ZDDP. Addition of all OFMs with ZDDP reduced COF values but wear behaviour varied among these OFMs. Blend

of FM1 with ZDDP increased wear significantly but decreased COF value in comparison with BO + ZDDP. Similarly lubricant blend of FM 4 and FM 8 with ZDDP reduced high COF value of ZDDP but in wear performance FM 4 increased wear significantly and FM 8 reduced wear extraordinarily. The lowest COF value was observed with the lubricant blend of FM 10 and ZDDP and the highest COF value was recorded with the blend of FM14 and ZDDP but both OFMs worked synergistically with ZDDP and reduced the wear factor value.

In this developing scenario the friction and wear relationship is described by organising them in four groups and these are,

- High friction/Low wear
- High friction/High wear
- Low friction/Low wear
- Low friction/High wear

High friction/Low wear are assigned to lubricant blends having COF value between 0.071 and 0.14 and wear factor value between 0.0 and 1.26.

High friction/High wear are assigned to lubricant blends having COF value between 0.071 and 0.14 and wear factor value between 1.27 and 2.6.

Low friction/Low wear are assigned to lubricant blends having COF value between 0.0 and 0.70 and wear factor value between 0.0 and 1.26.

Low friction/High wear are assigned to lubricant blends having COF value between 0.0 and 0.70 and wear factor value between 1.27 and 2.6.

Figure 6-3 illustrates position of the lubricant blends in above-mentioned four groups as per respective friction and wear performance. The wear performance of BO + ZDDP is used as a centre point in assigning them High and Low wear groups. Maximum number of lubricant blends with different OFMs are grouped in the High friction/Low wear group. The blend of FM 14, which showed the highest friction, and the blend of FM 8, which produced the best AW capability, are also assigned to this group. The lubricant blend having FM 1, which increased the wear factor value significantly are placed in High friction/High wear group.

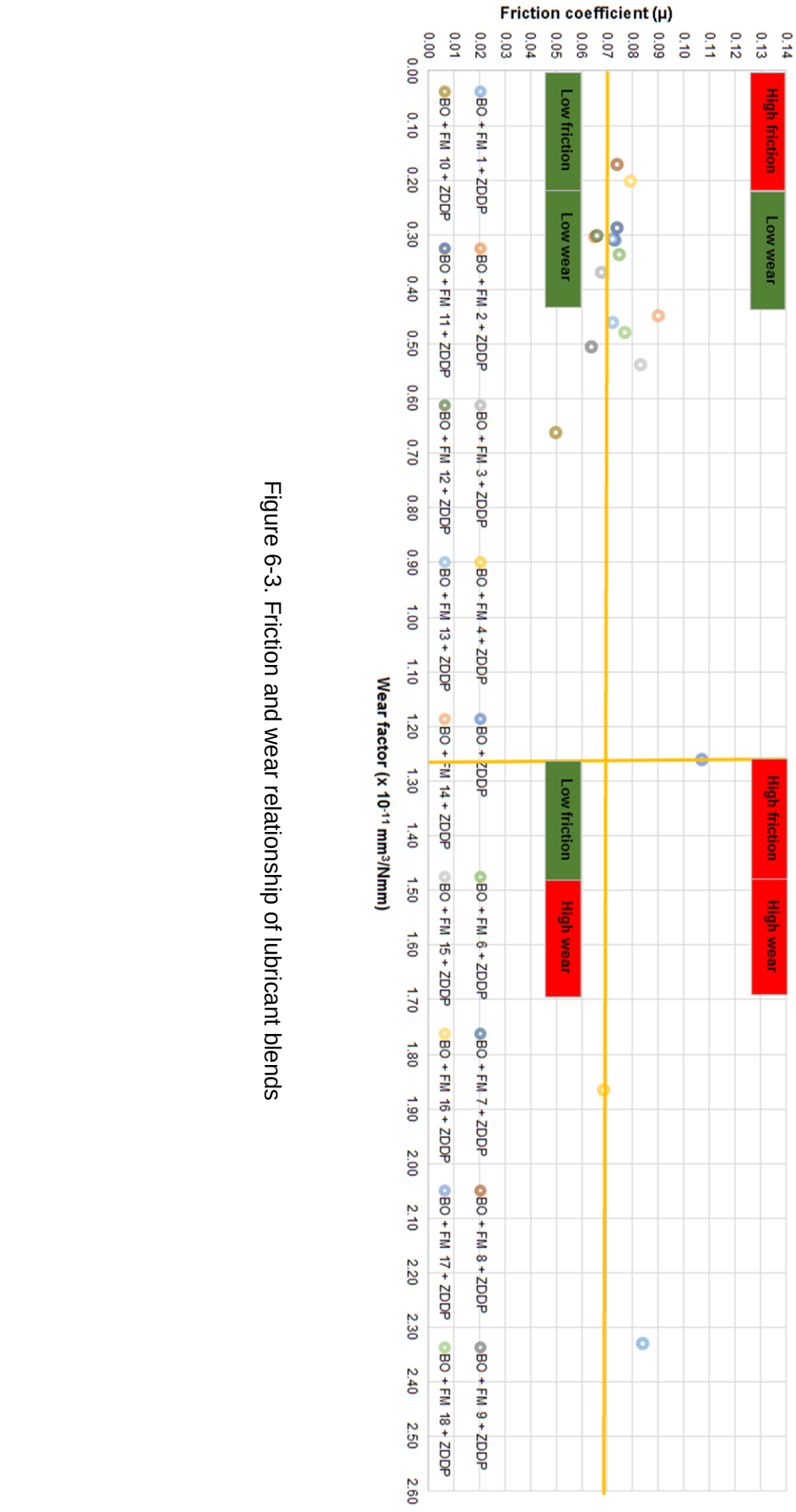

Figure 6-3. Friction and wear relationship of lubricant blends

The lubricant blend of FM 10, which showed the lowest COF value and remarkable AW capability, are placed in Low friction/Low wear group. The lubricant blend of FM 4, which showed antagonistic wear behaviour and significantly increased the wear factor value, is positioned in Low friction/High wear group.

Shortlisting of OFMs are based on friction and wear relationship. Because of this grouping, it was revealed that tribological performance of few OFMs are above or below the friction and wear benchmarks. Based on friction and wear performance five blend of OFMs were picked from these groups (1 top lubricant blend from each group i.e. FM 1, FM 4, FM 10 and FM 14) plus blend of FM 8 and ZDDP because it showed the best AW performance.

6.4 Concentration effect on friction and wear

Five OFMs were shortlisted and these were mainly fatty amines (FAs) with different structure and chain lengths whereas one friction modifier (i.e. FM 10) was fatty alcohol. These OFMs were blended with ZDDP in 0.5:1 and 1:1 molar ratio of FM to ZDDP. The detailed blending procedure is included in the Experimental Methods and Materials chapter (i.e. Chapter 5). The concentration of ZDDP was constant in all formulations (i.e. 0.55 wt. %). The BO used in lubricant blends was group III mineral oil having a kinematic viscosity value of 4.4 cSt at 100 °C.

The addition of the OFMs in the lubricant blend disturb the AW performance of ZDDP [30]. The increase in the concentration of the OFMs further worsen the wear performance of ZDDP [162][33]. Amines interact synergistically with ZDDP up to a specific concentration but above that concentration the synergism starts to convert into antagonism and consequently wear increases significantly [162]. The tribological results in section 6.2 revealed that the addition of the OFMs did not necessarily increase wear as few OFMs interacted synergistically with ZDDP and reduced wear. The friction and wear evaluation of the different lubricant blends with two different concentrations of the OFMs (i.e. 0.5:1 and 1:1 molar ratio of OFM to ZDDP), exposed the impact of the increase in the concentration of the OFMs on the tribological performance of ZDDP.

6.4.1 Friction analysis

Each test was two-hours long (continuous test) and was repeated three times to confirm the repeatability. The COF values were calculated from the average friction values of the last thirty minutes of each test. Figure 6-4 shows the combined friction behaviour of binary additive systems in which five OFMs were blended with ZDDP in 0.5:1 and 1:1 molar ratio of FM to ZDDP along with BO + ZDDP.

The friction results showed that BO + ZDDP had the highest COF (i.e. 0.11), as expected due to the uneven morphology of the phosphate tribofilm formed by ZDDP [15], [16], [22], [61], [155]. The friction results of the lubricant blend having 0.5:1 molar ratio of FM to ZDDP revealed that the blend of FM 14 with ZDDP showed the highest COF (i.e. 0.09), whereas the blend of FM 8 with ZDDP exhibited the lowest value of COF (i.e. 0.068). The blend of FM 4 showed the second highest COF (i.e. 0.081). The blends of FM 1 and FM 10 with ZDDP showed a similar COF (i.e. 0.072) but with a slightly different standard deviation value. The increase in the concentration of the OFM in the blend (i.e. 1:1 molar ratio of FM to ZDDP) slightly modified the COF values. The blend of FM 14 with ZDDP showed the highest COF value (i.e. 0.09) followed by the blend of FM 1 with ZDDP (i.e. 0.08). The blends of FM 4 and FM 8 produced very much similar COF values (i.e. 0.069 and 0.074). The blend of FM 10 with ZDDP showed the lowest COF (i.e. 0.05) among all the OFMs.

The friction results of the lubricant blends with both concentrations (i.e. 0.5:1 and 1:1 molar ratio of the FM to ZDDP), indicated one common trend, which is the reduction in the ZDDP boundary friction but the extent of this reduction, is varied. The increase in the concentration of the OFM in the blends with ZDDP did not necessarily reduce the COF value, as with few OFMs the COF values slightly increased. The lubricant blends having FM 4 and FM 10 further reduced the COF with the increase in the concentration of the OFM. On the other hand, the increase in concentration of FM 1 and FM 8 in the lubricant blend further increased the COF values. The lubricant blend having FM 14 showed a similar friction behaviour with both concentrations of FM.

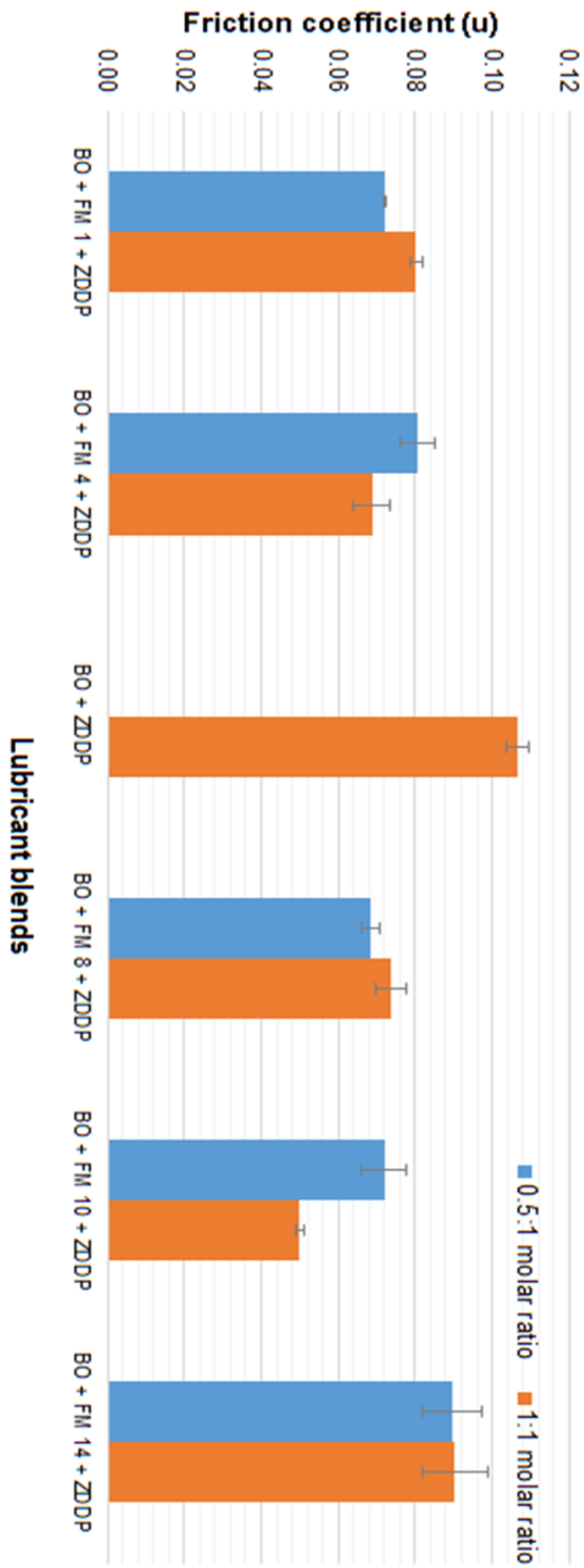

Figure 6-4. Combine friction behaviour of lubricant blends in 0.5:1 and 1:1 molar ratio of FM to ZDDP

6.4.2 Wear analysis

The addition of the OFM in the lubricant blend interferes with the ZDDP capability to form AW film [22], [61], [159]. The tribological testing of the lubricant blends having five different OFMs in two different concentrations with ZDDP produced some interesting wear results. Figure 6-5 shows the combined wear behaviour of the lubricant blends having five different OFMs blended with ZDDP in 0.5:1 and 1:1 molar ratio of FM to ZDDP. The wear result of BO + ZDDP is also added for reference purpose.

The wear results of the lubricant blends having 0.5:1 molar ratio of FM to ZDDP revealed that the lubricant blend having FM 1 with ZDDP significantly increased the wear factor value followed by the lubricant blend having FM 4. The blend of FM 8 and ZDDP showed the best AW performance by reducing the wear factor value followed by the blends of FM 10 and FM 14. The wear results indicated both synergistic and antagonistic wear trends. The wear factor value of BO + ZDDP was found 1.30. The lubricant blends of FM 1 and FM 4 showed antagonistic wear behaviour by increasing the wear factor value to 3.13 and 1.62, respectively. The lubricant blends having FM 8, FM 10 and FM 14 showed synergistic wear behaviour by reducing the wear factor value to 0.45, 0.60 and 0.65, respectively. The increase in concentration of the OFM in the blend (i.e. 1:1 molar ratio of FM to ZDDP), showed similar wear trends as observed previously with 0.5:1 molar ratio of FM to ZDDP. The lubricant blend having FM 1 and ZDDP produced the highest wear whereas the blend having FM 8 and ZDDP reduced wear significantly. The lubricant blend of FM 1 and FM 4 with ZDDP showed antagonism by increasing the wear factor value to 2.54 and 1.87, respectively. This behaviour of the OFMs indicated that the AW capability of ZDDP is disturbed and consequently wear increased. The blends FM 8, FM 10 and FM 14 with ZDDP showed synergistic wear behaviour. The wear factor value is reduced remarkably to 0.33, 0.57 and 0.44, respectively.

The friction and wear results revealed that increase in wear does not necessarily lead to an increase in the COF value or vice versa and it is very difficult to develop any dependency between friction and wear.

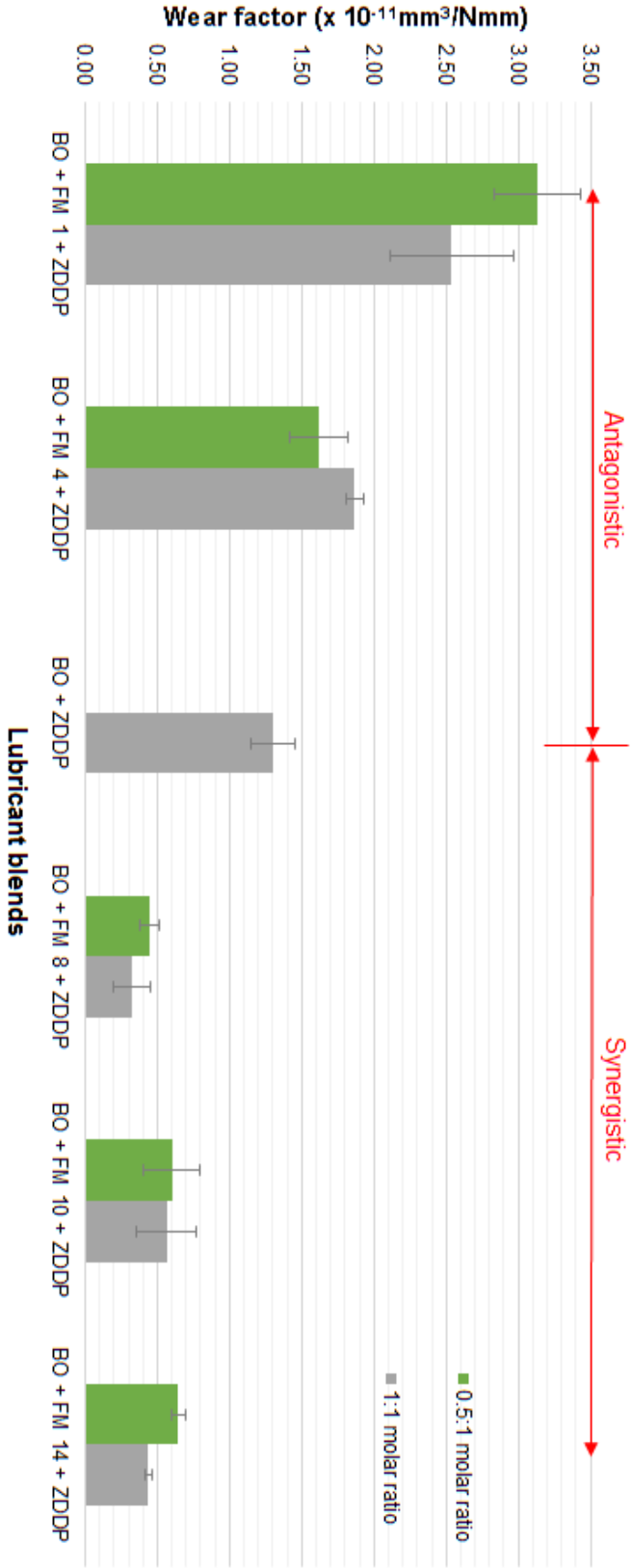

Figure 6-5. Combine wear behaviour of lubricant blends in 0.5:1 and 1:1 molar ratio of FM to ZDDP

The friction behaviour of the lubricant blends showed that the addition of the OFMs with ZDDP in both concentrations (i.e. 0.5:1 and 1:1 molar ratio FM to ZDDP) reduced the COF value. More or less all the OFMs had a positive effect on the friction performance. The wear result indicated some interesting wear trends. The addition of the OFMs with ZDDP in both concentrations (i.e. 0.5:1 and 1:1 molar ratio FM to ZDDP), showed two different wear behaviours. The addition of FM 1 and FM 4 with ZDDP significantly increased wear, whereas the addition of FM 8, FM 10 and FM 14 reduced wear remarkably. The wear results suggested that OFMs do not necessarily increase or decrease the AW performance when blended with ZDDP. The wear results also proposed that increase in the concentration do not necessarily improve the wear performance of lubricant blend having OFMs and ZDDP.

The concentration effect of each individual OFM (i.e. 0.5:1 and 1:1 molar ratio of FM to ZDDP) on the tribofilm morphology of ZDDP is included in the next chapter.

6.5 Summary

This chapter covered the tribological screening of seventeen OFMs with ZDDP. Based on friction and wear performance five OFMs are shortlisted for further study. This chapter also discussed the concentration effect of shortlisted OFMs on the tribological performance of ZDDP. OFMs were blended with ZDDP in 1:1 molar ratio of FM to ZDDP. Tribological testing was performed on TE 77 (high frequency friction machine), in which pin specimen reciprocated physically against a fixed plate specimen. The friction and wear result revealed that,

- The lubricant blend of BO + ZDDP offered the highest COF value
- Addition of OFMs in the blend with ZDDP reduced COF value
- Blend of FM 14 with ZDDP showed the highest COF value whereas blend of FM 10 showed the lowest COF value
- The interaction of OFMs with ZDDP reduced COF value but it predominantly disturbed AW performance of ZDDP
- The blend of FM 1 and FM 4 with ZDDP showed antagonism and as a result increased wear factor value significantly whereas blend of FM 8 showed the best AW capability
- The lubricant blends are assigned to four friction and wear groups as per friction and wear performance
- On the basis of friction and wear performance five blend of OFMs were picked from these groups (i.e. 1 top lubricant blend from each group plus blend of FM 8 and ZDDP because it showed the best AW performance)
- The friction result of lubricant blends in both concentrations (i.e. 0.5:1 and 1:1 molar ratio of FM to ZDDP), indicated one common trend which was reduction in ZDDP boundary friction, however extent of reduction is varied
- Increase in concentration of OFM in the lubricant blend with ZDDP not necessarily reduced COF value
- The blend of FM 14 in both concentrations showed the highest COF value

- The wear results of lubricant blends having both concentrations of OFM (i.e. 0.5:1 and 1:1 molar ratio of OFM to ZDDP) indicated some interesting wear trends
- The blend of FM 1 and FM 4 in both concentrations with ZDDP increased wear factor value significantly
- The blend of FM 8, FM 10 and FM 14 in both concentrations worked synergistically with ZDDP
- The wear result revealed that FAs not necessarily increased or reduced wear when blended with ZDDP
- The wear result suggested that increase in concentration of OFM in the lubricant blend not necessarily improved the wear performance
- The friction and wear relationship revealed that increase in wear not necessarily lead to increase in COF value or vice versa and it is difficult to develop any dependency between friction and wear

Chapter 7
OFMs interaction with ZDDP; effect on concentration on tribofilm morphology

7.1 Introduction

ZDDP forms a thick, unevenly distributed and primarily solid-like reaction films on interacting steel surfaces [15], [25], [28], [29], [63], [65]. These glassy phosphate pads are liable to limit the asperity-to-asperity contact and also bear the load between the interacting asperities [25], [27], [99]. The addition of OFMs in the lubricant oil disturb the anti-wear (AW) film formation capability of ZDDP [22], [61], [116], [163]. The increase in the concentration of the OFM further deteriorates the wear performance of ZDDP [33], [116]. The combined friction and wear results in Chapter 6 indicated that the addition of the OFMs with ZDDP predominantly affected the AW performance of ZDDP and as a result the wear behaviour of some lubricant blends shifted from significant reduction in wear to massive increase in wear. In this situation, it is important to analyse the impact of change in concentration of OFM on the tribofilm morphology of ZDDP. This chapter primarily focus on the concentration effect of the shortlisted OFMs on the tribofilm topography of ZDDP.

7.2 Tribofilm morphology

Figure 7-1 shows the wear track appearing on plate specimen as a result of the tribological interaction between pin and plate. The tribofilm is formed under reciprocating pure sliding conditions. Two positions on the plate specimen are selected for morphological analysis (i.e. middle and start/end of the wear track). These two positions are selected to analyse the impact of change in concentration of OFMs along with the effect of speed on the tribofilm morphology of ZDDP. The AFM is used to analyse the microscopic features of the tribofilm topography formed by the different lubricant blends on the plate specimen. An area of 30 µm x 30 µm across the middle and start/end of the wear track are scanned in the peak force-tapping mode. Surface parameters (i.e. root mean square surface roughness (R_q) and the largest of the individual peak to valley height (R_{max})), of each tribofilm topography are also measured.

Details about the experimental setup of the AFM analysis is included in Experimental Methods and Materials chapter (Chapter 5).

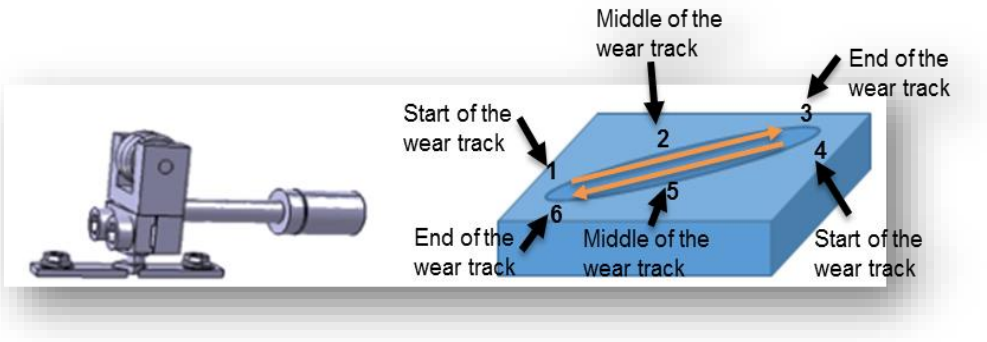

Figure 7-1. Schematic of pin, plate interface and wear track positions [188]

7.3 ZDDP tribofilm morphology

The AW tribofilm formed by ZDDP is heterogeneous in terms of topography due to its ridge and valley regions [15], [26], [27], [98]. This pad-like structure of ZDDP has been widely reported in literature [15], [26], [27]. Studies [15], [18], [28], [29], [58], [70], [72]–[74], [90] proposed that the ZDDP tribofilm mainly comprised of a bi-layer phosphate structure. The bulk of the film which is near the substrate is composed of short chain- length phosphates while the top layer of the tribofilm primarily consists of longer chain-length phosphate species. Figure 7-2 shows a high resolution (HR) AFM topographical image of the tribofilm formed by ZDDP at the middle of the wear track. The bright contrast in the image represents regions of high topography while the dark contrast represents areas of lower topography. During the tribological experiment, the sliding direction of the pin specimen over the plate is from the top to bottom of the image. The topographical image of the tribofilm formed by ZDDP is not homogenous and consists of two distinct regions, (i.e. ridges, the elevated parts and valleys, the shallow parts) [15], [26], [27], [98]. The elevated regions are islands of tribofilm commonly known as AW pads [25][20]. The primary function of these pads is to bear load and limit the contact between interacting surfaces [26], [62]. The regions between adjacent pads are known as valleys. The valleys are the areas of low topography

having minimum or no AW films and usually accumulated the wear debris [26], [62].

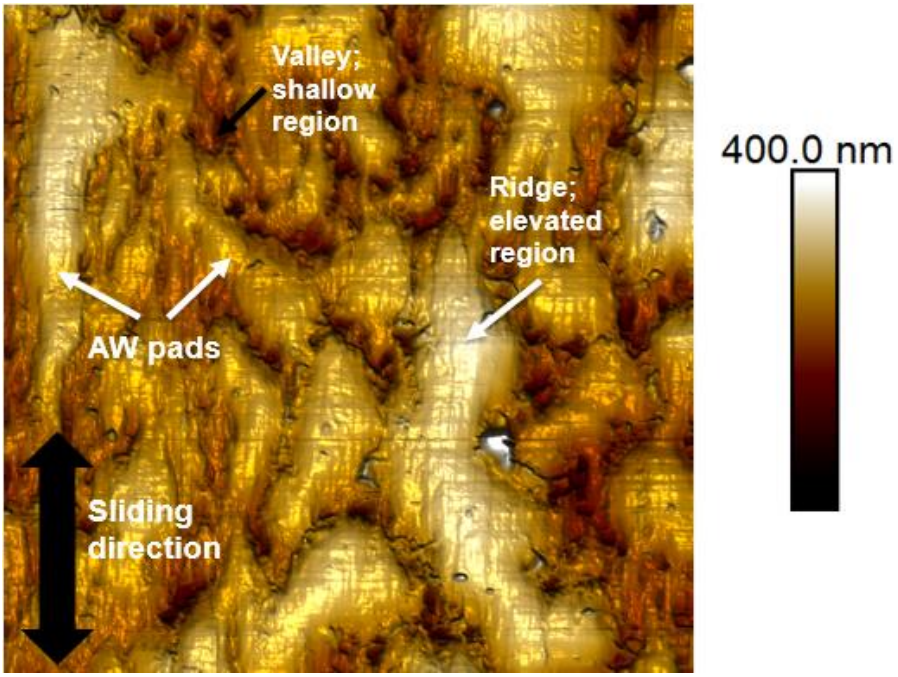

Figure 7-2. Tribofilm topography of BO + ZDDP (image size 30 x 30 μm^2)

The topographical image in Figure 7-3 shows that the tribofilm formed by ZDDP mainly comprised of well-defined large and a few small phosphate pads. These large phosphate pads are elongated in the sliding direction and have an exceptionally smooth surface. The topographical images show that the smaller pads are comparatively less elongated in the sliding direction with average pad size of around 2 µm to 5 µm. The elongated large pads are elevated, smooth, composed of longer chain phosphates and support a noteworthy amount of load whereas the smaller pads are unable to support a significant amount of load [25]–[27], [99]. These phosphate pads are mainly formed on asperities and are liable to limit the asperity-to-asperity contact where interacting surfaces rubbed with each other [25], [27], [99], whereas the valley regions contains adsorbed or partially decomposed ZDDP by products [26], [62], [99].

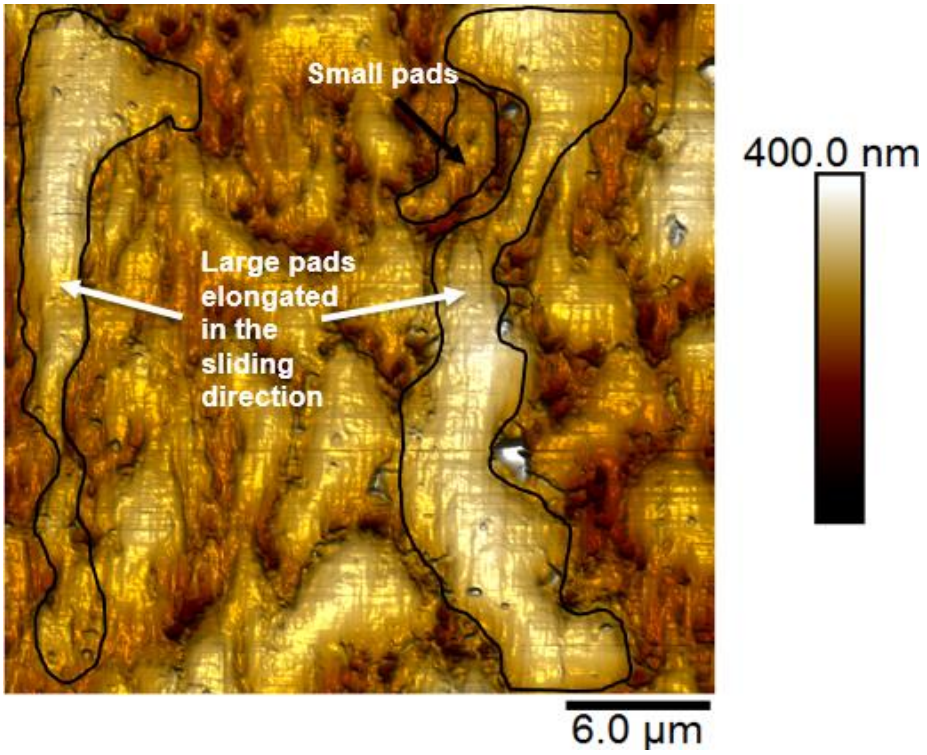

Figure 7-3. Large and small pads in ZDDP tribofilm topography

Figure 7-4 shows a comparison between the tribofilm morphology formed by the lubricant blend of BO + ZDDP at the middle and start/end of the wear track.

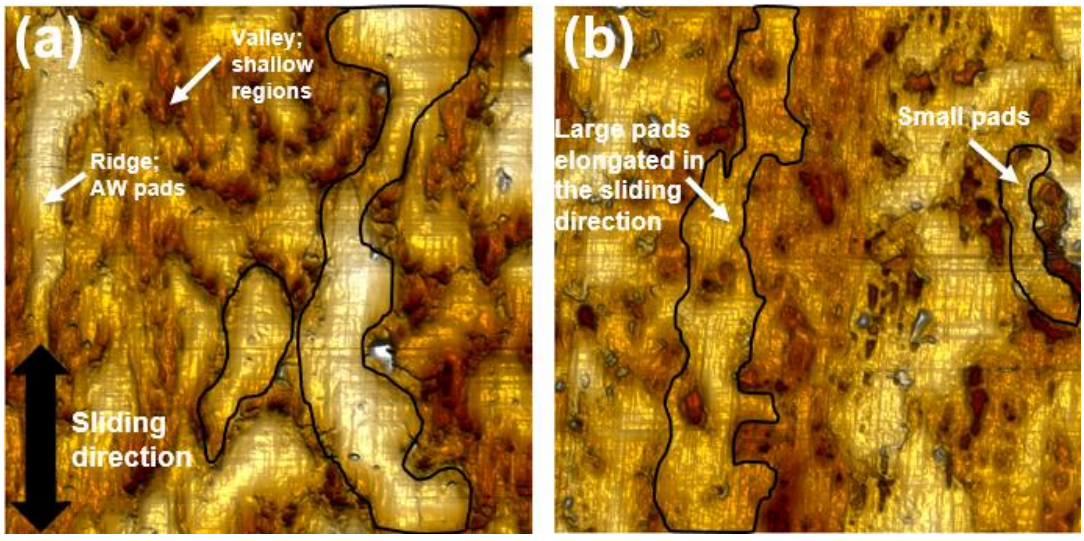

Figure 7-4. Tribofilm topography of BO + ZDDP at two different locations
(a) Middle of the wear track (b) Start/end of the wear track

The AFM image in Figure 7-4 (a) shows that the tribofilm formed at middle of the wear track composed of large phosphate AW pads along with few small phosphate pads. The large pads are elongated in the sliding direction with a length from a few micrometres to about 25 µm and these pads are appeared to be higher than than the surrounding features. The small pads are less elongated in the sliding direction and comparatively not as high as the large pads. Figure 7-4 (b) shows the topographical image of the tribofilm formed at start/end of the wear track. The AFM scan showed a very similar topographical configuration as observed in the image captured from the middle of the wear track. The tribofilm is mainly composed of large and small AW pads. The large pads are elongated in the sliding direction whereas the small pads are not elongated like the large pads.

The AFM line profile analysis in Figure 7-5 and Figure 7-6 show that the tribofilm at the middle of the wear track has a higher average R_q value, (i.e. 30 nm), in-comparison to the start/end of the wear track (i.e. 20 nm). The results also showed higher average R_{max} value at the middle of the wear track (i.e. 173 nm) in-comparison to the start/end of the wear track (i.e. 127 nm). The AFM images showed that topography of the tribofilms are not significantly modified between the middle and start/end of the wear track. Both images showed the formation of large AW pads elongated in the sliding direction along with the formation of small pads though these are fewer in number. Table 7.1 and 7.2 show the average R_q and R_{max} values at the middle and start/end of the wear track.

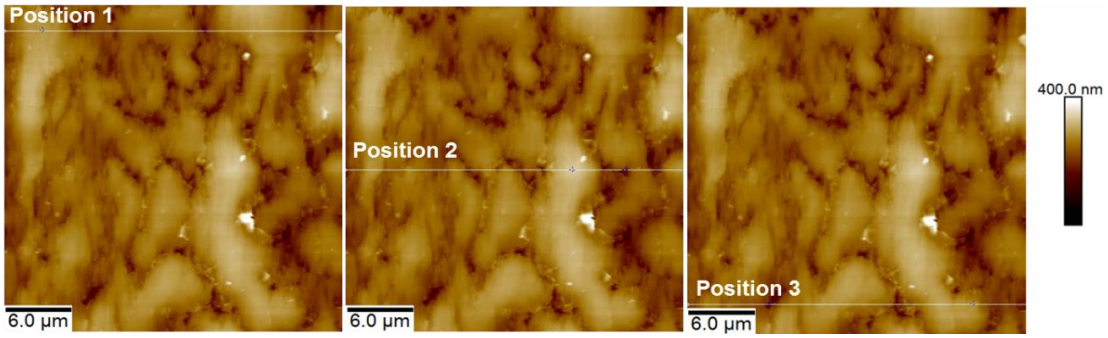

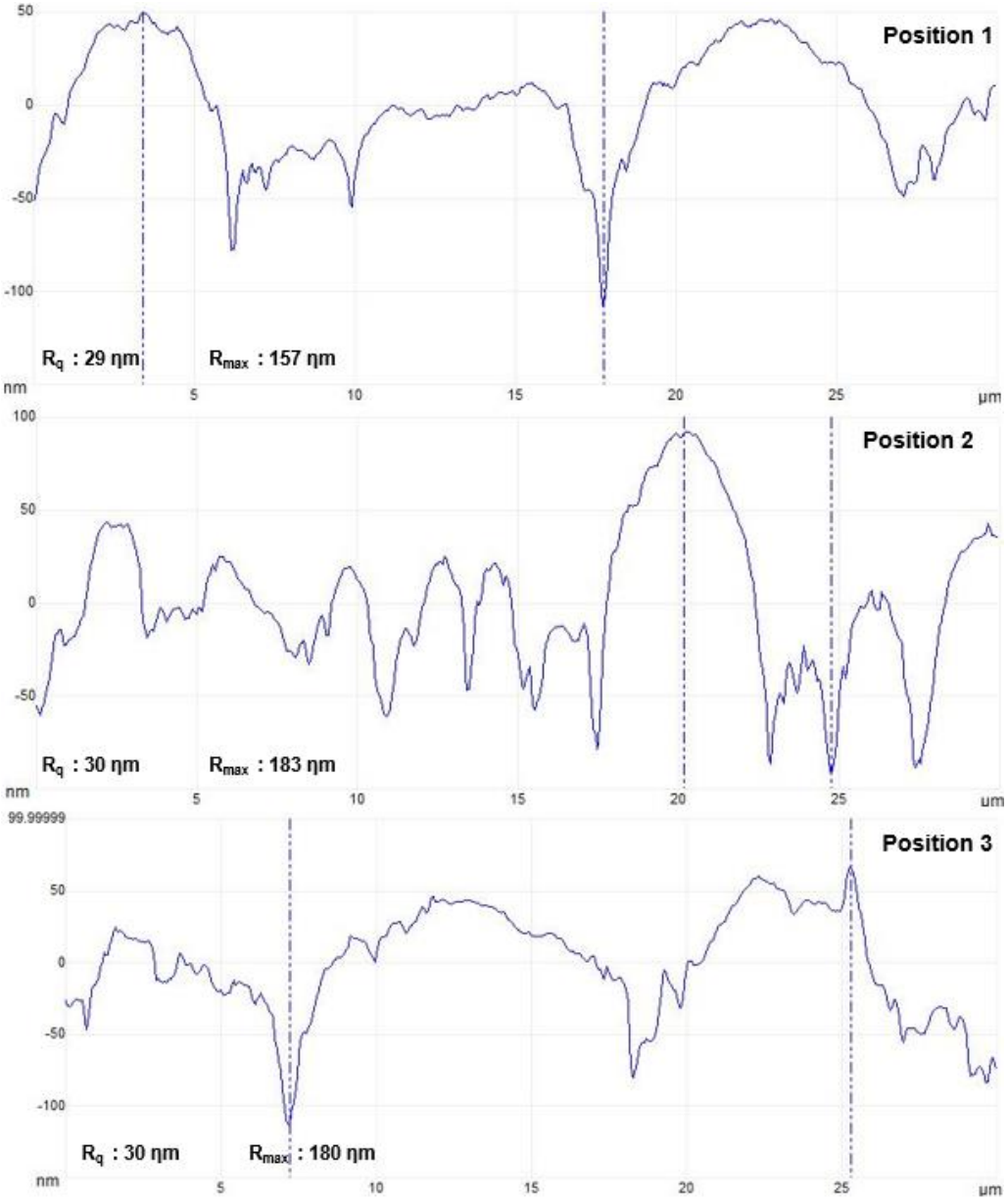

Figure 7-5. Line profile analysis at the middle of the wear track

Table 7-1. Surface roughness analysis at the middle of the wear track

Roughness parameters	Position 1	Position 2	Position 3	Average	Std. deviation
R_q (nm)	29	30	30	30	0.6
R_{max} (nm)	157	183	180	173	14.2

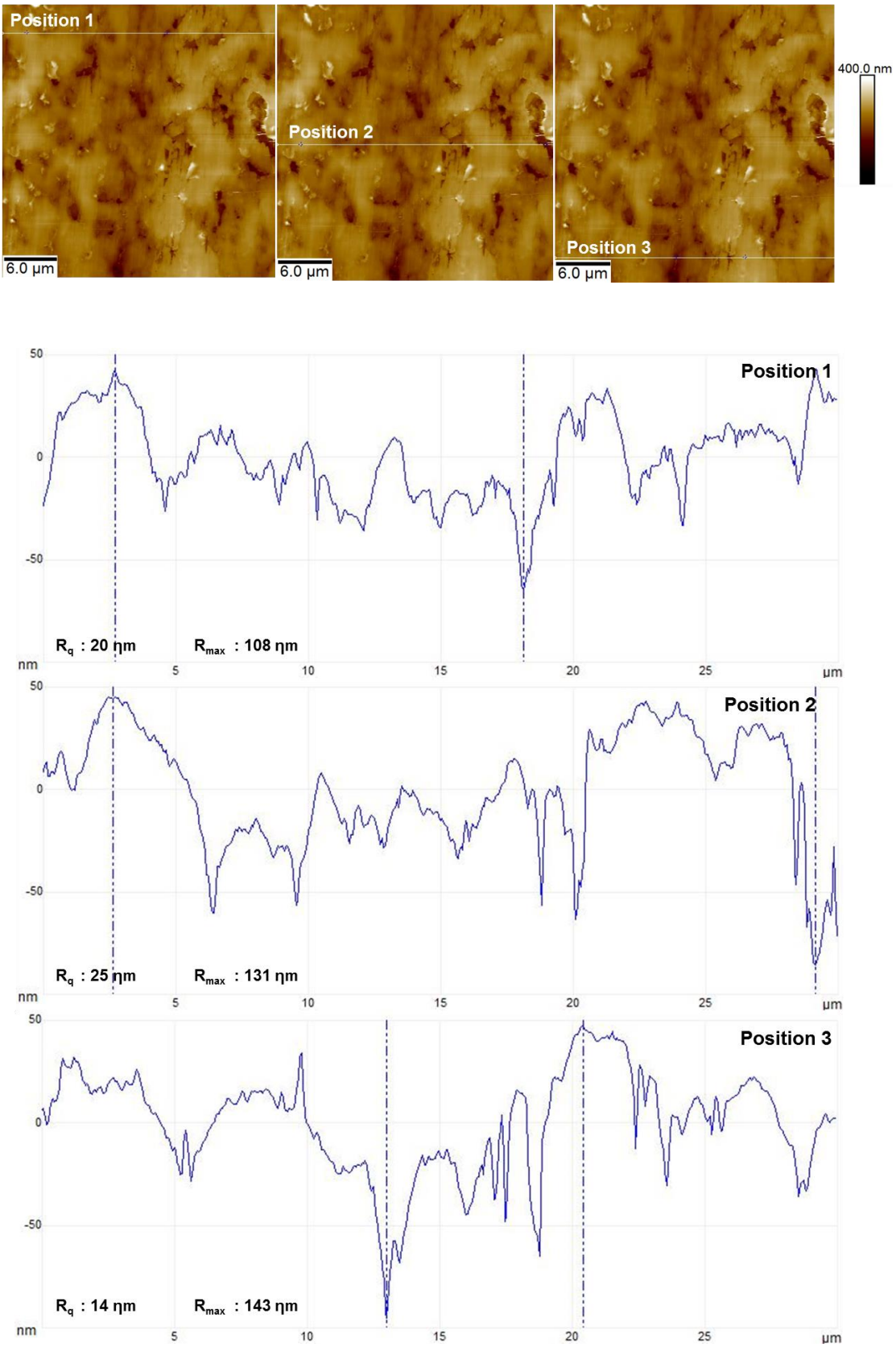

Figure 7-6. Line profile analysis at the start/end of the wear track

Table 7-2. Surface roughness analysis at the start/end of the wear track

Roughness parameters	Position 1	Position 2	Position 3	Average	Std. deviation
R_q (nm)	20	25	14	20	5.5
R_{max} (nm)	108	131	143	127	17.8

The tribofilm at middle of the wear track is comparatively more evolved (i.e. having more prominent phosphate pads). These AW pads are consistently to be higher than the surrounding in-comparison to the pads at start/end of the wear track. The qualitative analysis showed that both tribofilm topographies are more or less similar but from the quantitative results it seems that the tribofilm at middle of the wear track are more established with higher R_{max} and R_q values.

7.4 Morphology of the tribofilm formed by the addition of OFM with ZDDP

The AFM images revealed that the tribofilms formed at the middle of the wear track are comparatively more evolved in terms of tribofilm features (i.e. ridges and valley regions). The qualitative and quantitative analysis of the image showed that the tribofilm topography (i.e. ridges and valleys) and roughness parameters are also more established at the middle position of the wear track. In this situation, it is interesting to analyse the effect of the addition of OFMs with ZDDP on the tribofilm morphology at middle of the wear track.

7.4.1 Concentration effect of FM 1 on tribofilm morphology

The wear results (Chapter 6) showed that the AW performance of ZDDP is massively shifted with the addition of OFMs in two different concentrations. Few OFMs when added with ZDDP improved the AW performance of ZDDP while some other OFMs reduced the AW capability of ZDDP.

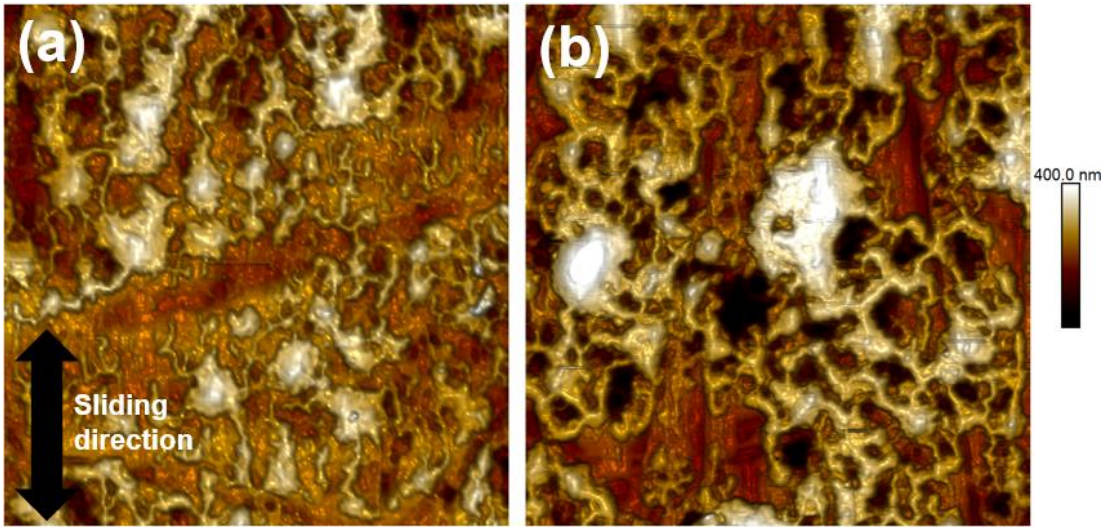

Figure 7-7. Tribofilm topographies of BO + FM 1 + ZDDP
(a) 0.5:1 molar ratio of FM to ZDDP (b) 1:1 molar ratio of FM to ZDDP

Figure 7-7 compares the tribofilm topographies formed by the addition of FM 1 (i.e. coco amine) in two different concentrations (i.e. 0.5:1 and 1:1 molar ratio of FM to ZDDP). The area of each captured image was 30 µm x 30 µm. The AFM images showed that addition of FM 1 in the blend massively modified the tribofilm topographies of ZDDP (Figure 7-3). Both topographies (i.e. 7-7(a) and 7-7(b)) found very much similar to each other which indicated a minimal impact of the change in the concentration of FM 1 on the tribofilm topography of ZDDP. The large elongated AW pads completely disappeared from the film topography and only smaller pads are observed. These smaller phosphate pads scattered around the image and appeared to be higher than the surrounding features. These smaller pads are slightly elongated in the sliding direction. The conversion of the large phosphate pads into smaller pads exhibited a significant shift in the tribofilm topography.

Figure 7-8 and 7-9 show the line profile analysis of the tribofilm formed with the addition of FM 1 with ZDDP. The tribofilm roughness (R_q) value increased with the addition of FM 1 in the blend in comparison to the roughness value of the tribofilm formed by BO + ZDDP. R_q value is increased from 30 nm (BO + ZDDP) to 33 nm and 38 nm with the addition of FM 1 in two different concentrations (i.e. 0.5:1 and 1:1 molar ratio of FM to ZDDP). The addition of coco amine in the blend with ZDDP nominally changed the maximum peak to valley height (R_{max}) values of the tribofilm.

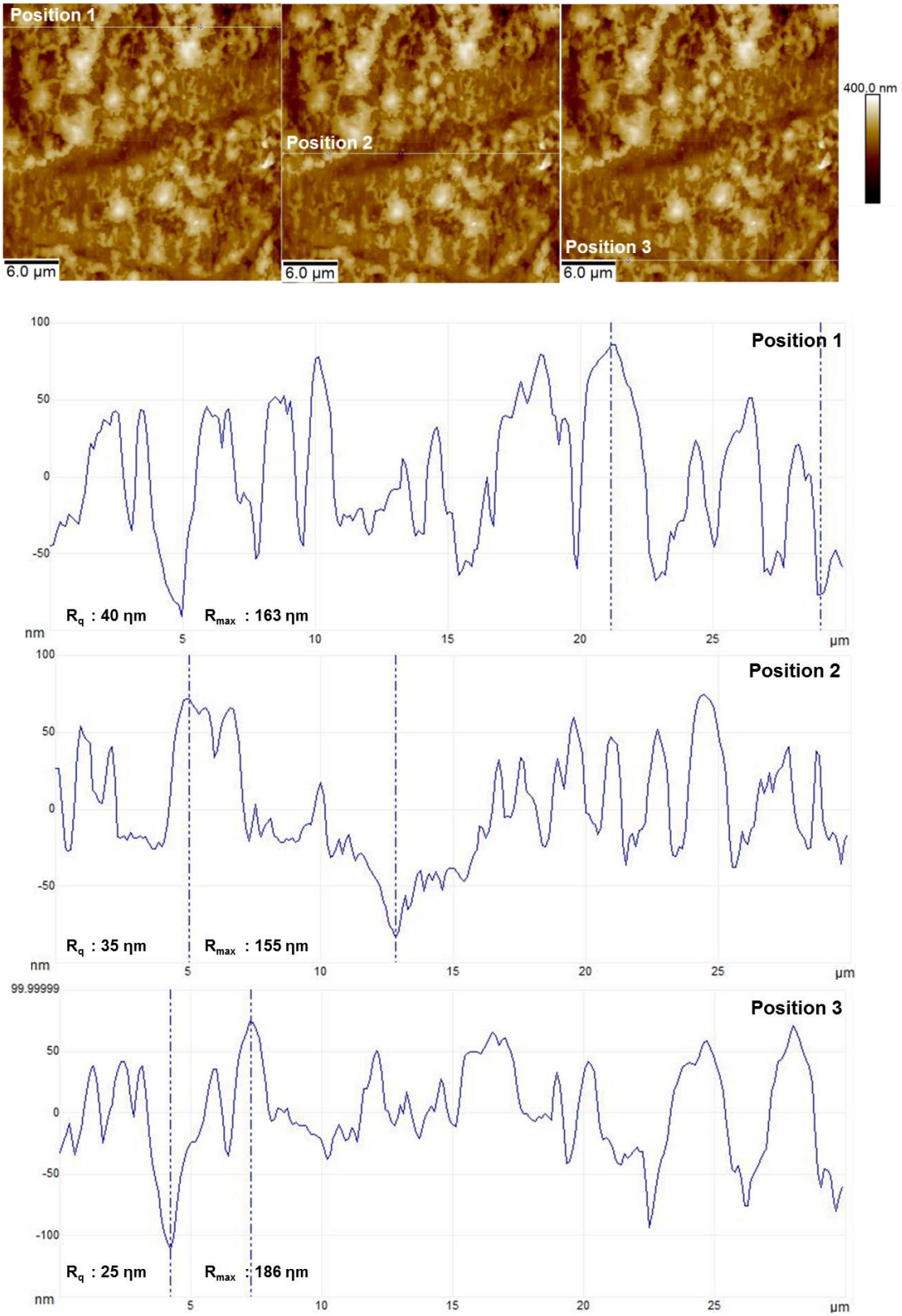

Figure 7-8. Line profile analysis of the tribofilm formed by BO + FM 1 + ZDDP having 0.5:1 molar ratio of FM to ZDDP

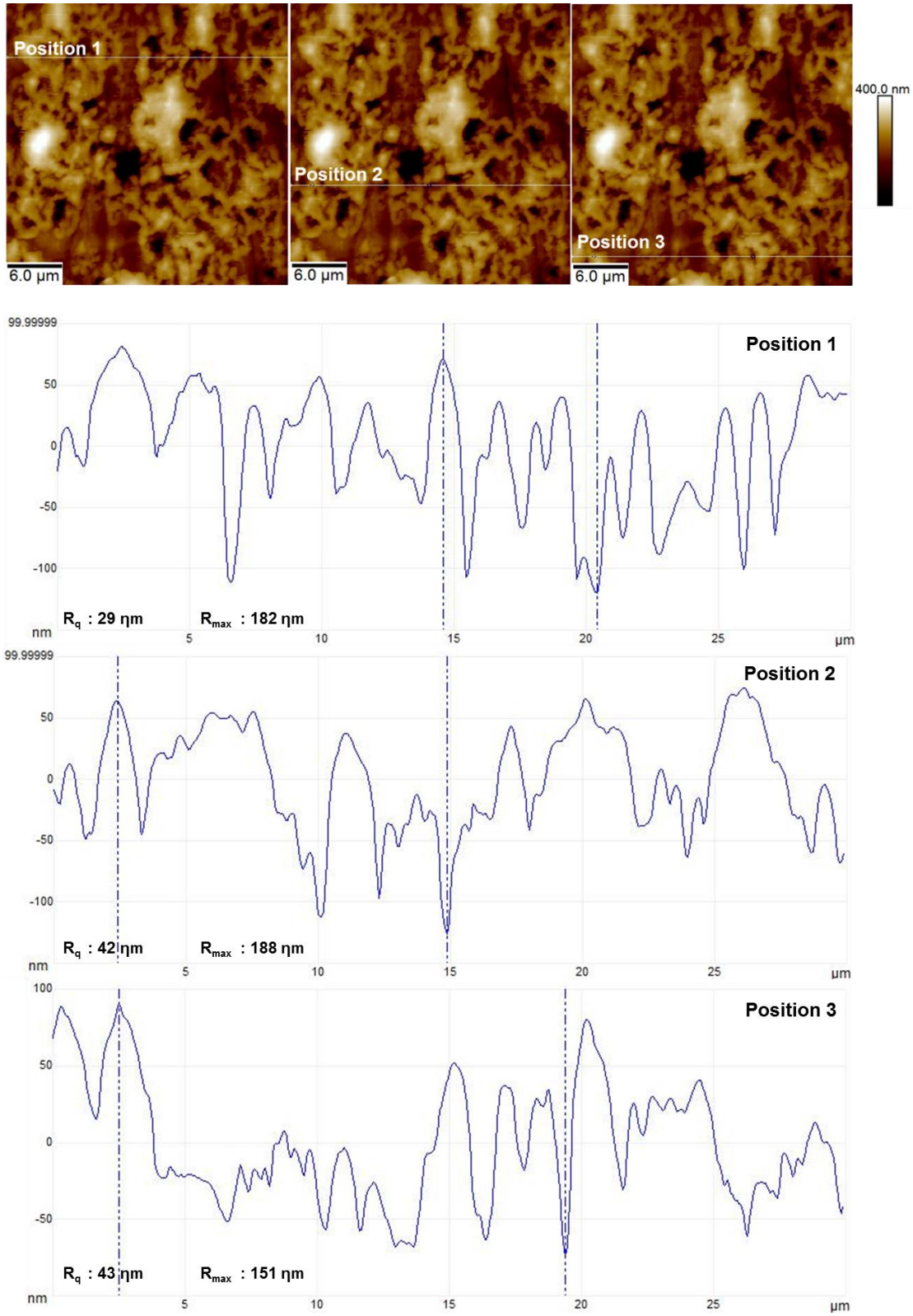

Figure 7-9. Line profile analysis of the tribofilm formed by BO + FM 1 + ZDDP having 1:1 molar ratio of FM to ZDDP

The complete comparison of average R_q and R_{max} values of BO + ZDDP along with the addition of coco amine in the blend is specified in Table 7-3. The AFM

measurement showed that addition of coco amine with ZDDP modified the tribofilm topography along with tribofilm roughness, which ultimately affected the tribological performance of ZDDP.

Table 7-3. Surface roughness analysis of the tribofilm with the addition of FM 1

Lubricant blend	R_q (nm)	Std. deviation	R_{max} (nm)	Std. deviation
BO + ZDDP	30	0.6	173	14.2
BO + FM 1 + ZDDP (0.5:1)	33	7.6	168	16.1
BO + FM 1 + ZDDP (1:1)	38	7.8	174	20

7.4.2 Concentration effect of FM 4 on tribofilm morphology

The AFM scans in Figure 7-10 shows that addition of FM 4 (i.e. ethoxylated hydrogenated tallow amine) in the blend massively modified the tribofilm topography of ZDDP. Figure 7-10 (a) and 7-10 (b) compare the tribofilm topographies formed by the addition of FM 4 in two different concentrations (i.e. 0.5:1 and 1:1 molar ratio of OFM to ZDDP). The AFM images showed that the addition of FM 4 in the blend with ZDDP significantly modified the tribofilm topography but at the same time both AFM images showed very similar tribofilm topographies which indicated a negligible impact of change in concentration of FM 4 on the tribofilm topography. The large elongated AW phosphate pads (as observed in the tribofilm formed by BO + ZDDP) completely transformed into smaller pads with the addition of FM 4 in the blend. These AW pads appeared to be higher than the surrounding features but in general the pad size is considerably reduced. The increase in concentration of FM 4 in the blend with ZDDP further squeezed the phosphate pads. The reduction in overall pad dimensions with increase in the concentration of FM 4 indicated availability of excess concentration of FM 4 in the blend which significantly affected the AW tribofilm formation capability of ZDDP.

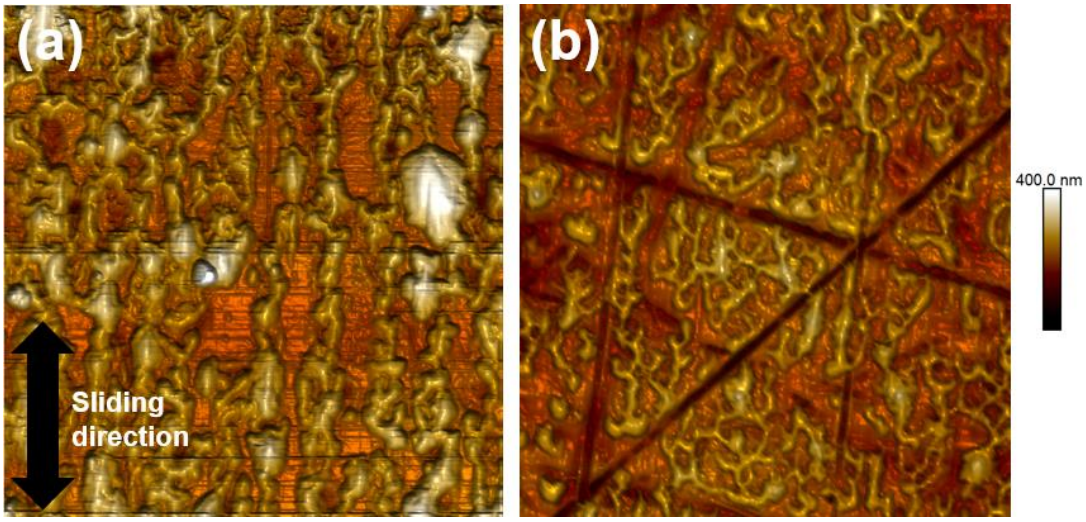

Figure 7-10. Tribofilm topographies of BO + FM 4 + ZDDP

(a) 0.5:1 molar ratio of FM to ZDDP (b) 1:1 molar ratio of FM to ZDDP

Figures 7-11 and 7.12 show the line profile analysis of the tribofilm formed with the addition of FM 4 with ZDDP. The tribofilm roughness (R_q) value did not change remarkably with the addition of FM 4 in the blend in-comparison to the tribofilm formed by BO + ZDDP. The result showed that the average Rq value persisted around 25 nm with the addition of FM 4 in both concentrations. Significant reduction in the R_{max} value is recorded with the addition of FM 4 in the blend with ZDDP. Little effect on R_{max} value is observed with increase in concentration of FM 4 in the lubricant blend.

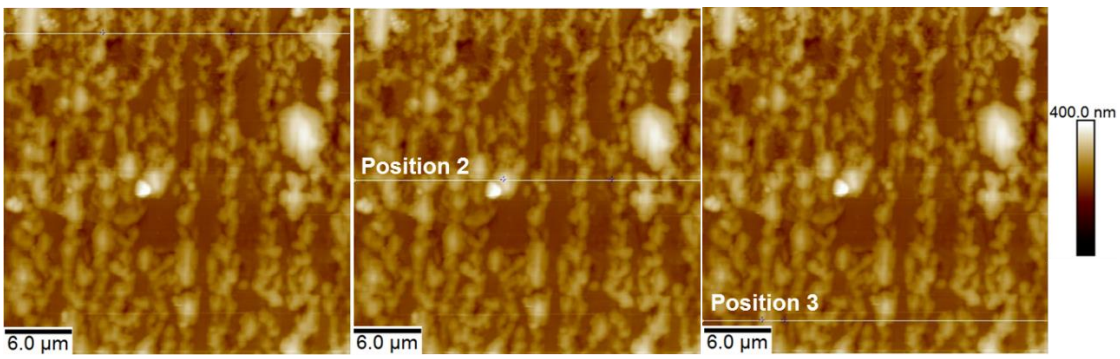

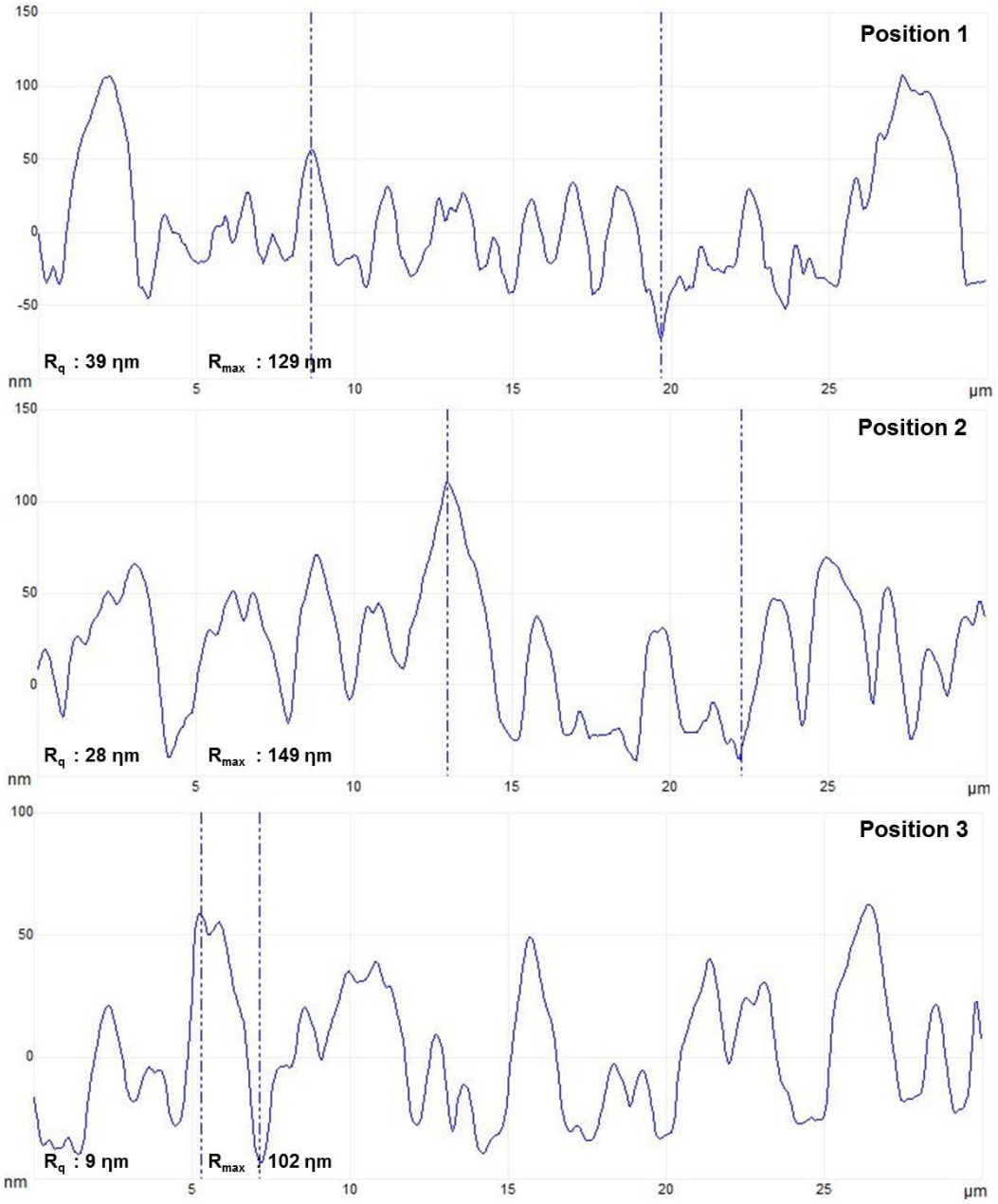

Figure 7-11. Line profile analysis of the tribofilm formed by BO + FM 4 + ZDDP having 0.5:1 molar ratio of FM to ZDDP

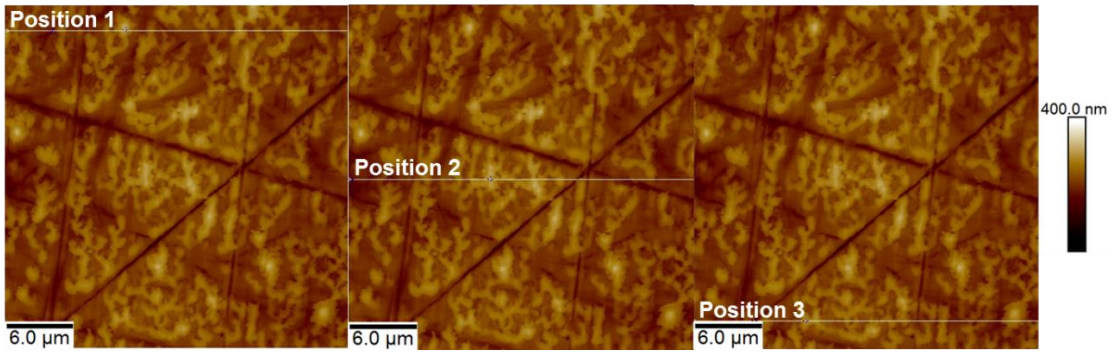

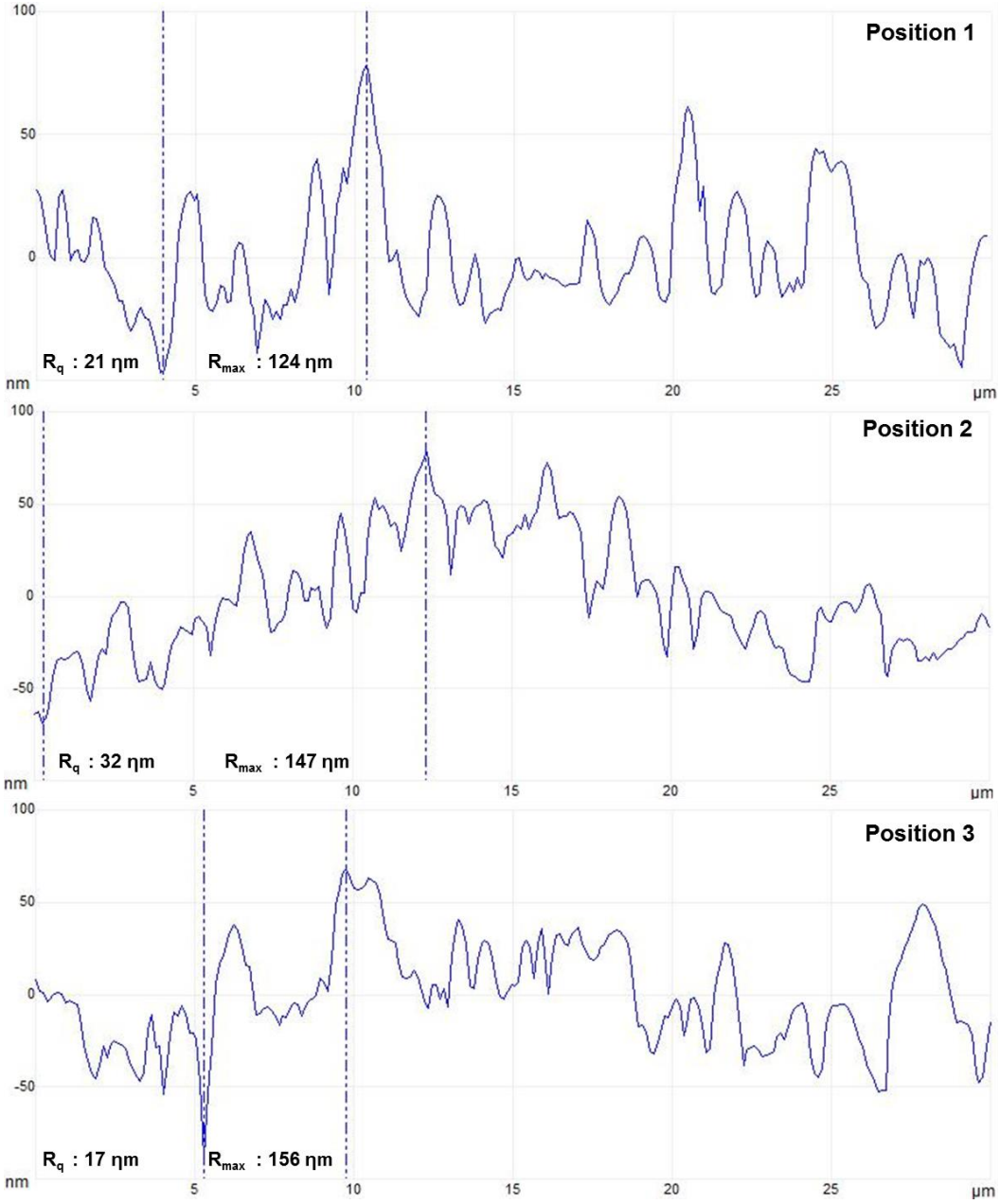

Figure 7-12. Line profile analysis of the tribofilm formed by BO + FM 4 + ZDDP having 1:1 molar ratio of FM to ZDDP

The complete comparison of R_q and R_{max} values of the lubricant blends are specified in Table 7-4. The AFM analysis revealed that the addition of FM 4 in the blend with ZDDP massively modified the tribofilm topography and as a result large elongated phosphate pads are completely transformed into much smaller pads. The minimal effect on the film roughness value is recorded with the addition of FM 4 in the blend with ZDDP. However, the R_{max} value is significantly reduced, which could be due to reduction in the film thickness.

Table 7-4. Surface roughness analysis of the tribofilm with the addition of FM 4

Lubricant blend	R_q (nm)	Std. deviation	R_{max} (nm)	Std. deviation
BO + ZDDP	30	0.6	173	14.2
BO + FM 4 + ZDDP (0.5:1)	25	15	127	24
BO + FM 4 + ZDDP (1:1)	23	7.8	142	17

7.4.3 Concentration effect of FM 8 on tribofilm morphology

Figure 7-13 compares the tribofilm topographies formed by the addition of FM 8 (i.e. tallow amine), at two different concentrations (i.e. 0.5:1 and 1:1 molar ratio of FM to ZDDP). The AFM images showed that the addition of FM 8 in the blend with ZDDP modified the tribofilm morphology.

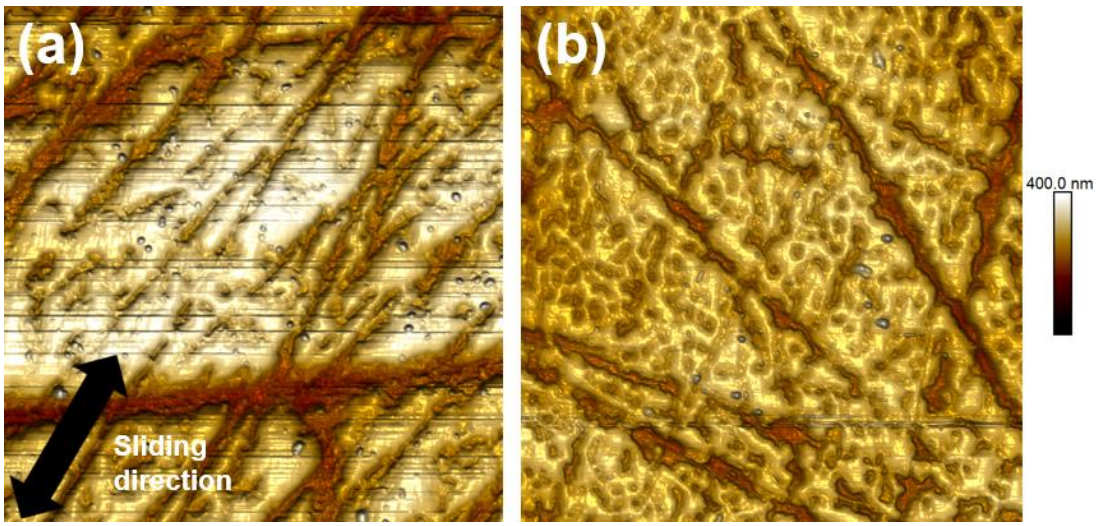

Figure 7-13. Tribofilm topographies of BO + FM 8 + ZDDP

(b) 0.5:1 molar ratio of FM to ZDDP (b) 1:1 molar ratio of FM to ZDDP

The AFM scan in Figure 7-13 (a) shows that addition of FM 8 slightly modified the tribofilm topography of BO + ZDDP. The large phosphate pads squeezed but still elongated in the sliding direction. The phosphate pads appeared to be higher than the surrounding features but not as high as observed in the tribofilm topography of BO + ZDDP (Figure 7-3). The AFM image in

Figure 7-13 (b) shows a significant modification with increase in concentration of FM 8 in the blend (i.e. 1:1 molar ratio of OFM to ZDDP). The large elongated phosphate pads are transformed into a smaller cluster of pads. These cluster of pads still looked to be higher than the surrounding features.

Figure 7-14 and 7-15 show the line profile analysis of the tribofilm formed with the addition of FM 8 with ZDDP. The tribofilm roughness (R_q) value decreased with the addition of FM 8 in the blend with ZDDP in-comparison to the roughness value of the tribofilm formed by BO + ZDDP. The result showed that the R_q value decreased from 30 nm (BO + ZDDP) to 23 nm and18 nm respectively with the addition of FM 8 in the lubricant blend (0.5:1 and 1:1 molar ratio of FM to ZDDP). Significant reduction in the R_{max} value is also recorded with the addition of FM 8 in the blend with ZDDP. Negligible effect on R_{max} value is noticed with increase in concentration of FM 8 in the lubricant blend with ZDDP.

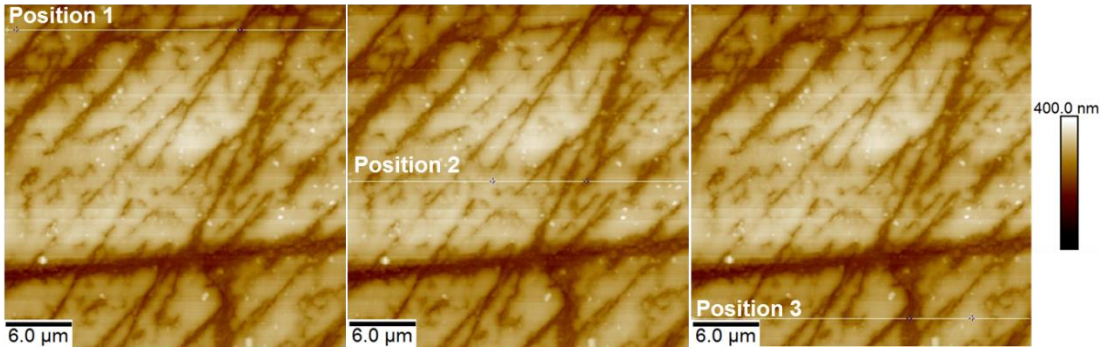

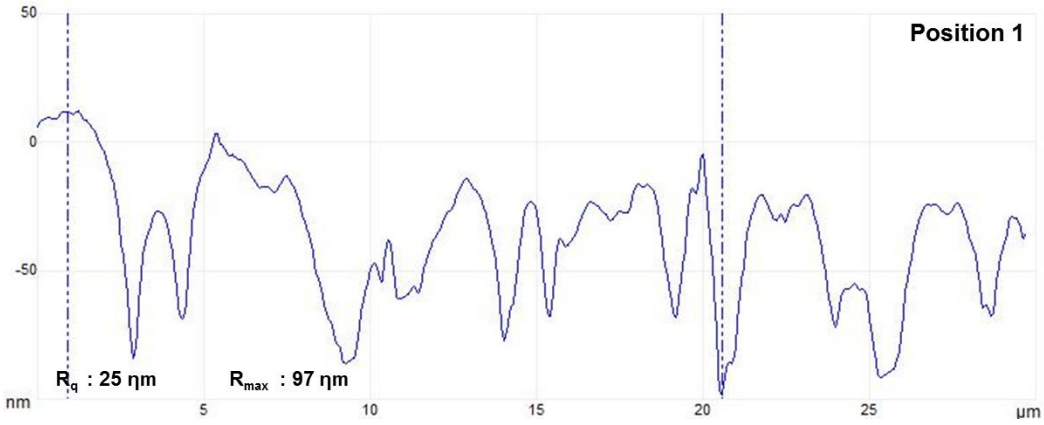

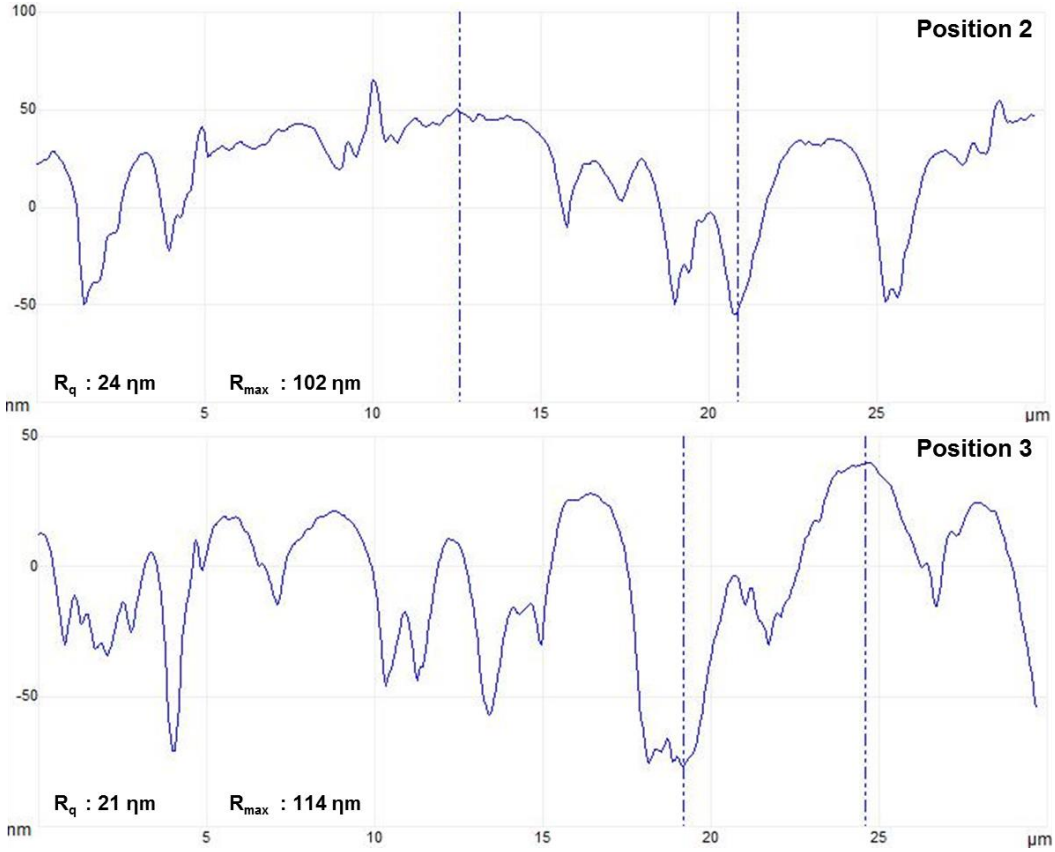

Figure 7-14. Line profile analysis of the tribofilm formed by BO + FM 8 + ZDDP having 0.5:1 molar ratio of FM to ZDDP

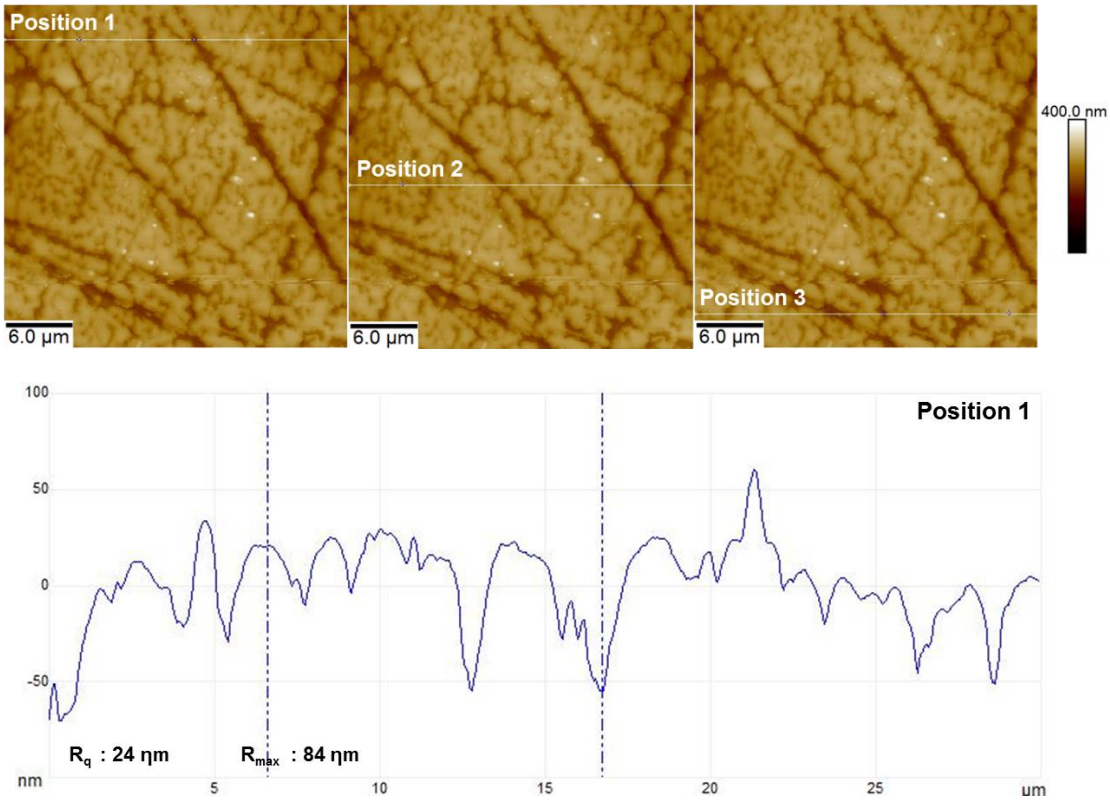

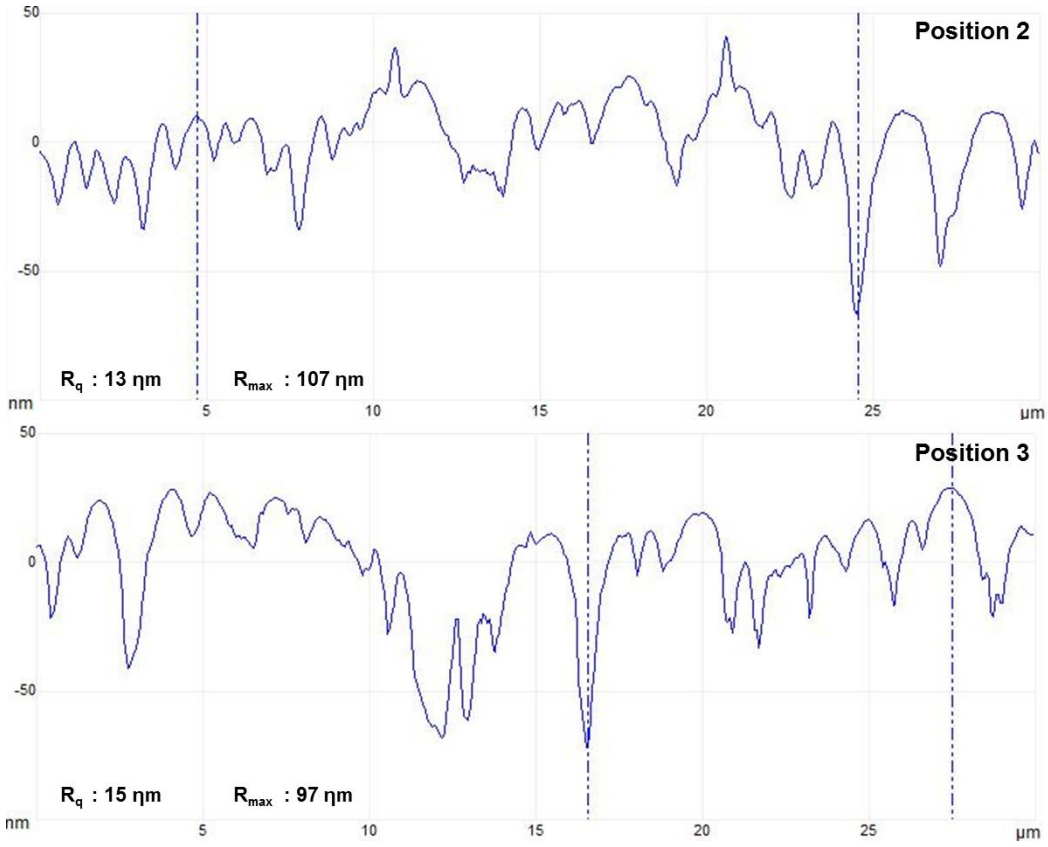

Figure 7-15. Line profile analysis of the tribofilm formed by BO + FM 8 + ZDDP having 1:1 molar ratio of FM to ZDDP

The addition of FM 8 in the blend with ZDDP reduced the tribofilm R_q and R_{max} values. The complete comparison of average R_q and R_{max} values of BO + ZDDP along with the addition of FM 8 in the blend is specified in Table 7-5.

Table 7-5. Surface roughness analysis of the tribofilm with the addition of FM 8

Lubricant blend	R_q (nm)	Std. deviation	R_{max} (nm)	Std. deviation
BO + ZDDP	30	0.6	173	14.2
BO + FM 8 + ZDDP (0.5:1)	23	2	104	9
BO + FM 8 + ZDDP (1:1)	18	6	96	12

The reduction in R_q and R_{max} values and the modification in the tribofilm topography indicated that the film formation capability of ZDDP is disturbed as

a result of the interaction with FM 8. The AFM image (Figure 7-13) specified an increase in the amine impact with the increase in the concentration of tallow amine in the blend. The significant decrease in the R_{max} value is possibly indicated reduction in the film thickness due to interaction of FM 8 with ZDDP.

7.4.4 Concentration effect of FM 10 on tribofilm morphology

The AFM scans in Figure 7-16 shows the tribofilm topographies formed by the addition of FM 10 (i.e. alcohol ethoxylate), in the blend with ZDDP. Figure 7-16 (a) and 7-16 (b) compare the tribofilm topographies formed by the addition of FM 10 in two different concentrations. The AFM images showed that the addition of FM 10 in the blend with ZDDP significantly modified the tribofilm topography. The AW pads are elongated in the sliding direction but in terms of size, these pads are transformed into shorter species. Increase in concentration of FM 10 in the blend further reduced size of the AW pads but these AW pads appeared to be higher than the surrounding features.

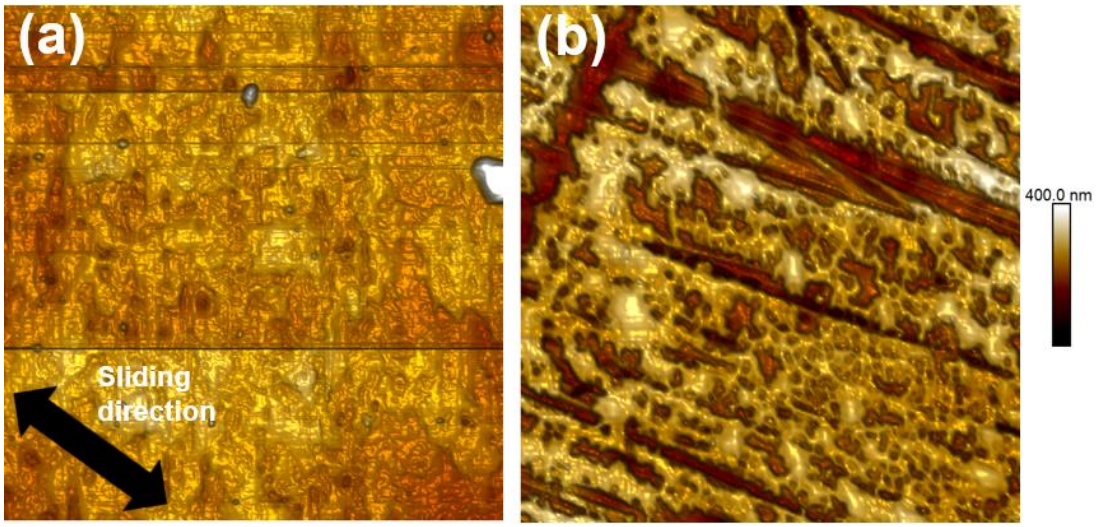

Figure 7-16. Tribofilm topographies of BO + FM 10 + ZDDP

(a) 0.5:1 molar ratio of FM to ZDDP (b) 1:1 molar ratio of FM to ZDDP

Figure 7-17 and 7-18 show the line profile analysis of the tribofilm formed with the addition of FM 10 and ZDDP. The tribofilm roughness (R_q) value is decreased with addition of FM 10 in the blend. The result showed that the R_q value decreased from 30 nm (BO + ZDDP) to 11 nm and 15 nm respectively with the addition of FM 10 in 0.5:1 and 1:1 molar ratio of the FM to ZDDP.

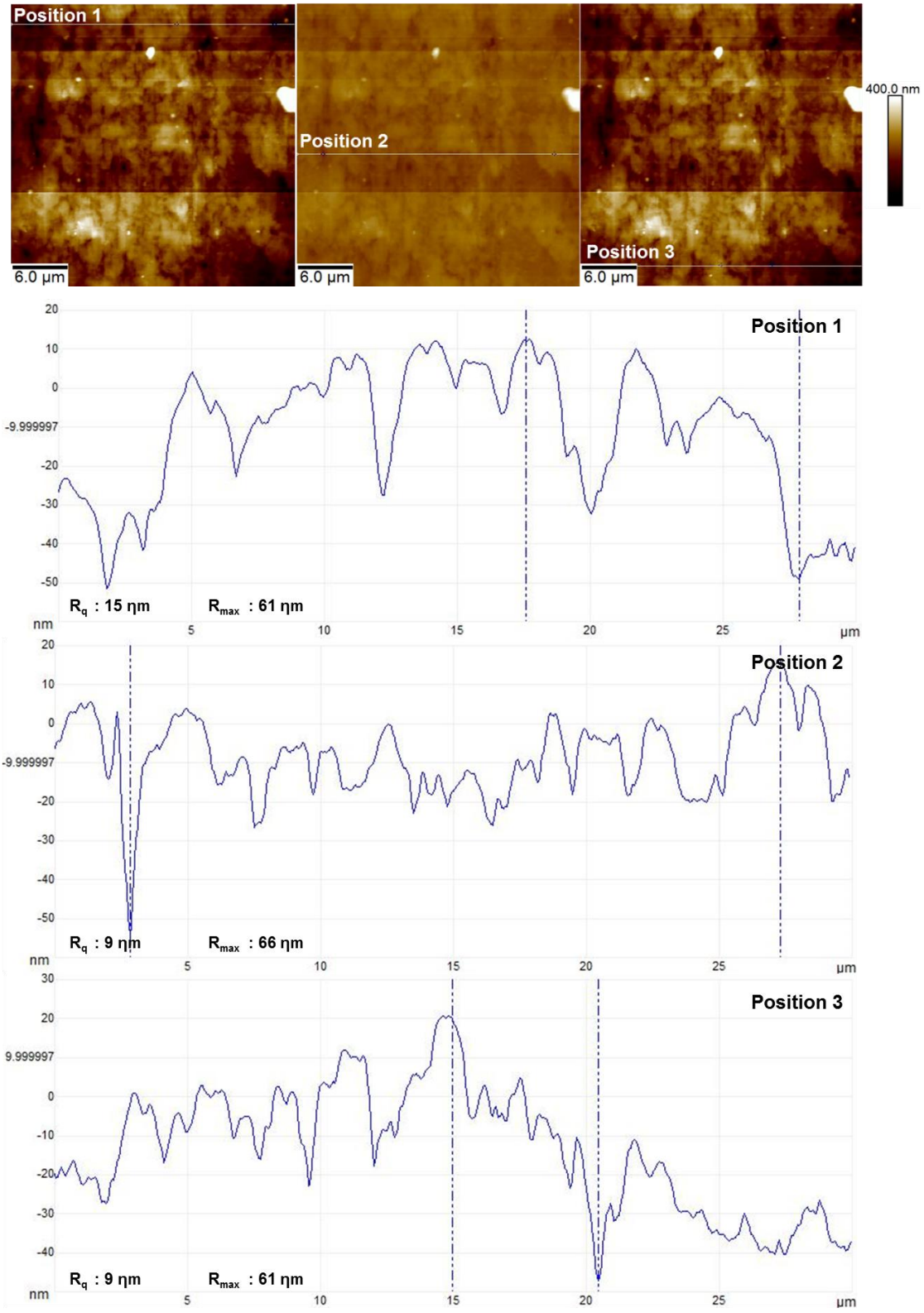

Figure 7-17. Line profile analysis of the tribofilm formed by BO + FM 10 + ZDDP having 0.5:1 molar ratio of FM to ZDDP

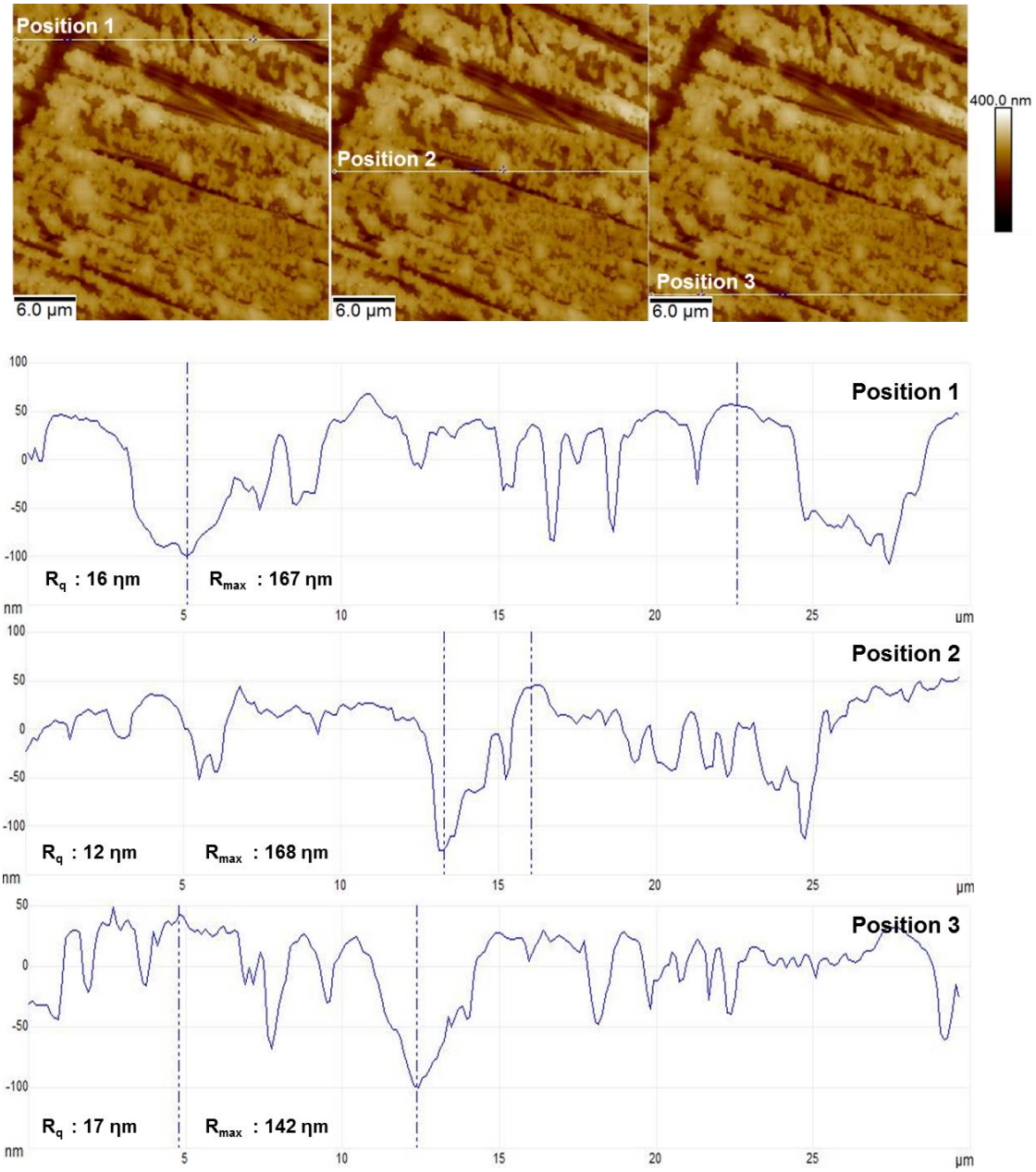

Figure 7-18. Line profile analysis of the tribofilm formed by BO + FM 10 + ZDDP having 1:1 molar ratio of FM to ZDDP

The addition of FM 10 in the blend with ZDDP also reduced the maximum peak to valley height (R_{max}) values in comparison to BO + ZDDP. The addition of FM 10 (0.5:1 molar ratio of the FM to ZDDP), remarkably reduced R_{max} value but with increase in the concentration of FM 10 in the lubricant blend (1:1 molar ratio of the FM to ZDDP), the R_{max} value is increased significantly. The addition of FM 10 modified the tribofilm topography of ZDDP just like amine friction modifiers. The AW pads found elongated in the sliding direction but they are squeezed in overall dimension. The siginificant modification in the

tribofilm topography of ZDDP highlighted the impact of the FM 10 on the film formation capability of ZDDP. The complete comparison of the R_q and R_{max} values of BO + ZDDP along with the addition of FM 10 in the blend is presented in Table 7-6.

Table 7-6. Surface roughness analysis of the tribofilm with the addition of FM 10

Lubricant blend	R_q (nm)	Std. deviation	R_{max} (nm)	Std. deviation
BO + ZDDP	30	0.6	173	14.2
BO + FM 10 + ZDDP (0.5:1)	11	4	63	3
BO + FM 10 + ZDDP (1:1)	15	3	159	15

7.4.5 Concentration effect of FM 14 on tribofilm morphology

Figure 7-19 compares the tribofilm topographies formed by the addition of FM 14 (i.e. ester of tri-ethanol amine with tallow fatty acid), in two different concentrations (i.e. 0.5:1 and 1:1 molar ratio of OFM to ZDDP). The addition of FM 14 in the blend with ZDDP significantly modified the tribofilm topography in comparison with the film formed by BO + ZDDP.

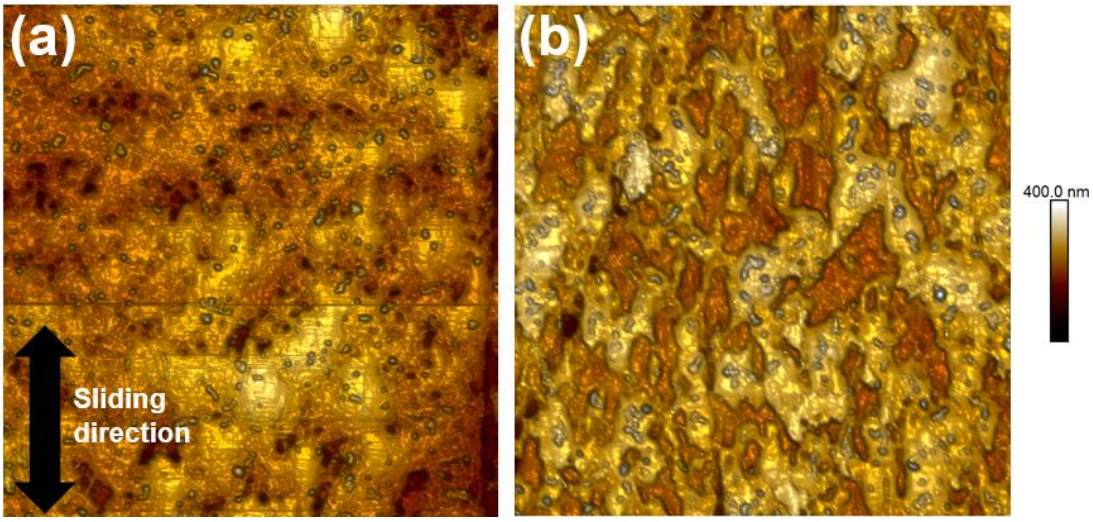

Figure 7-19. Tribofilm topographies of BO + FM 14 + ZDDP

(a) 0.5:1 molar ratio of FM to ZDDP (b) 1:1 molar ratio of FM to ZDDP

The AFM images in Figure 7-19 (a) show that the addition of FM 14 slightly modified the tribofilm topography of BO + ZDDP. The large phosphate pads are slightly squeezed but still elongated in the sliding direction. The phosphate pads height is appeared to be reduced in-comparison to the topography of BO + ZDDP (Figure 7-3). Figure 7-19 (b) show the impact of the increase in the concentration of FM 14 in the blend with ZDDP. The increase in concentration of FM 14 massively modified the tribofilm topography. The large elongated phosphate pads formed by BO + ZDDP completely transformed into smaller strips but still elongated in the sliding direction. The pad sizes are significantly reduced but they still appeared to be higher than the surrounding features.

Figure 7-20 and 7-21 show the line profile analysis of the tribofilm formed with the addition of FM 14 and ZDDP. The tribofilm roughness (R_q) value decreased with the addition of FM 14 in-comparison with the roughness value of the tribofilm formed by BO + ZDDP. The result showed that the R_q value decreased from 30 nm (BO + ZDDP) to 15 nm and 19 nm respectively with the addition of FM 14 in 0.5:1 and 1:1 molar ratio of FM to ZDDP. The addition of FM 14 in the blend with ZDDP also reduced the maximum peak to valley height (R_{max}) values in-comparison to the tribofilm formed by BO + ZDDP. The line profile analysis showed that the addition of FM 14 (0.5:1 molar ratio of FM to ZDDP), remarkably decreased the R_q and R_{max} values but with the increase in concentration of FM 14 in the lubricant blend (1:1 molar ratio of FM to ZDDP), the R_q and R_{max} values are slightly increased. The variation in the tribofilm topography indicated that the addition of FM 14 in the blend affected the AW film formation capability of ZDDP. The complete comparison of the R_q and R_{max} values of the blend is specified in Table 7-7.

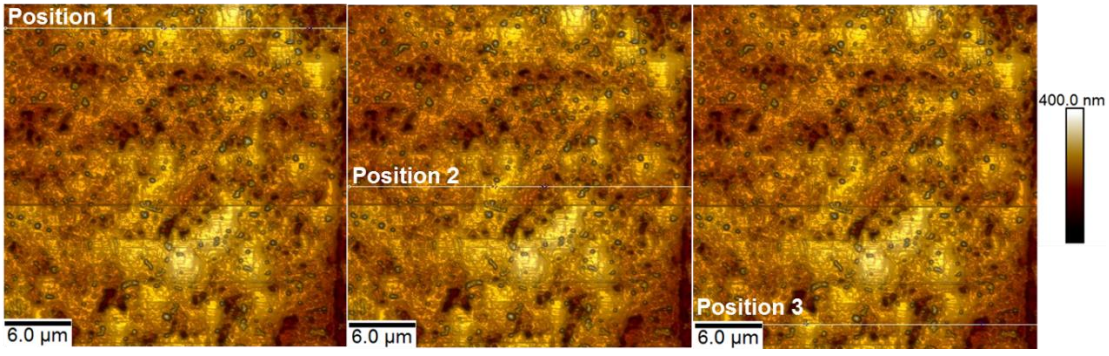

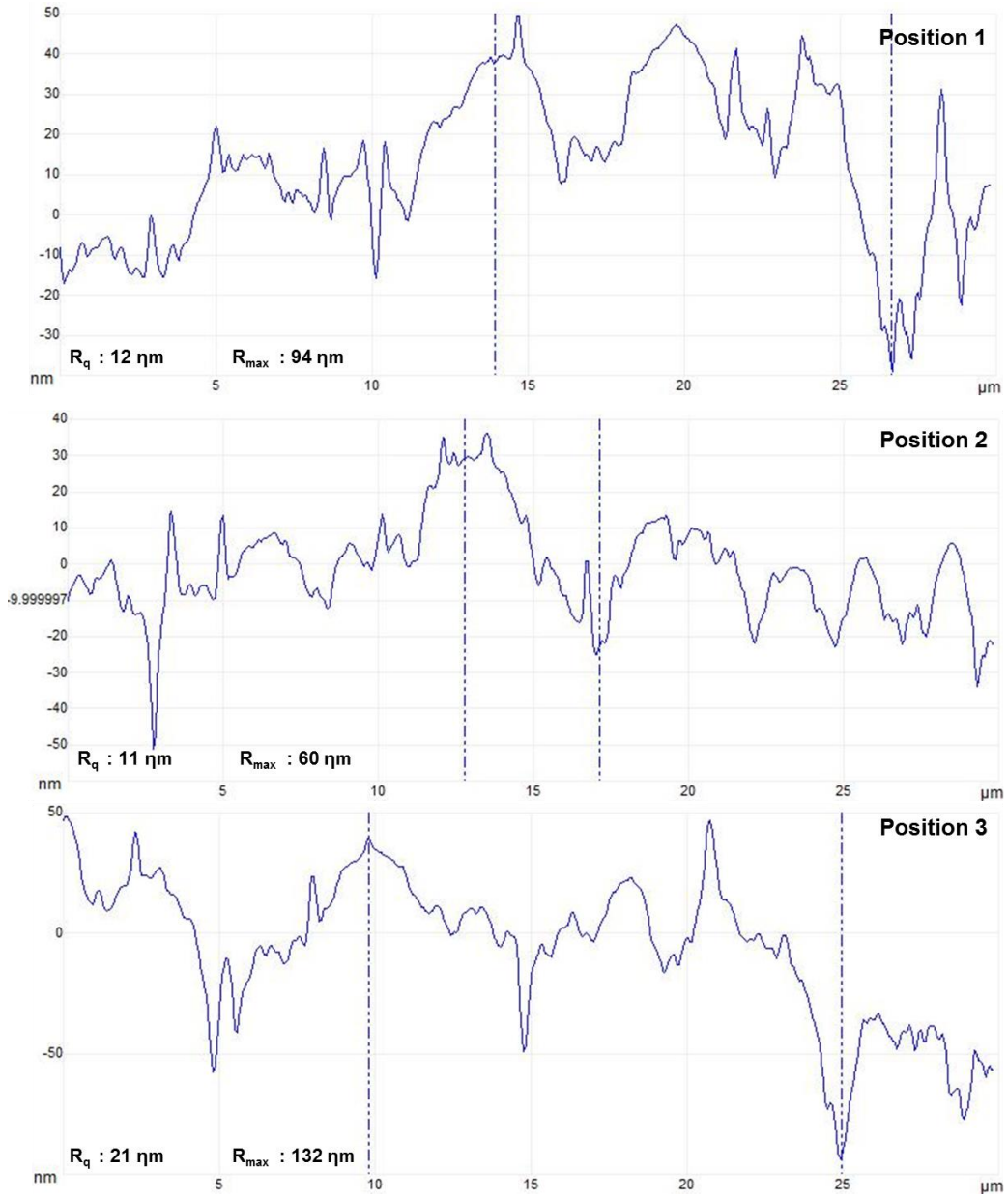

Figure 7-20. Line profile analysis of the tribofilm formed by BO + FM 14 + ZDDP having 0.5:1 molar ratio of FM to ZDDP

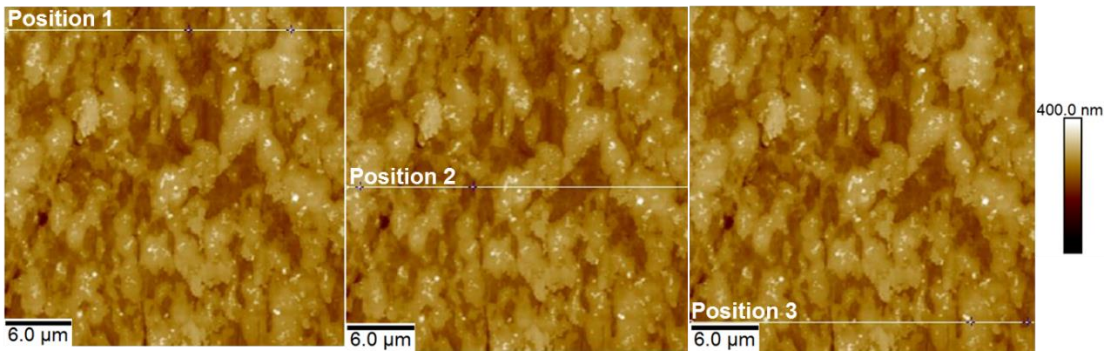

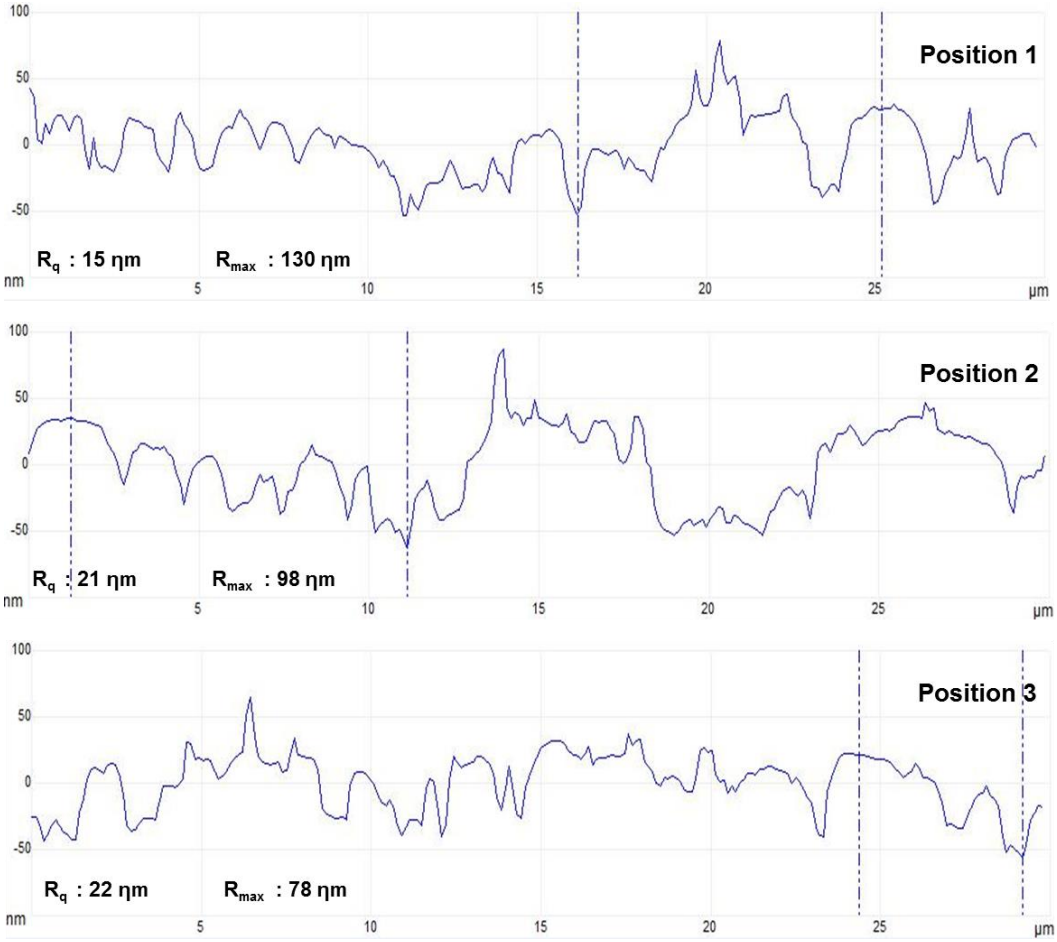

Figure 7-21. Line profile analysis of the tribofilm formed by BO + FM 14 + ZDDP having 1:1 molar ratio of FM to ZDDP

Table 7-7. Surface roughness analysis of the tribofilm with the addition of FM 14

Lubricant blend	R_q (nm)	Std. deviation	R_{max} (nm)	Std. deviation
BO + ZDDP	30	0.6	173	14.2
BO + FM 14 + ZDDP (0.5:1)	15	6	96	36
BO + FM 14 + ZDDP (1:1)	19	4	102	26

The AFM results suggested that addition of OFM with ZDDP (in both concentrations) significantly modified the tribofilm topography of ZDDP. The modification in the tribofilm topography of ZDDP indicated that addition of

OFM at some extent disturbed the tribofilm formation capability of ZDDP. It is interesting to analyse whether the chemical composition of the tribofilm is also modified with the addition of OFM in the blend with ZDDP. However, the OFMs in both concentrations (i.e. 0.5:1 and 1:1 molar ratio of OFM to ZDDP), affected the AW film topography of ZDDP but the difference between these modifications are not found significant. Therefore, the tribofilms formed by 1:1 molar ratio of FM to ZDDP are analysed to explore the chemical and elemental composition of the tribofilm. The elemental mapping and chemical composition of the tribofilm formed by the addition of OFM in 1:1 molar ratio of FM to ZDDP are presented in next chapter.

7.5 Summary

This chapter primarily focused on the concentration effect of OFMs on the tribofilm morphology of ZDDP. The tribological testing was performed on a TE 77 high frequency friction machine, in which a pin specimen reciprocated physically against a fixed plate specimen. The AFM was used to analyse the microscopic features of the tribofilm topography formed by the different lubricant blends on the plate specimen.

The tribofilm topography results revealed that:

- The tribofilm formed by ZDDP is heterogeneous and comprised of ridges (i.e. elevated part) and valley (i.e. shallow part)
- The elevated regions are islands of tribofilm commonly known as AW pads. The primary function of these pads is to bear load and limit the contact between interacting surfaces
- The large phosphate pads are elongated in the sliding direction and have exceptionally smooth surface.
- The smaller pads were less elongated in the sliding direction with average pad size of 2 µm to 5 µm
- The qualitative and quantitave analysis of the image exposed that the tribofilm features (i.e. ridges and valley regions and roughness parameters) are more established at middle position of the wear track.
- The addition of OFM in both concentrations (i.e. 0.5:1 and 1:1 molar ratio of FM to ZDDP) modified the tribofilm topography and roughness parameters
- The extent of modification in the tribofilm topography and roughness parameters varies with the different OFMs
- The OFMs in both concentrations (i.e. 0.5:1 and 1:1 molar ratio of OFM to ZDDP), affected the AW film topography of ZDDP but the difference between these modifications are not found significant
- The tribofilms formed by 1:1 molar ratio of OFM to ZDDP will be further analysed to explore the chemical and elemental composition of the tribofilm

Chapter 8
Organic friction modifier ZDDP interaction; Composition of the tribofilm

8.1 Introduction

Tribological analysis of five shorlisted lubricant blends with two different concentrations of OFMs (i.e. 0.5:1 and 1:1 molar concentrations of FM to ZDDP), produced some attention-grabbing tribological results. More or less all OFMs showed a positive effect on the friction performance. The wear results displayed some interesting wear trends. The addition of FM 1 and FM 4 with ZDDP significantly increased wear, whereas the addition of FM 8, FM 10 and FM 14 reduced wear remarkably. The AFM results displayed that the addition of OFM modified the tribofilm topogrpahy which possibly disturbed the tribological performance of ZDDP. Surprising wear responses of ZDDP (i.e. increasing or decreasing wear value), in-comparison with the wear behaviour of BO + ZDDP, indicated that the modification in the tribofilm morphology is possibly due to change in,

- Elemental composition of the tribofilm
- Chemical composition of the tribofilm

This chapter is focused on the modifications emerged in the elemental/chemical composition of the tribofilm by the addition of OFM with ZDDP (1:1 molar ratio of FM to ZDDP).

8.2 Elemental composition and mapping of the tribofilm

The AFM topographical images in Chapter 7 showed that the tribofilm formed by the lubricant blend of ZDDP mainly comprised of well-defined large and few small AW phosphate pads. The primary function of these pads are to bear load and limit the contact between interacting surfaces [26], [62]. This AW tribofilm is mainly composed of long and short chain phosphates along with zinc and iron sulphides [57], [90], [91]. In a typical ZDDP tribofilm, the top most surface has low or no iron (Fe) content but the bottom part of the tribofilm near the substrate possess the highest Fe content [58], [70]. The chemical

composition of the tribofilm formed by BO + ZDDP is used as a reference to analyse the impact of addition of OFM in the blend.

EDX is a good technique to assess the elemental composition but it is a bulk sensitive method, which penetrates deeper than the tribofilm thickness. Since EDX probes the substrate, it can provide elemental composition of the substrate as well [191]. The SEM-EDX analysis was performed on the plate specimens tested with all lubricant blends along with BO + ZDDP. SEM-EDX analysis were performed more than one position due to non-uniform tribofilm formation on the wear track. Only those results are added in this section which showed relatively better presence of key elements of the tribofilm (i.e. P, S, Zn and O). Later on, the XPS analysis of the tribofilms are also added in this chapter.

8.2.1 SEM-EDX analysis

Figure 8-1 shows the SEM-EDX analysis of the tribofilm formed by BO + ZDDP. The elemental mapping confirmed a strong presence of P, S, Zn and O, which indicated the possible formation of a zinc phosphate tribofilm inside the wear track. The results indicated that the elemental intensity of Zn is higher than P and S. The EDX spectrum also showed a strong presence of the substrate element (i.e. Fe) as this technique probes the substrate [191].

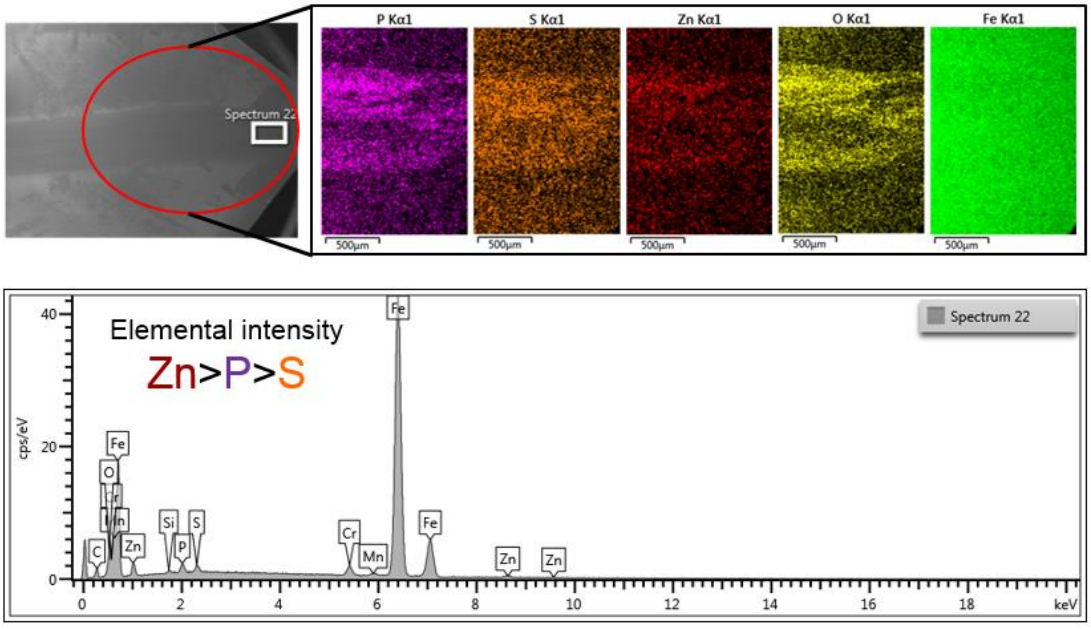

Figure 8-1. The elemental mapping and EDX spectrum of the ZDDP tribofilm

Figure 8-2 presents the elemetal mapping and EDX spectrum of the tribofilm formed by the addition of FM 1 (i.e. coco amine), in the lubricant blend with ZDDP. The elemental mapping results showed a major shift in the elemental composition of the tribofilm due to the addition of FM 1 in the lubricant blend. The results showed that the overall presence of P, S, Zn and O is relatively reduced. The EDX spectrum revealed that the relative intensity of S is increased in comparison to P and Zn. The change in the elemental intensity indicated a possible modification in the tribofilm elemental composition in-comparison to the tribofilm formed by BO + ZDDP as presented above in Figure 8-1.

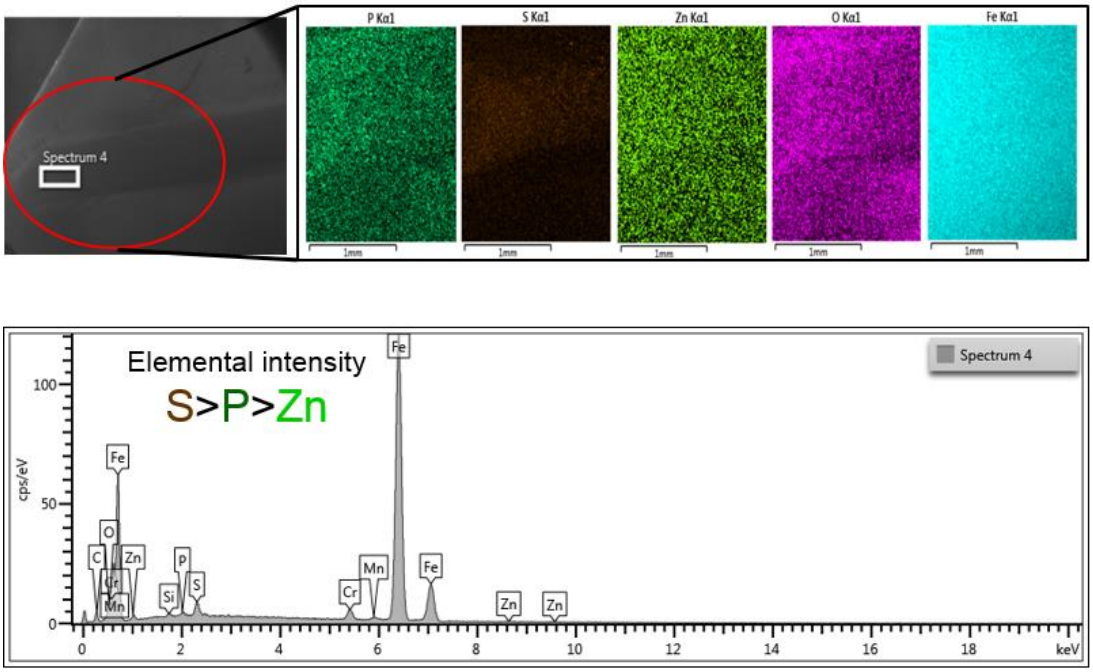

Figure 8-2. The elemental mapping and EDX spectrum of the tribofilm formed by BO + FM 1 + ZDDP

Figure 8-3 shows the elemental mapping and composition of the tribofilm formed with the addition of FM 4 (i.e. ethoxylated hydrogenated tallow amine) in the lubricant blend with ZDDP. A stronger presence of S in-comparison to Zn and P is found in the elemental mapping. The EDX spectrum confirmed that the intensity of S is higher in-comparison to Zn and P.

The elemental mapping and EDX spectrum of the tribofilm formed with the addition of FM 8 (i.e. tallow amine) with ZDDP is presented in Figure 8-4. The

elemental mapping showed a strong presence of S and Zn, which indicated that the tribofilm formed with the addition of FM 8 is S and Zn-dominated. The EDX spectrum exhibited a stronger intensity of S and Zn in-comparison to P.

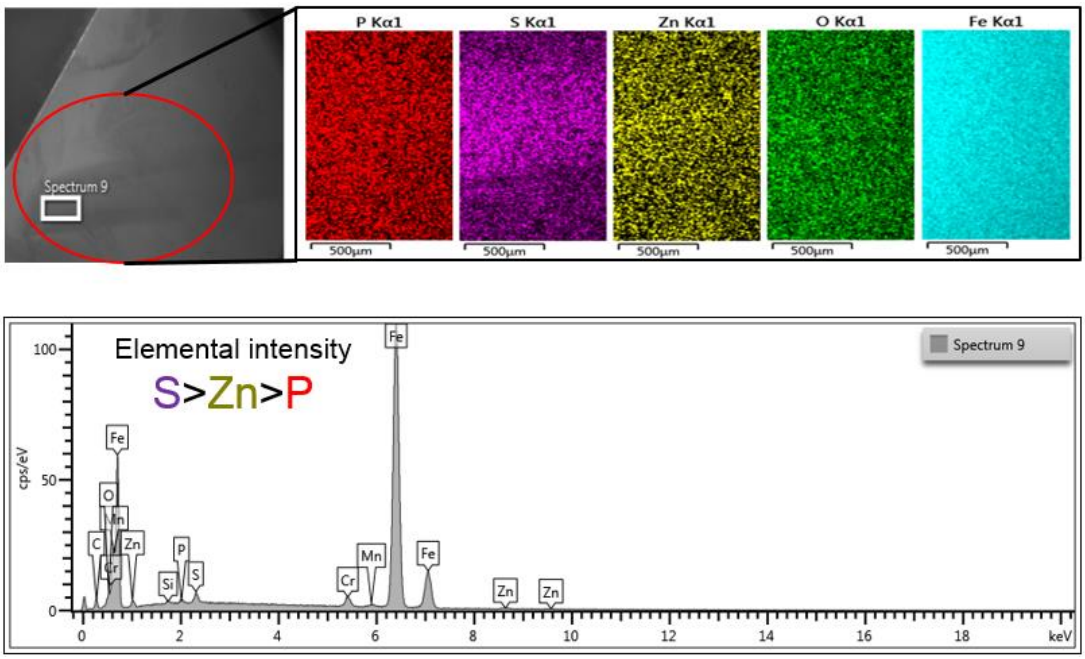

Figure 8-3. The elemental mapping and EDX spectrum of the tribofilm formed by BO + FM 4 + ZDDP

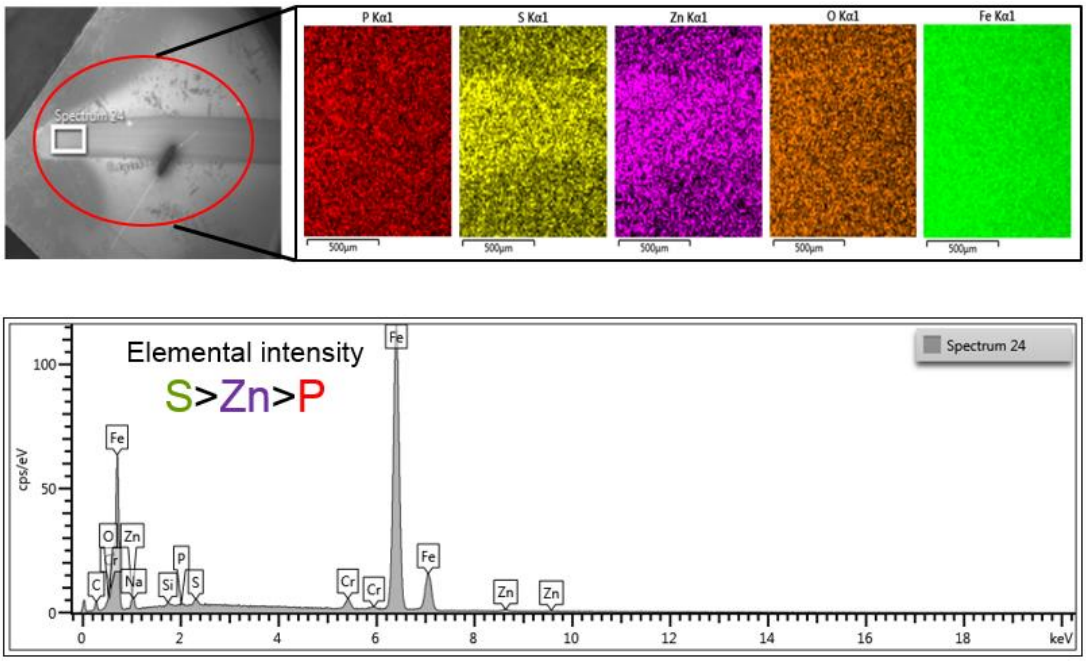

Figure 8-4. The elemental mapping and EDX spectrum of the tribofilm formed by BO + FM 8 + ZDDP

The results indicated a modification in the tribofilm elemental composition with the addition of FM 8 in-comparison to BO + ZDDP. The EDX spectrum also indicated a strong presence of the substrate element (i.e. Fe).

The elemental mapping and EDX spectrum of the tribofilm formed with the addition of FM 10 (i.e. alcohol ethoxylate) with ZDDP is displayed in Figure 8-5. The mapping result showed a stronger presence of Zn, P, S- and O, which indicated the formation of zinc phosphate tribofilm inside the wear track. The mapping results revealed that the elemental composition of the tribofilm is not significantly modified with the addition of FM 10 in-comparison to the tribofilm formed by BO + ZDDP. The EDX results confirmed that the tribofilm formed by the addition of FM 10 is Zn and P-dominated with a relatively reduced elemental intensity of S- in the tribofilm.

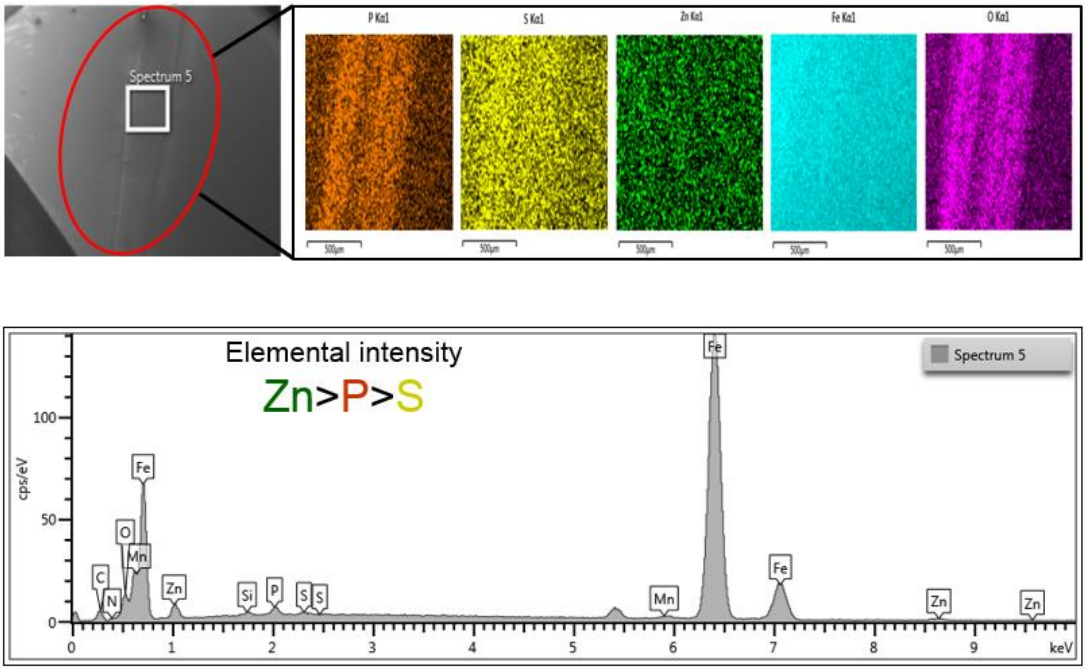

Figure 8-5. The elemental mapping and EDX spectrum of the tribofilm formed by BO + FM 10 + ZDDP

Figure 8-6 presents the elemental mapping and EDX spectrum of the tribofilm formed with the addition of FM 14 (i.e. ester of triethanol amine with tallow fatty acid) with ZDDP. The mapping result showed presence of Zn, S, P and -O. The EDX spectrum confirmed that the tribofilm formed with addition of FM 14 is Zn- dominated. The elemental intensity of P- is relatively reduced in

comparison to Zn, which indicated a modification in elemental composition of the tribofilm. The EDX results in both Figures 8-5 and 8-6 showed a strong presence of substrate element (i.e. Fe).

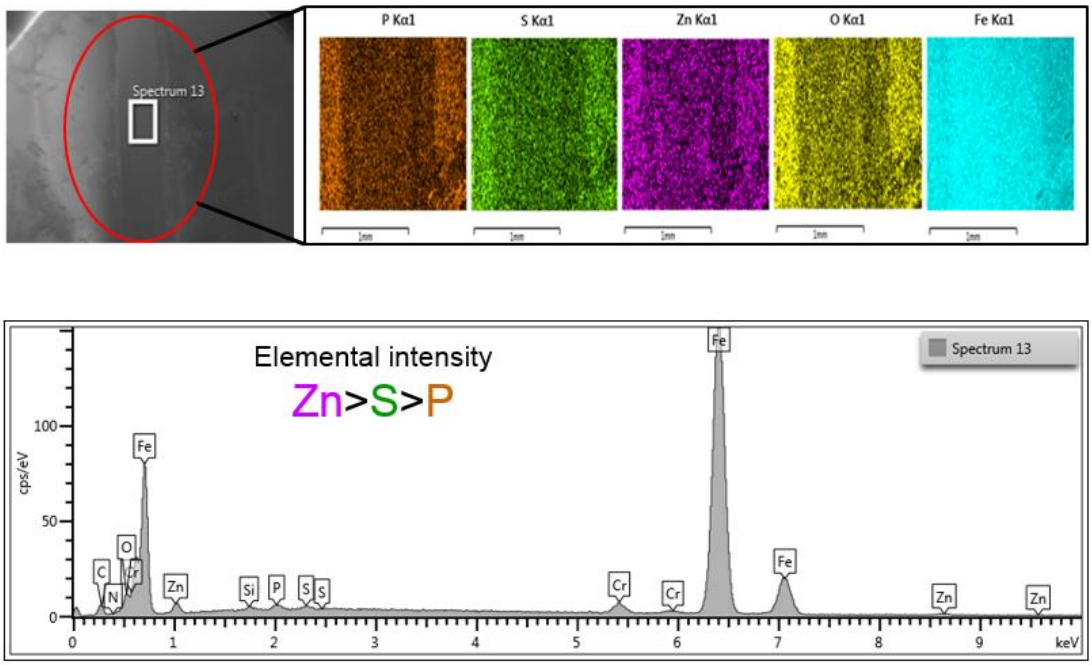

Figure 8-6. The elemental mapping and EDX spectrum of the tribofilm formed by BO + FM 14 + ZDDP

The SEM-EDX analyses clearly showed that the tribofilm formed by BO + ZDDP is enriched with P, S, Zn and O. The tribofilm formed with the addition of different amines are mostly found to be S and Zn-dominated with a reduction in the elemental intensity of P in-comparison to BO + ZDDP. The tribofilm formed by the addition of FM 10 showed elemental composition simlar to BO + ZDDP. The results apparently revealed that the addition of OFMs with ZDDP modified the tribofilm elemental composition.

8.3 Chemical composition and quantification of the tribofilm

The elemental composition results confirmed that the EDX technique penetrated well across the tribofilm and provided elemental composition of the substrate [191]. The XPS analysis is included in this chapter because it is a surface sensitive technique, which provides precise information about the tribofilm chemical composition [201], [202].

The primary reasons for inclusion of the XPS analyses is to;

- Supplement EDX results
- Analyse chemical composition of the tribofilms formed by BO + ZDDP and blends of OFM with ZDDP by identifying the exact species

Etching of the tribofilm surfaces are also conducted during this study in order to mitigate any contamination effect and to further,

- Analyse the change in elemental concentration across the tribofilm
- Analyse the chemical structure of the tribofilm

8.3.1 Tribofilm characterisation using XPS

The high-resolution (HR) XPS scans of selected elements (i.e. P 2p, O 1s, S 2p, Zn 2p, Zn 3s and N 1s) of the tribofilms are included in this chapter. After detailed XPS analysis of the top 5-8 nm of the tribofilm surface, the tribofilm is etched. Comparison of the XPS data from the top most surface of the tribofilm with the chemical species found after few etching cycles provided a good indication about modification in the chemical structure of the tribofilm.

8.3.1.1 Chemical composition and quantification of the tribofilm formed by ZDDP

The elemental mapping and EDX spectrum of the tribofilm formed by BO + ZDDP (Figure 8-1) revealed strong presence of Zn, P, S and O inside the wear track. Figure 8-7 shows HR XPS scans of selected elements (i.e. O 1s, P 2p, Zn 3s, Zn 2p and S 2p), of the tribofilm formed by BO + ZDDP. The C 1s signal is resolved into four Gaussian components. The major component appeared at 284.8 eV assigned to aliphatic carbon and used for energy calibration purpose [82], [191]. The O 1s signal is also resolved into two components. The major component at 531.49 eV is assigned to the terminating O incorporated in the phosphate chain (-P=O and P-O-M, in this case M refers to Zn metal) and is termed as Non-Bridging Oxygen (NBO) [77], [203], [207]–[210]. The other component at 533 eV is assigned to the O that binds phosphate group in the phosphate chain (P-O-P) and is termed as Bridging Oxygen (BO) [203], [208]–[210]. A metal oxide peak was not detected in the O 1s signal.

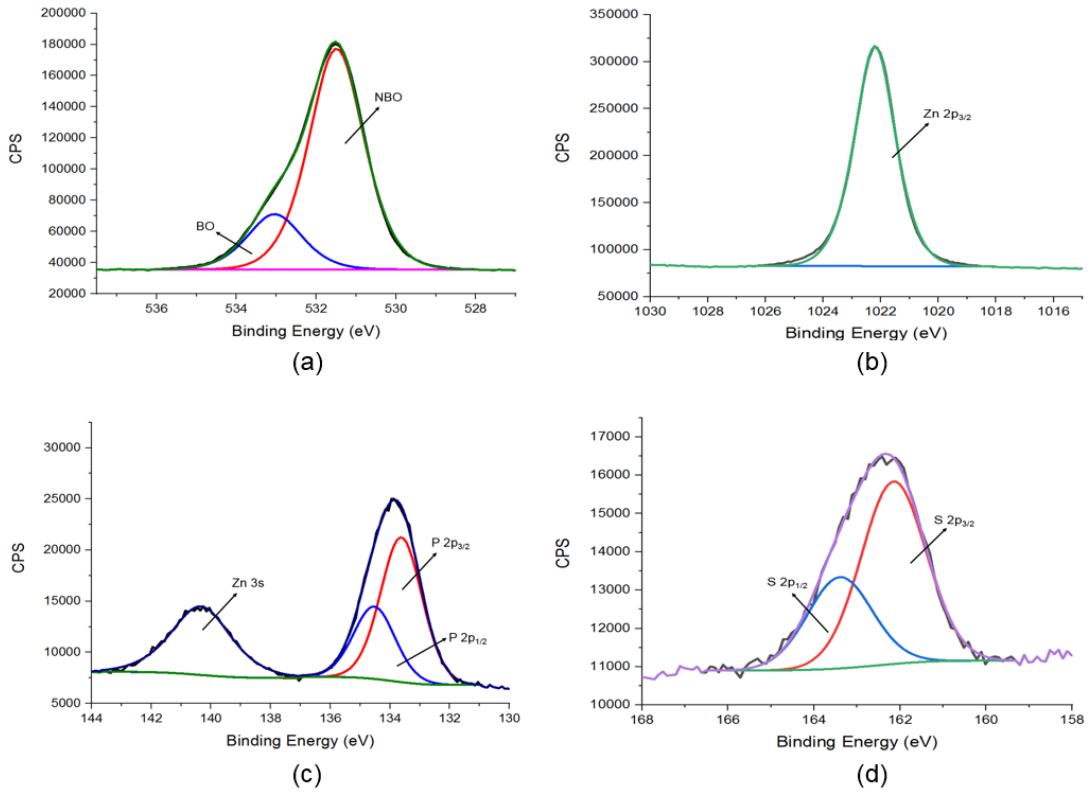

Figure 8-7. HR XPS spectra of the key elements in ZDDP tribofilm

(a) O 1s (b) Zn $2p_{3/2}$ (c) P 2p and Zn 3s (d) S 2p

The Zn 2p signal is detected at 1022.19 eV which is assigned to either ZnS, ZnO [199], [211] or zinc phosphate glass formation [208]. The P 2p signal is originated from the phosphate chains embedded in the tribofilm. The P $2p_{3/2}$ and P $2p_{1/2}$ components are detected at 133.65 and 134.49 eV. These binding energy (BE) values are assigned to either pyrophosphate or polyphosphate [77], [203], [212], [213]. The Zn 3s signal is detected at 140.39 eV. The S 2p signal is deconvoluted in two components. The S $2p_{3/2}$ and S $2p_{1/2}$ components are found at 162.15 and 163.40 eV. These BE values are assigned to sulphides present in the tribofilm [199], [211]. The incorporation of S in the tribofilm indicated the formation of metal sulphides [15], [82], [211]. These BE values also corresponded to S which partly substitutes O from phosphate chain and form zinc (thio)phosphate [76] and it is difficult to distinguish between metal sulphides and (thio)phosphate as the peaks overlap due to small shift in BE value [76].

Figure 8-8 shows a depth-profile of the tribofilm formed by the lubricant blend of ZDDP. The depth-profile graph revealed the presence of high amount of C

and O along with Zn, P and S on top most surface of the tribofilm. Low or no amount of Fe (Iron) was found on the top most surface of the tribofilm. Presence of key elements of the tribofilm and absence of Fe indicated that zinc phosphate film is well established. The concentration of P, Zn and O is decreased with subsequent etching cycles (i.e. around every 40 seconds), whereas no significant change in S concentration is observed. The Fe concentration increased significantly with the etching time, which indicated that Fe from the substrate material is building up in the tribofilm [214]. The concentration of C is decreased considerably after etching, which also confirmed that the initial high concentration of C was due to surface contamination [72].

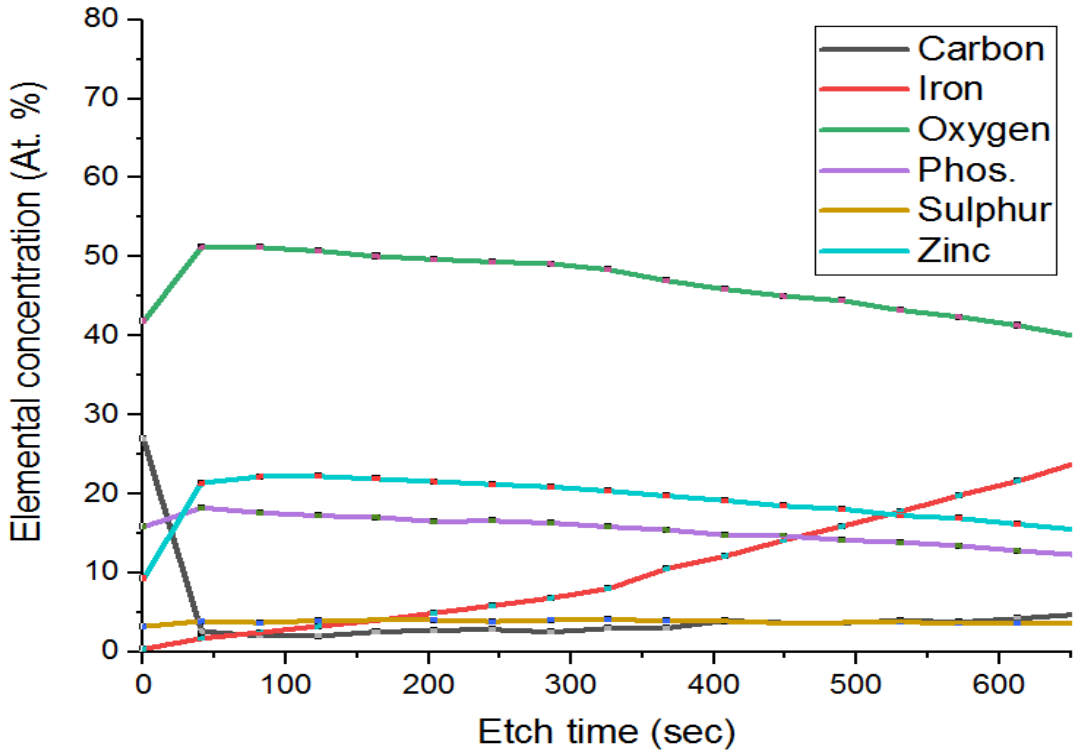

Figure 8-8. The XPS depth profile of ZDDP tribofilm

Table 8-1 shows the elemental concentration ratios after each sputter cycle in ZDDP tribofilm. The data shows a drop in P/S, P/Zn, P/O and P/Fe elemental ratios from the top most surface to deeper in the tribofilm (towards the substrate), whereas Zn/S and Fe/S concentration ratios increased deeper in the tribofilm.

Table 8-1. Elemental concentration ratios after each sputter cycle in ZDDP tribofilm

Etch. time (sec)	P/S	P/Zn	P/O	P/Fe	Zn/S	Fe/S
0	4.91	1.72	0.38	43.89	2.86	0.11
40.7	4.72	0.85	0.36	10.72	5.53	0.44
81.8	4.79	0.79	0.34	7.22	6.03	0.66
122.6	4.35	0.78	0.34	5.31	5.61	0.82
163.5	4.23	0.78	0.34	4.29	5.45	0.99
203.9	4.08	0.77	0.33	3.35	5.34	1.22
244.9	4.30	0.78	0.34	2.84	5.50	1.51
285.9	4.03	0.78	0.33	2.39	5.17	1.69
326.3	3.88	0.78	0.33	1.97	4.99	1.97
367.3	3.90	0.78	0.33	1.47	4.98	2.66
408.3	3.80	0.77	0.32	1.22	4.94	3.13
449.3	4.03	0.80	0.33	1.04	5.07	3.88
490.3	3.81	0.78	0.32	0.89	4.87	4.29
531.3	3.65	0.80	0.32	0.78	4.55	4.69
572.3	3.76	0.80	0.32	0.68	4.73	5.56

8.3.1.2 Chemical composition and quantification of the tribofilm formed by addition of FM 1 and ZDDP

The EDX results exhibited that the overall presence of P, S, Zn and O is relatively reduced due to the addition of FM 1 (i.e. coco amine) and ZDDP in the blend. The results showed that the addition of FM 1 with ZDDP hindered the formation of phosphate tribofilm to some extent. The XPS scan in Figure 8-9 shows the presence of key elements of the tribofilm inside the wear track. The major components in O 1s signal are assigned to NBO and BO from phosphate chains in the tribofilm [77], [203], [207]–[210]. A metal oxide peak is also detected in O 1s signal [199], [203], [211], [215]–[217]. The P 2p signal is deconvoluted in two components (i.e. P $2p_{3/2}$ and P $2p_{1/2}$). The BE values of P $2p_{3/2}$ and P $2p_{1/2}$ components are assigned to phosphates in the tribofilm [77], [203], [211]–[213]. The Zn 3s peak is recorded next to the P 2p signal.

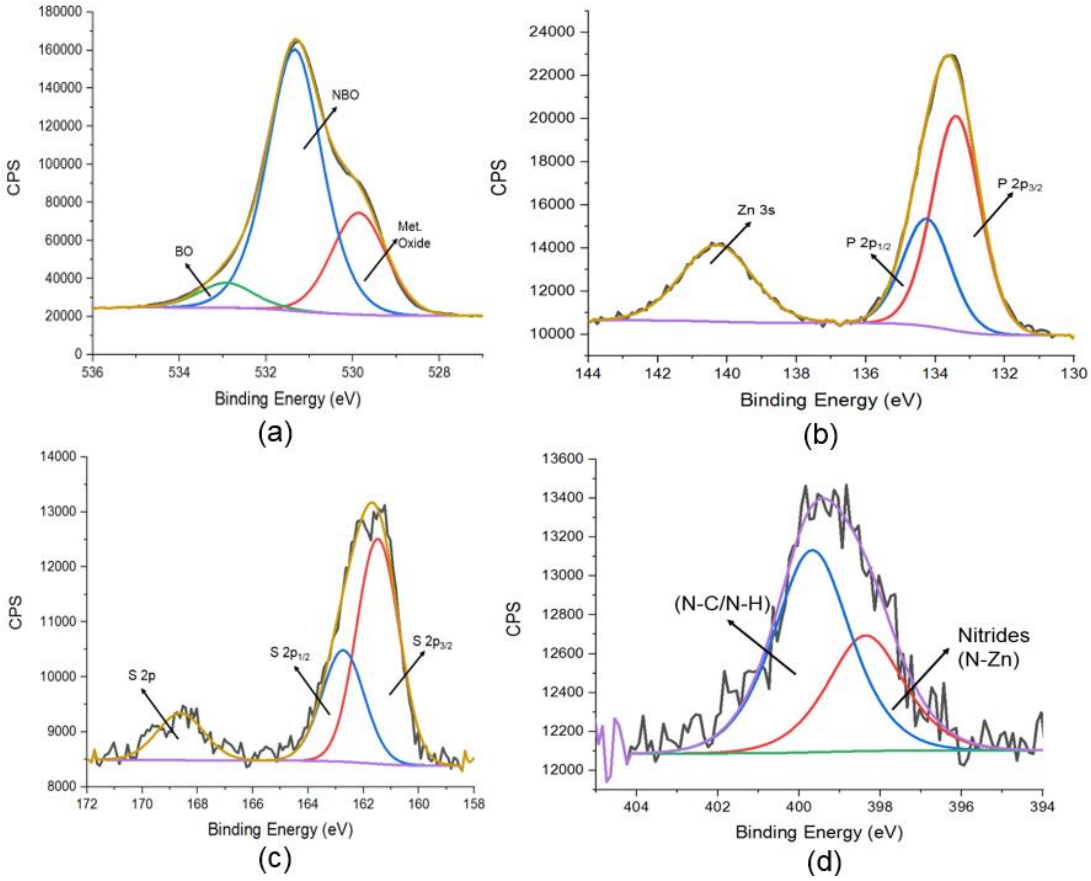

Figure 8-9. HR XPS spectra of the key elements in BO + FM 1 + ZDDP tribofilm

(a) Oxygen 1s (b) P 2p and Zn 3s (c) S 2p (d) N 1s

The S 2p signal is deconvoluted in to S $2p_{3/2}$ and S $2p_{1/2}$ components which are assigned to sulphides [199], [211] and or S which partly substitute O from the phosphate chain and form zinc (thio)phosphate [76]. The sulphate peak is also detected in the same BE window which is originated from S in oxidation state of +VI [91]. The N 1s peak is difficult to interpret due to the very limited availability of specific standards [174]. The N 1s peak is deconvoluted into two components. The first component is assigned to nitrides (N-Zn) and second component to N-C/N-H bonds [174], [211]. Evolution of the metal oxide peak in O 1s signal and interaction of N with Zn indicated that chemical composition of tribofilm is modified. Figure 8-10 shows the depth-profiling graph of the tribofilm formed by BO + FM 1 + ZDDP. The depth profiling of the tribofilm revealed that the overall concentration of P, Zn and O is comparatively decreased whereas S and Fe concentration is increased with the addition of FM 1 and ZDDP in the lubricant blend.

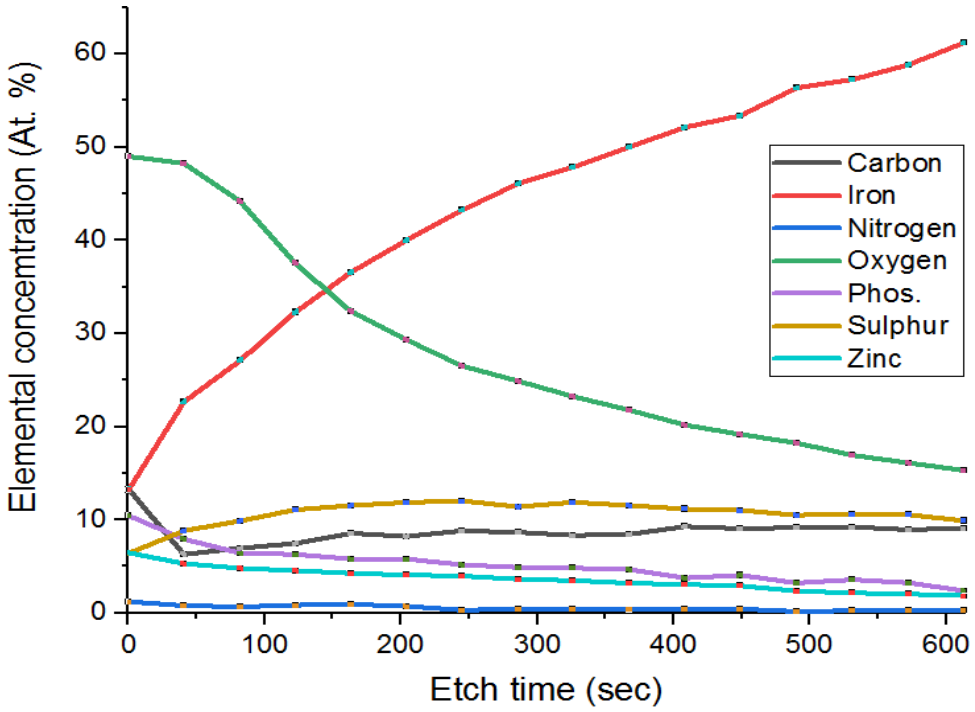

Figure 8-10. The depth profile of the tribofilm formed by BO + FM 1 + ZDDP

The presence of an iron oxide peak at the top surface of the tribofilm and the sharp increase in the Fe concentration with etching time indicated that Fe from the substrate material is rapidly building up in the tribofilm [214]. Another major difference is the significant increase in the S concentration and its incorporation throughout the tribofilm. The etching result displayed that C concentration decreased significantly after sputtering but comparatively a higher C concentration is recorded in-comparison to the tribofilm formed by BO + ZDDP. Table 8-2 presents the elemental concentration ratios of the key elements of the tribofilm. Data showed a substantial decrease in P/S, P/Fe and Zn/S and nearly similar P/Zn and P/O elemental ratios from the top most surface to deeper in the tribofilm (towards the substrate).

8.3.1.3 Chemical composition and quantification of the tribofilm formed by addition of FM 4 and ZDDP

EDX results revealed that the tribofilm formed with addition of FM 4 (i.e. ethoxylated hydrogenated tallow amine) and ZDDP in the lubricant blend is S and Zn dominated. The elemental mapping result indicated that the addition of FM 4 modified the tribofilm composition. The XPS analysis in Figure 8-11 shows the chemical composition of the key elements of the

tribofilm. Prominent signal from the key elements shows the existence of the tribofilm inside the wear track.

Table 8-2. Elemental concentration ratios after each sputter cycle in the tribofilm formed by addition of FM 1

Etch. time (sec)	P/S	P/Zn	P/O	P/Fe	Zn/S	Fe/S
0	1.49	1.62	0.21	0.79	0.92	1.88
40.7	0.90	1.50	0.16	0.35	0.60	2.57
81.8	0.65	1.34	0.15	0.24	0.49	2.74
122.6	0.57	1.39	0.17	0.19	0.41	2.92
163.5	0.50	1.36	0.18	0.16	0.37	3.17
203.9	0.49	1.42	0.20	0.15	0.34	3.37
244.9	0.43	1.31	0.19	0.12	0.33	3.60
285.9	0.43	1.35	0.20	0.11	0.32	4.04
326.3	0.40	1.39	0.21	0.10	0.29	4.03
367.3	0.41	1.46	0.21	0.09	0.28	4.33
408.3	0.34	1.23	0.19	0.07	0.27	4.66
449.3	0.37	1.39	0.21	0.08	0.26	4.84
490.3	0.31	1.36	0.18	0.06	0.22	5.36
531.3	0.34	1.66	0.21	0.06	0.20	5.39
572.3	0.31	1.60	0.20	0.06	0.19	5.58

The major components in O 1s signal are assigned to NBO and BO from phosphate chains in the tribofilm [77], [203], [207]–[210]. A metal oxide peak is also detected in O1s signal [199], [203], [211], [215]–[217]. The P 2p signal is originated from the phosphate chains embedded in the tribofilm and is deconvoluted into P $2p_{3/2}$ and P $2p_{1/2}$ components. The Zn 3s peak is found next to P 2p signal. The S 2p signal is deconvoluted in to S $2p_{3/2}$ and S $2p_{1/2}$ components which are assigned to sulphides [199], [211] and or S which partly substitutes O from phosphate chain and form zinc (thio)phosphate [76]. The sulphate peak is also detected in the same BE window which is originated from S in oxidation state of +VI [91], [199], [211]. The N 1s signal is resolved in two components. BE of the first component is assigned to N-C/N-H group

and the second to NH_2/NH_3 salt [165], [174]. The deconvolution of N 1s signal revealed the formation of amine and ammonium salt which could contribute to amine/ammonium phosphate formation [165], [187]. Evolution of the metal oxide peak in O 1s signal and possible formation of amine/ammonium phosphate specified that the tribofilm chemical composition is modified.

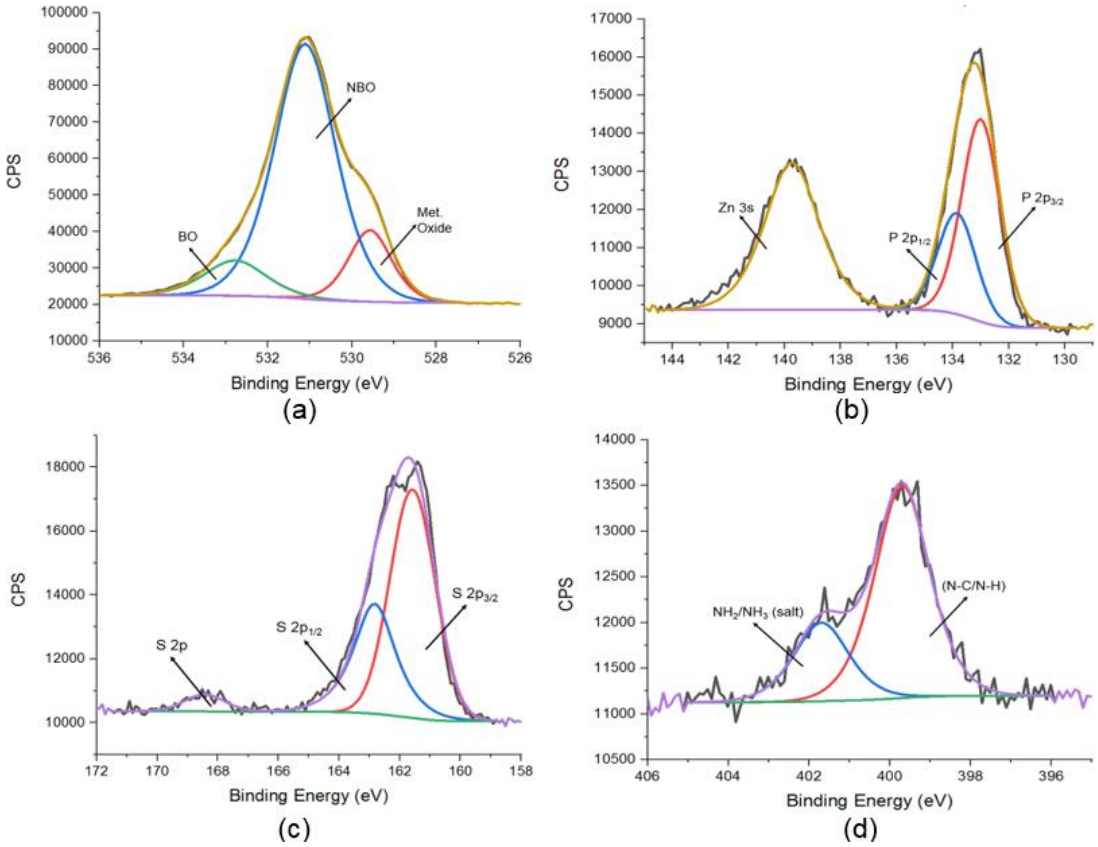

Figure 8-11. HR XPS spectra of the key elements in BO + FM 4 + ZDDP tribofilm (a) O 1s (b) P 2p and Zn 3s (c) S 2p (d) N 1s

Figure 8-12 shows the depth-profiling graph of the tribofilm formed by the lubricant blend of BO + FM 4 + ZDDP. The depth profiling of the tribofilm revealed that the overall concentration of P, Zn and O is comparatively decreased whereas S and Fe concentrations are increased. After subsequent etching cycles the concentration of P, Zn and O is decreased remarkably whereas the Fe concentration is increased sharply (as observed previously with the addition of FM 1 and ZDDP). The significant increase in Fe concentration indicated that the Fe from the substrate material is rapidly building up in the tribofilm [214]. The graph also showed that the S content

increased remarkably and it is incorporated throughout the tribofilm. The S-incorporation suggested the formation of more sulphide species [15], [82], [199]. The result showed the presence of excess Fe as compared to Zn deeper in the tribofilm, which indicated possible formation of more Fe species. N is incorporated in top part of the tribofilm and possibly contributed in formation of amine/ammonium phosphate [165], [187]. The elemental concentration ratios in Table 8-3 presented a significant decrease in P/S, P/Zn, P/Fe and Zn/S ratios in depth of the tribofilm, whereas a minor decrease in P/O elemental concentration is also recorded.

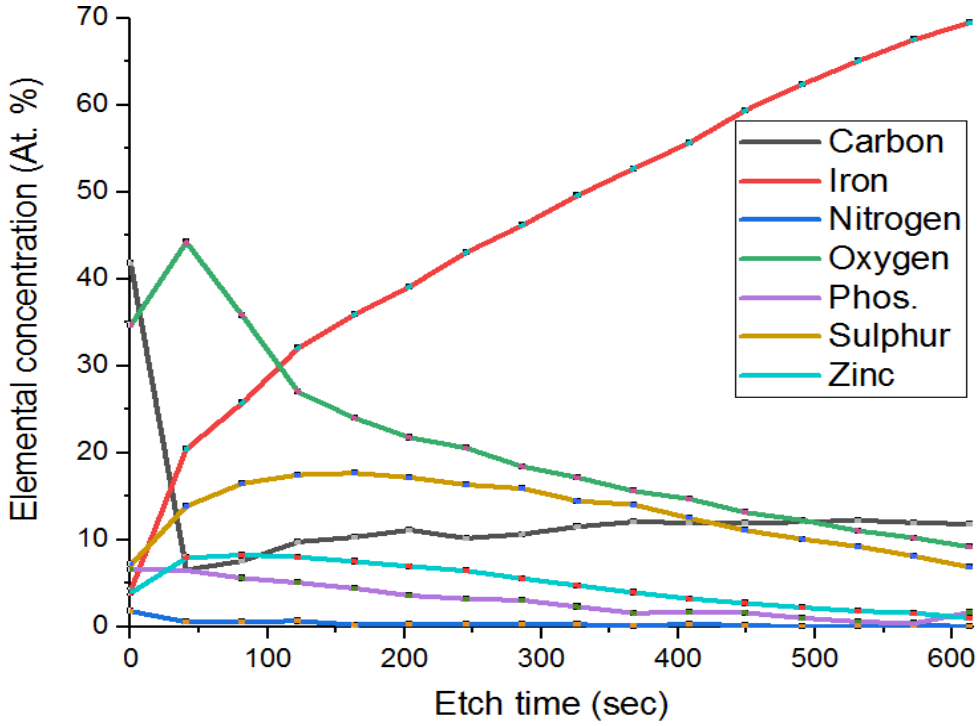

Figure 8-12. The depth profile of the tribofilm formed by BO + FM 4 + ZDDP

8.3.1.4 Chemical composition and quantification of the tribofilm formed by addition of FM 8 and ZDDP

The EDX elemental mapping of the tribofilm formed by the addition of FM 8 (i.e. tallow amine) showed a strong presence of S and Zn, which indicated that the tribofilm formed with the addition of FM 8 is S and Zn dominated. Detail XPS analysis of the key elements of the tribofilm in Figure 8-13 shows presence of the tribofilm inside the wear track. The O 1s signal is resolved in three components. The major peak is corresponded to NBO from phosphate.

The other peak at higher BE is assigned to BO from phosphate. A small metal oxide peak is also detected in the O 1s signal.

Table 8-3. Elemental concentration ratio after each sputter cycle in the tribofilm formed by addition of FM 4

Etch. time (sec)	P/S	P/Zn	P/O	P/Fe	Zn/S	Fe/S
0	0.87	1.70	0.19	1.59	0.51	0.54
40.7	0.47	0.82	0.15	0.32	0.57	1.48
81.8	0.34	0.68	0.16	0.22	0.50	1.56
122.6	0.29	0.63	0.19	0.16	0.46	1.83
163.5	0.25	0.59	0.18	0.12	0.42	2.03
203.9	0.21	0.51	0.16	0.09	0.41	2.28
244.9	0.20	0.50	0.16	0.07	0.39	2.64
285.9	0.19	0.55	0.17	0.07	0.35	2.90
326.3	0.16	0.48	0.13	0.05	0.33	3.43
367.3	0.11	0.40	0.10	0.03	0.28	3.75
408.3	0.13	0.51	0.11	0.03	0.26	4.46
449.3	0.14	0.59	0.12	0.03	0.25	5.37
490.3	0.10	0.46	0.08	0.02	0.22	6.18
531.3	0.06	0.31	0.05	0.01	0.20	7.04
572.3	0.05	0.25	0.04	0.01	0.20	8.31

The P 2p signal is deconvoluted in P 2p3/2 and P 2p1/2 components. The Zn 3s peak is noticed next to the P 2p signal. The presence of strong Zn 3s signal indicated a modification in the phosphate chain length compared to the tribofilm formed by BO + ZDDP. The S 2p signal is deconvoluted into S $2p_{3/2}$ and S $2p_{1/2}$ components. These BE values are assigned to sulphides in the tribofilm [199], [211] and or S which partly substitutes O from the phosphate chain and form zinc (thio)phosphate [76]. The N 1s signal is resolved in two components. BE of the first component correspond to N-C/N-H group and second component to NH2/NH3 salt [165], [174].

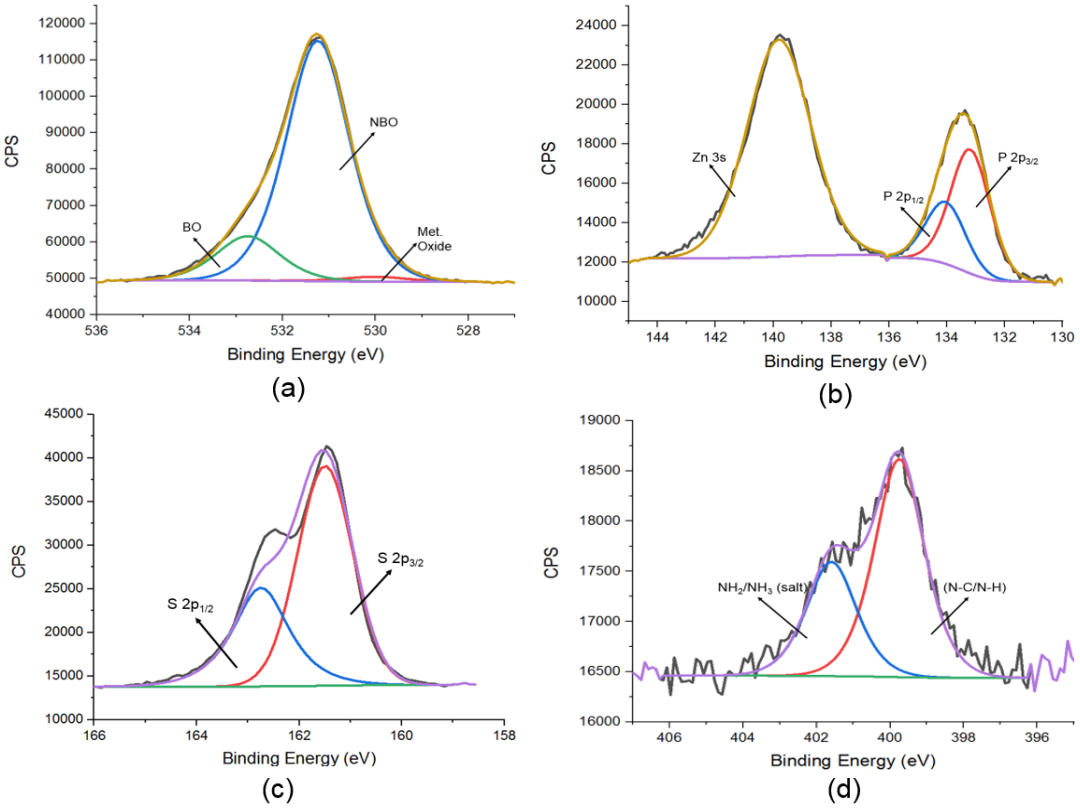

Figure 8-13. HR XPS spectra of the key elements in BO + FM 8 + ZDDP tribofilm (a) O 1s (b) P 2p and Zn 3s (c) S 2p (d) N 1s

Figure 8-14 shows the depth-profiling graph of the tribofilm formed with the addition of FM 8. The graph presented that the overall elemental concentration of P and O is reduced with the addition of FM 8. The tribofilm found to be rich in S and Zn but they showed entirely different incorporation trend as compared to the tribofilm formed by BO + ZDDP (Figure 8-8). The Fe concentration is increased considerably with the etching time (as observed previously with the addition of FM 1 and FM 4 with ZDDP), which indicated that Fe from the substrate material is rapidly building up in the tribofilm [214]. Though sputtering significantly decreased C concentration but still higher C content is detected in-comparison to BO + ZDDP tribofilm. The elemental concentration ratios in Table 8-4 exhibited a minor decrease in P/S, P/Zn and P/O elemental ratios from the top surface to deeper in the tribofilm (near the substrate), whereas an increase in Zn/S and Fe/S elemental concentration ratio are also observed.

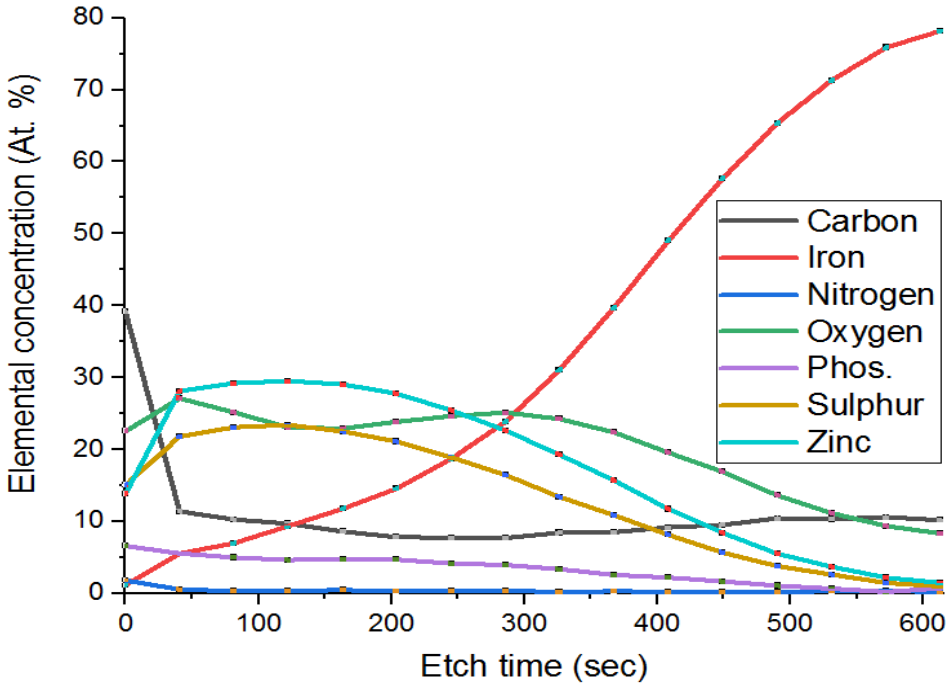

Figure 8-14. The depth profile of the tribofilm formed by BO + FM 8 + ZDDP

8.3.1.5 Chemical composition and quantification of the tribofilm formed by addition of FM 10 and ZDDP

The elemental mapping of the tribofilm formed with the addition of FM 10 (i.e. alcohol ethoxylate) and ZDDP in the blend displayed a stronger presence of Zn, P, S and O. Interestingly the elemental composition of the tribofilm is not significantly modified with the addition of FM 10 and ZDDP in the lubricant blend. Figure 8-15 shows the XPS scans of key elements of the tribofilm (i.e. O 1s, P 2p, Zn 3s, S 2p and Zn 2p), which confirmed the presence of the tribofilm inside the wear track. The O 1s signal is deconvoluted in to NBO and BO from the phosphate chain. A small metal oxide peak is also detected in O 1s signal. The Zinc 2p signal is assigned to ZnS, ZnO [199] or zinc phosphate glass formation [208]. The P 2p signal is originated from the phosphate chains of the tribofilm and is resolved into P $2p_{3/2}$ and P $2p_{1/2}$ components. The Zn 3s peak is found next to P 2p signal. The S 2p signal is deconvoluted into S $2p_{3/2}$ and S $2p_{1/2}$ components. The BE values of S 2p components are assigned to sulphides [199] and or S which partly substitute O- from phosphate chain and form zinc (thio)phosphate [76].

Table 8-4. Elemental concentration ratios after each sputter cycle in the tribofilm formed by addition of FM 8

Etch. time (sec)	P/S	P/Zn	P/O	P/Fe	Zn/S	Fe/S
0	0.44	0.48	0.29	5.84	0.93	0.08
40.7	0.25	0.20	0.20	1.00	1.29	0.25
81.8	0.22	0.17	0.20	0.72	1.26	0.30
122.6	0.20	0.16	0.20	0.50	1.26	0.40
163.5	0.21	0.16	0.21	0.40	1.29	0.52
203.9	0.22	0.17	0.20	0.32	1.32	0.69
244.9	0.22	0.16	0.17	0.22	1.35	0.99
285.9	0.24	0.17	0.16	0.17	1.38	1.45
326.3	0.25	0.17	0.14	0.11	1.44	2.31
367.3	0.24	0.16	0.11	0.06	1.45	3.65
408.3	0.27	0.19	0.11	0.04	1.44	6.03
449.3	0.29	0.20	0.10	0.03	1.48	10.17
490.3	0.28	0.19	0.08	0.02	1.46	17.29
531.3	0.25	0.18	0.06	0.01	1.42	27.44
572.3	0.15	0.10	0.02	0.00	1.51	52.69

Figure 8-16 shows the XPS depth-profiling graph of the tribofilm formed by the lubricant blend of FM 10 and ZDDP. The depth-profiling graph revealed very interesting results. The addition of FM 10 modified the elemental composition of the tribofilm as compared to BO + ZDDP but the extent of modification is not found comparatively significant as observed with the addition of other OFMs. The results demonstrated that the elemental concentration of P, S and O in the tribofilm are found more or less very similar to BO + ZDDP. Zn concentration is comparatively reduced but similar incorporation trend is observed across the tribofilm. The elemental concentration ratios in Table 8-5 shows a decrease in P/S, P/Zn, P/O and P/Fe ratios from the top surface to deeper in the tribofilm, whereas a considerable increase in the Zn/S is also recorded. The presence of excess Fe in the depth of the tribofilm indicated a possible formation of Fe species (i.e. iron sulphide).

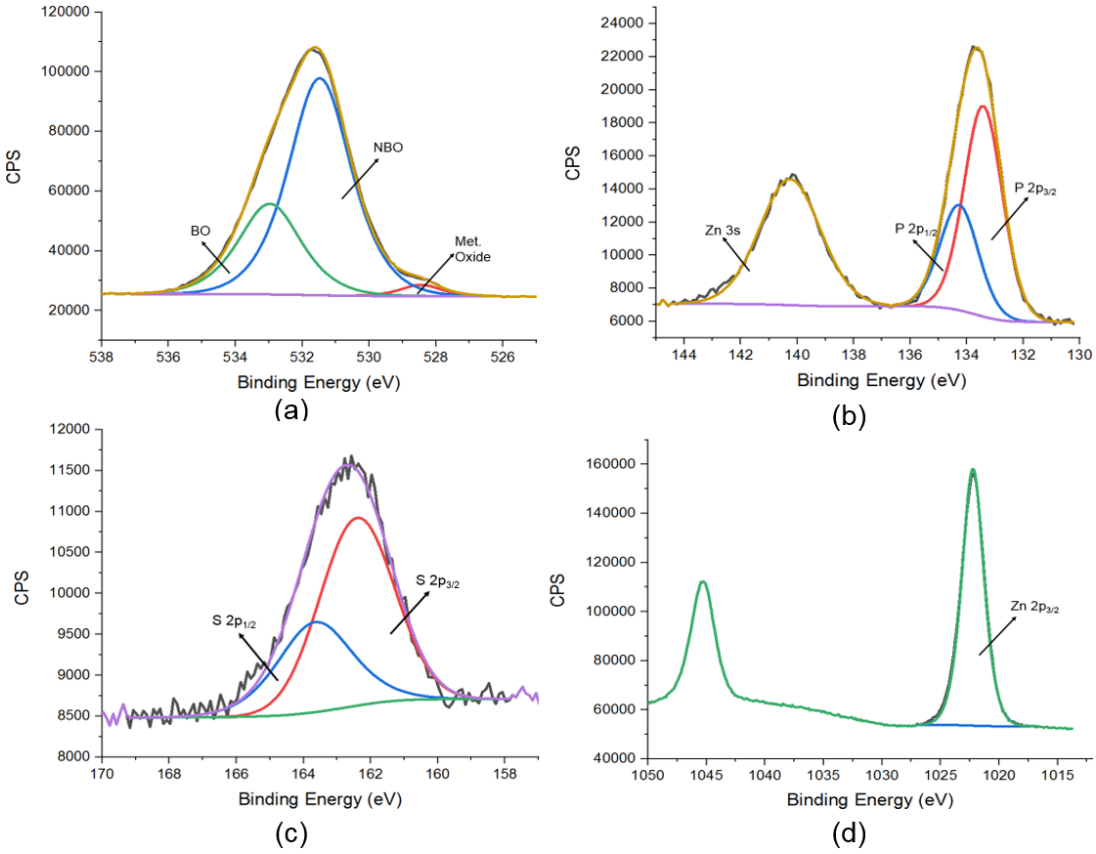

Figure 8-15. HR XPS spectra of the key elements in BO + FM 10 + ZDDP tribofilm

(a) O 1s (b) P 2p and Zn 3s (c) S 2p (d) Zn $2p_{3/2}$

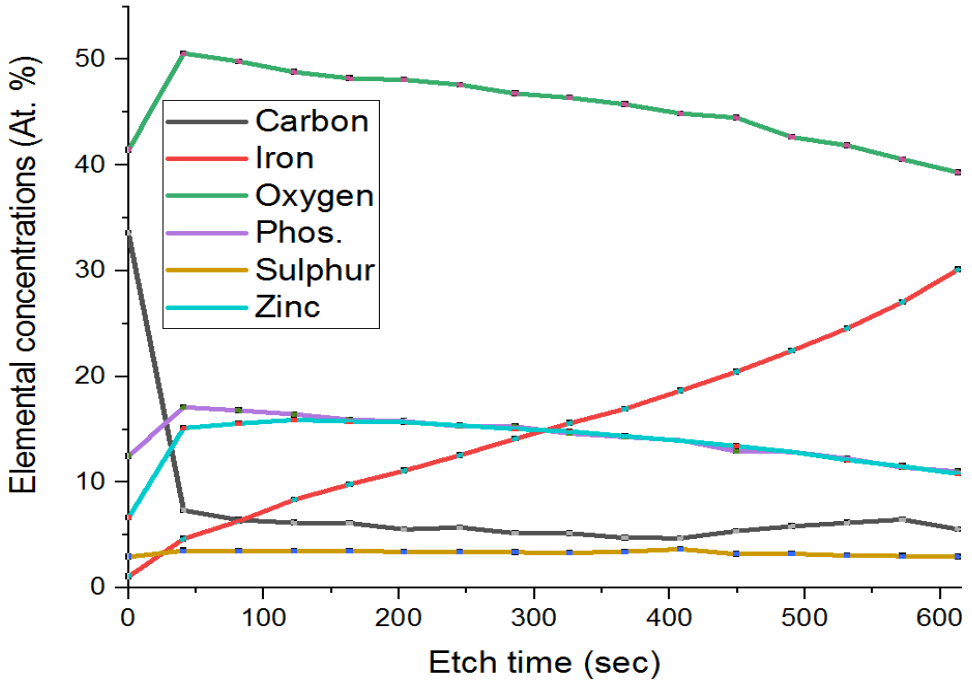

Figure 8-16. The depth profile of the tribofilm formed by BO + FM 10 + ZDDP

Table 8-5. Elemental concentration ratios after each sputter cycle in the tribofilm formed by addition of FM 10

Etch. time (sec)	P/S	P/Zn	P/O	P/Iron	Zn/S	Iron/S
0	4.50	1.88	0.30	11.57	2.39	0.39
40.7	4.83	1.13	0.34	3.68	4.27	1.31
81.8	4.77	1.08	0.34	2.65	4.42	1.80
122.6	4.72	1.03	0.34	1.97	4.57	2.40
163.5	4.52	1.01	0.33	1.62	4.47	2.78
203.9	4.62	1.01	0.33	1.42	4.60	3.26
244.9	4.47	1.00	0.32	1.22	4.49	3.67
285.9	4.53	1.01	0.33	1.08	4.47	4.19
326.3	4.42	0.99	0.32	0.94	4.47	4.71
367.3	4.15	0.99	0.31	0.84	4.17	4.93
408.3	3.81	1.00	0.31	0.75	3.80	5.09
449.3	4.03	0.96	0.29	0.63	4.18	6.37
490.3	3.98	1.00	0.30	0.57	3.98	6.95
531.3	4.00	1.01	0.29	0.50	3.96	8.03
572.3	3.77	0.99	0.28	0.42	3.81	8.96

8.3.1.6 Chemical composition and quantification of the tribofilm formed by addition of FM 14 and ZDDP

The elemental mapping of the tribofilm formed with the addition of FM 14 (i.e. ester of triethanol amine with tallow fatty acid) and ZDDP in the blend displayed a strong presence of Zn and P. The elemental intensity of S is relatively reduced in-comparison to Zn and P. Figure 8-17 shows the XPS scans of the key elements of the tribofilm (i.e. O 1s, P 2p, Zn 3s, S 2p and N 1s). The O 1s signal is deconvoluted into NBO and BO from the phosphate chain. A small metal oxide peak is also detected in the O 1s signal. The P 2p signal is originated from the phosphate chains in the tribofilm and deconvoluted into P $2p_{3/2}$ and P $2p_{1/2}$ components. The Zn 3s peak is found next to P 2p signal. The S 2p signal is deconvoluted into S $2p_{3/2}$ and S $2p_{1/2}$ components. The BE values of S 2p components are assigned to sulphides

[199], [211] and or S which partly substitute O from the phosphate chain and form zinc (thio)phosphate [76].

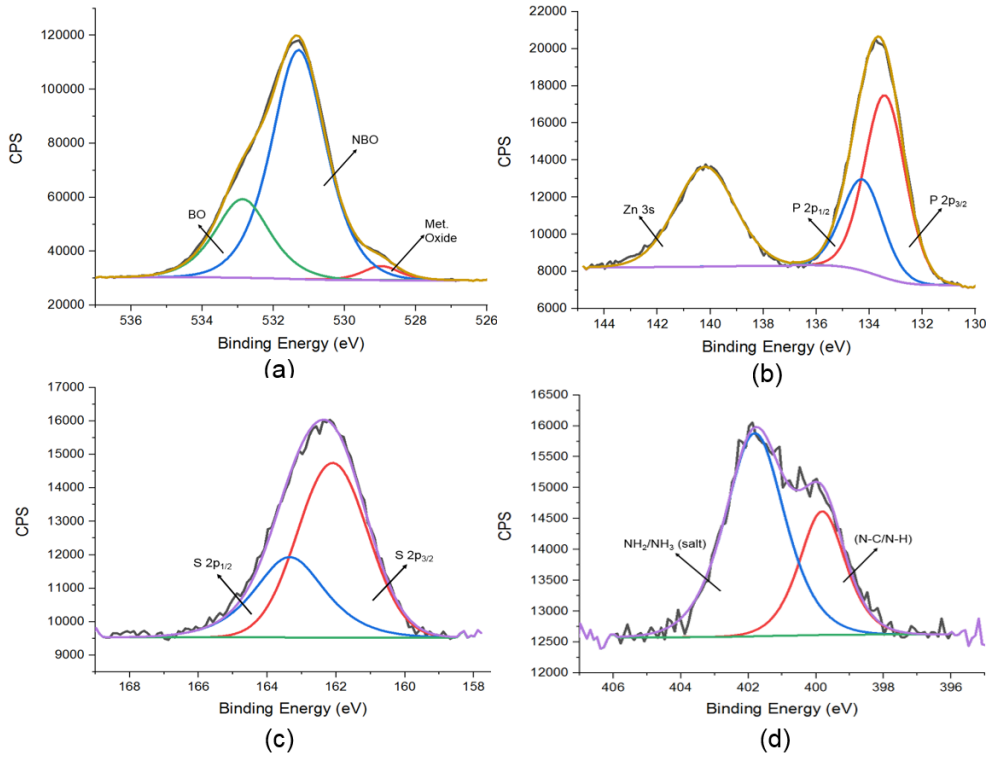

Figure 8-17. HR XPS spectra of the key elements in BO + FM 14 + ZDDP tribofilm

(a) O 1s (b) P 2p and Zn 3s (c) S 2p (d) N 1s

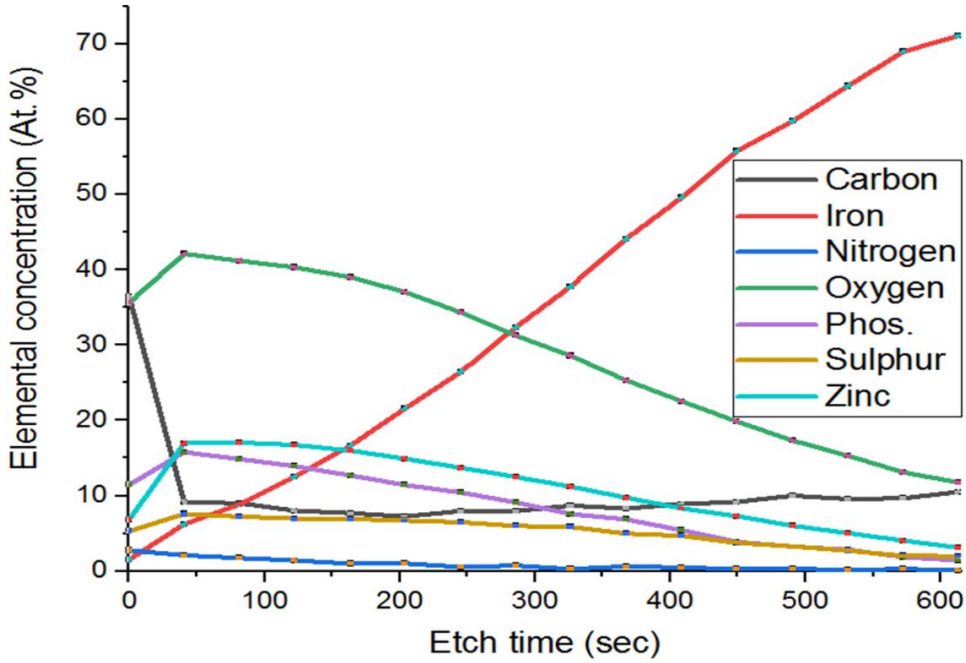

Figure 8-18. The depth profile of the tribofilm formed by BO + FM 14 + ZDDP

The N 1s signal is resolved into two components which corresponds to N-C/N-H group and NH_2/NH_3 salt [165], [174]. Figure 8-18 shows the XPS depth-profiling graph of the tribofilm formed by BO + FM 14 + ZDDP. The results revealed that the overall concentration of P, Zn, and O is reduced. The tribofilm is found comparatively rich in S, which is incorporated across the tribofilm in the form of sulphides species. The Fe concentration increased sharply with the etching time.

Table 8-6. Elemental concentration ratios after each sputter cycle in the tribofilm formed by addition of FM 14

Etch. time (sec)	P/S	P/Zn	P/O	P/Fe	Zn/S	Fe/S
0	2.07	1.67	0.32	7.51	1.24	0.28
40.7	2.08	0.93	0.38	2.53	2.23	0.82
81.8	2.06	0.87	0.36	1.68	2.36	1.23
122.6	1.99	0.83	0.35	1.11	2.39	1.80
163.5	1.83	0.79	0.33	0.76	2.30	2.40
203.9	1.70	0.77	0.31	0.53	2.22	3.21
244.9	1.61	0.76	0.30	0.40	2.11	4.06
285.9	1.52	0.73	0.29	0.28	2.08	5.40
326.3	1.29	0.67	0.26	0.20	1.91	6.43
367.3	1.38	0.70	0.27	0.16	1.96	8.84
408.3	1.15	0.65	0.24	0.11	1.77	10.52
449.3	1.03	0.53	0.20	0.07	1.95	14.87
490.3	0.98	0.54	0.19	0.05	1.82	17.98
531.3	1.05	0.56	0.19	0.04	1.86	23.76
572.3	0.92	0.46	0.14	0.03	2.00	33.97

Table 8-6 shows a decrease in P/S, P/Zn, P/O and P/Fe elemental concentration ratios from the top surface to the deeper in the tribofilm, whereas an increase in Zn/S and Fe/S elemental concentration ratio are also recorded. The presence of sufficient Fe in the bottom layer of the tribofilm suggested a possible formation of more Fe species.

8.4 Binding energy values of key elements of the tribofilm and tribofilm elemental comparison

The composition and length of the phosphate chains vary across the tribofilm [82], [84], [218] and these variations affect the tribological performance of the tribofilm [15], [206]. The chemical shift of P 2p signal towards lower BE value and an increase in Zn concentration in the bulk of the tribofilm confirmed a modification in the phosphate chain length [77], [186], [204]. Table 8-7 shows the BE values of key constituents of the tribofilm.

Table 8-7. Binding energy values of key elements at top surface of the tribofilm

Element		**BO + ZDDP + (eV)**	**FM 1 (eV)**	**FM 4 (eV)**	**FM 8 (eV)**	**FM 10 (eV)**	**FM 14 (eV)**
O 1s	NBO	531.49	531.34	531.11	531.24	531.48	531.29
	BO	533.04	532.92	532.78	532.75	532.97	532.87
O 1s	Fe_xO_y/ ZnO	----	529.86	529.57	530.0	528.46	528.97
P $2p_{3/2}$	P_xO_y	133.65	133.4	133.0	133.2	133.62	133.41
S $2p_{3/2}$	Fe_xS_y/ ZnS	162.15	161.9	161.61	161.49	162.40	162.10
S 2p	Sulphate	----	167.55	168.43	----	----	----
Zn $2p_{3/2}$	ZnO/ ZnS	1022.19	1021.71	1021.76	1021.77	1022.24	1021.90
Zn 3s		140.33	140.28	139.78	139.82	140.37	140.19
N 1s	N-Zn	----	398.35	----	----	----	----
	N-C/N-H	----	399.67	399.7	399.75	----	399.81
	NH_2/NH_3	----	----	401.7	401.59	----	401.81
ΔBE (Zn 3s – P $2p_{3/2}$)		6.68	6.88	6.78	6.62	6.75	6.78

The addition of OFM in the blend with ZDDP chemically shifted the P $2p_{3/2}$ component towards the lower BE values but the Zn 3s peak value is more or

less detected at a very similar positions. The Zn 3s – P $2p_{3/2}$ difference suggested that the addition of OFM in the blend with ZDDP modified the glass composition [77], [186], [204] of the tribofilm and this change varies with the addition of different OFMs in the blend with ZDDP. The BE of P $2p_{3/2}$ signal is found between 133.0-133.62 eV, which does not corresponds to long chain phosphate [204], [208], [217]. The tribofilm formed by the addition of different OFMs are expected to be a mix of pyrophosphate and orthophosphate [204].

The XPS depth profiling graphs (Figures 8-10, 8-12, 8-14, 8-16 and 8-18), showed that addition of OFM with ZDDP affected the elemental incorporation which ultimately disturbed the tribofilm formation capability of ZDDP. Figure 8-19 shows the incorporation of the key constituents of the tribofilms formed by blend of OFM and ZDDP along with BO + ZDDP. Figure 8-19 (a) shows that the concentration of P in the tribofilm is reduced with the addition of N containing OFMs in the blend with ZDDP. The P concentration is slightly reduced with the addition of FM 10 (i.e. alcohol ethoxylate) in the blend with ZDDP and furthermore it followed a similar P incorporation trend as observed in the tribofilm formed with the lubricant blend of BO + ZDDP. Figure 8-19 (b) shows that the tribofilm formed with the addition of N containing OFMs are found rich in S. Interestingly blend of FM 10 with ZDDP showed very similar incorporation trend as found in the tribofilm formed by BO + ZDDP.

Figure 8-19 (c) shows the Zn incorporation in the tribofilms formed with the addition of OFMs and ZDDP. Highest concenrtration of Zn is observed with the lubricant blend of FM 8 and ZDDP, whereas the tribofilm formed with the addition of FM 14 with ZDDP offered comparatively less Zn concentration. The Zn concentration in tribofilms having FM 8 and FM 14 reduced steeply and hence less concentration of Zn is available near the substrate as compare to top half of the tribofilm. The lubricant blend of FM 10 and ZDDP followed same pattern of Zn incorporation as produced by BO + ZDDP with reduced concentration. The tribofilm formed with the addition of FM 1 and FM 4 showed less concentration of Zn through out the tribofilm. Figure 8-19 (d) shows the O incorporation graph in the tribofilms. The blend of BO + ZDDP offered highest concentration of O and interestingly addition of FM 10 with ZDDP slightly reduced O concentration in the tribofilm. The concentration of O is reduced sharply with the addition of N based OFMs in the blend.

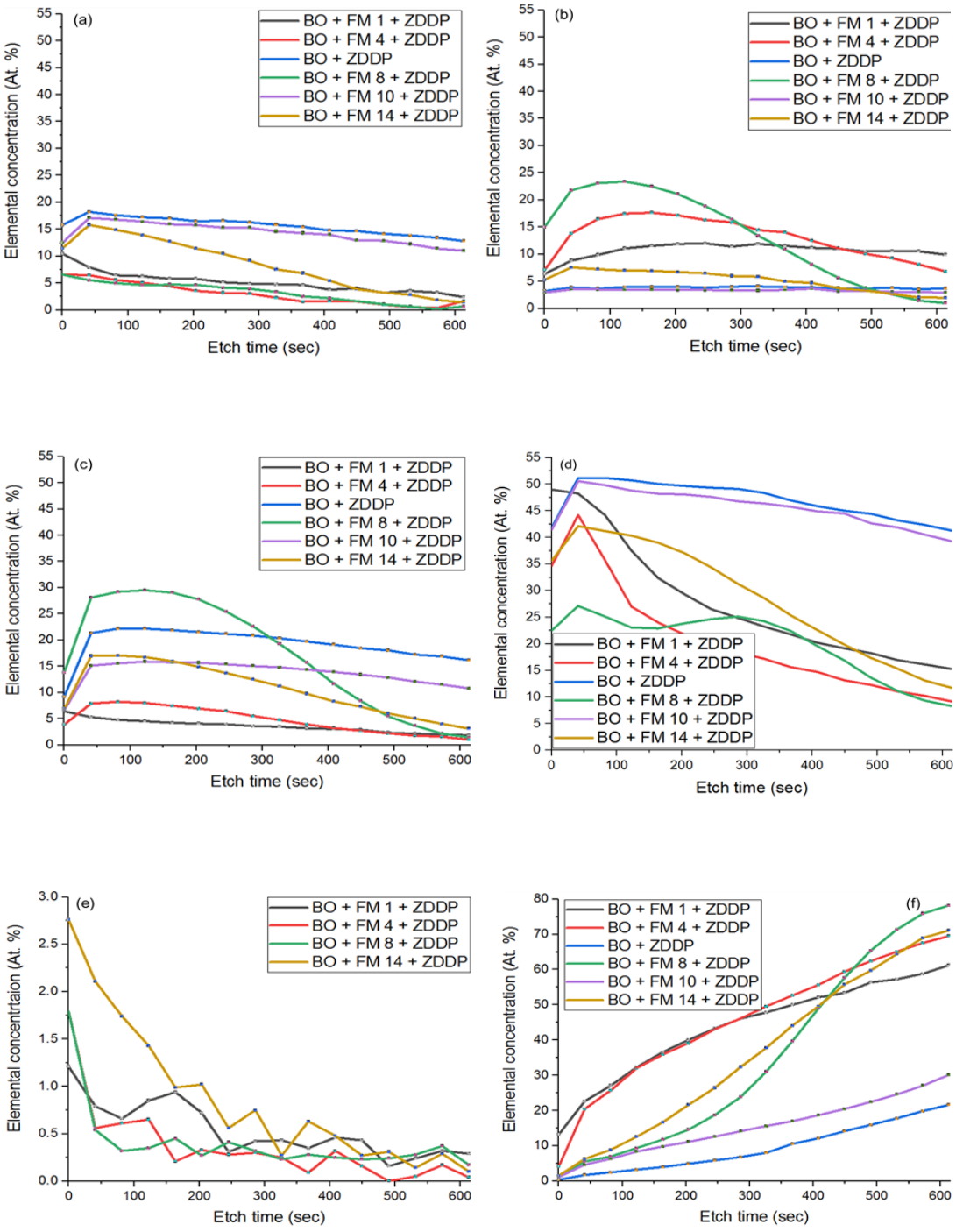

Figure 8-19. The depth profile of key constituents of the tribofilms

(a) Phosphorous (b) Sulphur (c) Zinc (d) Oxygen (e) Nitrogen (f) Iron

Figure 8-19 (e) shows that N is well incorporated through out the tribofilm. The highest concentration of N is recorded in the trobiflm formed with the addition of FM 14 and ZDDP in the lubricant blend. Similar N incorporation trends are observed in the tribofilm formed with the addition of FM 4 and FM 8, whereas

slightly different incorporation behaviour of N is observed in the tribofilm formed with the blend having FM 1 and ZDDP. The Fe incorporation graph showed in Figure 8-19 (f). The tribofilm formed with BO + ZDDP showed no Fe content at the top most surface but with subsequent etching Fe concentration is increased. The Fe concentration is observed at the top most surface of the tribofilm with the addition of OFMs in the blend with ZDDP. Furthermore, significant increase in Fe concentration is recorded with subsequent etching cycles.

8.5 Phosphorous chemical structure with tribofilm thickness

The XPS analysis of P 2p signal from the top most surface of the tribofilm and the P species found after few etching cycles provided a good indication about modification in P chemical structure. Figure 8-20 shows the XPS scan of P 2p signal (at the top most surface and after few etching cycles) of the tribofilm formed by BO + ZDDP. No significant modification in the chemical state of P 2p signal is observed even after few etching cycles. Figures 8-21, 8-22, 8-23, 8-24 and 8-25 show the XPS scans of P 2p signal of the tribofilm formed by the addition OFMs and ZDDP in the lubricant blend.

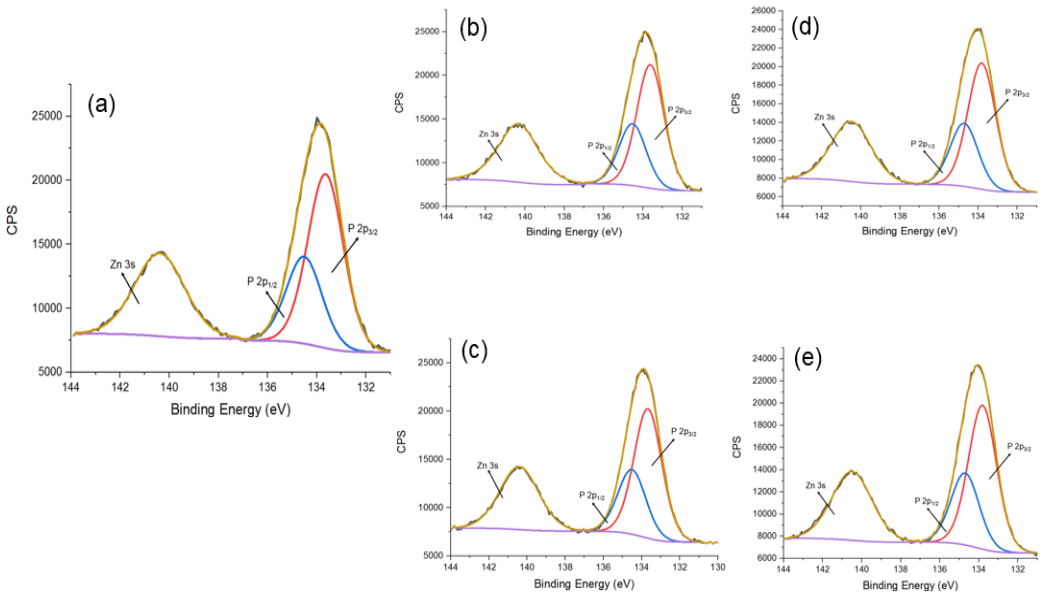

Figure 8-20. The XPS scan of P 2p signal of the tribofilm formed by BO + ZDDP

(a) Upper most surface (before etching) (b) After 1st etching cycle (c) After 2nd etching cycle (d) After 3rd etching cycle (e) After 4th etching cycle

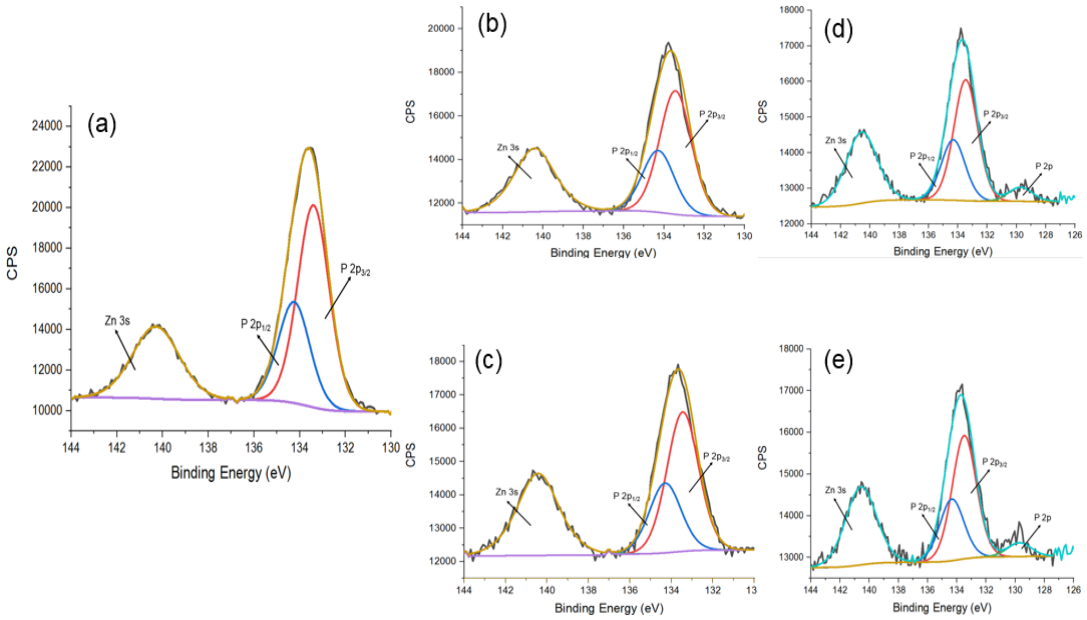

Figure 8-21. The XPS scan of P 2p signal of the film formed by BO + FM 1 + ZDDP

(a) Upper most surface (before etching) (b) After 1st etching cycle (c) After 2nd etching cycle (d) After 3rd etching cycle (e) After 4th etching cycle

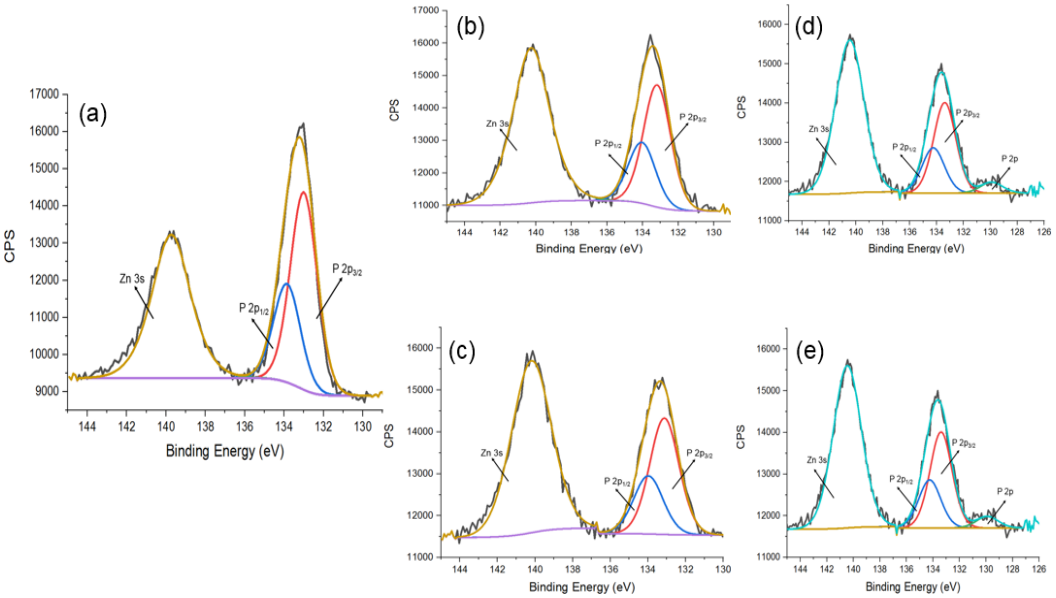

Figure 8-22. The XPS scan of P 2p signal of the film formed by BO + FM 4 + ZDDP

(a) Upper most surface (before etching) (b) After 1st etching cycle (c) After 2nd etching cycle (d) After 3rd etching cycle (e) After 4th etching cycle

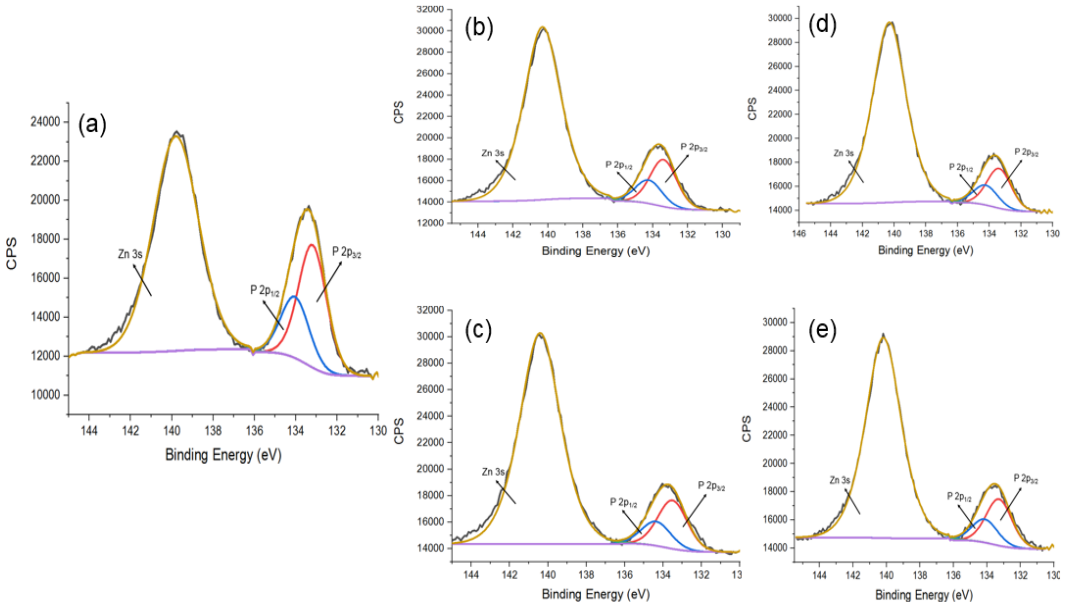

Figure 8-23. The XPS scan of P 2p signal of the film formed by BO + FM 8 + ZDDP

(a) Upper most surface (before etching) (b) After 1st etching cycle (c) After 2nd etching cycle (d) After 3rd etching cycle (e) After 4th etching cycle

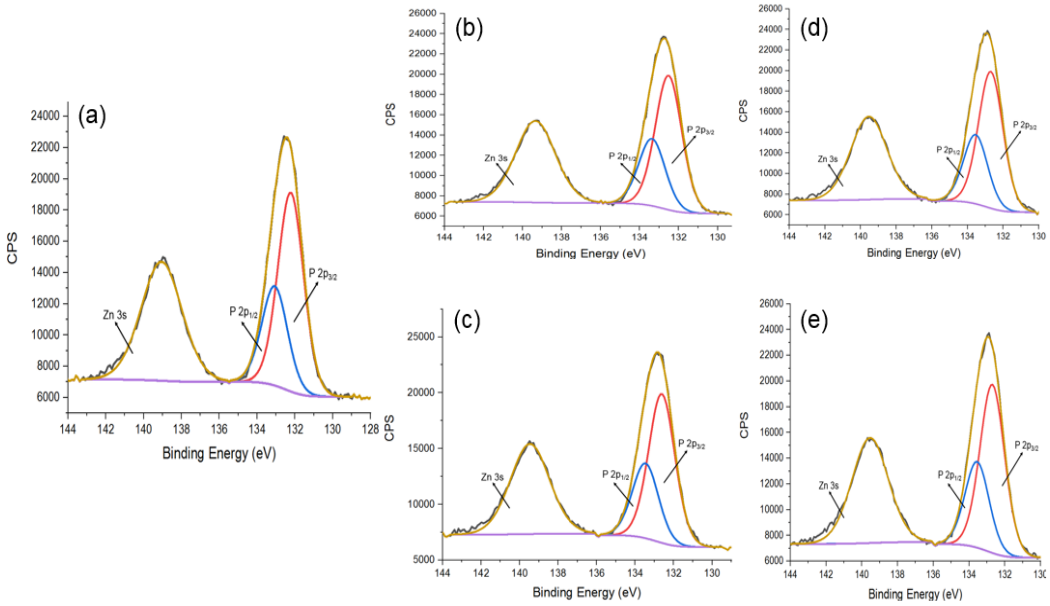

Figure 8-24. The XPS scan of P 2p signal of the film formed by BO + FM 10 + ZDDP

(a) Upper most surface (before etching) (b) After 1st etching cycle (c) After 2nd etching cycle (d) After 3rd etching cycle (e) After 4th etching cycle

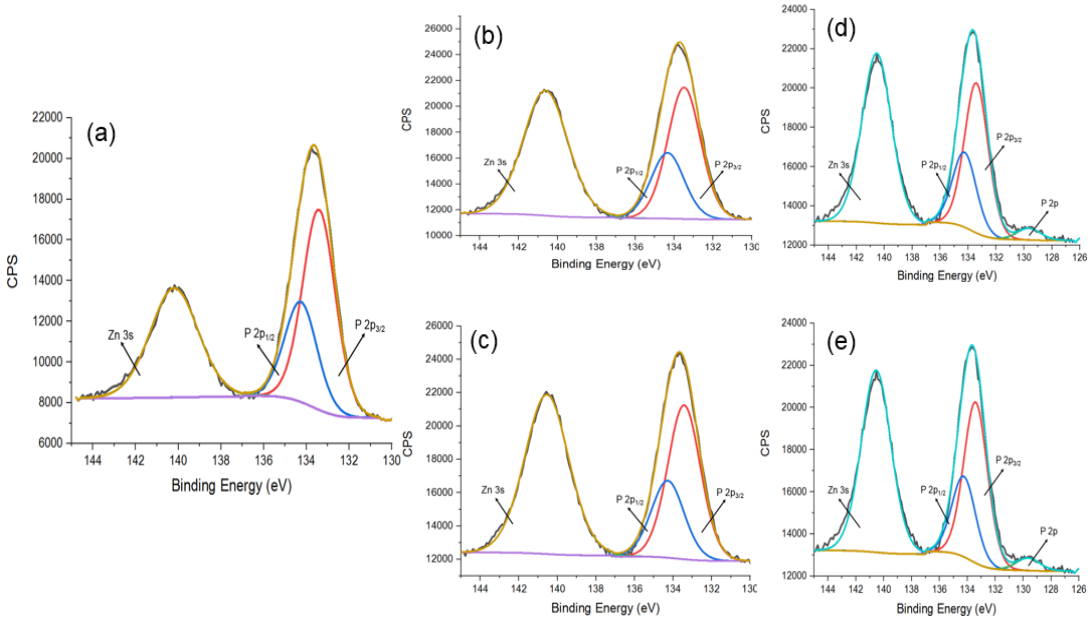

Figure 8-25. The XPS scan of P 2p signal of the film formed by BO + FM 14 + ZDDP

(a) Upper most surface (before etching) (b) After 1st etching cycle (c) After 2nd etching cycle (d) After 3rd etching cycle (e) After 4th etching cycle

The etching results confirmed that addition of few OFMs modified the chemical state of P 2p signal deeper in the tribofilm. After few etching cycles an additional phosphorous peak is observed in the same BE window just before the phosphate peak. The results in Figures 8-21, 8-22 and 8-25 showed an additional peak after 3rd and 4th etching cycles. These tribofilms are formed by the addition of FM 1, FM 4 and FM 14 with ZDDP in the lubricant blend.

Table 8-8. Binding energy values of additional P 2p peak detected in the tribofilms

Etching cycle	BO + ZDDP + (eV)	FM 1 (eV)	FM 4 (eV)	FM 8 (eV)	FM 10 (eV)	FM 14 (eV)
After 3rd etching cycle	……	129.73	129.91	……	……	129.70
After 4th etching cycle	……	129.72	129.80	……	……	129.65

The BE values of the additional peak are assigned to iron phosphide/zinc phosphide [199], [211], [219]. No additional peak is detected in the tribofilms formed by the addition of FM 8 and FM 10 as showed in Figure 8-23 and

8-24. Table 8-8 shows the BE values of the additional peak detected in the tribofilms formed by FM 1, FM 4 and FM 14.

The XPS results revealed that the addition of OFM with ZDDP modified the elemental/chemical composition of the tribofilm. This modification in chemical composition of the tribofilm affected the AW capability of ZDDP but the level of disturbance again varied from one friction modifier to other. The interaction of a couple of OFMs with ZDDP contributed to a significant increase in the wear factor value whereas the interaction of some of the OFMs showed synergism with ZDDP and reduced the wear factor value remarkably. The possible interaction mechanisms of these OFMs will be discussed in the last chapter.

8.6 Summary

This chapter covered the modifications emerged in the elemental/chemical composition of the tribofilm by the addition of OFM with ZDDP (1:1 molar ratio of FM to ZDDP). The initial part of this chapter focussed on the elemental composition of the tribofilm formed by the addition of OFM with ZDDP using SEM-EDX analysis. Since EDX penetrates well across the tribofilm thickness and can provide elemental composition of the substrate, the XPS was used to complement the EDX results.

The elemental mapping results confirmed that,

- The tribofilm formed by BO + ZDDP showed strong elemental intensity of Zn, P, S and O. The strong presence of these key tribological elements inside the wear track confirmed the formation of phosphate film
- Addition of FM 1 with ZDDP modified the elemental intensity of the tribofilm and as a result S concentration is increased
- Addition of FM 4 with ZDDP showed a stronger presence of S in comparison to Zn and P. The EDX result revealed that the tribofilm formed with the addition of FM 4 with ZDDP is S dominated
- Addition of FM 8 with ZDDP displayed a strong presence of S and Zn, which indicated that the tribofilm formed with the addition of FM 8 is S-dominated
- Addition of FM 10 with ZDDP indicated the formation of zinc phosphate tribofilm inside the wear track. The mapping results indicated that the elemental composition of the tribofilm is not significantly modified with the addition of FM 10 in the blend with ZDDP
- Addition of FM 14 with ZDDP showed a strong presence of Zn, S and P. The EDX spectrum confirmed that the tribofilm formed with the addition of FM 14 in the blend with ZDDP is Zn-dominated

Overall addition of OFMs modified the elemental composition of the tribofilm in-comparison to the tribofilm formed by BO + ZDDP.

The XPS results confirmed that,

- ZDDP formed tribofilm inside the wear track. No metal oxide peak was found in O 1s signal
- The depth profile graph showed a decrease in P, Zn and O concentration, whereas no significant change in S concentration is observed
- The tribofilm formation capability of ZDDP is disturbed due to addition of FM 1 in the blend and as a result metal oxide peak is detected in O 1s signal. Interaction of N, with Zn and phosphate indicated that amine FM disturbed the zinc phosphate formation capability of ZDDP at some extent
- The depth-profiling of the tribofilm revealed that overall concentration of P, Zn and O is comparatively reduced whereas S and Fe content increased. Fe concentration is increased significantly with the etching time
- The tribofilm formation capability of ZDDP was disturbed due to addition of FM 4 and as result O 1s signal showed prominent metal oxide peak
- The depth-profile graph showed that concentration of P, Zn and O is decreased remarkably whereas tribofilm found rich in S and Fe. The depth profiling result showed availability of more Fe deeper in the tribofilm. The N is incorporated up to middle of the tribofilm and may contribute the possible formation of amine/ammonium phosphate
- Modification in chemical composition of the tribofilm formed with the addition of FM 8 and ZDDP in the blend. Presence of strong Zn 3s signal indicated modification in phosphate chain length as compared to tribofilm formed by BO + ZDDP. Deconvolution of the N 1s signal revealed formation of N-C/N-H bond, which could contribute to amine/ammonium phosphate formation
- The depth profiling results revealed that overall concentration of P and O is reduced. The tribofilm found to be rich in S and Zn. The XPS scan confirmed that S is primarily present in the form of sulphides, which means possibly more metal sulphide species may form deeper in the tribofilm

- The presence of metal oxide peak in O 1s signal indicated that the tribofilm formed by blend of FM 10 with ZDDP is relatively less effective as compared to BO + ZDDP
- The depth-profiling graph revealed that addition of FM 10 in the blend with ZDDP slightly modify the elemental composition of the tribofilm. Result displayed that elemental concentration and incorporation trend of P, S and O across the tribofilm is more or less very much similar as observed in the tribofilm formed by BO + ZDDP
- The presence of metal oxide peak in O 1s signal indicated that addition of FM 14 with ZDDP in the blend modified the tribofilm composition. The P 2p signal indicated formation of pyrophosphate or polyphosphate, whereas the BE of S 2p components are assigned to sulphides and or sulphur which partly substitute oxygen from the phosphate chains and form zinc (thio)phosphate. The deconvolution of N 1s signal revealed formation N-C/N-H bond, which could contribute to amine/ammonium phosphate formation
- The depth profiling results revealed that overall concentration of P, Zn, O and S is reduced. Tribofilm was found rich in S, which is incorporated across the tribofilm in the form of metal sulphides. The Fe concentration is increased sharply with the etching time
- The etching of the tribofilm formed with the addition of N containing OFMs (except FM 8), suggested evolution of new phosphorous peak in the same BE window just before P 2p peak. These BE values are assigned to iron phosphide/zinc phosphide

Chapter 9
Organic friction modifier ZDDP interaction; sequential film formation and chemical composition of the tribofilm

9.1 Introduction

Addition of OFM and ZDDP in the lubricant blend modified the morphology and elemental/chemical composition of the tribofilm (discussed in Chapter 7 and 8). The EDX/XPS results confirmed that addition of OFM modified the elemental/chemical composition of the tribofilm and this modification varied from one OFM to other which ultimately reflected in the wear behaviour. The tribofilm formed with the addition of amine FMs and ZDDP in the lubricant blend found rich in S and Zn instead of P (Chapter 8). This results chapter is specifically designed to explore the interaction of amine based FMs (i.e. FM 1, FM 4, FM 8 and FM 14) with ZDDP and for this purpose, the sequential film formation tests were conducted.

9.2 Sequential tribofilm formation

The sequential film formation tests were designed to explore the possible sequence of film formation with single additive systems. In these tribological tests, the tribofilm is initially formed with BO + ZDDP in the first half of the test and then in the second half of the test the lubricant oil (i.e. BO + ZDDP) is replaced with BO + OFM and the tribofilm is formed on top of the pre-formed ZDDP tribofilm or vice versa. These tests were conducted for three different time durations (i.e. 30, 60 and 120 minutes). A detailed test methodology was presented in Experimental Methods and Materials chapter (i.e. Chapter 5). The basic purpose of these tests are,

- To analyse the friction behaviour of BO + OFM and BO + ZDDP in sequential film formation and on the steel surface
- To analyse the overall impact of sequential film formation tests on wear performance
- To analyse modification in elemental composition of the tribofilm and possible film formation mechanism

Tribological tests were performed on TE 77 (high frequency friction machine). Working details of TE 77 machine, test parameters and experimental setup are discussed in Chapter 5.

9.2.1 Friction and wear behaviour of FM 1 and ZDDP

Figures 9-1(a), 9-1(b) and 9-1(c) display the friction behaviour of FM 1 (i.e. coco amine) and ZDDP in the sequential film formation experimental set up for three different time durations (i.e. 30, 60, 120 minutes). The friction result of BO + FM 1 + ZDDP (continuous test for the entire duration) is also included for comparison purposes. The friction results revealed that for all test durations blend of BO + FM 1 showed higher coefficient of friction (COF) on the steel surface (very close to the COF value of ZDDP on the steel surface) but relatively lower COF on top of pre-formed ZDDP tribofilm. The results exhibited that FM 1 has the capability to form a film on top of the ZDDP tribofilm. The tribofilm formed by BO + ZDDP offered higher COF (i.e. around 0.1), on the steel surface but on top of the pre-formed film of FM 1, the COF value is decreased. Reduction in COF value indicated possible hindrance in the film formation potential of ZDDP. The tribofilm formed by the blend of BO + FM 1 + ZDDP showed very similar COF as observed by BO + ZDDP on top of the pre-formed film of BO + FM 1 (60 and 120 minutes). The similar friction behaviour of these two lubricant blends specified possible interaction sequence.

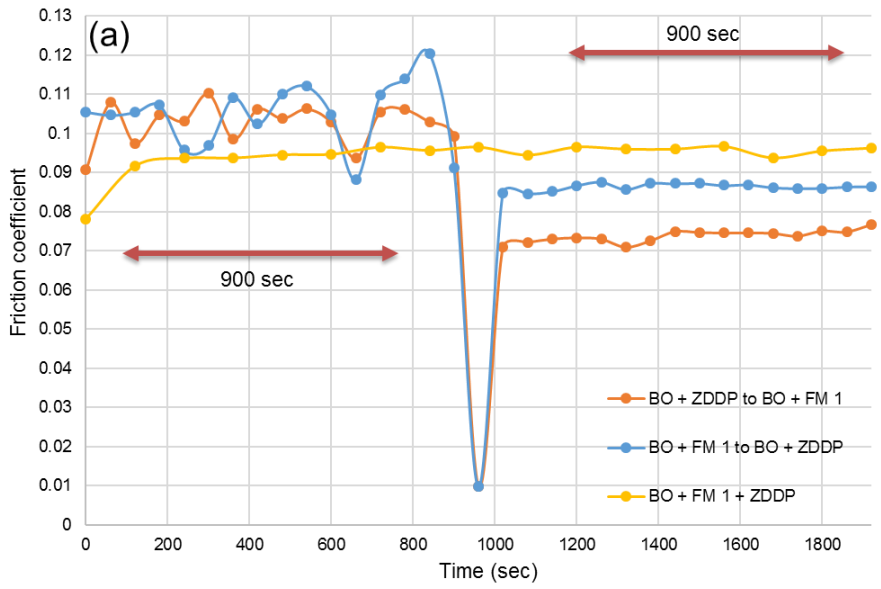

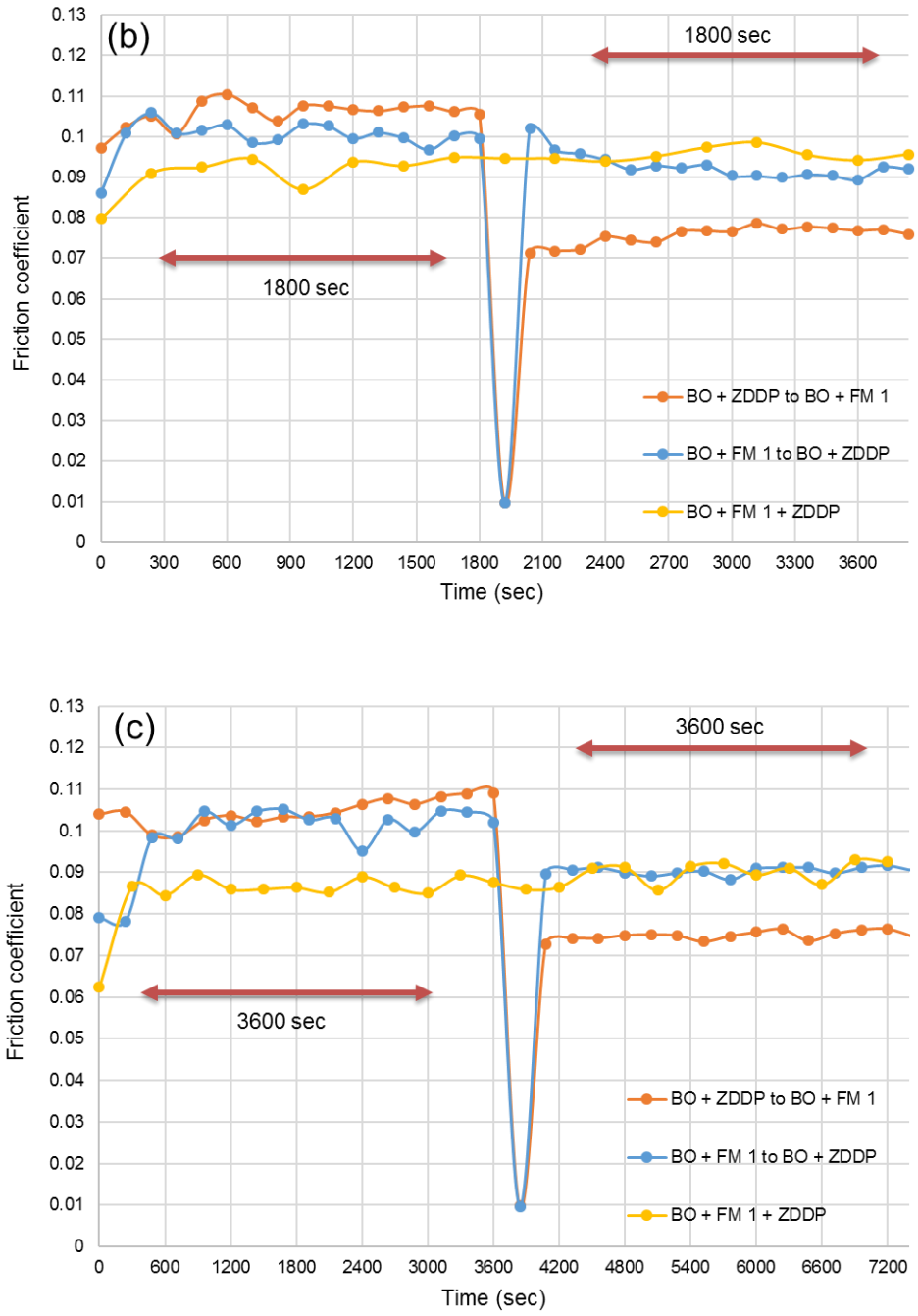

Figure 9-1. The friction behaviour of FM 1 and ZDDP along with BO + FM 1 + ZDDP

(a) 1800 sec (b) 3600 sec (c) 7200 sec

The wear result in Figure 9-2 shows a fascinating result. The sequential tribological tests produced more or less similar wear results. For the continuous test (i.e. BO + FM 1 + ZDDP), the wear volume is substantially higher than the sequential film formation tests between ZDDP and FM 1. This will be discussed later in this thesis.

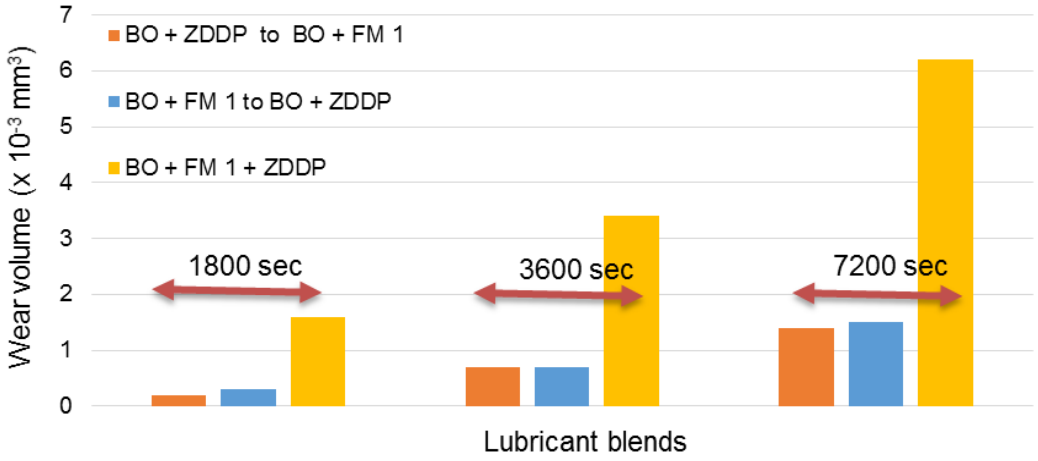

Figure 9-2. The wear behaviour of FM 1 and ZDDP along with BO + FM 1 + ZDDP

9.2.2 Friction and wear behaviour of FM 4 and ZDDP

Figures 9-3(a), 9-3(b) and 9-3(c) show the friction behaviour of FM 4 (i.e. ethoxylated hydrogenated tallow amine) and ZDDP in tests using the sequential film formation experimental set up for three time durations. The friction result of BO + FM 4 + ZDDP (continuous test for the entire duration) is also included for comparison purposes. The interaction of FM 4 and ZDDP produced slightly different friction behaviour as compared to the sequential film formation tests of FM 1 and ZDDP.

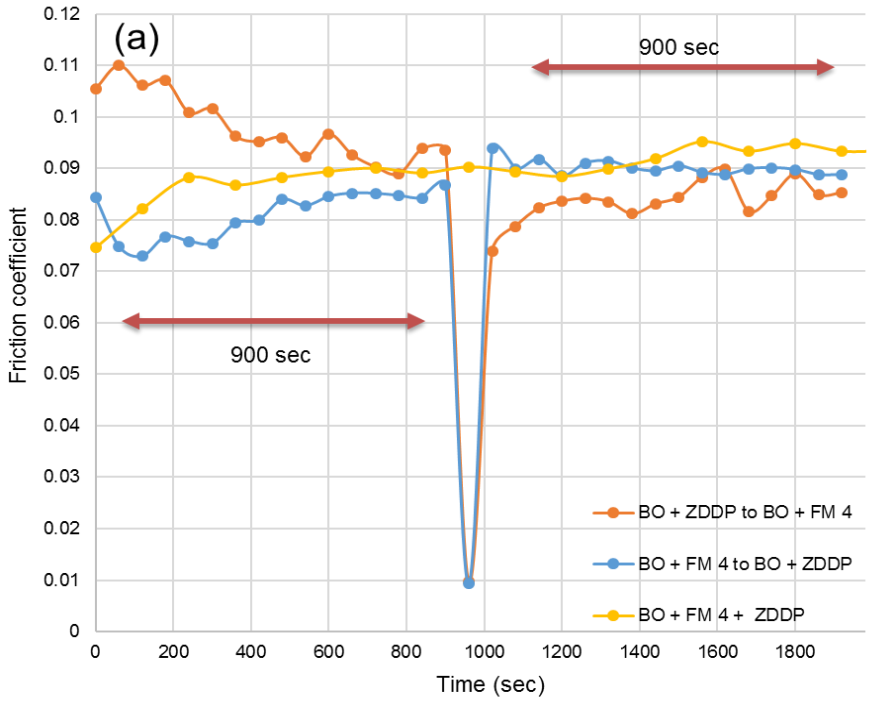

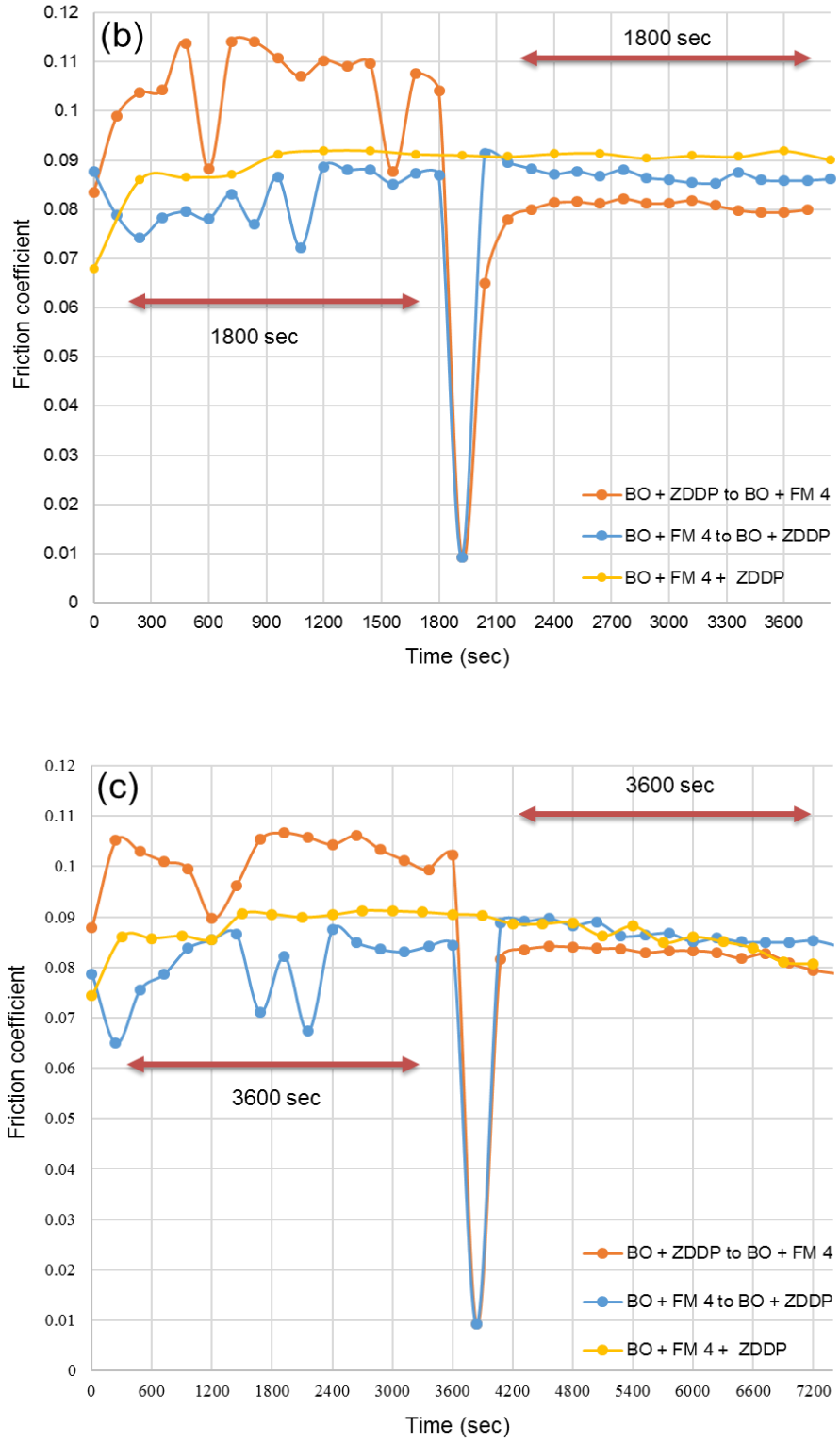

Figure 9-3. The friction behaviour of FM 4 and ZDDP along with BO + FM 4 + ZDDP

(a) 1800 sec (b) 3600 sec (c) 7200 sec

The lubricant blend of FM 4 showed relatively low COF on the steel surface. Furthermore, on top of pre-formed ZDDP tribofilm, the COF value is further

decreased. The friction results clearly exhibited that FM 4 has the capability to form a film on top of the ZDDP tribofilm and reduce the high COF value. The tribofilm formed by BO + ZDDP showed higher COF on the steel surface but on top of pre-formed film of BO + FM 4, an even lower COF value is recorded. Reduction in the COF value of ZDDP on top of a pre-formed layer of FM 4 indicated some disturbance in formation of the zinc phosphate film. The friction results clearly revealed that the blend of BO + FM 4 + ZDDP exhibited COF value very close to the value exhibited by the film formed by BO + ZDDP on top of the pre-formed layer of BO + FM 4. Resemblance in friction response of these two tribofilms indicated that the sequential film formed by FM4 and ZDDP have similar interaction mechanisms.

The wear result in Figure 9-4 shows very similar wear behaviour as observed previously with FM 1. The sequential tribological tests produced similar wear results. For the continuous test (i.e. BO + FM 4 + ZDDP), the wear volume is substantially higher than the sequential film formation tests between ZDDP and FM 4.

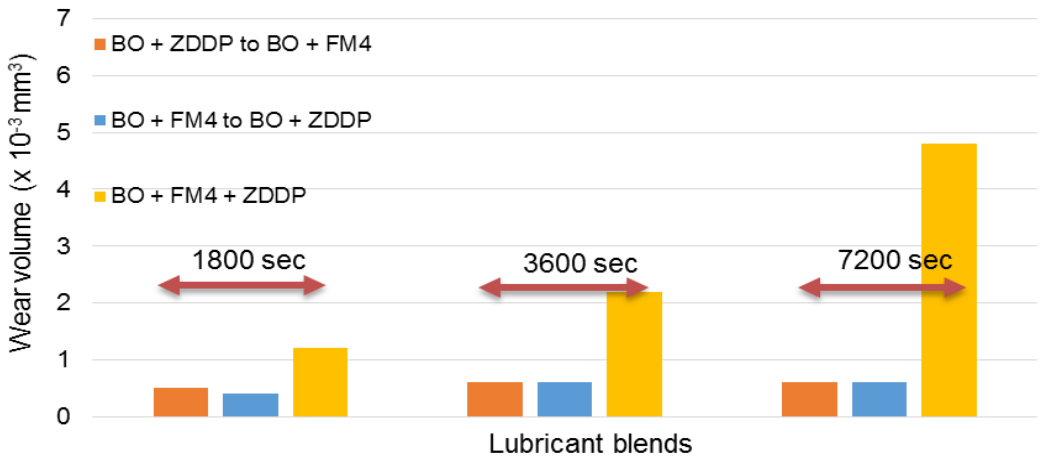

Figure 9-4. The friction behaviour of FM 1 and ZDDP along with BO + FM 4 + ZDDP

9.2.3 Friction and wear behaviour of FM 8 and ZDDP

The friction behaviour of FM 8 (i.e. tallow amine) and ZDDP in tests using the sequential film formation experimental set up for three time durations are showed in Figures 9-5(a), 9-5(b) and 9-5(c). The friction result of BO + FM 8 + ZDDP (continuous test for the entire duration) is also included in

this graph. The lubricant blend of BO + FM 8 showed higher COF on steel surface (very close to the COF value produced by the BO + ZDDP tribofilm). The COF value is reduced when FM 8 formed a film on the surface having pre-formed ZDDP tribofilm, which indicated that FM 8 has the capability to form a film on top of ZDDP tribofilm.

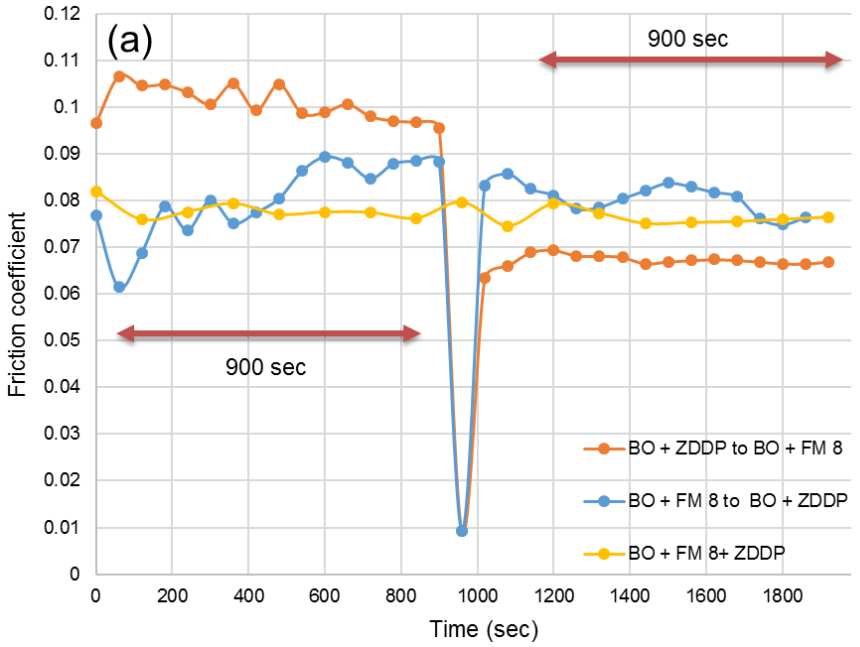

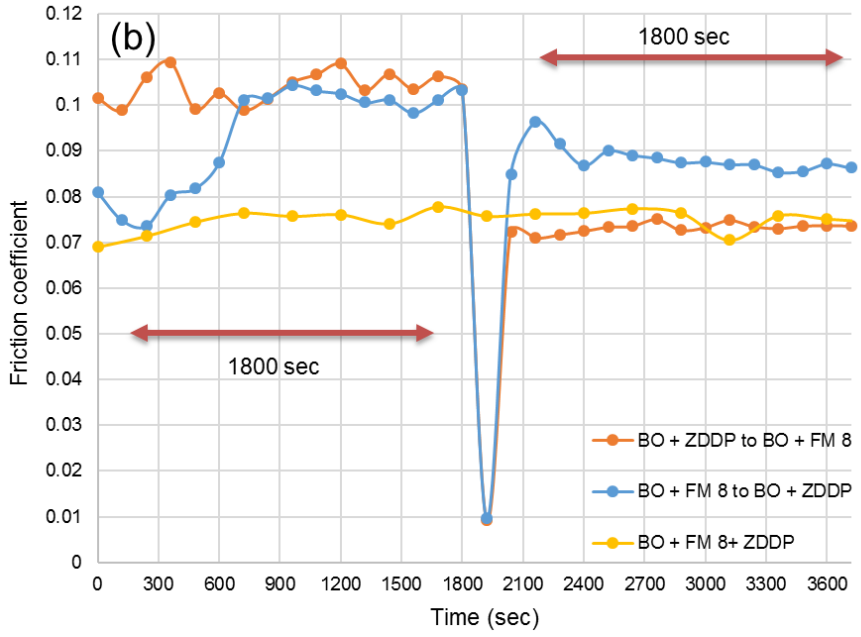

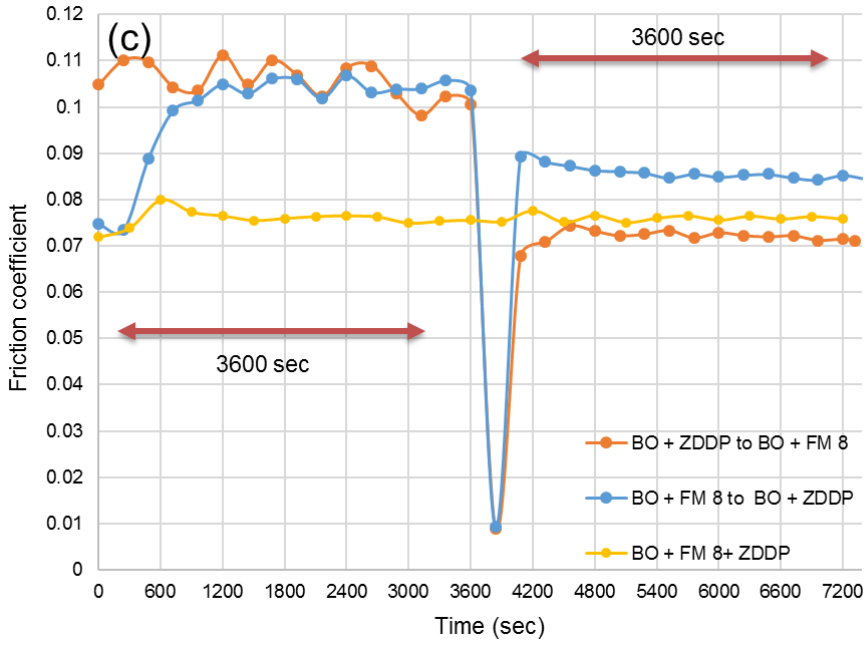

Figure 9-5. The friction behaviour of FM 8 and ZDDP along with BO + FM 8 + ZDDP

(a) 1800 sec (b) 3600 sec (c) 7200 sec

The blend of BO + ZDDP offered higher COF value on the steel surface but the COF value is reduced when zinc phosphate film is formed on top of a film formed by FM 8. Similar friction behaviour was observed with FM 1 and FM 4 and it indicated that FM 8 also has the potential to restrict the tribofilm formation capability of ZDDP. The COF value of BO + FM 8 + ZDDP (continuous test) found close to the friction values exhibited by BO + FM 8 on top of pre-formed ZDDP tribofilm (60 and 120 minutes) in sequential film formation tests, which indicated similarities in the interaction sequence between FM 8 and ZDDP.

The wear graph in Figure 9-6 shows different wear behaviour from previous two amine FMs (i.e. FM 1 and FM 4). FM 8 and ZDDP displayed very similar wear volume in both scenarios whether FM 8 or ZDDP formed film first on the steel surface. When both additives were there for the entire test period, the wear was much lower. Synergistic wear behaviour between FM 8 and ZDDP suggested that FM 8 offered low or no interference in tribofilm formation capability of ZDDP but it interacted with the zinc phosphate film and modified its chemical composition.

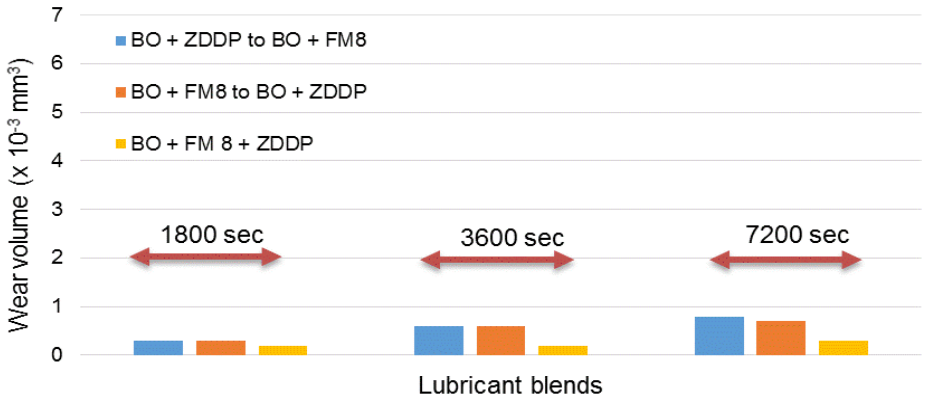

Figure 9-6. The wear behaviour of FM 8 and ZDDP along with BO + FM 8 + ZDDP

9.2.4 Friction and wear behaviour of FM 14 and ZDDP

The friction behaviour of FM 14 (i.e. triethanol amine with tallow fatty acid) and ZDDP in tests using sequential film formation experimental set up are showed in Figures 9-7(a), 9-7(b) and 9-7(c). The friction results of BO + FM 14 + ZDDP (continuous test for the entire duration) is also included for the comparison purpose. The blend of BO + FM 14 displayed similar COF values whether it formed film on the steel surfaces or surfaces having pre-formed ZDDP tribofilm. This friction behaviour indicated that FM 14 has the capability to form a film without any influence of surface. The tribofilm formed by BO + ZDDP showed higher COF on steel surface but COF value is reduced when zinc phosphate film is formed on top of the film formed by BO + FM 14.

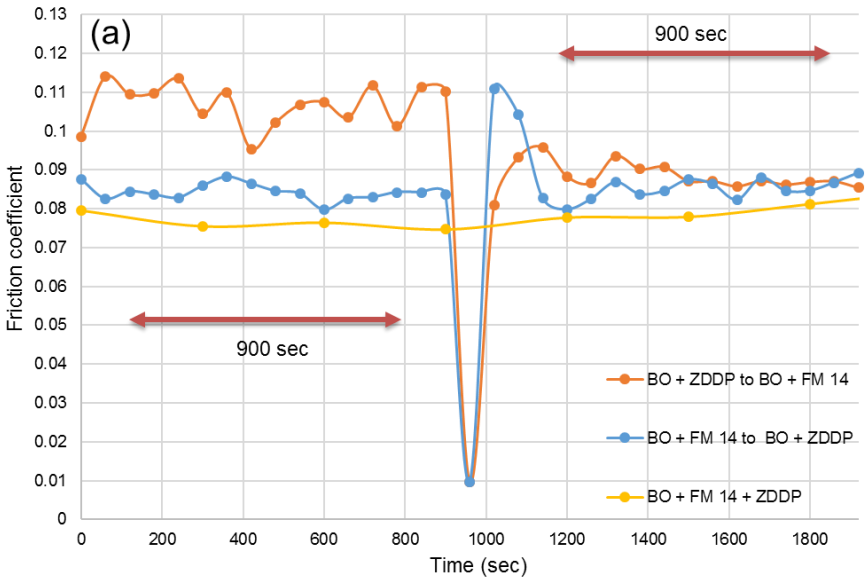

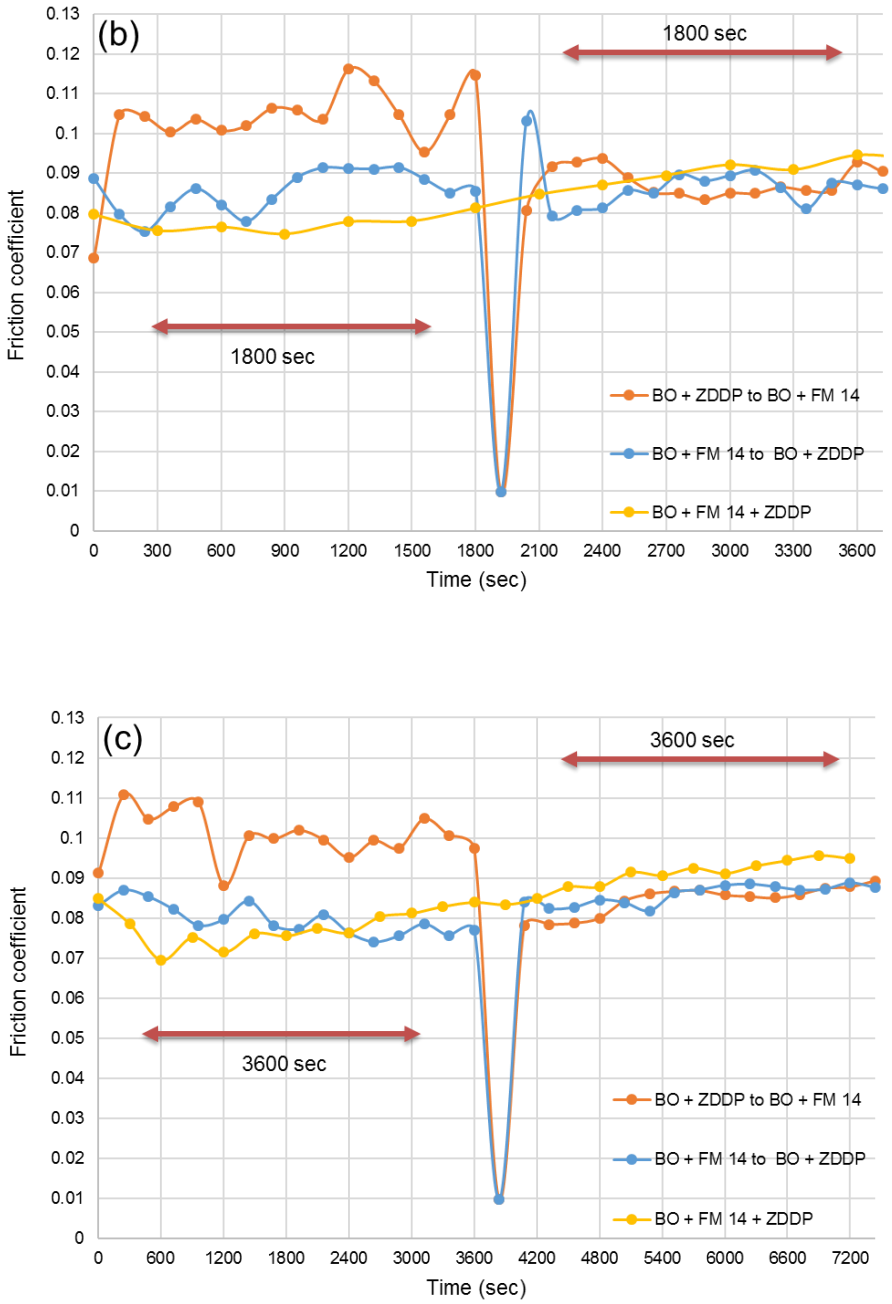

Figure 9-7. The friction behaviour of FM 14 and ZDDP along with BO + FM 14 + ZDDP

(a) 1800 sec (b) 3600 sec (c) 7200 sec

The friction results indicated that the blend of FM 14 has influenced or restricted the tribofilm formation capability of ZDDP. Similar COF values are observed whether blend of BO + FM 14 formed a film on top of the ZDDP tribofilm or ZDDP form a film on top of film formed by FM 14. Interestingly the blend of BO + FM 14 + ZDDP (continuous tests) displayed COF value close to the values observed in tests using sequential film formation experimental

set up. The similarity in friction behaviour in different tribological interactions indicated that interaction sequence between FM 14 and ZDDP is similar regardless of any influence of surface or mixing of both additives together in lubricant blend.

The wear graphs in Figure 9-8 shows similar wear trend whether FM 14 or ZDDP got the opportunity to form a film first on steel surface. Overall wear volume is increased in tribological tests using sequential film formation tests in comparison to other amine FMs (FM 1, FM 4 and FM 8). In continuous tribological test (i.e. BO + FM 14 + ZDDP), synergistic wear behaviour is observed but wear volume is slightly increased in comparison to FM 8 (which also showed synergistic wear behaviour).

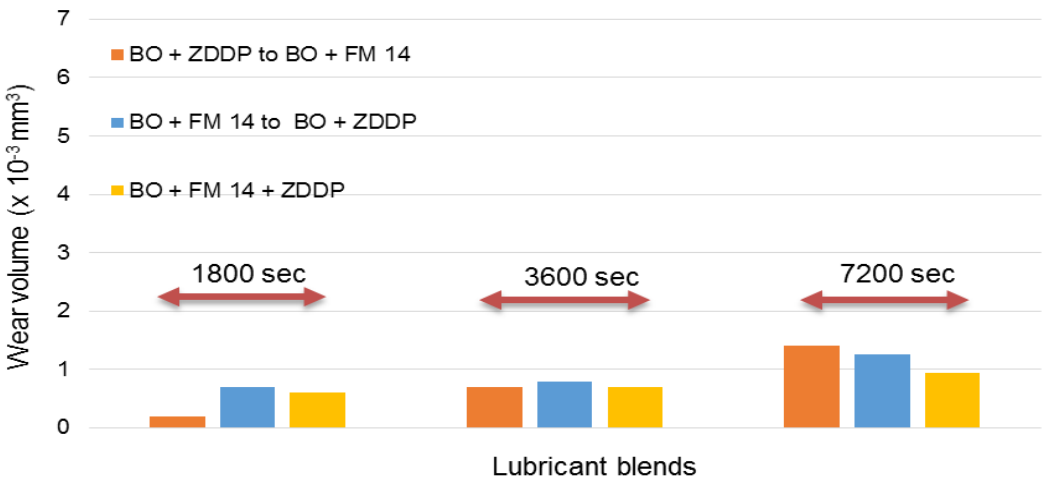

Figure 9-8. The wear behaviour of FM 14 and ZDDP along with BO + FM 14 + ZDDP

The overall findings from the sequential film formation experiments between amine FMs and ZDDP is summarized below;

- The COF value is reduced when amine FMs formed film on top of ZDDP tribofilm
- FM 1 displayed higher COF value on the steel surfaces as compared to FM 4, FM 8 and FM 14
- ZDDP showed higher COF values on the steel surfaces as compared to surfaces having a pre-formed amine FMs (i.e. FM 1, FM 4, FM 8 and FM 14) films

- FM 1 and FM 4 increased the wear volume significantly in continuous tribological testing
- FM 8 and FM 14 exhibited effective AW performance in continuous tribological testing

9.3 Chemical composition and quantification of the tribofilm

The tribofilm characterisation has been carried out to analyse the effect of amine FM on pre-formed ZDDP tribofilm (i.e. BO + ZDDP to BO + OFM). The XPS technique was used to analyse the tribofilms as it is a surface sensitive technique that provides information precisely about the tribofilm chemical composition [201], [202]. The XPS analysis was conducted to,

- Analyse chemical composition of the tribofilms formed as a result of tests using sequential film formation experimental set up

Etching of the tribofilm surfaces was also conducted in order to mitigate any contamination effect and to further,

- Analyse changes in elemental concentration across the tribofilm surface

The high resolution (HR) XPS scans of selected elements (i.e. P 2p, O 1s, S 2p, Zn 3s and N 1s) of the tribofilms are included in this chapter. After detailed XPS analysis of the top 5-8 nm of the tribofilm surface, the tribofilm is etched. The approximate etching time for each layer of the tribofilm was 160 seconds. The depth profile data provided the elemental quantification and changes in elemental concentration in the tribofilms formed because of sequential film formation tests.

9.3.1 Chemical composition of the tribofilm formed by ZDDP and FM 1

The XPS scans in Figure 9-9 shows presence of the key elements of the tribofilm inside the wear track. The O 1s signal is deconvoluted in two components. The major peak at has been assigned to the non-bridging oxygen (NBO) from the phosphate chains [77], [203], [207]–[210] and the other peak at the higher binding energy (BE) corresponds to the bridging

oxygen (BO) from the phosphate chains in the tribofilm [203], [208]–[210]. A metal oxide peak at the top surface of the tribofilm was not found, indicating that the tribofilm formed by ZDDP is well established and even changing oil did not influence the pre-formed ZDDP tribofilm. A metal oxide peak was detected in the tribofilm formed by BO + FM 1 + ZDDP (continuous test Chapter 8). The P 2p signal is deconvoluted in two components (i.e. P $2p_{3/2}$ and P $2p_{1/2}$). The BE values of both components clearly indicated that the tribofilm is not composed of long chain phosphates [204], [208], [217]. The Zn 3s peak is recorded next to P 2p signal. The S 2p spectra are also deconvoluted in two components (i.e. S $2p_{3/2}$ and S $2p_{1/2}$) [203]. The BE values of these two components are assigned to sulphides [199], [211], metal sulphides [15] and also as S which partly substitutes O from the phosphate chains and forms zinc (thio)phosphate [15], [76].

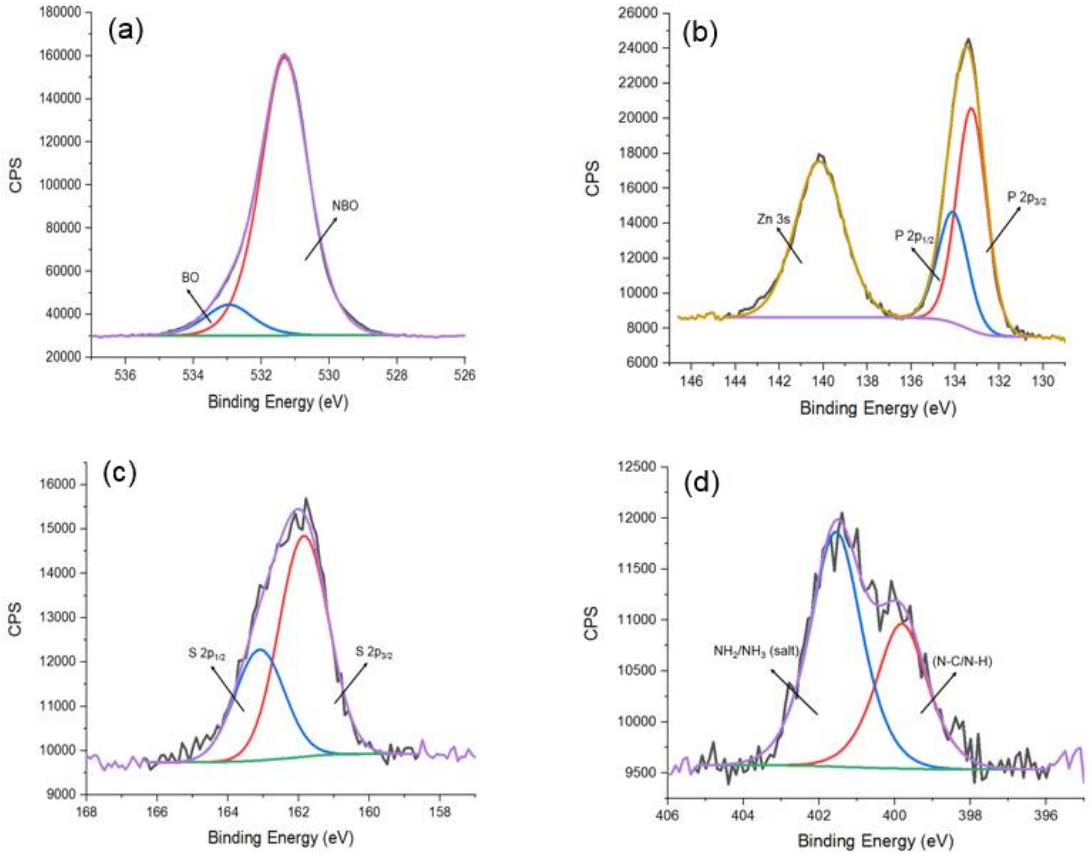

Figure 9-9. HR XPS spectra of key elements of the tribofilm formed by ZDDP and FM 1 in sequential film formation tests

(a) O 1s (b) P 2p and Zn 3s (c) S 2p (d) N 1s

The N 1s signals are resolved in two components. The first component is assigned to N-C/N-H group and second component to NH_2/NH_3 salt [174][165]. No bonding of nitrogen (N) with zinc (Zn) found in sequential tribological testing. A zinc nitride peak was detected in continuous tribological test of the lubricant blend having FM 1 and ZDDP in BO (Chapter 8).

9.3.2 Chemical composition of the tribofilm formed by ZDDP and FM 4

The XPS results in Figure 9-10 confirms presence of the key elements of the tribofilm inside the wear track. The O 1s signal is deconvoluted in two peaks which are assigned to NBO [77], [203], [207]–[210] and BO from the phosphate chains in the tribofilm [203], [208]–[210]. A metal oxide peak at the top surface of the tribofilm was not found. A metal oxide peak was detected in the tribofilm formed by BO + FM 4 + ZDDP (continuous test Chapter 8). This change in chemical composition indicated that FM 4 has low or no influence on the pre-formed ZDDP tribofilm.

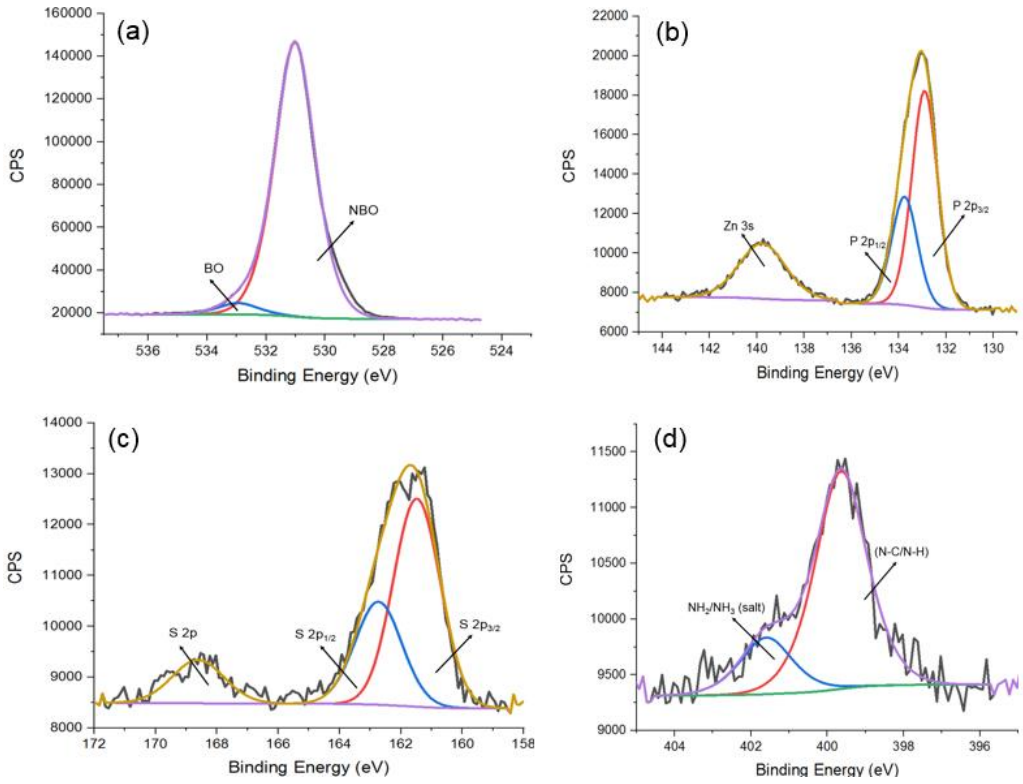

Figure 9-10. HR XPS spectra of key elements of the tribofilm formed by ZDDP and FM 4 in sequential film formation tests

(a) O 1s (b) P 2p and Zn 3s (c) S 2p (d) N 1s

The P 2p signal is deconvoluted in P $2p_{3/2}$ and P $2p_{1/2}$ components. The BE values of P $2p_{3/2}$ and P $2p_{1/2}$ components clearly indicated that tribofilm is not composed of long chain phosphates [204], [208], [217]. The S 2p signals are also resolved in S $2p_{3/2}$ and S $2p_{1/2}$ components. The BE values of S $2p_{3/2}$ and S $2p_{1/2}$ components are assigned to sulphides [199], metal sulphides [15] and also as S which partly substitute O from the phosphate chains and forms zinc (thio)phosphate [15], [76]. Another peak is also detected in the same BE window which corresponds to S in oxidation state of +VI (i.e. sulphate) [91], [199], [211]. The sulphate peak is only detected at top surface of the tribofilm, whereas in depth of the tribofilm only sulphide species are detected.

The N 1s signals are resolved in two components. The first component is assigned to N-C/N-H group and second component to NH_2/NH_3 salt [165], [174]. Chemical state of N 1s signal in the sequential film formation tests found very similar to one observed in the tribofilm formed by the blend of BO + FM 4 + ZDDP (continuous test Chapter 8). However, area ratio of chemical species is changed (i.e. N-C/N-H group changed from 73% to 78.7% and NH_2/NH_3 salt it is changed from 27% to 21.2%).

9.3.3 Chemical composition of the tribofilm formed by ZDDP and FM 8

The XPS results in Figure 9-11 shows presence of key elements of the tribofilm inside the wear track in sequential film formation tests. The O 1s signal is deconvoluted in two peaks which are assigned to NBO from the phosphate chains [77], [203], [207]–[209] and BO that binds phosphate group in the phosphate chains [203], [208]–[210]. A metal oxide peak is not detected in O 1s signal. The P 2p signal is deconvoluted in to P $2p_{3/2}$ and P $2p_{1/2}$ components. The BE value of P $2p_{3/2}$ signal clearly indicated that the tribofilm is not composed of long chain phosphates [204], [208], [217]. The S 2p signal is deconvoluted in two components (i.e. S $2p_{3/2}$ and S $2p_{1/2}$). The BE values of S $2p_{3/2}$ and S $2p_{1/2}$ components are assigned to sulphides [199], metal sulphides [15] and or S which partly substitute O from the phosphate chains and form zinc (thio)phosphate[15], [76]. Another peak is detected in same BE window which corresponds to S in oxidation state of +VI (i.e. sulphate) [91], [199], [211]. The XPS results showed that sulphate peak only exists at the top

surface of the tribofilm, whereas deeper in the tribofilm only sulphide species are detected.

The N 1s signals are resolved in two components. The first component is assigned to N-C/N-H group and second assigned to NH_2/NH_3 salt [165], [174]. Similar chemical state of N was observed in the tribofilm formed by BO + FM 8 + ZDDP (continuous test Chapter 8). However, area ratio of chemical species is changed (i.e. N-C/N-H group changed from 65.6% to 51% and NH_2/NH_3 salt it is changed from 34.4% to 49%), which indicated a modification in N interaction with ZDDP.

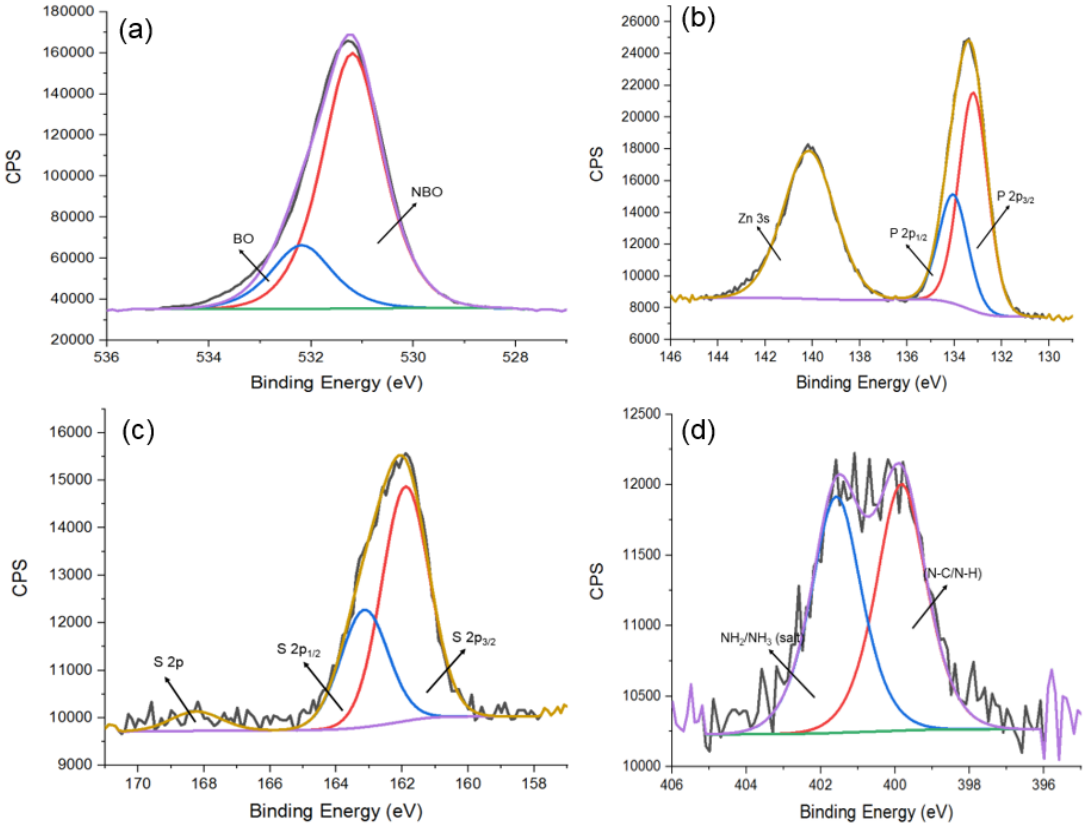

Figure 9-11. HR XPS spectra of key elements of the tribofilm formed by ZDDP and FM 8 in sequential film formation tests

(a) O 1s (b) P 2p and Zn 3s (c) S 2p (d) N 1s

9.3.4 Chemical composition of the tribofilm formed by ZDDP and FM 14

The XPS scans in Figure 9-12 shows the presence of key elements of the tribofilm inside the wear track. The O 1s signal is deconvoluted in to NBO from

the phosphate chains [77], [203], [207]–[210] and BO that binds phosphate group in the phosphate chains [203], [208]–[210]. A metal oxide peak is not detected in O 1s signal. A metal oxide peak was detected in the tribofilm formed by BO + FM 14 + ZDDP (Chapter 8). The P 2p signal is deconvoluted in to P $2p_{3/2}$ and P $2p_{1/2}$ components. The BE value of P $2p_{3/2}$ signal clearly indicated that the tribofilm is not composed of long chain phosphates [204], [208], [217]. The S 2p spectra is deconvoluted in to S $2p_{3/2}$ and S $2p_{1/2}$ components. The BE values of S 2p components are assigned to sulphides [199], metal sulphides [15] and or S which partly substitute O from the phosphate chains and form zinc (thio)phosphate[15], [76]

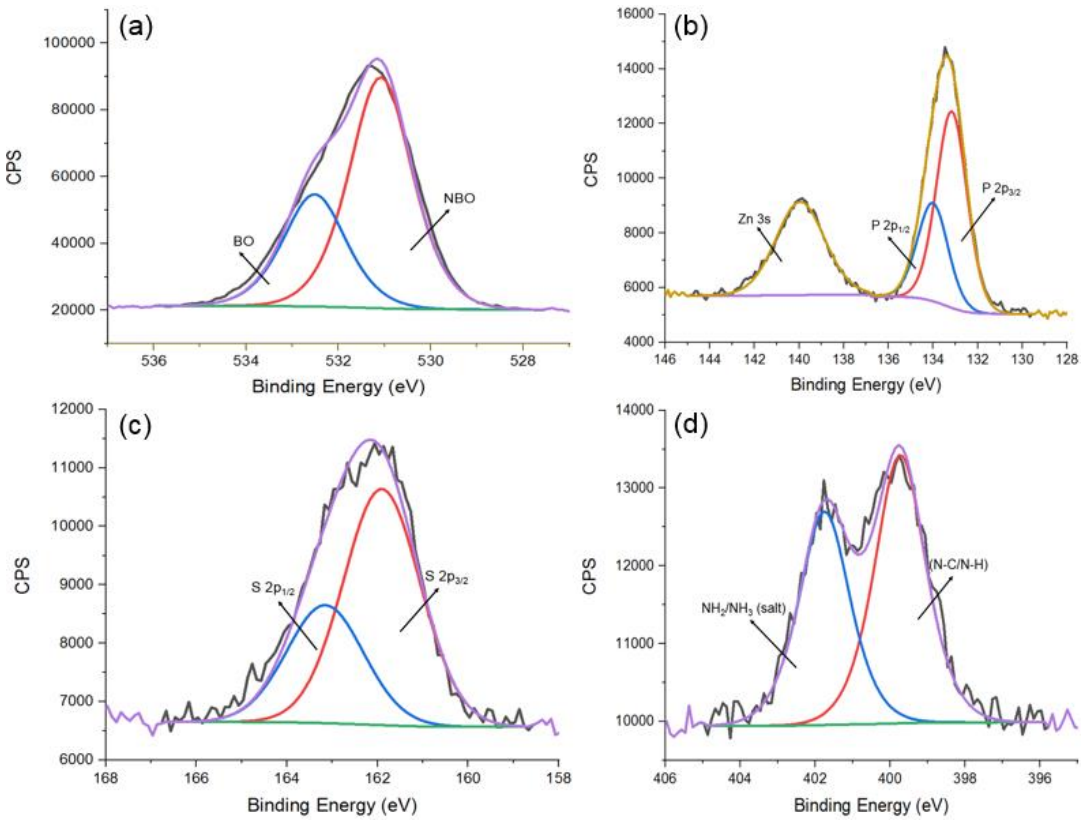

Figure 9-12. HR XPS spectra of key elements of the tribofilm formed by ZDDP and FM 14 in sequential film formation tests

(a) O 1s (b) P 2p and Zn 3s (c) S 2p (d) N 1s

The N 1s signal is resolved in two components. The first component is assigned to N-C/N-H groups and the second component is assigned to NH_2/NH_3 salts [165], [174]. Same chemical state of the N was observed in the

tribofilm formed by BO + FM 14 + ZDDP (continous test Chapter 8). However, area ratio of chemical species are changed (i.e. N-C/N-H group 32.2% to 55.4% and NH_2/NH_3 salt 67.8% to 44.7%), in these two different tribological system.

9.4 Tribofilm elemental concentration in sequential film formation tests

The depth profile was carried out to analyse the elemental concentrations across the tribofilm surfaces. Figure 9-13 shows the XPS depth profiling graphs in sequential film formation tests along with the elemental concentration of BO + ZDDP (for comparison).

Figure 9-13 (a) shows etching profile of the P in tribofilms formed in sequential film formation tests. In sequential film formation tests, P concentration is decreased as compared to tribofilm formed by BO + ZDDP. However, extent of reduction in P concentration varied with addition of different amine FMs on top of a pre-formed ZDDP tribofilm. Interestingly, P incorporation trends in sequential film formation tests found different from the tribofilm formed by the tribological system having amine FM and ZDDP together in BO (continuous test Chapter 8).

The etching results in Figure 9-13 (b) shows slight increment in the S concentration in sequential film formation tests in comparison to significant increase in tribological system having amine FMs and ZDDP together in BO (continuous test Chapter 8). Overall, the tribofilms formed in sequential film formation tests were not found rich in S.

The etching profile of Zn in sequential tribological tests is showed in Figure 9-13 (c). The elemental concentration results confirmed that Zn concentration is slightly suppressed in comparison to the tribofilm formed by lubricant blends having amine FM and ZDDP in BO (continuous test Chapter 8). Reduction in Zn concentration clearly indicated minimum interaction of amine FMs with pre-formed ZDDP tribofilm.

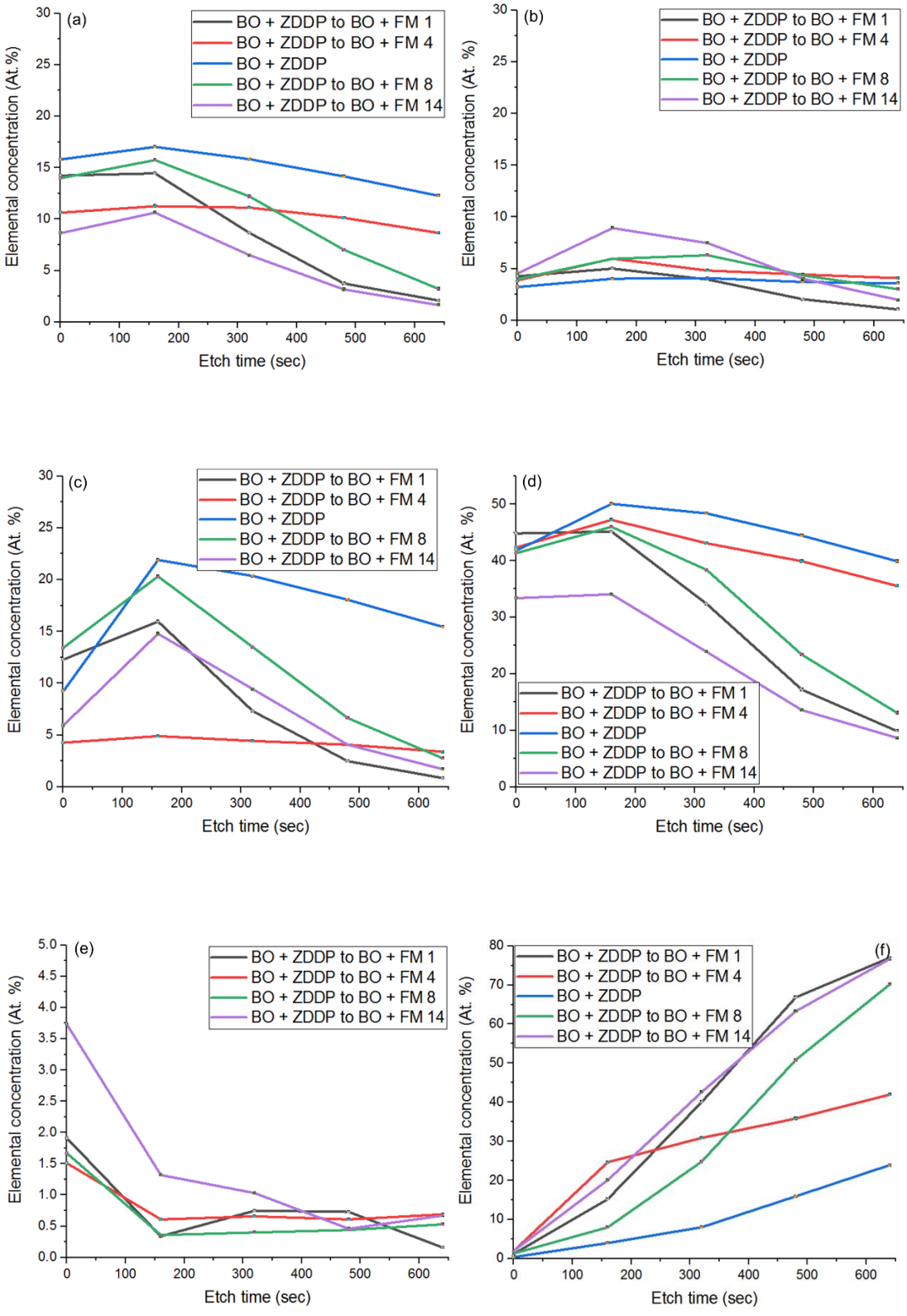

Figure 9-13. The depth profile of the tribofilms formed in sequential film formation tests

(a) Phosphorous (b) Sulphur (c) Zinc (d) Oxygen (e) Nitrogen (f) Iron

Figure 9-13 (d) shows O incorporation graph in the tribofilms formed in sequential film formation tests. The elemental concentration results showed reduction in concentration of O across the tribofilm. However, extent of reduction in O concentration is varied with different amine FMs. Graph showed comparatively more O concentration in top half of the tribofilm as compared to tribofilms formed by lubricant blends having amine FM and ZDDP together in BO (continuous test Chapter 8).

Figure 9-13 (e) shows N incorporation graph in sequential film formation. Graph showed that N is incorporated throughout the tribofilm which possibly indicated interaction of nitrogen with zinc phosphate tribofilm formed by ZDDP and consequently modify chemical composition of the tribofilm [22], [220]. The Fe incorporation trend in Figure 9-13 (f) revealed significant increase in Fe content towards the substrate. Low or no Fe content was detected on top surface of the tribofilm. However, increase in Fe concentration with subsequent etching cycles is also recorded in the tribofilm formed by BO + ZDDP.

Sequential tribological tests revealed capability of amine FMs to interact with the pre-formed ZDDP tribofilm [22], [164]. Because of this interaction, elemental composition of the tribofilms is modified but the extent of modification varied with different amine FMs. The depth profile graphs showed increase in Fe concentration deeper in the tribofilm (towards the substrate). An increase in Fe concentration indicated that the effectiveness of ZDDP tribofilm is compromised due to interaction with amine FMs.

9.5 Binding energy values of key elements of the tribofilm and phosphate film formation

The HR XPS results and etching profile showed variation in chemical/elemental composition of the tribofilm which affected the tribological performance of the tribofilm [15], [206]. Table 9-1 outlines the BE values of key elements of the tribofilm formed because of sequential film formation tests. The BE values of the key elements of the tribofilm formed by ZDDP is also added for reference purpose. The XPS results showed a chemical shift of P 2p signal because of tribological interaction of amine FMs with the pre-

formed ZDDP tribofilms. The data showed that the P $2p_{3/2}$ component is chemically shifted towards lower BE values. The BE difference between Zn 3s signal and P $2p_{3/2}$ signal suggested that tribological interaction of amine FMs with the pre-formed ZDDP tribofilm modified the glass composition [77], [186], [204].

Table 9-1. Binding energy values of key elements at top surface of the tribofilm

Element		**BO + ZDDP to (eV)**	**BO + FM 1 (eV)**	**BO + FM 4 (eV)**	**BO + FM 8 (eV)**	**BO + FM 14 (eV)**
O 1s	NBO	531.49	531.1	531.02	531.19	531.09
	BO	533.04	532.95	532.95	532.19	532.52
P $2p_{3/2}$	P_xO_y	133.65	133.25	132.9	133.20	133.16
S $2p_{3/2}$	Fe_xS_y/ ZnS	162.15	161.85	161.48	161.89	161.91
S 2p	Sulphate	----	----	168.61	168.24	----
Zn $2p_{3/2}$	ZnO/ ZnS	1022.19	1022.0	1021.75	1022.04	1021.88
Zn 3s	----	140.33	140.17	139.77	140.15	139.95
N 1s	N-C/N-H	----	399.81	399.64	399.83	399.73
	NH_2/NH_3	----	401.55	401.6	401.58	401.75
ΔBE (Zn 3s – P $2p_{3/2}$)		6.68	6.92	6.87	6.95	6.79

This chapter discussed the tribological interaction of the pre-formed ZDDP tribofilm with amine FMs. Surface characterisation of the tribofilms are also included in this chapter to analyse modifications in chemical/elemental composition of the tribofilm formed by ZDDP because of sequential interaction tests. Next chapter will summarise all the key results and on the basis of these results present possible interaction mechanisms between amine FMs and ZDDP.

9.6 Summary

This result chapter is specifically focused on interaction sequence of amine FMs (i.e. FM 1, FM 4. FM 8 and FM 14) with ZDDP and for this purpose sequential film formation tests were conducted. In these tribological tests, tribofilm is initially formed with BO + ZDDP in first half of the test and then in second half of the test tribological interaction is performed on top of pre-formed film with BO + OFM or vice versa. Friction and wear results confirmed that,

- The COF value is further reduced when OFMs formed film on top of ZDDP tribofilm
- FM 1 displayed higher COF on the steel surface as compared to FM 4, FM 8 and FM 14
- ZDDP showed higher COF on the steel surface as compared to surface having pre-formed OFMs (i.e. FM 1, FM 4, FM 8 and FM 14) film
- FM 1 and FM 4 increased the wear volume significantly in continuous tribological testing
- FM 8 and FM 14 exhibited the effective friction and wear performance and even along with ZDDP synergism is observed

The XPS technique was used to analyse the chemical composition of the tribofilms formed during sequential tribological tests (i.e. BO + ZDDP to BO + OFM). Etching of the tribofilm surfaces was also conducted to further analyse changes in the elemental concentration across the tribofilm thickness. The XPS results confirmed that,

- The tribofilm formation capability of ZDDP is not massively disturbed in sequential film formation tests with amine FMs. A metal oxide peak is not detected in O 1s signal indicating that the ZDDP tribofilm is effective
- The chemical state of N 1s signal is found to be different in sequential film formation test between ZDDP and FM 1 from what was observed in the tribofilm formed by BO + FM 1 + ZDDP (continuous test Chapter 8)
- The chemical state of N 1s signal found very much similar in sequential film formation tests between ZDDP and FM 4/FM 8/FM 14 as observed

previously in the case of tribofilm formed by the lubricant blends having amine FMs and ZDDP in BO (continuous test Chapter 8)

The etching/depth profile was carried out to analyse the elemental concentrations across the tribofilm surfaces. In sequential film formation tests,

- The P concentration is decreased as compared to tribofilm formed by BO + ZDDP
- The S concentration is increased but significant increase was not recorded as observed in tribological system having amine FMs and ZDDP together in BO (continuous test Chapter 8)
- The Zn concentration is suppressed in comparison to the tribofilm formed by lubricant blends having amine FM and ZDDP in BO (continuous test Chapter 8)
- The O concentration is suppressed across the tribofilm. However, extent of suppression in O concentration is varied with different amine FMs
- The N is incorporated throughout the tribofilm which possibly indicated interaction of N with zinc phosphate tribofilm
- A sharp increase in Fe concentration was observed with the subsequent etching cycles
- The P $2p_{3/2}$ component is chemically shifted towards lower BE values. The BE difference between Zn 3s and P $2p_{3/2}$ suggested that tribological interaction of amine FMs with the pre-formed ZDDP tribofilm modified the glass composition

Chapter 10
Discussion

10.1 Overview

This chapter discusses the most important results obtained throughout this study. The points included in this chapter based on trends and indications acquired from the results and then linked with the available literature relating to the interactions between OFMs and ZDDP. This chapter is split in two parts.

The first part focuses on the tribological interaction of,

1. OFMs and ZDDP in base oil (BO)
2. ZDDP and amine FMs in sequential film formation tests

The second part covers,

3. The film formation mechanism of amine FM on a steel surface
4. The interaction between amine FMs and ZDDP
5. The wear behaviour and interaction mechanisms

10.2 Tribological interaction of OFMs and ZDDP

ZDDP exhibits a high boundary friction [15], [22] but due to its excellent AW performance almost all engine oil formulations contain ZDDP [15]–[18], [52]. ZDDP performs this function by forming the zinc phosphate films which limits the contact between interacting surfaces [27], [28], [58], [62]. Similarly, OFMs form a film on interacting surfaces by physical adsorption or chemical reaction [22], [104], [105], [116], [119], [121], [130] and as a result of this action OFMs reduce the metallic junction growth and hence solid adhesion [104], [105], [137]. The AW performance of ZDDP is affected by its interaction with other additives including OFMs [22], [61], [159]. Few additives interact synergistically with ZDDP and improve its AW performance, whereas some others additives work antagonistically with ZDDP [30], [162], [172]. The wear results (Chapter 6) confirmed that the addition of OFM with ZDDP affect the AW film formation capability of ZDDP, which shifted the wear factor values from significantly high wear to remarkably low wear.

Miklozic et al. [22] studied the tribological behaviour of different OFMs and ZDDP by using mini traction machine (MTM) and high-frequency reciprocating rig (HFRR). The experimental results of Miklozic et al. [22] confirmed that amine FMs significantly disturbed the film formation capability of ZDDP which consequently reduced the film thickness [16], [22]. The wear results (from HFRR) showed that amine FM severely damage the AW film formed by ZDDP and invalidates the effectiveness of ZDDP tribofilm [22]. Lundgren and Ericsson [166] investigated the tribological performance of ZDDP and FA molecules and concluded that FAs not only reduce boundary friction but also disturb the film formation capability of ZDDP and remove ZDDP film from the surface [61]. The significant increase in performance of FAs was recorded when little concentration of molybdenum dialkyldithiocarbamate (MoDTC) was added in the solution [166]. Furthermore, addition of FA in the mixture of organic molybdate amid and ZDDP reduced COF value from 0.04 to 0.02 [167]. Ratoi et al. [16] investigated the influence of other additives on ZDDP tribofilm by using mini-traction machine (MTM) with optical interference (i.e. SLIM attachment). They found that presence of other additives restricted the ability of ZDDP to form AW film and consequently tribological interaction produced thinner tribofilm. Figure 10-1 shows the film thickness and wear behaviour of different lubricant. These results are in agreement with the friction and antagonistic wear behaviour of lubricant blends having OFMs and ZDDP (Chapter 6).

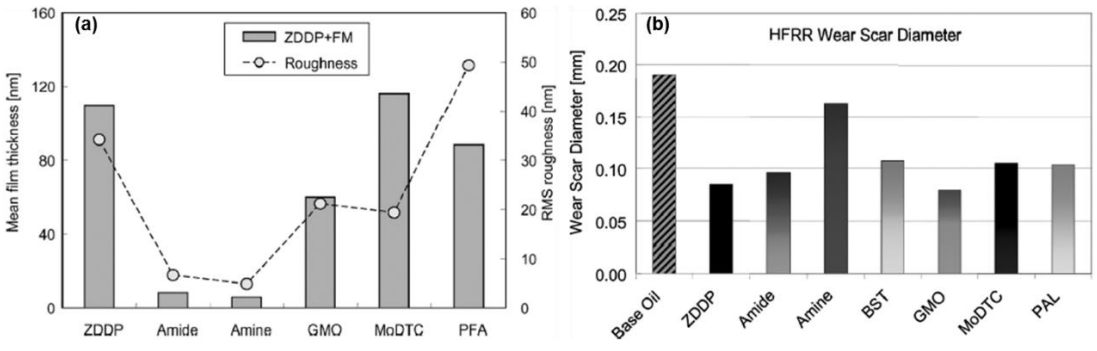

Figure 10-1. Tribological behaviour of ZDDP and OFMs along with ZDDP alone [22]

(a) Film thickness and surface roughness (b) Wear measurement

The oleyl amine [16] and oleyl amide [61] reduce the friction COF value without showing antagonism to AW film formed by ZDDP. Rounds [162] investigated the effect of lauryl amine on AW performance of ZDDP by using four-ball wear test machine. He established that wear remain low after the addition of Lauryl amine in lubricant blend having ZDDP in-comparison to WSD of ZDDP in the BO (i.e. 0.24 mm). Furthermore, beyond the critical concentration of lauryl amine, the WSD value increased significantly. Using reciprocating sliding tribometer, Massoud et al. [124] investigated the effect of ZDDP on lubrication mechanism of linear fatty amines (FAs). They found that blend of most of the amines with ZDDP improved AW performance of ZDDP with the wear scar width (WSW) very close to the Hertz diameter of 87 µm. The experimental results of previous studies [124], [162] are in agreement with the synergistic wear results of lubricant blends having OFMs and ZDDP (Chapter 6). Morina et al. [191] investigated the friction and wear behaviour of MoDTC along with ZDDP by using reciprocating pin on plate apparatus. Tribological results of the investigation confirmed that presence of ZDDP in the lubricant blend increased AW capability of MoDTC. The wear factor value decreased from 0.25 (BO + MoDTC) to 0.19 (BO + MoDTC + ZDDP). The synergistic wear result of MoDTC and ZDDP is also in agreement with the synergistic wear behaviour of amine FMs in presence of the ZDDP.

10.2.1 Tribofilm topography

The tribofilm topographical results (Chapter 7) confirmed that addition of OFM and ZDDP in the lubricant blend modified the tribofilm topography. The topographical results are in agreement with Ratoi et al. [16]. Using MTM-SLIM machine, they established that addition of other additives along with ZDDP modified the tribofilm topography [16]. The topographical images of the tribofilm formed by ZDDP (Chapter 7) were composed of two distinct regions, ridges (elevated parts) and valleys (shallow parts) [20], [26], [27], [62]. The large pads were elongated in the sliding direction having a length extending up to ~ 25 µm. These AW pads were elevated, smooth and found higher than the surrounding features (Chapter 7). Using the AFM, Graham et al. [27] recommended that the larger AW pads are elongated in the sliding direction, around 20 µm in length. These pads are relatively smooth and appeared higher than the nearby regions, which mean these AW pads may support

noteworthy amount of load. The smaller pads are not elongated in the sliding direction and comparatively not as high as the large pads [27]. The X-ray photoelectron emission microscopy (X-PEEM) of ZDDP tribofilm showed formation of long chain phosphate on high topographical areas (i.e. surface of larger AW pads), whereas mixture of long and short chain phosphate on low topographical regions [62]. Nicholls and colleagues [62] proposed that formation of long chain phosphate on high topography are linked with load bearing capability of the surface, which possibly facilitate the cross-linking between phosphate chain. Topographical result of the tribofilm formed by ZDDP (Chapter 7) is in agreement with the published studies [27], [62].

The addition of FM 1 (i.e. coco-amine) and FM 4 (i.e. ethoxylated tallow amine) with ZDDP produced an antagonistic wear behaviour, which means that wear increased significantly (Chapter 6). The larger elongated ZDDP AW pads [27], [62] completely disappeared from the film topography and all we observed were smaller pads, which were contained and not elongated in the sliding direction (Chapter 7). These AW pads were scattered around the AFM images and appeared higher than the surrounding features. The topographical results of the tribofilm formed with the addition of FM 1 and FM 4 in the lubricant blends are in agreement with the investigation of ZDDP tribofilm conducted by Graham and colleagues [27]. They confirmed that smaller pads are not elongated in the sliding direction [27] and also unable to support noteworthy amount of load [27], [62].

However, Ratoi and colleagues [16] stated that the tribofilm formed by ZDDP along with BLO (ZDDP + other additives but no FM) are composed of AW pads elongated in the sliding direction. They also suggested that the tribofilm formed by BLO composed of non-uniformly distributed AW pads in-comparison to uniformly distributed AW pads found in BO + ZDDP [16]. The addition of FM 8 (i.e. tallow-amine), FM 10 (i.e. alcohol- ethoxylate) and FM 14 (i.e. ester of tri-ethanol amine with tallow fatty acid) with ZDDP produced synergistic wear behaviour (Chapter 6). Addition of aforementioned OFMs transformed larger zinc phosphate pads (i.e. observed in topography of BO + ZDDP) into shorter species but still elongated in the sliding direction. These AW pads found comparatively shorter (in height) to the pads formed by BO + ZDDP but still appeared higher than the surrounding features

(Chapter 7). These elongated AW pads limit the asperity-to-asperity contact and support the load during tribological interaction. Graham et al. [27] characterize the ZDDP AW film and suggested that elongated pads in the sliding direction are usually higher than the surrounding topographies and supposedly share the load during tribological interaction. Nicholls et al. [62] also characterize the ZDDP tribofilm and stated that centre of these pads are stiffer than the corners and hence responsible to keep interacting asperities apart.

10.2.2 Tribofilm elemental composition

The tribofilm formed by ZDDP is composed of two-layer structure (i.e. long chain on the top and short chain phosphates in the bottom) [15], [18], [58], [70], [72]–[74]. The phosphate structure of the tribofilm contain zinc and iron cations at the interface between the tribofilm and metal substrate [26]. The sulphides are also incorporated in the tribofilm and these are present as zinc sulphide and iron sulphide mainly near the substrate [57], [90], [91]. The addition of the OFMs with ZDDP in the lubricant blend modified the tribofilm morphology (Chapter 7). The EDX mapping results (Chapter 8) confirmed that addition of OFMs in lubricant blends also modified the tribofilm elemental composition. The tribofilms formed by the addition of amine FMs with ZDDP was rich in sulphur (S) with low phosphorous (P) concentration. The tribochemical interaction between these two additives modified the elemental intensity of key elements of the tribofilm in-comparison to the tribofilm formed by BO + ZDDP (Chapter 8). Interestingly, the tribofilm formed with the addition of FM 10 (i.e. alcohol ethoxylate) showed a similar elemental incorporation to that observed with the blend of BO + ZDDP. Table 10-1 presents the order of the elemental intensity of the elements found in the tribofilms formed by BO + ZDDP and lubricant blends having OFMs with ZDDP.

The elemental intensity trends established that the addition of amine FMs with ZDDP increased S-concentration and suppressed P-concentration in the tribofilm. Matsui et al. [32] investigated the effect of polar compounds (i.e. polymethacrylates (PMA)) along with a dispersant compound on the formation of ZDDP tribofilm. Using a ball- on-disc type tribometer, they found that the tribofilm formed with the addition of dimethylaminomethacrylate (PMA-N) and dispersant compound (amino functionalised compound) was

high in S-concentration with less P-concentration. Furthermore, the tribofilm formed with the addition of addition of 2-hydroxyethylmethacrylate (PMA-OH) was found similar in elemental concentration as formed by BO + ZDDP. The modification in elemental intensity with the addition of amino-containing compounds and similar elemental composition to that formed by BO + ZDDP with the addition of hydroxyl containing compound are in agreement with the elemental composition results (Chapter 8). Addition of amino-containing compounds restricted the tribofilm formation and also modified the elemental structure of the tribofilm with high S-concentration [34].

Table 10-1. Order of the tribofilm elemental intensity formed by different lubricant blends

S.No	Lubricant blend	Elemental intensity
1	BO + ZDDP	**Zn > P > S**
Antagonism		
2	BO + FM 1 + ZDDP	**S > P > Zn**
3	BO + FM 4 + ZDDP	**S > Zn > P**
Synergism		
4	BO + FM 8 + ZDDP	**S > Zn > P**
5	BO + FM 10 + ZDDP	**Zn > P > S**
6	BO + FM 14 + ZDDP	**Zn > S > P**

In another study Matsui et al. [31] characterise the tribofilms formed by addition of different ash-less compounds with ZDDP in the lubricant blend. The Auger Electron Spectroscopy (AES) analysis of the tribofilms having an amino group (PMA-N, dispersant and dimethyoctadecylamine (DMODA)), showed substantial increase in relative S-concentration and notable reduction in relative P-concentration. However, AES analysis is based on very small

spot size (i.e. in micrometre) but still with this limitation, AES analysis provide an approximate level of elemental intensity. Figure 10-2 shows AES analysis of the tribofilms formed with the addition of different ash-less compounds with the ZDDP. The AES result of the tribofilms are in agreement with the elemental composition of the tribofilms formed with the addition of OFMs with ZDDP (Chapter 8).

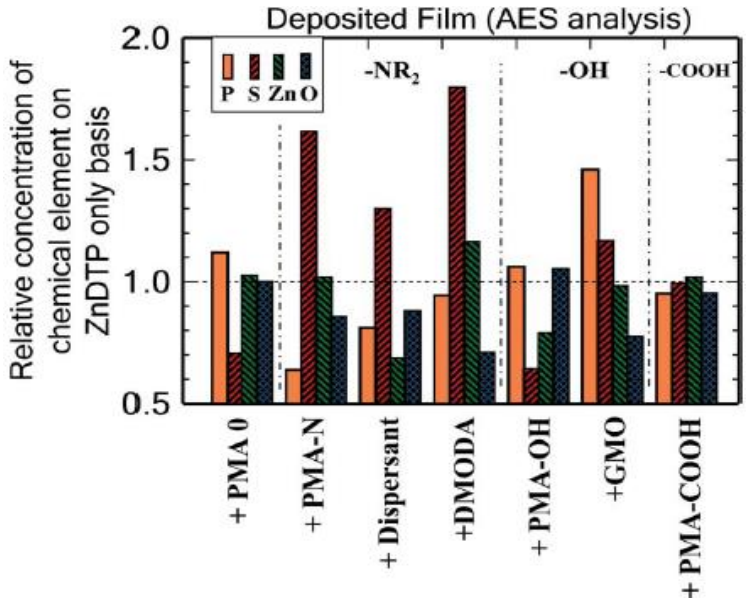

Figure 10-2. The relative concentration of the key elements of the tribofilm formed with the addition of different ash-less compounds and ZDDP [31]

10.2.3 Tribofilm chemical composition and depth profile

The surface analysis (XPS) results from the top 5-8 nm of the tribofilm surface confirmed presence of the key constituents of the tribofilm formed by BO + ZDDP (Chapter 8). A strong presence of P 2p, O 1s, S 2p, Zn 2p and Zn 3s signals confirmed presence of tribofilm inside the wear track mainly composed of phosphates and sulphides [15], [18], [91], [57], [58], [70], [72]–[74], [82], [90]. The binding energy (BE) of P $2p_{3/2}$ component was assigned to pyrophosphate [77], [203], [204], [212], [213]. The iron oxide peak was not detected in O 1s signal which is in agreement with the studies [58], [174], which means that the tribofilm is effective in terms of overcoming wear mechanism or mechanisms. The BE of S $2p_{3/2}$ component was assigned to sulphides [199] and or S which partly substitutes O from the phosphate chains

and form zinc (thio)phosphate [76]. However, by using the XPS technique it is difficult to distinguish between metal sulphides and (thio)phosphate as the peaks overlaps due to the small shift in BE value [76]. The incorporation of S throughout the tribofilm (Chapter 8) supported the formation of sulphide species [15], [82]. The BE value of Zn 2p spectrum was assigned to ZnS, ZnO [199] and zinc phosphate [208]. Previous studies [72], [89] suggested that Zn is incorporated in the tribofilm as ZnO instead of ZnS.

The tribochemical interaction between ZDDP and amine FMs affected the elemental composition and consequently the chemical composition of the tribofilm (Chapter 8). The XPS analysis of the top 5-8 nm of the tribofilm surface (Chapter 8), showed presence of the iron oxide peak in O 1s signal with addition of the different OFMs with ZDDP. However, the concentration of the iron oxide peak varied with the different OFMs. The etching results (Chapter 8), confirmed presence of the iron (Fe) at the top surface of the tribofilm. The significant increase in the Fe concentration with the subsequent etching cycles indicated that Fe from the substrate material was building up in the tribofilm. Zhang et al. [214] suggested that sharp increase in Fe concentration with etching cycles specified that iron from the substrate is accumulating in the film. The etching results of the tribofilms formed with the addition of amine FMs in the lubricant blend with ZDDP (Chapter 8) are in agreement with the depth profile data [32]. Massoud et al. [124] reported the contribution of a metallic oxide peak in the tribofilm but not specifically discussed the formation of the iron oxide peak in top most surface of the tribofilm.

The XPS results (Chapter 8) confirmed that P-concentration in the tribofilms was suppressed with the addition of the different amine FMs. The oxygen (O) incorporation in the tribofilms was also suppressed and it followed a similar trend to that of P, which is expected due to the formation of phosphates in the tribofilm. This is in agreement with previous studies [31], [32], [174], which suggested that nitrogen (N) containing compounds restricted the formation of P based tribofilm. Based on AES analysis, Matsui et al. [32] supported the two layer structure of ZDDP tribofilm [76]. They named the top layer the '*deposited film'* in which P concentration remain almost stable while in underneath layer (i.e. *gradient layer*) the P, Zn and O-

concentration slowly reduced towards the substrate and Fe concentration is increased. Massoud et al. [124] and Soltanahmadi et al. [91] analysed the etching profile of the tribofilm formed with the addition of amine FM and ZDDP in the lubricant blend and established that presence of amine FMs suppressed the key tribofilm elements (i.e. P, Zn and S). This is an indication that addition of amine FM in the lubricant blend induced thinner AW film on the surface.

The zinc phosphate film formation capability of ZDDP was slightly suppressed due to its interaction with FM 10 (i.e. alcohol ethoxylate). This is also in agreement with the investigation conducted by Matsui et al. [31] in which they reported that presence of hydroxyl polar group slightly reduced the tribofilm formation capability of ZDDP.

10.2.3.1 Role of sulphur in tribofilm composition

The etching profile data of the tribofilms (Chapter 8) uphold previous studies [32], [34] that the tribofilms formed as a result of the interaction between the amine FMs and ZDDP are primarily S driven instead of P. The driving force behind the S enhancement in the tribofilm is still unknown [32]. The depletion in the P and O concentrations and at the same time the increase in the S-concentration in the tribofilms confirmed modification in the tribofilm chemical composition, which is in agreement with previous AES analysis of the tribofilm [31], [32]. The sulphate peak detected at top surface of the tribofilm formed with the addition of FM 1 and FM 4 with ZDDP, whereas the XPS results confirmed the formation of only sulphide species in depth of the tribofilm (i.e. towards the substrate). Soltanahmadi et al. [91] investigated the effect of amine FM on the properties of ZDDP tribofilm by using MTM tribometer. The XPS analysis of the tribofilm confirmed formation of the sulphate peak (S VI) on the top surface of the tribofilm and contribution of sulphide (S II) in depth of the tribofilm, which is in agreement with the XPS results (Chapter 8). The formation of the oxidised S species (i.e. sulphate) in the tribofilm is not very well understood, though few studies [206], [221] suggested that the formation of sulphate species inside the wear track is because of water contamination or it may arise due to the presence of S containing additive in the blend [91].

The etching profile (Chapter 8), showed an increment in the Fe concentration and a reduction in the Zn concentration near the substrate. Decrease in P/S

ratio from the top surface to deeper in the tribofilm (near the substrate), suggesting more contribution of the sulphide in the middle and bottom of the tribofilm in comparison to the top layer of the tribofilm (Table 8.2, 8.3, 8.4 and 8.6). The XPS results (Chapter 8) confirmed the formation of sulphide species deeper in the tribofilm (towards the substrate). The sulphide contribution in depth of the tribofilm are mainly comprised of zinc sulphide/iron sulphide (Chapter 8). The iron sulphides are formed as a result of acid-base reaction between nascent surface/iron particles with the remaining organic sulphur species in the lubricant [58], [222]. The XPS result from the Fe spectra confirmed formation of the iron sulphides along with iron oxides. The formation of iron sulphide species during the tribological interaction between amine FMs and ZDDP suggested severe wear conditions in the local contact zone [76] because the iron sulphide has the ability to protect the interacting surfaces from oxidation, scuffing and abrasive wear between interacting surfaces [3], [58], [222], [223]. The incorporation of S in the tribofilm also supported formation of ZnS in the tribofilm [82].

10.2.3.2 Role of zinc in tribofilm composition

Zinc phosphate tribofilms interact with the iron oxide particles on the surface of the substrate and as a result of this tribochemical reaction iron oxide is eliminated from the surface and zinc oxide is formed [26], [58], [70]. The XPS results (Chapter 8), confirmed the presence of zinc oxide at the top surface and zinc sulphide [199], [211] in depth of the tribofilm (near the substrate). The zinc sulphide formation can take place because of interaction between organic sulphur species and zinc oxide according to HSAB principle or it may form directly in case phosphate chain contain sulphur atom ((thio)phosphate) [58]. Recently, Massoud et al. [124] discussed the interaction of linear FAs with ZDDP and mentioned that presence of octadecylamine and ZnO in the lubricant blend may lead to the formation of ZnO-amine complexes or possibly hard-core reverse micelles (in which FA molecules are firmly attached to the zinc oxide core) [180]. These micelles form a ZnO rich tribofilm on the interacting asperities, which reduces wear [124].

The lubricants blend having FM 8, FM 10 and FM 14 with ZDDP produced synergistic wear results (Chapter 6). The highest concenrtration of Zn was observed with the addition of FM 8 with ZDDP. The XPS result (Chapter 8)

confirmed presence of relatively strong Zn 3s then P 2p signal, which suggested an increase in the amount of Zn in-comparison to phosphate in the tribofilm. This finding is in agreement with the previous study [124]. The blend of FM 14 with ZDDP offered comparatively less concentration of Zn but both of these amine FMs, which offered synergistic wear behaviour, followed the similar Zn incorporation trends. The formation of Zn enrich tribofilm and reduction in wear is in agreement with the investigation of Massoud et al. [124]. The blends of OFM with ZDDP, which offered antagonistic wear behaviour (i.e. FM 1 and FM 4), showed comparatively less incorporation of Zn throughout the tribofilm. The reduction in the Zn concentration indicated limited formation of Zn species in the tribofilm.

10.2.3.3 Role of nitrogen in tribofilm composition

Because of nature of the OFMs, it is particularly interesting to understand the role of the N species in the tribofilm composition. The etching results (Chapter 8) confirmed N incorporation throughout the tribofilm but with relatively reduced concentration deeper in the tribofilm. The XPS results (Chapter 8) indicated that N interacted with zinc phosphate film on the top surface and deeper in the tribofilm to some extent. The N incorporation results of the tribofilms having amine FMs and ZDDP are in agreement with the studies [91], [169], which suggested that N based FMs interact with phosphate film on top surface and also deeper in the tribofilm. However, a recent study [124] reported presence of N only at the top most surface of the tribofilm. An important aspect of the interaction of amine FMs and ZDDP (Chapter 8) was formation of N-C/N-H bonds in chemisorbed amine FMs [144], [171]. The blend of FM 1 and ZDDP (which produced the highest wear), also formed zinc nitride (N-Zn) along with N-C/N-H bonds (Chapter 8). This is in agreement with the XPS result of a previous work [174], which stated that N 1s signal in the tribofilm (formed as a result of tribochemical interaction between ZDDP and succinimide), resolved in N-C peak, zinc nitride peak and succinimide group.

The X-ray absorption near edge structure spectroscopy (XANES) analysis [169], [187] reported contribution of ammonium phosphate or amine phosphate [165] in the tribofilm, formed as a result of interaction between ZDDP and dispersant. The formation of ammonium phosphate [169] or/and

amine phosphate is a result of chemisorption or reaction between amine group with zinc phosphate film or decomposed ZDDP by-products [165]. The studies [165], [187] suggested that presence of N-C/N-H bonds may disturb the formation of zinc phosphate tribofilm and possibly lead to form amine/ammonium phosphate. The amines are strong bases and have capability to act as a Brønsted–Lowry base by binding with a proton (H^+) and forming a protonated compounds [146]. The protonated compounds ($R\text{-}NH_3$) are weak acids [171] and phosphates are hard bases [76]. According to the HSAB principle, amines react with phosphate ions and form amine/ammonium phosphate [171]. Previous studies [164], [165], [169], [187] proposed that tribochemical interaction between amine and ZDDP by-products also produce additional cations which could facilitate the formation of short chain length zinc phosphate tribofilm.

It could be possible that severe antagonistic wear behaviour of FM 1 is related with the formation of zinc nitride (N-Zn) in the tribofilm (Chapter 8). Addition of FM 4 in the blend with ZDDP also increased wear factor value but wear result was comparatively better than FM 1 (Chapter 8). Interestingly, the XPS analysis not detected zinc nitride peak (in N 1s signal) in the tribofilm formed with the addition of FM 4 and ZDDP in the lubricant blend.

10.2.4 Tribofilm composition and phosphate chain length

The wear results (Chapter 6), confirmed that addition of FM 1 and FM 4 showed antagonistic wear behaviour. The addition of FM 1 and FM 4 in the blend with ZDDP significantly increased the Fe concentration across the tribofilm. The P/Fe ratio (Table 8.2 and 8.3) of the tribofilms specified that the Fe content in the tribofilm increased significantly whereas the P/O and Zn/S ratios were decreased in comparison to the tribofilm formed by BO + ZDDP (Table 8.1). The modification in the elemental ratios established that the tribofilms formed by the blend having FM 1 and FM 4 with ZDDP were incapable of overcoming wear in the contact zone. The addition of FM 8, FM 10 and FM 14 with ZDDP showed a synergistic wear behaviour. The P/Fe ratios (Table 8.4, 8.5, 8.6) of the tribofilms decreased from the top surface towards the substrate. The sharp increase in the Fe concentration with etching cycles is in agreement with the study [214]. Interestingly, the first few nanometres of the respective tribofilms contained less Fe contents. Higher

P/O elemental ratio in comparison to FM 1 and FM 4 (which showed antagonistic wear) indicated better availability of the phosphate in the tribofilm. The increase in Zn/S and decrease in P/S and P/Zn elemental ratios from top most surface of the tribofilm towards the substrate suggested formation of more zinc sulphide [171]. Massoud et al. [124] proposed formation of ZnO from decomposition of basic ZDDP, which may incorporate in the tribofilm and deposit on the steel surface. The availability of excess cations (i.e. Fe and Zn) specified formation of more sulphide species than phosphates deeper in the tribofilm. These results are in agreement with the previous studies [164], [165], [169], [187], which stated that presence additional cations in the tribofilm could enable the decomposition of ZDDP to short chain length phosphates.

Measuring the phosphate chain length based on the ratio of BO to NBO becomes very complex for the tribofilms formed with the blend of OFM and ZDDP [58]. This complexity arises due to interference of the oxide groups (i.e. hydroxides, carbonate, sulphate etc.), with the P-O-P oxygen peak [174], [224] and because of this reason it is unpredictable to assess the change in the phosphate chain length on the basis of the BO/NBO ratio. Another indication of the changes in the chain length is based on the P 2p signal which shifts towards higher BE for longer chain phosphates or vice versa [77], [186], [204], whereas the Zn 3s signal does not chemically shifts [186], [204]. Hence measuring the phosphate chain length based on the ΔBE value between the P $2p_{3/2}$ and Zn 3s is more reliable with less uncertainties for complex lubricant blends [186].

The BE value of the P $2p_{3/2}$ component of P 2p signal in the tribofilm formed by BO + ZDDP or with the addition of OFMs in the blend with ZDDP (Chapter 8) found around 133.0-133.6 eV. The BE of P $2p_{3/2}$ component corresponding to long chain phosphate is reported between 134-135 eV [204], [208], [217]. The XPS results (Chapter 8) confirmed that interaction between the amine FMs and ZDDP shifted the P $2p_{3/2}$ component towards lower BE values and furthermore this change in the BE values was even more than the respective ΔBE value of (Zn 3s – P $2p_{3/2}$). The XPS results of the tribofilms formed with the addition of OFMs in the blend with ZDDP (Chapter 8), showed availability of excess metal oxides in the tribofilm, which shifted P $2p_{3/2}$ component towards the lower BE values. This result is in agreement with the

studies [77], [204] suggested that presence of metal oxide in the tribofilm decrease the phosphate chain length. The chemical shift toward lower BE values established that the resultant product (i.e. amine/ammonium phosphate) comprised of shorter chain phosphates. This result also uphold the studies [164], [169], [187] proposed that tribochemical interaction between amine and ZDDP by-products also produce additional cations (due to presence of ammonium ion in the tribofilm) which could enable the decomposition of ZDDP to short chain length phosphates. FM 10 displayed a similar elemental concentration as found in the tribofilm formed by BO + ZDDP but the presence of iron oxide peak in the O 1s signal suggested a modification in the tribofilm chemical composition with the addition of FM 10 in the blend.

The tribofilm etching results (Chapter 8) showed the formation of metal phosphide (i.e. iron phosphide/zinc phosphide) peak [211], [225], [226] in the same BE window of P 2p signal. The metal phosphide peaks detected in the tribological systems having FM 1, FM 4 and FM 14 with ZDDP in BO. The metal phosphide peak was not found in the tribofilm formed with the addition of FM 8 and FM 10 with ZDDP. Furthermore, etching results of the ZDDP tribofilm also showed no metal phosphide peak. Etching can change the chemical state of the species due to ion bombardment [82], [174] but still with this limitation the formation of metal phosphide peak (i.e. in lubricant blends having FM 1, FM 4 and FM 14) indicated that phosphate film could possibly disintegrated deeper in the tribofilm near the substrate.

Philippon et al. [225] investigated the tribochemical interaction of phosphite additives on steel surface. The XPS analysis of the tribofilm formed with the addition of tributylphosphite (TBPi) in liquid phase lubrication (LPL) confirmed the formation of phosphates on top most surface of the tribofilm whereas after etching iron phosphide peak also detected in the same BE window along with phosphates. The tribofilm formed by trimethylphosphite (TMPi) in gas phase lubrication (GPL) without ion etching confirmed formation of iron phosphide peak approximately at 129.2 eV [225], [226]. The BE of iron phosphide peak on the Fe $2p_{3/2}$ spectrum found very close to metallic iron component approximately at 707 eV [225], [226]. The XPS results of the phosphite tribofilms are in agreement with the etching results of the tribofilms (Chapter 8) showed the formation of metal phosphide peak.

On the basis of XPS results, Philippon et al. [227] confirmed formation of the iron phosphide only inside the tribological contact zone. The formation of iron phosphide in the tribofilm is a thermally activated process initiated at or above 300 °C [228]. This thermally activated process facilitate breaking of the P—O bond and interaction of atomic phosphorous with nascent iron surface (after removing the iron oxide layer during tribological interaction) [225], [227], [228]. The in-situ surface spectroscopy analysis [229] proposed formation of the thin iron phosphide film on steel surface in presence of the phosphite additives. This thin film is very effective in reducing friction [219], adhesion and high shear strength of iron [229]. Bouchet et al. [219] using combine GPL experimental results and XPS analysis confirmed that presence of the phosphorous is effective in reducing sliding friction between Fe surfaces. The phosphites produce more P in-comparison to phosphates (due to presence of O in its structure), which restrict adsorption and molecular detachment of P. Therefore, phosphites significantly reduce surface friction.

10.3 Tribological interaction in sequential film formation

The friction results of the sequential film formation tribological tests (Chapter 9), revealed that the FM 1 and FM 8 exhibited higher COF value compared to other blends of amine FMs (i.e. FM 4 and FM 14) on steel surface. Interestingly, formation of the amine FMs film on top of the pre-formed ZDDP tribofilm decreased the high COF value of ZDDP tribofilm. Miklozic et al. [22] confirmed that the tribological interaction of N based OFMs with pre-formed ZDDP tribofilm immediately reduce boundary friction. Furthermore, N based FMs also reduce friction in the mixed lubrication regime. Using MTM-SLIM tribometer, Dawczyk et al. [61], recognised that the amine FMs immediately interact with pre-formed ZDDP tribofilm, reduce boundary friction and also remove part of the ZDDP tribofilm. The reduction in COF value of ZDDP tribofilm is in agreement with the friction results (Chapter 9). Figure 10-3 shows friction behaviour of amine FMs (with different level of saturation) with pre-formed ZDDP tribofilm.

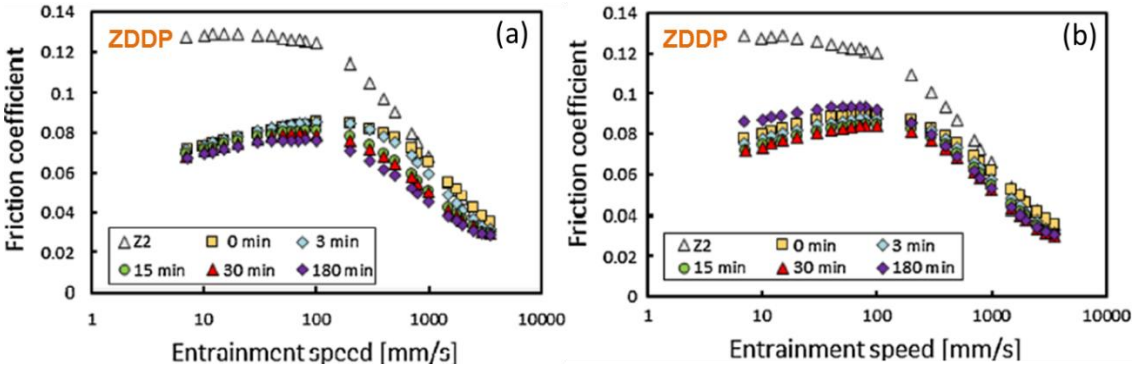

Figure 10-3. The Stribeck friction graphs of the pre-formed ZDDP tribofilm interacted with amine FMs [61]

(▲Z2 represent the ZDDP tribofilm after 3 hours of rubbing)

(a) Saturated amine FM (b) Mixture of saturated and unsaturated amine FM

ZDDP showed a higher COF value on the steel surface and comparatively lower COF values on the top of the amine FMs. The wear results (Chapter 9), suggested a similar wear volume whether ZDDP or amine FMs formed a film first and other additive formed a film on top of the first additive. However, the wear volume slightly varies from one amine FM to another. Tribological results confirmed that ZDDP has the capability to form a tribofilm on the top of an amine film and similarly the amine FMs have the capability to form a film on top of a pre-formed zinc phosphate film formed by ZDDP.

10.3.1 Tribofilm elemental composition

The sequential interaction of the amine FMs with the pre-formed ZDDP tribofilm modified the elemental composition of the tribofilm (Chapter 9). The decrease in the P, Zn and O concentrations demonstrated the competency of the amine FMs to interact with the pre-formed zinc phosphate film formed by ZDDP (Chapter 9). Based on XANES analysis, Dawczyk et al. [61] established that ZDDP AW film mainly consist of zinc orthophosphate and rubbing this pre-formed ZDDP tribofilm in amine FM removed part of the zinc-orthophosphate film [64], [220]. Reduction in zinc concentration indicated possible modification in the tribofilm chemical composition with less formation of zinc oxide, zinc sulphide and zinc phosphate. The etching results (Chapter 9) confirmed that the tribofilms formed in the sequential interaction tests (i.e. amine film on top of ZDDP tribofilm) were not S enriched. The modification in the S incorporation across the tribofilms suggested a clear shift

in the interaction mechanism when the amine FMs interact with the pre-formed ZDDP film. The N incorporation throughout the tribofilms (Chapter 9) proposed the interaction of N with the zinc phosphate film and consequently modified the chemical structure and composition of the tribofilm [22], [61]. The presence of low or no Fe on the top 5-8 nm of the tribofilm surface indicated a formation of well-established zinc phosphate tribofilm on the steel surface (Chapter 9).

10.3.2 Tribofilm chemical composition

The chemical structure of the tribofilm formed due to the interaction of the amine FM on the top of the pre-formed phosphate film brought some fascinating results. The XPS scan of the top 5-8 nm of the film (Chapter 9) confirmed a strong presence of P 2p, O 1s, S 2p, Zn 2p and Zn 3s signals and hence presence of zinc phosphate tribofilm inside the wear track which are mainly composed of phosphates [18], [82]. The absence of a metal oxide peak in the O 1s signal confirmed that rubbing of the ZDDP tribofilm in amine FM was unable to disturb the AW effectiveness of the film. The BE values of the P $2p_{3/2}$ component in all the tribofilms confirmed that they were not comprised of longer chain phosphates. Previous studies [204], [208], [217] identified that the BE value of the P $2p_{3/2}$ component in longer chain phosphates are in the range of 134.1 – 135.0 eV. The BE data (Chapter 9) confirmed that the P 2p signal was shifted towards lower BE values as a result of interaction between the amine FMs and the pre-formed ZDDP tribofilm. Studies [77], [204], [230], recommended that presence of excess metal oxides in the tribofilm shifted the P $2p_{3/2}$ component towards lower BE values. Using XPS analysis, Crobu et al. [204] recognized that the chemical shift of the P $2p_{3/2}$ component towards lower BE values indicated shortening in the phosphate chain length. Yamaguchi et al. [169] using XANES analysis, confirmed that interaction of N based additive with ZDDP produce excess cation in the tribofilm, which is needed to convert long chain phosphates to shorter chain phosphates.

Difference in elemental and chemical composition of the tribofilm formed in both tribological systems (i.e. BO interaction and sequential film formation tests), indicated that the tribological system influenced the interaction mechanisms between amine FMs and ZDDP. Comparatively less suppression in the concentration of key elements of the tribofilm confirmed that in

sequential film formation tests the ZDDP film established on the steel surface but still the amine FMs interacted with the pre-formed ZDDP tribofilm and affected the overall composition of the tribofilm (Chapter 9). Significant suppression in P and Zn concentration in BO interaction tests (continuous test Chapter 8) confirmed that amine FMs restricted ZDDP ability to form AW film and consequently affect its AW capability.

10.4 Film formation of amine FMs on steel surface

OFMs are amphiphilic surfactants with polar end group at one end [116] which form a self-assembled ultra-thin film on the rubbing asperities [106], [116]. OFMs rapidly form films on the interacting surfaces but the film formation rate is dependent on diffusion of the OFMs molecules from oil to the rubbing asperities [106], [117]. OFMs adsorb physically or react chemically with the metal surfaces through their head group on the interacting asperities with the hydrogen chain extending in the lubricant [105], [116], [119]. The role of the polar groups [61] is of vital importance in the effectiveness of the OFMs [104], [118], [231]. OFMs form a film in an orderly manner having closely packed molecules, attached with each other [116], [121].

The amine molecular film is a combination of physical adsorption and chemical reaction with the steel surface [104], [147], [148]. The fatty amines (FAs) possess an affinity with iron oxide surfaces and quickly form chemisorbed films on the iron oxide surfaces [144]. The fatty amine (FA) molecules form thick monolayers even at low concentrations in the solvent [144]. The formation of the surface adsorbed film minimises the metal-to-metal contact and forms a low shear strength plane along the sliding direction, thereby reducing the COF value [67], [104], [105], [116], [131]. The molecular dynamics simulation proposed that the films formed by the FA molecules are approximately 16-20 Å thick [144], [150] with a molecular tilt angle somewhere between 30° and 60° with respect to the metal oxide surface [116], [144], [150]. Salmeron [232] studied the microscale processes in alkane chain monolayer film using AFM and surface force apparatus (SFA). He proposed that contact pressure in the tribological contact zone influence the tilt angle of the FA molecules on the Fe surfaces. The extreme contact pressure reduces

the tilt angle between the FA molecules and Fe surface, which ultimately blocks the metal surface and suppress the adsorption of other additives.

Recently, Nalam et al. [116] investigated the adsorption behaviour of amine FMs on the steel surface using a quartz crystal microbalance (QCM) and AFM. The experimental results demonstrated that FAs generally form horizontally oriented weakly adsorbed boundary film on the steel surfaces. The unsystematic adsorption of FA molecules, presence of weak interaction forces between FA molecules and steel surface and short equilibrium time may lead the development of boundary film composed of multilayer or mono layer with a tilt angle around 17°. The lateral force microscopic analysis [116] showed that FA derivatives having high adsorption rate constants, quickly replace the worn out molecules and maintain low COF value during tribological interaction.

10.4.1 Factor affecting the performance of amine FMs

The chemical structure and alkyl chain length, polarity of the head group, presence of multiple functional groups, degree of saturation, concentration, and solubility of the OFMs determine the thickness and density of the adsorbed molecules on the interacting surfaces [104], [116], [118], [120], [122], [131]. Other external factors such as temperature, pressure, metallurgical composition of the substrate may also influence on the performance of the amine FMs [106], [118], [130]. Spikes [104] specified that OFMs having straight chain chemical structure, saturated bonds and small head groups form strong monolayers with closely packed molecules.

FM 1 (i.e. coca amine) and FM 8 (i.e. tallow amine) both have a straight chain hydrocarbon structure. However, FM 1 molecules consist of a relatively shorter hydrocarbon chain length in comparison to FM 8 molecules. The amines are the highly polar surfactants due to large dipole moment of a lone pair of electron in its structure [146]. The amines may act as a Lewis base (a nucleophile) because of a lone pair of electron which can bond with an electrophile [145], [146]. The N atom in the amine group can donate a lone pair of electron to surface Fe (III) ions [116], [144], [145] and as a result of this reaction, amine form a film on the iron oxide surfaces [144]. The presence of strong van der Waals interactions between alkyl chains may lead to the

formation of monolayers on the metal surface [131], [138], [233]. The Steric hindrance between alkyl group on opposing interacting surfaces produce a low shear strength plane which facilitate the sliding process [234]. Jahanmir [120] stated that increase in the alkyl chain length decrease the COF value and it may be due to increase in the lateral cohesive forces between methyl groups of neighbouring saturated alkyl chain [131]. Kenbeek et al. [119] specified in a review study that increase in alkyl chain length increase the thickness of the molecular film.

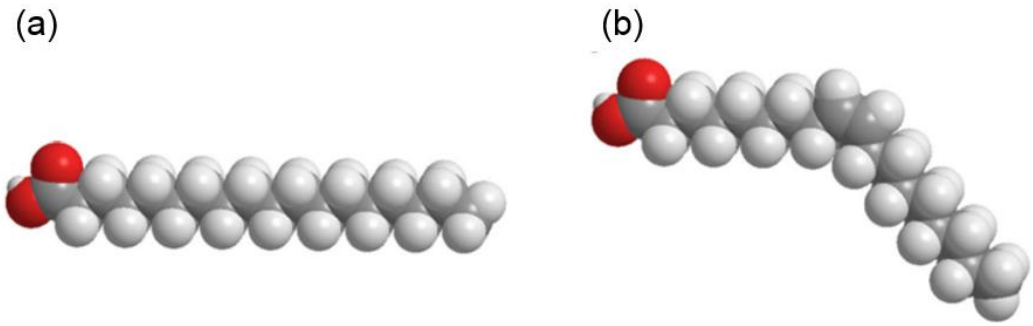

Figure 10-4. Modification in structural configuration due to *cis*-double bond [140]
(a) Saturated stearic acid (b) Unsaturated oleic acid

The degree of unsaturation in the alkyl chain also affect the amine interaction behaviour with ZDDP [133]. The tribological performance of primary saturated stearylamine is found to be relatively better than that of primary unsaturated oleyl amine [124], [133]. The unsaturation in the molecules promotes higher steric hindrance in comparison to saturated hydrocarbons which affects the adsorption of the OFMs and hence the tribological performance [131], [144]. The cis-to-trans ratios of both FMs (i.e. FM 1 and FM 8) not disclosed but the provided chemical structure indicated the presence of *cis*-double bond in both FMs. The chemical configuration of the FM 8 molecules confirmed a higher degree of unsaturation in comparison to the configuration of the FM 1 molecules. The existence of *cis*-double bond in the respective FA molecules introduces kinks in the structure [171]. The presence of kinks tilts the hydrocarbon chain towards the metal surface and reduces the packing density of the molecular film [140], [171]. The unsaturated OFMs form disorderly and

loosely packed molecular film [131]. Figure 10-4 shows the difference in the structural configuration of a saturated molecule and an unsaturated molecule.

The reduction in the packing density affects the adsorption capability of the amine molecule and also blocks the free surface that other additives may use to form a film on the metal surface [116], [140]. The higher steric hindrance in unsaturated alkyl hydrocarbons is due to presence of *cis*-double bond which affects the friction performance [104], [131], [140], [235]. The saturated amine molecules form well organised molecular films on the top of the iron oxide with a tilt angles at 30-50° range [144]. The FM 1 and FM 8 molecules have a high degree of unsaturation in the chemical structure but they probably follow the similar film adsorption model as the saturated amine molecules with the exception of the less densely packed molecular film and the modification in the tilt angle of the alkyl group towards the metal surface. Figure 10-5 shows the film formation schematic of FM 1 and FM 8 on the steel surface.

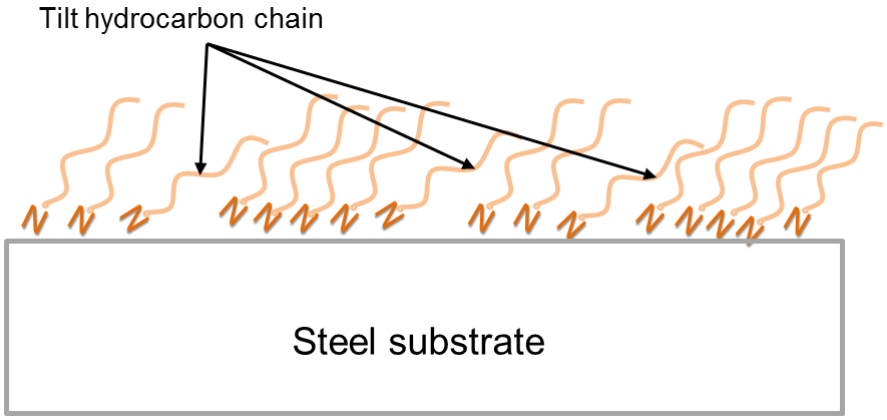

Figure 10-5. Adsorption process of FM 1 and FM 8 on the steel surface during rubbing

The amine ethoxylates are formed as a result of a reaction of the primary FA with ethylene oxide [236]. Ethoxylation improves the solubility and anti-corrosion characteristics [237]. The presence of functional groups in the amine FMs promotes chelation and consequently adsorption [104], [116], [131]. The film formation of FM 4 (i.e. ethoxylated hydrogenated tallow amine) is slightly complex due to presence of OH (hydroxyl group) group in the chemical structure. FM 4 possibly follows two adsorption pathways on the metal

surface. The O is more electronegative than N which means that O─H bonds are more polar than N─H bonds [146].

- The first pathway is the physical adsorption of the two hydroxyl groups on the iron oxide surface [105], [238] and/or interaction of the hydroxyl groups with the iron oxide surface [171]. The hydroxyl group carries strong nucleophilic properties thus interacts with Fe (III) cations (positive sites) and form chemical bonding between O in the hydroxyl group and Fe in the iron oxide surface layer [171]
- The second pathway is the chemisorption process of N atom through the donation of lone pair of electron to surface Fe (III) ions [116], [144], [145]. As a result of the amine-iron interaction, the molecular film form on the iron oxide surface [144]

The two pathway interactions of the FM 4 with the iron oxide surfaces improves the adsorption performance and film coverage of the amine molecules on the iron oxide surface [163], [171]. Soltanahmadi et al. [171] proposed that the larger head group of ethoxylated amine facilitate the amine molecules to occupy the maximum surface area and improve the film coverage. Figure 10-6 shows the film formation schematic of FM 4 on the steel surface.

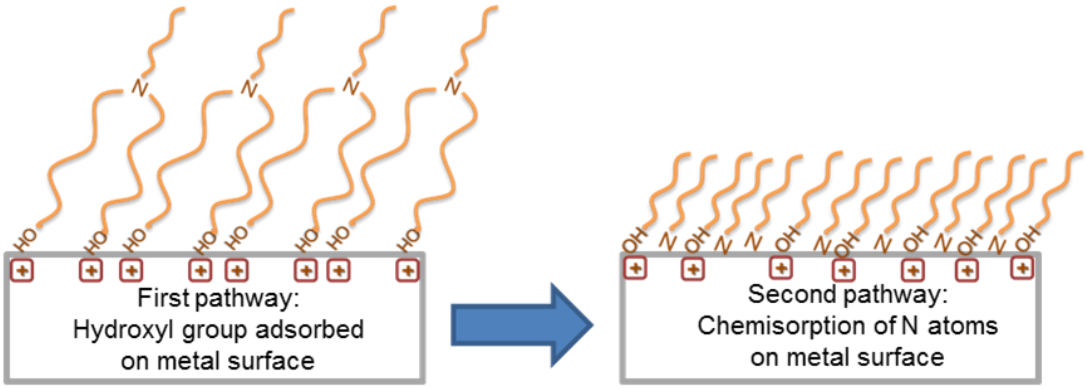

Figure 10-6. Adsorption process of FM 4 on the steel surface during rubbing

FM 14 (ester of tri-ethanol amine with tallow fatty acid) is designed to improve the adsorption capability and consequently the friction properties of the

composition [105]. The chemical structure of FM 14 indicates the existence of *cis*-double bonds, which can introduce kinks in the structure. The presence of kinks tilts the hydrocarbon chains towards the metal surface and reduces the packing density of the molecular film [140], [171]. The film formation of FM 14 is more complex due to presence of hydroxyl (OH) and ester (OC–O–R) groups. Figure 10-7 shows the film formation schematic of FM 14 on the steel surface.

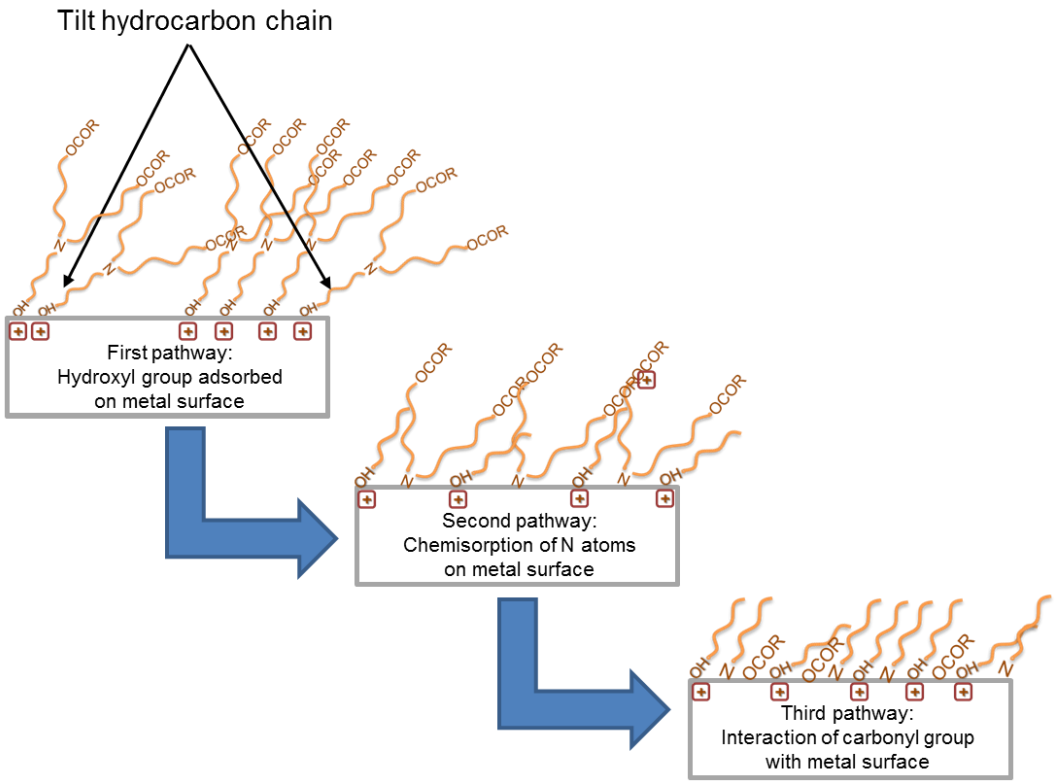

Figure 10-7. Adsorption process of FM 14 on the steel surface during rubbing

FM 14 possibly followed three adsorption pathways on the metal surface.

- The first pathway is physical adsorption of hydroxyl head group on iron oxide surface [105], [238] and/or interaction of hydroxyl group with iron oxide surface [171]. The hydroxyl group which carries strong nucleophilic properties interact with Fe (III) cations (positive sites) and form a chemical bond between O in hydroxyl group and Fe in iron oxide surface layer [171]

- The second pathway is the chemisorption process of N atom through donation of a lone pair of electron to surface Fe (III) ions [116], [144], [145]. As a result of amine-iron interaction, the molecular film form on the iron oxide surface [144]
- The third pathway involved interaction of ester group with the iron oxide surface layer. The carbonyl (C=O) group in ester has competency to proceed Lewis acid-base reaction with the hydroxyls on the iron oxide surface [239]

Infrared reflection absorption spectroscopy (IRRAS) analysis [239], suggested that ester containing organic compounds physically adsorb through carbonyl group and form hydrogen bond with the substrate material [240], [241]. Zachariah et al. [131] identified that physical adsorption proceed through formation of hydrogen bonding with the oxygen of the metal surface. Presence of multiple functional groups in chemical structure promote chelation and improve adsorption on metal surfaces [116], [131]. Furthermore, increase in steric hindrance because of multiple functional groups may also affect the adsoroption kinetics of the OFMs [131].

10.5 Interaction between amine FMs and ZDDP

The addition of amine FMs in the lubricant blend modified the chemical composition of the tribofilm formed by BO + ZDDP. Interestingly, the tribofilms formed in the sequential interaction tests showed different elemental incorporation trends in-comparison to the tribofilms with lubricant blends having amine FMs and ZDDP together in the BO (tribofilm etching results Chapter 8 and Chapter 9). Dissimilarity in the elemental incorporation indicated a difference in interaction mechanism in both tribological systems. The AW performance of ZDDP is affected by its interaction with other additives including OFMs [22], [61], [159]. The amines and amid are effective OFMs and both reduce friction in boundary and mixed lubrication regimes [22]. MTM tribological test [61] confirmed that the ethoxylated amine FMs have the capability to reduce the high boundary friction of pre-formed ZDDP tribofilm. The sequential interactions friction results (Chapter 9), showed that not only

ethoxylated but non-ethoxylated amine FMs also have the capability to form a film on the top of the pre-formed ZDDP tribofilm and reduce COF value.

In the absence of ZDDP, amines form a film through donation of lone pair of electron to surface Fe (III) ions [116], [144], [145]. The addition of amines with ZDDP in the BO affect the AW film formation capability of ZDDP [22], [61], [116], [163]. The amines with sp^3 hybridization act as a Lewis base and can donate a lone pair of electron [145]. In the presence of ZDDP in lubricant oil, amines act as a ligand and form amine-ZDDP complex through Zn atom in ZDDP [22], [30]–[33], [64], [124], [171]–[173]. The FAs affect the AW film formation of ZDDP by delaying or slowing down the film formation mechanism [22], [30], [33], [164]. The rate of decomposition of ZDDP decreased in the presence of amines as it takes more time to decompose [30], [162]. The sequential film formation test results (Chapter 9) showed that ZDDP have the capability to form a tribofilm on the top of the film formed by the amine FMs but with reduced COF value.

The antagonistic wear behaviour of FM 1 and synergistic wear response of FM 8 (Chapter 8) specified that some other factors e.g. the alkyl chain length, polarity of the head group, presence of multiple functional groups, degree of saturation and solubility etc. [104], [116], [118], [120], [122], [131] influence the interaction of the amine FMs with ZDDP. The molecular structure and alkyl chain lengths are very crucial for the extent of ZDDP-amine interaction. Studies [30], [61], [124] identified that primary alkyl amines showed the maximum amine interaction with ZDDP and it is possibly due to the chelation of Zn^{2+} ions from zinc-phosphate film [22], [61]. Amendments in the primary amine structure by introducing branch or branches having chains and double bonds in the structure reduces the amine interaction significantly [30], [162], [175]. The presence of unsaturation in alkyl chain affects the amine interaction behaviour with ZDDP [133]. The tribological performance of primary saturated stearylamine is found to be relatively better than that of primary unsaturated oleyl amine [124], [133]. Loehle et al. [117] linked the differences in the tribological performance with the formation of self-assembled films and suggested that unsaturated molecules form more disordered self assembled films than saturated molecules.

10.5.1 Interaction mechanism of amine FMs

The tribological behaviour and elemental incorporation analysis of both tribological systems suggested few interaction mechanisms. One or more than one interaction mechanisms may be involved in the tribofilm formation of the lubricant blend having amine FMs and ZDDP in BO [22], [34], [164]. These interaction mechanisms include,

- ❖ Preferential adsorption and blocking effect of adsorb additive
- ❖ Reaction with decomposed ZDDP by-products
- ❖ ZDDP amine complex formation

10.5.1.1 Preferential adsorption and blocking effect of adsorb additive

The sequential film formation tests explored the preferential adsorption and blocking effect scenario between ZDDP and amine FMs. In this mode of interaction one additive take the lead and preferentially adsorbs on the metal surface (completely or partially) and then the second additive has only option to form a film on top of the pre-formed film or find limited metal surface to form a film in the case of partial adsorption of the first additive. Previous studies [22], [33], [34], [164], [174] documented that N containing additives have the capability to preferentially adsorb on the metal surfaces and as a result reduce ZDDP derived tribofilm [34]. Figure 10-8 shows schematic illustration of preferential adsorption interaction mechanism.

In this interaction mechanism, the preferentially adsorbed additive create a blocking effect for the second additive and disturb its film formation capability on the metal surface. MTM experimental results [34] established that addition of DMODA with ZDDP significantly reduce COF value, whereas addition of dispersant increased COF value. Interestingly, both N containing additives reduced the ZDDP derived tribofilm [34]. The tribological result recognised that preferential adsorption of DMODA on steel surface reduced COF value [34]. The increase in COF value indicated that dispersant additive not preferentially formed film on the steel surface and/or high contact pressure/shear in the tribological contact zone completely remove the molecular film and supposedly molecular film is unable to quickly replace the worn out molecules [116]. The electron probe microanalysis (EPMA) [34]

confirmed that addition of dispersant suppressed the P content in the tribofilm, which means that dispersant produced a blocking effect on ZDDP tribofilm formation. Fujita and Spikes [220] using MTM-SLIM optical interference images established that rubbing in dispersant solution remove the pre-formed ZDDP tribofilm [22], which possibly means that only part of the tribofilm exist on the steel surface.

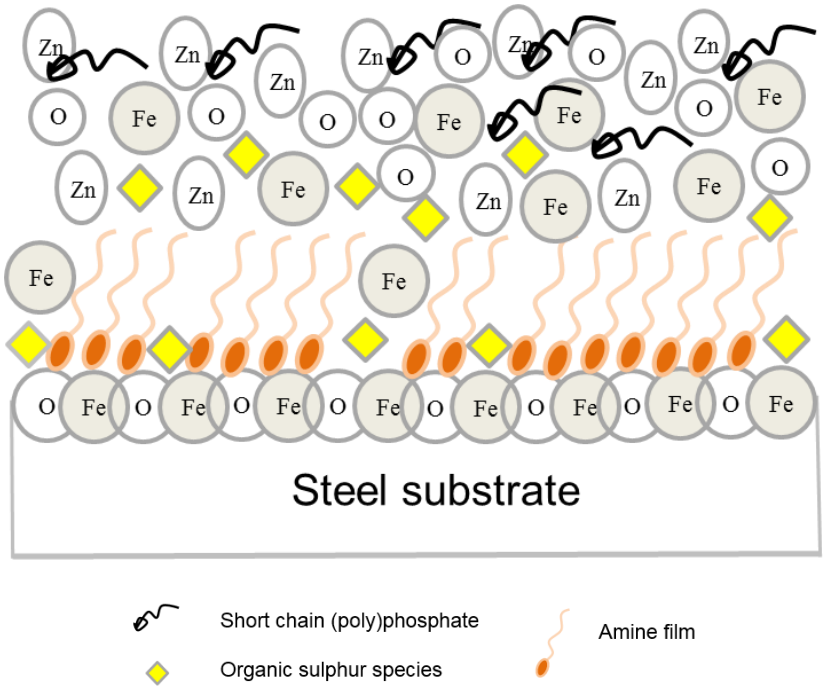

Figure 10-8. Schematic of preferential adsorption interaction mechanism between amine FM and ZDDP

10.5.1.2 Reaction with decomposed ZDDP by products

The decomposition of ZDDP is a mechanochemical process which is dependent on the availability of shear and heat in the surface contact zone [63], [65], [92], [95]. The decomposition of ZDDP produces zinc phosphate deposits on the metal surface, which can react with iron oxide (in case of the steel substrate) and produce Fe/Zn phosphate along with zinc-oxide [58], [70]. The presence of amine FM in the blend accelerates the hydrolysis of neutral ZDDP and produces zinc oxide in two stage chemical reaction [124], [177], [178] provided that the available temperature is up and above 100 °C [124], [179]. The amine FMs and zinc oxide in the lubricants may lead to the

formation of ZnO-amine complexes or possibly reverse micelles (in which the FA molecules are firmly attached with the zinc oxide core) [124], [180]. These micelles form a ZnO rich tribofilm on the interacting asperities, which reduces the wear [124]. The amine group also has the capability to form complex with zinc cation and consequently seep it out from the zinc phosphate glass [22]. Figure 10-9 shows the interaction mechanism of amine FM with decomposed ZDDP by products.

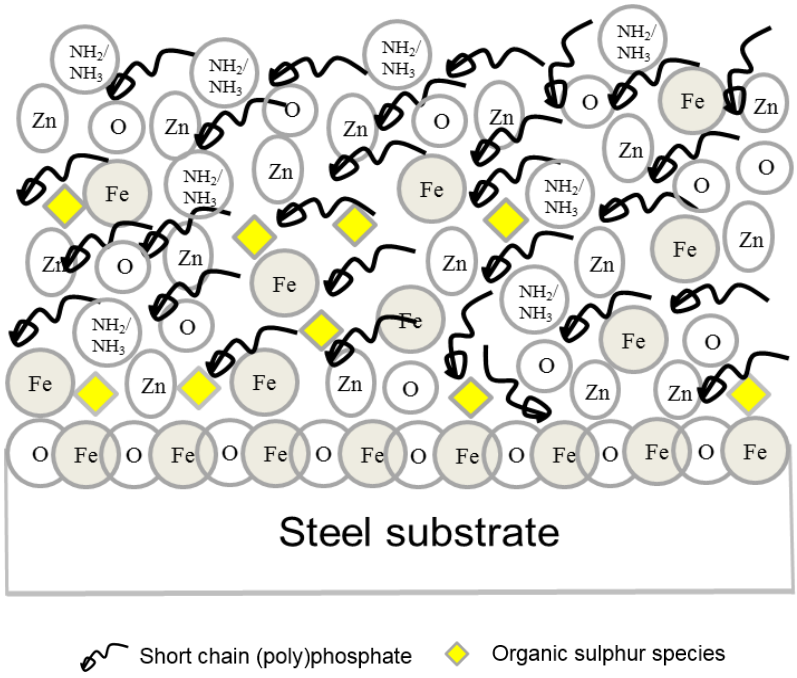

Figure 10-9. Schematic illustration of interaction mechanism of amine FMs with the ZDDP by products

The XPS results (Chapter 8), confirmed the deconvolution of N 1s signal in N-C/N-H groups. Previous studies [165], [171], [242] established that N-C/N-H groups has the capability to chemisorb on the metal surfaces having zinc-phosphate deposits and form amine/ammonium phosphate. The lubricants having N based additives and ZDDP produce a tribofilm comprised of amine/ammonium phosphate as a result of tribochemical interaction between the amine group and decomposed ZDDP by-products [165], [169], [171], [187]. The tribochemical interaction between amine and ZDDP by-products also produce additional cations [164], [165], [169], [187]. The

presence of excess cation in the tribofilm depolymerise the longer chain phosphates into shorter chain phosphates [169]. The chemical shift in P 2p signal in the tribofilms (Chapter 8) were possibly due to the formation of amine/ammonium phosphate because of the interaction between N-C/N-H groups and decomposed ZDDP by-products [165], [187].

10.5.1.3 ZDDP amine complex formation

The amine FMs affect the AW film formation of ZDDP by delaying or slowing down the film formation mechanism [22], [30], [33], [164]. Matsui et al. [31], by using AES results confirmed that addition of the additives (having amino functional group) in the lubricant blend with ZDDP remarkably reduced P-concentration in the deposited film. The presence of amine FMs in the lubricant blend can suppress the ZDDP decomposition rate and consequently the ZDDP molecules take longer time to decompose and form zinc phosphate film [30], [162]. The simplest amine (i.e. NH_3) has central N atoms which are sp^3 hybridized [145]. The amines with sp^3 hybridization are more likely to donate a lone pair of electrons then amines with sp^2 hybridization and act as a Lewis base [145]. In presence of ZDDP in the lubricant oil, amines act as a ligand because of a lone pair of electron [33], [171] and form amine-ZDDP complex through Zn atom in the lubricant blend [31], [33].

Previous studies [22], [30], [173], [31]–[33], [64], [91], [124], [171], [172] proposed that the amine FMs interact with ZDDP molecule in the BO and produce metal complexes which are bigger in size and lead to higher steric hindrance, which consequently reduces the adsorption on the metal surface [171]. The phosphorous nuclear magnetic resonance (P-NMR) spectrum [31] analysis confirmed that addition of amino functional group modified the compound ratio of basic to neutral ZDDP. The decrease in original value of neutral ZDDP is supposed to be due to formation of coordination complex between amino functional group and Zn atom in neutral ZDDP. Previous study [243] reported that formation of coordination complex with Zn atom in basic ZDDP is highly unlikely due to its tetrahedral structure along with six dithiophosphates (DTP) ligands around it. The ZDDP-amine complexes are in equilibrium with both the reactants and the degree of complex formation is dependent on basicity of the amines [33]. The ZDDP-amine complexes reduce

the concentration of the free ZDDP molecules available in the BO which affect the ZDDP film formation capability [171].

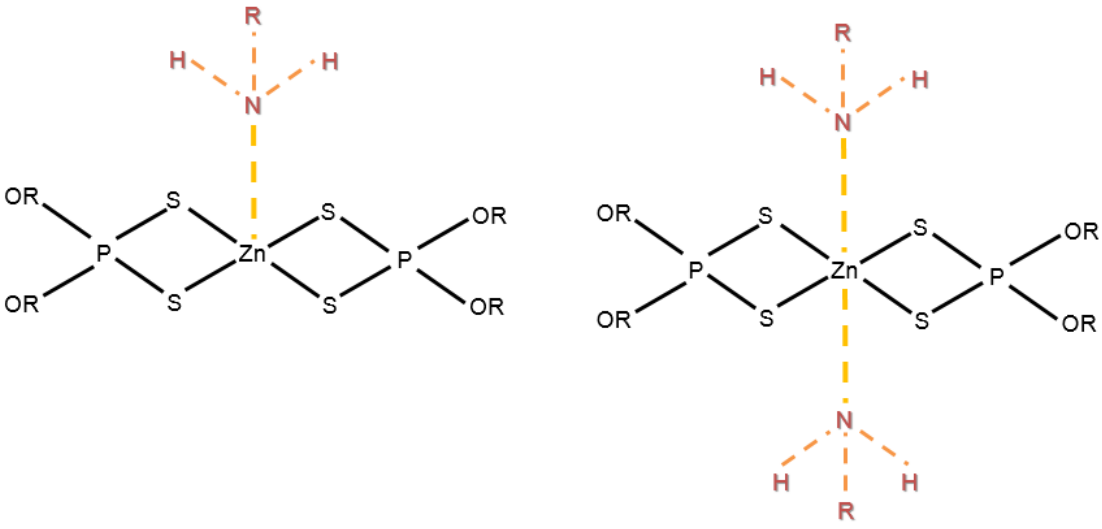

1:1 ZDDP-amine metal complex 1:2 ZDDP-amine metal complex

Figure 10-10. ZDDP-amine complex formation [33]

The molecular structure and alkyl chain lengths are very crucial for extent of the ZDDP-amine interaction [30], [61], [124] and it also influence the tendency of complex formation of amines with ZDDP. The amines having limited steric hindrance around the N atom form 1:2 complexes with ZDDP, medium hindrance amines form 1:1 complexes while large hindrances around N atom form no complexes [33]. Figure 10-10 shows the ZDDP amine complex formation.

10.5.2 Wear behaviour and interaction mechanisms

The wear results (Chapter 6) showed that the addition of amine FMs with ZDDP produced synergistic or antagonistic wear behaviour. The tribofilm topographical results (Chapter 7) confirmed that the addition of amine FMs with ZDDP modified the tribofilm topography. The XPS results (Chapter 8 and Chapter 9) revealed a modification in the elemental/chemical composition of the tribofilm, which ultimately reflected in wear behaviour. The tribological test results and surface characterization of the tribofilm made it clear that the addition of amine FMs disturbed the ZDDP's AW film formation capability and

the extent of this disturbance varied from one FM to other. The XPS results also suggested that the different amine FMs interact with ZDDP in different fashion and furthermore the interaction mechanism of amine FMs varied from one FM to other.

10.5.2.1 Antagonistic wear behaviour and film formation mechanism

The addition of FM 1 and FM 4 with ZDDP in BO reduced the COF value in comparison to the tribofilm formed by BO + ZDDP but at the same time increased the wear factor value significantly (Chapter 6). The elemental incorporation results (Chapter 8 and Chapter 9) showed a clear modification in the tribofilm elemental structure because of the interaction of the amine FMs with ZDDP in BO (continuous test) and in sequential film formation tests. The modification in the elemental concentration of the key elements of the tribofilm affected the AW performance of ZDDP.

The elemental incorporation comparison of FM 1 with ZDDP in both tribological systems confirmed the modification in the elemental composition of the tribofilm. Interestingly both tribological systems produced different elemental incorporation trends and this dissimilarity in the tribofilm elemental composition suggested a difference in the interaction mechanism between FM 1 and ZDDP. However, both tribological systems suppressed concentrations of P, Zn and O in the tribofilms but the sequential film formation tests comparatively showed more concentration of these elements. The tribofilm formed in sequential film formation tests was not S driven as observed in the tribological system having FM 1 and ZDDP in BO (continuous test). The sequential film formation tests also suppressed N incorporation in the tribofilm, which indicated a limited interaction of N across the tribofilm. The elemental composition analysis categorically showed that both tribological systems followed different interaction mechanisms.

The elemental incorporation comparison of FM 4 with ZDDP in both tribological systems showed a modification in the elemental composition of the tribofilm. BO interaction of both additives (continuous test) significantly reduced P, Zn and O concentrations throughout the tribofilm. The tribofilm formed as a result of BO interaction was S dominated [32], [34]. The sequential film formation tests supported the argument that ZDDP

preferentially forms a film on the steel surface but the tribological interaction of FM 4 can disturb the pre-formed zinc phosphate film, which consequently modified the P, Zn and O concentrations. The sequential film formation tests showed a much better film formation capability of ZDDP in-comparison to the interaction of FM 4 with ZDDP in BO (continuous test). Another key difference was the incorporation of N throughout the tribofilm. The sequential film formation tests suppressed the N incorporation in-comparison to the tribofilm formed in the BO interaction of both additives (continuous test). The N-incorporation in the tribofilm was the key difference in both tribological interaction systems. The variation in elemental incorporation established the difference in the interaction mechanisms.

The reduction in the COF value and the significant increase in wear supported any or both of these interaction mechanisms,

- Preferential adsorption and blocking effect of amine FM
- ZDDP amine complex formation

The elemental incorporation analysis of the sequential film formation tests showed higher concentration of P and Zn compared to those in the BO interaction of both additives (continuous test). The suppression in the P and Zn concentration supported the preferential adsorption of amine FM on the steel surface, which completely or partially blocked the surface. The reduction in the COF value also suggested that some adsorbed molecular film existed on the interacting asperities [34]. The tribological results (Chapter 9) confirmed the capability of ZDDP to form zinc phosphate film on the top of the amine film but this blocking effect partially reduced the ZDDP's AW film formation capability [34], [164], [174]. The reduction in the COF value, significant increase in wear and limited formation of the tribofilm suggested that the respective amine FMs (i.e. FM 1 and FM 4) preferentially adsorbed on metal surfaces [16], [34], [110], [111], [220].

The suppression in P and Zn concentrations in the tribofilm formed by the addition of FM 1 and FM 4 with ZDDP in respective BO interactions (continuous test), strongly supported the possibility of complexation between ZDDP and amine group in the BO [30]–[33], [164], [174], [244]. The amine FMs interact with ZDDP molecule in BO and produce metal complexes, which

are bigger in size and lead to higher steric hindrance [22], [30], [173], [31]–[33], [64], [91], [124], [171], [172] and reduce adsorption rate of ZDDP on the metal surface [171]. Matsui et al. [31] stated that the formation of coordination complex between amine FM and Zn atom (with the neutral ZDDP) decrease the content of neutral ZDDP but not disturb the chemical equilibrium state between neutral and basic ZDDP. The formation of coordination complex modify the decomposition temperature [31] which suppress the ZDDP decomposition rate and consequently ZDDP molecules take longer time to decompose and form AW film [30], [162]. The ZDDP-amine complexes reduce the concentration of free ZDDP molecules available in BO [31], [32], [171]. In this case the tribofilm is formed by the surplus ZDDP [30], which was reflected in terms of the suppression in the P and Zn concentrations. The results showed that one mechanism is not solely representing the complete film formation mechanism but possibly more than one mechanisms worked together [22], [34], [164].

FM 1 and FM 4 both followed a similar interaction mechanism to interact with ZDDP in BO (continuous test). Comparatively higher wear with the addition of FM 1 in the blend with ZDDP is possibly due to chemical structure and hydrocarbon chain length. FM 1 possesses straight chain structure with relatively shorter hydrocarbon chain length. The degree of unsaturation in FM 1 introduced kinks in the chemical structure, which tilt the hydrocarbon chain, reduce the packing density [140], [171] and block the free surface that ZDDP may use to form a film on the steel surface [116], [140]. The primary alkyl amines show the maximum amine interaction with ZDDP [30], [61], [124] and it is possibly due to the chelation of Zn^{2+} ions from zinc phosphate film [22], [61]. FM 4 is an ethoxylated hydrogenated long chain hydrocarbon. Ethoxylation improves solubility [237] and the presence of functional groups promotes chelation and consequently adsorption [104], [116], [131]. FM 4 molecule preferentially form a closely pack molecular film on the metal surface and is comparatively less interactive with ZDDP [104], [131]. Amendments in the primary amine structure by introducing branch or branches having chains, double bonds in the structure, aromatic rings reduce the amine interaction significantly [30], [162], [175]. Both amine FMs produce metal complexes with ZDDP and preferentially form a film on the metal surfaces. Difference in the

chemical structures affects their interaction with ZDDP and the molecular films formed by these additives on the metal surfaces (Figure 10-3 and 10-4).

10.5.2.2 Synergistic wear behaviour and film formation mechanism

The tribofilm formed by the lubricant blends having FM 8 and FM 14 with ZDDP showed a synergistic wear behaviour. The XPS results (Chapter 8 and Chapter 9) confirmed that both additives followed slightly different interaction pathways with ZDDP.

The BO interaction of FM 8 and ZDDP (continuous test), reduced the COF value and showed a synergistic wear behaviour, which means that the wear factor value decreased significantly. The elemental incorporation in both tribological systems significantly suppressed the P and O concentrations. The BO interaction (continuous test) massively increased the S and Zn concentrations in the tribofilm. The N incorporation in the tribofilms was the key difference in both tribological systems. The BO interaction of both additives (continuous test) showed more N-incorporation across the tribofilm whereas the sequential film formation tests displayed comparatively lesser incorporation. These interesting dissimilarities in the elemental incorporation behaviour suggested that both tribological systems followed different interaction mechanisms. The reduction in COF value and synergistic wear behaviour indicated the possibility of any or both of these interaction mechanisms and these are,

- ❖ Preferential adsorption and blocking effect of amine FM
- ❖ Reaction with decomposed ZDDP by-product

The tribofilm formed in sequential film formation tests displayed reduced concentration of P and Zn in comparison to the tribofilm formed by BO + ZDDP. Interestingly, the elemental incorporation trends followed the footprints of the tribofilm formed by BO + ZDDP. The BO interaction of both additives (continuous test), further suppressed the concentration of P in the tribofilm. The suppression in the P concentration indicated that presence of FM 8 in the blend disturbed the tribofilm formation capability of ZDDP. The reduction in COF value and the formation of a limited tribofilm possibly mean

that the FM 8 molecules preferentially adsorbed on the steel surface and disturbed the AW film formation capability of ZDDP [34], [164], [174].

The XPS results (continuous test Chapter 8) displayed presence of relatively strong Zn 3s then P 2p signal, which suggested an increase in the Zn and decrease in the phosphates in the tribofilm. A small metal oxide peak also detected in the O 1s signal. These modifications in chemical composition of the tribofilm proposed depletion in phosphate and formation of additional zinc-oxide in the tribofilm. Studies [124], [177], [178] proposed that presence of amine FM accelerate the hydrolysis of neutral ZDDP and transformed it into basic ZDDP. This newly formed basic ZDDP molecule decompose into neutral ZDDP and zinc-oxide (ZnO) provided that the available temperature is up and above 100 °C [124], [179]. The presence of amine FM and zinc-oxide in the lubricant may lead to the formation of ZnO-amine complexes or possibly reverse micelles (in which FA molecules are firmly attached to zinc-oxide core) [124], [180]. These micelles form ZnO rich tribofilm on the interacting asperities, which reduce wear [124] and improve the AW performance of the lubricant blend. The XPS results (continuous test Chapter 8), confirmed the deconvolution of the N 1s signal in the N-C/N-H group, which adsorbed on the surface having zinc phosphate deposits and formed amine/ammonium phosphate [165], [171], [242]. Previous studies [165], [169], [171], [187], [242] proposed that addition of N-based additives with ZDDP produce a tribofilm having amine/ammonium phosphate because of the interaction between the amine group and the decomposed ZDDP by-products.

The interaction of FM 14 and ZDDP in BO (continuous test) reduced COF value and showed a synergistic wear behaviour. The elemental incorporation analysis (Chapter 8 and Chapter 9) in both tribological systems significantly suppressed the P, Zn and O concentrations in comparison to the tribofilm formed by BO + ZDDP. The S concentration increased slightly in both tribological systems. The elemental incorporation analysis revealed that both tribological systems exhibited very similar elemental incorporation trends, which recognised that change in the tribological systems had no significant impact on the tribofilm elemental structure. The similarity in the elemental structure of the tribofilm emphasized that both tribological systems followed more or less similar interaction mechanisms. The reduction in COF value and

the synergistic wear behaviour showed the strong possibility of any or both of these interactions or film formation mechanisms and these are,

- ZDDP amine complex formation
- Reaction with decomposed ZDDP by-products

The similar elemental incorporation trends in both tribological systems negate the possibility of preferential adsorption and amine blocking effect. The suppression in the P and Zn concentration in-comparison to the tribofilm formed by BO + ZDDP strongly supported the possibility of complexation between the amine group and ZDDP in BO [30], [31], [33], [164], [173], [174], [244] which consequently restricted the ZDDP capability to form zinc phosphate tribofilm on the surface. The amine FMs interact with ZDDP molecule in the BO and produce metal complexes, which are bigger in size and lead to higher steric hindrance [22], [30], [173], [31]–[33], [64], [91], [124], [171], [172] and thus reduce adsorption rate of ZDDP on the metal surface [171]. The formation of coordination complex modify the decomposition temperature [31], which suppress the ZDDP decomposition rate and consequently ZDDP molecules take longer time to decompose and form AW film [30], [162]. The ZDDP-amine complexes reduce the concentration of free ZDDP molecules available in BO [31], [32], [171]. In this case the tribofilm is formed by the surplus ZDDP [30], which was reflected in terms of the suppression in the P and Zn concentrations.

The presence of the amine FMs accelerates the hydrolysis of neutral ZDDP and form basic ZDDP [124], [177], [178]. This newly form basic ZDDP molecule decompose into neutral ZDDP and zinc-oxide (ZnO), provided that the available temperature is up and above 100 °C [124], [179]. The presence of amine FM and zinc-oxide in the lubricant may form ZnO-amine complexes or possibly reverse micelles (in which FA molecules are firmly attached to zinc-oxide core) [124], [180]. These micelles form ZnO rich tribofilm on the interacting asperities, which reduces wear [124] and improves the AW performance of the lubricant blend. The sequential film formation test results (Chapter 9) showed that FM 14 has the capability to adsorb on top of the pre-formed ZDDP film and interact with the decomposed by-products of the ZDDP. The XPS results (continuous test Chapter 8), confirmed the deconvolution of

the N 1s signal in the N-C/N-H group. The N-C/N-H group has the capability to chemisorb on the metal surfaces having zinc phosphate deposits and form amine/ammonium phosphate [165], [169], [171], [187], [242]. The adsorption of the OFM on the ZDDP tribofilm may reduce the COF value just like the reduction in the COF value observed by the adsorption of the OFM molecules on the steel surfaces [110], [111]. The sequential film formation tests (Chapter 9) showed a reduction in COF value when the blend of FM 14 formed a film on the top of the pre-formed ZDDP tribofilm.

The addition of both amine FMs showed a synergistic wear behaviour but they followed different interaction mechanisms. The reaction with the ZDDP decomposed by-products is the common film formation mechanism found in both amine FMs. The results showed that one mechanism may not solely represent the complete film formation but possibly more than one mechanisms worked together in tribofilm formation [22], [34], [164].

Chapter 11
Conclusions and future work

This final chapter of the thesis contains fundamental conclusions derived from this study. These conclusions ranges from basic tribological behaviour of lubricant blends to morphology of the tribofilms, Interaction of additives in base oil (BO) to sequential film formation tests, elemental composition of the tribofilm to chemical structure of the tribofilm and finally interaction mechanism of amine FMs and ZDDP. Later on, this chapter also discuss areas, which needs further study / investigation, and these are included under future work.

11.1 Conclusions

During this study different experiments are designed, performed and their results (both tribological and surface analysis) are analysed to answer some open ended questions related with interaction of OFMs with ZDDP. Though tribological behaviour, film formation mechanism and morphology of the tribofilm formed by ZDDP is already discussed in literature but it is also included in this thesis to explore the tribological evolution inducted due to interaction of ZDDP with OFMs. The primary purpose of this study was to,

- Analyse the effect of OFMs on tribofilm morphology, durability, composition and film formation capability of ZDDP
- Understand tribochemical interaction between OFM and ZDDP

All tribological tests were performed in boundary lubrication regime which is the most critical and sever in terms of friction and wear in engine components. This study showed the feasibility of using amine FMs instead of MoDTC along with ZDDP. The most important finding of this study are as follows,

- Tribofilm formed with the addition of OFM with ZDDP produced encouraging friction results. Data showed reduction in COF values though reduction in COF value varies from one OFM to another
- Addition of OFMs with ZDDP in the blend primarily affected the AW performance of ZDDP and as a result wear factor value shifted from significant increase in wear to remarkable decrease in wear

- Addition of all OFMs (except FM 10) with ZDDP significantly modified the chemical composition of the tribofilm
- Addition of all amine FMs with ZDDP disturbed the tribofilm formation capability of ZDDP, modified the tribofilm topography and roughness parameters which ultimately affected the AW performance of ZDDP
- The tribofilm formed by addition of all amine FMs with ZDDP are found rich in sulphur instead of phosphorous
- All amine FMs have capability to form film on top of the pre-formed ZDDP tribofilm. Incorporation of N across the tribofilm indicated formation of amine phosphate and as a result COF value is decreased
- Amine FMs which showed synergistic wear behaviour (i.e. FM 8 and FM 14) produced zinc enriched tribofilm. The formation of ZnO-amine complex on the interacting asperities protect the interacting asperities and reduce wear
- Performance of amine FMs with ZDDP strongly dependent on its chemical structure, polarity, degree of saturation and presence of function group
- The preferential adsorption and blocking effect of amine FM and ZDDP amine complex formation are the interaction mechanism linked with the amine FMs which showed antagonistic wear behaviour
- The preferential adsorption and blocking effect of amine FM, reaction with the decomposed ZDDP by products and ZDDP amine complex formation are the interaction mechanisms found applicable with the amine FMs which showed synergistic wear behaviour

In conclusion, all amine FMs along with ZDDP successfully reduced COF values while couple of them significantly reduced wear as well. Due to remarkable tribological performance, amine FMs are favourable to replace MoDTC in engine oil formulation.

11.2 Future work

This research discussed the tribological behaviour of OFMs with ZDDP in two different tribological interaction systems. The modification in elemental composition and chemical structure of the tribofilm in-comparison to the

tribofilm formed by ZDDP is presented in this study. This study also proposed few interaction mechanisms between amine FMs and ZDDP which is based on tribological and surface analysis results. Though tribological and surface analysis results answered many questions regarding interaction between amine FMs and ZDDP but still there are few areas which needs further investigation and these includes,

- Effect of optimising the test parameters (i.e. reducing applied load and temperature) and analyse its impact on tribological behaviour, morphology and chemical structure of the tribofilm
- Analyse the effectiveness of interaction mechanisms (proposed in this study) and correlate it with the tribological behaviour
- Further enhance the proposed interaction mechanisms to elucidate
    - the formation of the S and Zn rich tribofilm
    - the S and Zn enhancing mechanism in the tribofilm
    - the significant increase in Fe content and its incorporation throughout the tribofilm
    - the formation of metal phosphides deeper in the tribofilm

Finally,

- Further develop and explore new interaction mechanisms between amine FMs and ZDDP

References

[1] G. Stachowiak and A. Batchelor, *Engineering Tribology*, 3rd Editio. Oxford: Elseveir, 2005.

[2] H. P. Jost and J. Schofield, “Energy Saving Through Tribology: a Techno-Economic Study.,” *Proc. - Inst. Mech. Eng.*, vol. 195, pp. 151–173, 1981.

[3] Gwidon W. Stachowiak and Andrew W. Batchelor, *Engineering Tribology*, 2nd ed. Woburn: Butterworth-Heneimamann, 2001.

[4] “Multiyear Program Plan : Reducing Friction and Wear in Heavy Vehicles Energy Efficiency and Renewable Energy Office of Transportation Technologies Office of Heavy Vehicle Technologies,” *Agenda*, 1999.

[5] K. Holmberg and A. Erdemir, “Global Impact of Friction on Energy Consumption , Economy and Environment,” pp. 181–185, 2015.

[6] K. Holmberg, P. Andersson, and A. Erdemir, “Global energy consumption due to friction in passenger cars,” *Tribol. Int.*, vol. 47, pp. 221–234, 2012.

[7] K. Holmberg, P. Andersson, N. Nylund, K. Mäkelä, and A. Erdemir, “Global energy consumption due to friction in trucks and buses,” *Tribiology Int.*, vol. 78, pp. 94–114, 2014.

[8] “Petrol and diesel car sales ban brought forward to 2035.” [Online]. Available: https://www.bbc.co.uk/news/science-environment-51366123. [Accessed: 10-Feb-2020].

[9] T. Haque, A. Morina, A. Neville, R. Kapadia, and S. Arrowsmith, “Non-ferrous coating/lubricant interactions in tribological contacts: Assessment of tribofilms,” *Tribol. Int.*, vol. 40, no. 10-12 SPEC. ISS., pp. 1603–1612, 2007.

[10] S. C. Tung and M. L. McMillan, “Automotive tribology overview of current advances and challenges for the future,” *Tribol. Int.*, vol. 37, no. 7, pp. 517–536, 2004.

[11] W. Martin and M. Ray, “A technical summary of Euro 6/VI vehicle emission standards,” *ICCT Brief. Pap.*, no. June, pp. 1–17, 2016.

[12] “Euro 6 emission standards.” [Online]. Available: http://www.autoexpress.co.uk/car-news/consumer-news/90816/euro-6-emissions-standards-what-do-they-mean-for-you. [Accessed: 30-Apr-2016].

[13] J. B. Heywood, *Internal combustion engine fundamentals*. McGraw-Hill, Inc, 1988.

[14] P. a. Willermet, D. P. Dailey, R. O. Carter, P. J. Schmitz, and W. Zhu, “Mechanism of formation of antiwear films from zinc dialkyldithiophosphates,” *Tribol. Int.*, vol. 28, no. 3, pp. 177–187, 1995.

[15] H. Spikes, “The history and mechanisms of ZDDP,” *Tribol. Lett.*, vol. 17, no. 3, pp. 469–489, 2004.

[16] M. Ratoi, V. B. Niste, H. Alghawel, Y. F. Suen, and K. Nelson, “The impact of organic friction modifiers on engine oil tribofilms,” *RSC Adv.*, vol. 4, no. 9, pp. 4278–4285, 2014.

[17] A. J. Gellman and N. D. Spencer, “Surface chemistry in tribology,” *Proc. Inst. Mech. Eng. Part J J. Eng. Tribol.*, vol. 216, no. 6, pp. 443–461, 2002.

[18] K. Ito, J. M. Martin, C. Minfray, and K. Kato, “Low-friction tribofilm formed by the reaction of ZDDP on iron oxide,” *Tribol. Int.*, vol. 39, no. 12, pp. 1538–1544, 2006.

[19] H. Spikes, “Low- and zero-sulphated ash, phosphorus and sulphur anti-wear additives for engine oils,” *Lubr. Sci.*, vol. 20, no. 2, pp. 103–136, 2008.

[20] J. Dawczyk, N. Morgan, J. Russo, and H. Spikes, “Film Thickness and Friction of ZDDP Tribofilms,” *Tribol. Lett.*, vol. 67, no. 2, pp. 1–15, 2019.

[21] K. M. Bodek and V. V. Wong, “The effects of sulfated ash, phosphorus and sulfur on diesel aftertreatment systems - A review,” *SAE Tech. Pap.*, pp. 2017–2035, 2007.

[22] K. T. Miklozic, T. R. Forbus, and H. A. Spikes, “Performance of Friction Modifiers on ZDDP-Generated Surfaces,” *Tribol. Trans.*, vol. 50, no. 3, pp. 328–335, 2007.

[23] M. Priest and C. M. Taylor, “Automobile engine tribology - approaching the surface,” *Wear*, vol. 241, no. 2, pp. 193–203, 2000.

[24] C. M. Taylor, “Automobile engine tribology-design considerations for efficiency and durability,” *Wear*, vol. 221, no. 1, pp. 1–8, 1998.

[25] H. Fujita and H. A. Spikes, “The formation of zinc dithiophosphate antiwear films,” *Proc. Inst. Mech. Eng. Part J J. Eng. Tribol.*, vol. 218, no. 4, pp. 265–278, 2004.

[26] M. A. Nicholls, T. Do, P. R. Norton, M. Kasrai, and G. M. Bancroft, “Review of the lubrication of metallic surfaces by zinc dialkyl-dithiophosphates,” *Tribol. Int.*, vol. 38, no. 1, pp. 15–39, 2005.

[27] J. F. Graham, C. Mccague, and P. R. Norton, “Topography and nanomechanical properties of tribochemical films derived from zinc dialkyl and diaryl dithiophosphates,” *Tribol. Lett.*, vol. 6, no. 3–4, pp. 149–157, 1999.

[28] M. Aktary, M. T. McDermott, and J. Torkelson, “Morphological evolution of films formed from thermooxidative decomposition of ZDDP,” *Wear*, vol. 247, no. 2, pp. 172–179, 2001.

[29] M. Aktary, M. T. McDermott, and G. a. McAlpine, “Morphology and nanomechanical properties of ZDDP antiwear films as a function of tribological contact time,” *Tribol. Lett.*, vol. 12, no. 3, pp. 155–162, 2002.

[30] F. G. Rounds, “Additive Interactions and Their Effect on the Performance of a Zinc Dialkyl Dithiophosphate,” *A S L E Trans.*, vol. 21, no. 2, pp. 91–101, 1978.

[31] Y. Matsui, S. Aoki, and M. Masuko, “Elucidation of the Action of Functional Groups in the Coexisting Ashless Compounds on the Tribofilm Formation and Friction Characteristic of Zinc Dialkyldithiophosphate-Formulated Lubricating Oils,” *Tribol. Trans.*, vol. 0, no. 0, pp. 1–9, 2017.

[32] Y. Matsui, S. Aoki, and M. Masuko, “Influence of coexisting functionalized polyalkylmethacrylates on the formation of ZnDTP-derived tribo film,” vol. 100, pp. 152–161, 2016.

[33] M. Shiomi, M. Tokashiki, H. Tomizawa, and T. Kuribayashi, “Interaction between Zinc Dialkyldithiophosphate and Amine,” *Lubr. Sci.*, vol. 1, no. 131, pp. 131–147, 1989.

[34] Y. Matsui, S. Aoki, O. Kurosawa, and M. Masuko, “Concert and Blocking Effects of Polar Compounds on the Friction Reduction and Tribofilm Formation of Zinc Dialkyldithiophosphate,” vol. 2, pp. 417–425, 2016.

[35] R. M. Mortier, M. F. FOX, and S. T. Orszulik, *Chemistry and Technology of Lubricant*, 3rd ed. Swindon, UK: Springer, 2010.

[36] Z. Pawlak, *Tribochemistry of Lubricating Oils*. London: Elsevier, 2003.

[37] H. M. Mobarak *et al.*, “The prospects of biolubricants as alternatives in automotive applications,” *Renew. Sustain. Energy Rev.*, vol. 33, pp. 34–43, 2014.

[38] D. S. (Hon. . Bharat Bhushan, Ph.D., *MODERN TRIBOLOGY HANDBOOK - Contents*. 2001.

[39] J. Yakadoum, *Materials and Surface Engineering in Tribology*. 2007.

[40] J. Booth, “The feasibility of using electrostatic charge condition monitoring for lubricant additive screening,” University of Southampton, 2008.

[41] F. Flow *et al.*, “Gas Turbine Fuel Systems and Fuels Surface Engineering Concepts,” 2015.

[42] S. M. Hsu and R. S. Gates, “Boundary lubricating films: Formation and lubrication mechanism,” *Tribol. Int.*, vol. 38, no. 3, pp. 305–312, 2005.

[43] T. F. J. Quinn, J. L. Sullivan, and D. M. Rowson, “Origins and development ambient temperatures,” *Wear*, vol. 94, pp. 175–191, 1984.

[44] S. Bair and F. Qureshi, “Observations of Shear Localization in Liquid Lubricants Under Pressure,” *J. Tribol.*, vol. 115, no. July, pp. 507–513, 1993.

[45] L. J. Gschwender, D. C. Kramer, and B. K. Lok, “Liquid Lubricants and Lubrication,” 2001.

[46] Smmt, “The Society of Motor Manufacturers and Traders Motor Industry Facts 2014,” p. 27, 2014.

[47] philipgomm, “Number of vehicles in the UK hits new high.” [Online]. Available: https://racfoundation.wordpress.com/2013/04/12/number-of-vehicles-in-uk-hits-new-high/. [Accessed: 27-Apr-2016].

[48] M. Hoshi, “Reducing friction losses in automobile engines,” *Tribol. Int.*, vol. 17, no. 4, pp. 185–189, 1984.

[49] “A history of leadership regarding emission.” [Online]. Available: http://www.scania.com/group/en/a-history-of-leadership-regarding-emissions/. [Accessed: 30-Apr-2016].

[50] E. A. Bardasz *et al.*, “Low Volatility ZDDP Technology : Part 2 - Exhaust Catalysts Performance in Field Applications,” *Victoria*, no. 724, 2007.

[51] Y. Enomoto and T. Yamamoto, “New materials in automotive tribology,” *Tribol. Lett.*, vol. 5, pp. 13–24, 1998.

[52] L. Taylor, a. Dratva, and H. a. Spikes, “Friction and Wear Behavior of Zinc Dialkyldithiophosphate Additive,” *Tribol. Trans.*, vol. 43, no. 3, pp. 469–479, 2000.

[53] H. Spedding and R. C. Watkins, “The antiwear mechanism of zddp’s. Part I,” *Tribol. Int.*, vol. 15, no. 1, pp. 9–12, 1982.

[54] N. Dörr *et al.*, “Correlation Between Engine Oil Degradation, Tribochemistry, and Tribological Behavior with Focus on ZDDP Deterioration,” *Tribol. Lett.*, vol.

67, no. 2, pp. 1–17, 2019.

[55] J. S. McQueen, H. Gao, E. D. Black, a. K. Gangopadhyay, and R. K. Jensen, “Friction and wear of tribofilms formed by zinc dialkyl dithiophosphate antiwear additive in low viscosity engine oils,” *Tribol. Int.*, vol. 38, no. 3, pp. 289–297, 2005.

[56] P. Njiwa *et al.*, “Zinc dialkyl phosphate (ZP) as an anti-wear additive: Comparison with ZDDP,” *Tribol. Lett.*, vol. 44, no. 1, pp. 19–30, 2011.

[57] Y. Shimizu and H. A. Spikes, “The Tribofilm Formation of ZDDP Under Reciprocating Pure Sliding Conditions,” *Tribol. Lett.*, vol. 64, no. 3, pp. 1–11, 2016.

[58] J. M. Martin, “Antiwear mechanisms of zinc dithiophosphate: a chemical hardness approach,” *Tribol. Lett.*, vol. 6, no. 1, pp. 1–8, 1999.

[59] A. M. Barnes, K. D. Bartle, and V. R. a Thibon, “A review of zinc dialkyldithiophosphates (ZDDPS): Characterisation and role in the lubricating oil,” *Tribol. Int.*, vol. 34, no. 6, pp. 389–395, 2001.

[60] B. a. Khorramian, G. R. Iyer, S. Kodali, P. Natarajan, and R. Tupil, “Review of antiwear additives for crankcase oils,” *Wear*, vol. 169, no. 1, pp. 87–95, 1993.

[61] J. Dawczyk, J. Russo, and H. Spikes, “Ethoxylated Amine Friction Modifiers and ZDDP,” *Tribol. Lett.*, pp. 1–15, 2019.

[62] M. a. Nicholls *et al.*, “Nanometer scale chemomechanical characterization of antiwear films,” *Tribol. Lett.*, vol. 17, no. 2, pp. 205–216, 2004.

[63] J. Zhang and H. Spikes, “On the Mechanism of ZDDP Antiwear Film Formation,” *Tribol. Lett.*, vol. 63, no. 2, pp. 1–15, 2016.

[64] H. Fujita, R. P. Glovnea, and H. A. Spikes, “Study of zinc dialkydithiophosphate antiwear film formation and removal processes, part I: Experimental,” *Tribol. Trans.*, vol. 48, no. 4, pp. 558–566, 2005.

[65] N. N. Gosvami, J. A. Bares,F. Mangolini, A. R. Konicek and R. W. C. D. G. Yablon, “Mechanisms of antiwear tribofilm growth revealed in situ by single-asperity sliding contacts.”

[66] M. L. S. Fuller, M. Kasrai, G. M. Bancroft, K. Fyfe, and K. H. Tan, “Solution decomposition of zinc dialkyl dithiophosphate and its effect on antiwear and thermal film formation studied by X-ray absorption spectroscopy,” *Tribol. Int.*, vol. 31, no. 10, pp. 627–644, 1998.

[67] J. Zhang and Y. Meng, “Boundary lubrication by adsorption film,” *Friction*, vol. 3, no. 2, pp. 115–147, 2015.

[68] D. A. E.S. Ferrari, K.J. Roberts, M. Sansone, “A multi-edge X-ray absorption spectroscopy study of the reactivity of zinc di-alkyl-di-thiophosphates anti-wear additives 2. In situ studies of steelroil interfaces,” *Wear*, vol. 236, pp. 259–275, 1999.

[69] Z. Pawlak and P. Yarlagadda, “The mechanical strength of phosphates under friction-induced cross-linking,” *… Achiev. …*, vol. 17, no. 1, pp. 201–204, 2006.

[70] J. M. Martin, T. Onodera, C. Minfray, F. Dassenoy, and A. Miyamoto, “The origin of anti-wear chemistry of ZDDP,” *Faraday Discuss.*, vol. 156, p. 311, 2012.

[71] T. K. W. Nicholas J. Mosey, Martin H. Mu¨ser, “Molecular Mechanisms for the Functionality of Lubricant Additives,” vol. 307, no. March, pp. 1612–1616, 2005.

[72] K. F. b Zhanfeng Yin t a, Masoud Kasrai a., Marina Fuller, G. Michael Bancroft and K. H. T. C, “Application of soft X-ray absorption spectroscopy in chemical characterization of antiwear films generated by ZDDP Part I: the effects of physical parameters,” *Wear*, vol. 202, p. pp.172-191, 1997.

[73] Z. Yin, M. Kasrai, G. ~ M. Bancroft ’, K. Fyfe, M. L. Colaianni, and K. H. Tan, “Application of soft X-ray absorption spectroscopy in chemical characterization of antiwear films generated by ZDDP Part II: the effect of detergents and dispersants,” *Wear*, vol. 202, pp. 192–201, 1997.

[74] A. Pourya Parsaeian, Ali Ghanbarzadeh , Marcel C. P. Van Eijk , Ileana Nedelcu and A. M. Neville, “A New Insight into the Interfacial Mechanisms Involved in the Formation of Tribofilm by Zinc Dialkyl Dithiophosphate,” 2017.

[75] A. Dorgham, P. Parsaeian, A. Neville, and K. Ignatyev, “In situ synchrotron XAS study of the decomposition kinetics of ZDDP triboreactive interfaces,” pp. 34168–34181, 2018.

[76] J. M. Martin, C. Grossiord, T. Le Mogne, S. Bec, and A. Tonck, “The two-layer structure of Zndtp tribofilms, Part I: AES, XPS and XANES analyses,” *Tribol. Int.*, vol. 34, no. 8, pp. 523–530, 2001.

[77] M. Crobu, A. Rossi, F. Mangolini, and N. D. Spencer, “Tribochemistry of Bulk Zinc Metaphosphate Glasses,” pp. 121–134, 2010.

[78] M. Ueda, A. Kadiric, and H. Spikes, “On the Crystallinity and Durability of

ZDDP Tribofilm," *Tribol. Lett.*, vol. 67, no. 4, pp. 1–13, 2019.

[79] E. Liu and S. D. Kouame, "An XPS Study on the Composition of Zinc Dialkyl Dithiophosphate Tribofilms and Their Effect on Camshaft Lobe Wear An XPS Study on the Composition of Zinc Dialkyl Dithiophosphate Tribofilms and Their Effect on Camshaft," vol. 2004, no. January 2016, 2014.

[80] M. Belin, J. M. Martin, and J. L. Mansot, "Role of iron in the amorphization process in friction-induced phosphate glasses," *Tribol. Trans.*, vol. 32, no. 3, pp. 410–413, 1989.

[81] C. Minfray *et al.*, "Experimental and Molecular Dynamics Simulations of Tribochemical Reactions with ZDDP: Zinc Phosphate–Iron Oxide Reaction," *Tribol. Trans.*, vol. 51, no. 5, pp. 589–601, 2008.

[82] C. Minfray, J. M. Martin, C. Esnouf, T. Le Mogne, R. Kersting, and B. Hagenhoff, "A multi-technique approach of tribofilm characterisation," vol. 448, pp. 272–277, 2004.

[83] J. Dawczyk, E. Ware, M. Ardakani, J. Russo, and H. Spikes, "Use of FIB to Study ZDDP Tribofilms," *Tribol. Lett.*, vol. 66, no. 4, 2018.

[84] C. Minfray, J. M. Martin, M. I. De Barros, T. Le Mogne, R. Kersting, and B. Hagenhoff, "Chemistry of ZDDP tribofilm by ToF-SIMS," *Tribol. Lett.*, vol. 17, no. 3, pp. 351–357, 2004.

[85] J. C. Bell, K. M. Delargy, and A. M. Seeney, "The Removal of Substrate Material through Thick Zinc Dithiophosphate Anti-Wear Films," *Tribol. Ser.*, vol. 21, no. C, pp. 387–396, 1992.

[86] G. C. Smith and J. C. Bell, "Multi-technique surface analytical studies of automotive anti-wear films," *Appl. Surf. Sci.*, vol. 144–145, pp. 222–227, 1999.

[87] F. G. Rounds, "Effects of Additives on the Friction of Steel on Steel - I. Surface Topography and Film Composition Studies," *ASLE Trans.*, vol. 7, no. November, p. Nov-23, 1964.

[88] S. Ii, A. O. Interactions, and F. G. Rounds, "Effects of Additives on the Friction of Steel on Steel II. Additive base oil interactons," vol. 8197, no. June, 2016.

[89] Z. Zhang, E. S. Yamaguchi, M. Kasrai, and G. M. Bancroft, "Tribofilms generated from ZDDP and DDP on steel surfaces: Part 2, growth, wear and morphology," *Tribol. Lett.*, vol. 19, no. 3, pp. 211–220, 2005.

[90] T. Haque, "Tribochemistry of lubricant additives on Non- Ferrous Coatings for Reduced Friction, Improved Durability and Wear in Internal Combustion

Engines," University of Leeds, 2007.

[91] S. Soltanahmadi, A. Morina, M. C. P. Van Eijk, I. Nedelcu, and A. Neville, "Investigation of the effect of a diamine-based friction modifier on micropitting and the properties of tribofilms in rolling-sliding contacts," *J. Phys. D. Appl. Phys.*, vol. 49, no. 50, 2016.

[92] A. Dorgham, P. Parsaeian, A. Azam, C. Wang, A. Morina, and A. Neville, "Single-asperity study of the reaction kinetics of P-based triboreactive fi lms," *Tribiology Int.*, vol. 133, no. September 2018, pp. 288–296, 2019.

[93] S. Gunsel, H. A. Spikes, M. Aderin, and S. G. Member, "In-Situ Measurement of ZDDP Films in Concentrated Contacts," vol. 2004, 2008.

[94] K. Varlot, J. M. Martin, C. Grossiord, R. Vargiolu, B. Vacher, and K. Inoue, "A dual-analysis approach in tribochemistry : application to ZDDP / calcium borate additive interactions," vol. 6, pp. 181–189, 1999.

[95] H. Spikes, "Stress-augmented thermal activation: Tribology feels the force," *Friction*, vol. 6, no. 1, pp. 1–31, 2018.

[96] A. Azam, A. Dorgham, P. Parsaeian, A. Morina, A. Neville, and M. C. T. Wilson, "The mutual interaction between tribochemistry and lubrication: Interfacial mechanics of tribofilm," *Tribol. Int.*, vol. 135, pp. 161–169, Jul. 2019.

[97] K. Hoshino, K. Yagishita, K. Tagawa, and H. Spikes, "Tribological properties of sulphur-free antiwear additives zinc dialkylphosphates (ZDPs)," *SAE Tech. Pap.*, vol. 5, no. 1, 2011.

[98] G. W. Canning *et al.*, "Spectromicroscopy of tribological films from engine oil additives . Part I . Films from ZDDP ' s," vol. 6, pp. 159–169, 1999.

[99] M. A. Nicholls, G. M. Bancroft, M. Kasrai, T. Do, B. H. Frazer, and G. De Stasio, "Nanometer scale chemomechanical characterizaton of antiwear films," *Tribol. Lett.*, vol. 17, no. 2, pp. 205–336, 2003.

[100] K. Topolovec-Miklozic, T. R. Forbus, and H. A. Spikes, "Film thickness and roughness of ZDDP antiwear films," *Tribol. Lett.*, vol. 26, no. 2, pp. 161–171, 2007.

[101] A. L. Aremu, "Tribochemistry of Boron-Containing Lubricant Additives on Ferrous Surfaces for Improved Internal Combustion Engine Performance," University of Leeds, 2017.

[102] O. L. Warren, J. F. Graham, P. R. Norton, J. E. Houston, and T. A. Michalske, "Nanomechanical properties of films derived from zinc dialkyldithiophosphate,"

Tribol. Lett., vol. 4, no. 2, pp. 189–198, 1998.

[103] J. S. Sheasby, T. a. Caughlin, and W. a. Mackwood, “The effect of steel hardness on the performance of antiwear additives,” *Wear*, vol. 201, no. 1–2, pp. 209–216, 1996.

[104] H. Spikes, “Friction Modifier Additives,” *Tribol. Lett.*, vol. 60, no. 1, 2015.

[105] Z. Tang and S. Li, “A review of recent developments of friction modifiers for liquid lubricants (2007-present),” *Curr. Opin. Solid State Mater. Sci.*, vol. 18, no. 3, pp. 119–139, 2014.

[106] J. Guegan, M. Southby, and H. Spikes, “Friction Modifier Additives , Synergies and Antagonisms,” *Tribol. Lett.*, vol. 67, no. 3, pp. 1–12, 2019.

[107] H. J. ie Feng1,*,†, Z. Fazheng1, and Ji Feng1 and Yao Junbing2, “Anti-wear performance of organomolybdenum compounds as lubricant additives,” *Lubr. Sci.*, vol. 19, p. pp.81–85, 2007.

[108] M. Müller, K. Topolovec-Miklozic, A. Dardin, and H. A. Spikes, “The design of boundary film-forming pma viscosity modifiers,” *Tribol. Trans.*, vol. 49, no. 2, pp. 225–232, 2006.

[109] M. Müller, J. Fan, and H. Spikes, “Design of functionalized PAMA viscosity modifiers to reduce friction and wear in lubricating oils,” *J. ASTM Int.*, vol. 4, no. 10, 2007.

[110] J. Fan, M. Müller, T. Stöhr, and H. A. Spikes, “Reduction of friction by functionalised viscosity index improvers,” *Tribol. Lett.*, vol. 28, no. 3, pp. 287–298, 2007.

[111] M. Tohyama, T. Ohmori, A. Murase, and M. Masuko, “Friction reducing effect of multiply adsorptive organic polymer,” *Tribol. Int.*, vol. 42, no. 6, pp. 926–933, 2009.

[112] S. Aoki, Y. Yamada, D. Fukada, A. Suzuki, and M. Masuko, “Verification of the advantages in friction-reducing performance of organic polymers having multiple adsorption sites,” *Tribol. Int.*, vol. 59, pp. 57–66, 2013.

[113] D. N. Khaemba, A. Neville, and A. Morina, “RSC Advances New insights on the decomposition mechanism of Molybdenum DialkyldiThioCarbamate (MoDTC): a Raman spectroscopic study †,” *RSC Adv.*, vol. 6, pp. 38637–38646, 2016.

[114] J. Hu, X. Wei, G. Dai, Y. Fei, F. Xie, and Z. Zong, “Tribological behaviors and mechanism of sulfur- and phosphorus-free organic molybdate ester with zinc

dialkyldithiophosphate," vol. 41, pp. 549–555, 2008.

[115] Y. Yamamoto and S. Gondo, "Friction and Wear Characteristics of Molybdenum Dithiocarbamate and Molybdenum Dithiophosphate," *Tribol. Trans.*, vol. 32, no. 2, pp. 251–257, 1989.

[116] P. C. Nalam, A. Pham, R. V. Castillo, and R. M. Espinosa-Marzal, "Adsorption Behavior and Nanotribology of Amine-Based Friction Modifiers on Steel Surfaces," *J. Phys. Chem. C*, vol. 123, no. 22, pp. 13672–13680, 2019.

[117] S. Loehle *et al.*, "Mixed lubrication with C18 fatty acids: Effect of unsaturation," *Tribol. Lett.*, vol. 53, no. 1, pp. 319–328, 2014.

[118] L. R. Rudnick, *Lubricant additives chemistry and applications*. 2003.

[119] D. Kenbeek, T. Buenemann, and H. Rieffe, "Review of Organic Friction Modifiers - Contribution to Fuel Efficiency?," *SAE Tech. Pap. 2000-01-1792*, no. 724, 2000.

[120] S. Jahanmir, "Chain length effects in boundary lubrication," vol. 102, pp. 331–349, 1985.

[121] H. Cheng and Y. Hu, "Influence of chain ordering on frictional properties of self-assembled monolayers (SAMs) in nano-lubrication," *Adv. Colloid Interface Sci.*, vol. 171–172, pp. 53–65, 2012.

[122] D. F. Ogletree and M. Salmeron, "Preparation and Characterization of Self-Assembled Multilayers of Octadecylamine on Mica from Ethanol Solutions," vol. 18, no. 1, pp. 3276–3281, 2003.

[123] V. Kocsis, J., Vilardo, J.S., Brown, J.R., Barrer, D.E. and P. E. . R.J., Mosier, "Tartaric acid derivatives in fuel compositions.," 2012.

[124] T. Massoud *et al.*, "Effect of ZDDP on lubrication mechanisms of linear fatty amines under boundary lubrication conditions," vol. 141, no. September 2019, 2020.

[125] S. Loehlé *et al.*, "Mixed lubrication of steel by C18 fatty acids revisited. Part I: Toward the formation of carboxylate," *Tribol. Int.*, vol. 82, no. PA, pp. 218–227, 2015.

[126] S. Loehlé *et al.*, "Mixed lubrication of steel by C18 fatty acids revisited. Part II: Influence of some key parameters," *Tribol. Int.*, vol. 94, pp. 207–216, 2016.

[127] H. Okabe, M. Masuko, and K. Sakurai, "Dynamic behavior of surface-adsorbed molecules under boundary lubrication," *ASLE Trans.*, vol. 24, no. 4, pp. 467–

473, 1981.

[128] S. Jahanmir and M. Beltzer, “Effect of Additive Molecular Structure on Friction Coefficient and Adsorption,” *J. Tribol.*, vol. 108, no. 1, p. 109, 1986.

[129] M. Ratoi, V. Anghel, C. Bovington, and H. A. Spikes, “Mechanisms of oiliness additives,” vol. 33, pp. 241–247, 2000.

[130] W. Li, C. Kumara, H. M. Meyer, H. Luo, and J. Qu, “Compatibility between Various Ionic Liquids and an Organic Friction Modifier as Lubricant Additives,” *Langmuir*, vol. 34, no. 36, pp. 10711–10720, 2018.

[131] Z. Zachariah, P. C. Nalam, A. Ravindra, A. Raju, A. Mohanlal, and K. Wang, “Correlation Between the Adsorption and the Nanotribological Performance of Fatty Acid‐Based Organic Friction Modifiers on Stainless Steel,” *Tribol. Lett.*, pp. 1–16, 2020.

[132] R. Simič and M. Kalin, “Adsorption mechanisms for fatty acids on DLC and steel studied by AFM and tribological experiments,” *Appl. Surf. Sci.*, vol. 283, pp. 460–470, 2013.

[133] S. Campen, J. Green, G. Lamb, D. Atkinson, and H. Spikes, “On the Increase in Boundary Friction with Sliding Speed,” pp. 237–248, 2012.

[134] J. P. Ewen, C. Gattinoni, N. Morgan, H. A. Spikes, and D. Dini, “Non equilibrium Molecular Dynamics Simulations of Organic Friction Modi fi ers Adsorbed on Iron Oxide Surfaces,” 2016.

[135] S. Campen, J. H. Green, G. D. Lamb, and H. A. Spikes, “In situ study of model organic friction modifiers using liquid cell AFM: Self-assembly of octadecylamine,” *Tribol. Lett.*, vol. 58, no. 3, 2015.

[136] A. Jaishankar, A. Jusufi, J. L. Vreeland, S. Deighton, J. Pellettiere, and A. M. Schilowitz, “Adsorption of Stearic Acid at the Iron Oxide/Oil Interface: Theory, Experiments, and Modeling,” *Langmuir*, vol. 35, no. 6, pp. 2033–2046, 2019.

[137] C. M. Allen and E. Drauglis, “Boundary layer lubrication: monolayer or multilayer,” *Wear*, vol. 14, no. 5, pp. 363–384, 1969.

[138] M. Ruths, S. Lundgren, K. Danerlöv, and K. Persson, “Friction of fatty acids in nanometer-sized contacts of different adhesive strength,” *Langmuir*, vol. 24, no. 4, pp. 1509–1516, 2008.

[139] V. Anghel, C. Bovington, and H. Spikes, “Thick-boundary-film formation by friction modifier additives,” *Lubr. Sci.*, vol. 00, no. August 1999, 1999.

[140] S. Campen, J. H. Green, G. D. Lamb, and H. a. Spikes, “In Situ Study of Model Organic Friction Modifiers Using Liquid Cell AFM; Saturated and Mono-unsaturated Carboxylic Acids,” *Tribol. Lett.*, vol. 57, no. 3, 2015.

[141] C. M. Allen and E. Drauglis, “Boundary layer lubrication: monolayer or multilayer,” *Wear*, vol. 14, no. 5, pp. 363–384, 1969.

[142] J. H. Choo, A. K. Forrest, and H. a. Spikes, “Influence of organic friction modifier on liquid slip: A new mechanism of organic friction modifier action,” *Tribol. Lett.*, vol. 27, no. 2, pp. 239–244, 2007.

[143] H. A. Spikes, “Slip at the wall - Evidence and tribological implications,” *Tribol. Ser.*, vol. 41, pp. 525–535, 2003.

[144] M. H. Wood, R. J. L. Welbourn, T. Charlton, A. Zarbakhsh, M. T. Casford, and S. M. Clarke, “Hexadecylamine Adsorption at the Iron Oxide − Oil Interface,” 2013.

[145] S. A. Lawrence, *Amines synthesis, properties and applications*, First. New York: Cambridge University Press, 2004.

[146] J. R. L . G . WA D E, *Organic chemistry*, 8th ed. New York: PEARSON, 2013.

[147] H. A. Spikes and A. Cameron, “A Comparison of adsorption and boundary lubricant failure.,” *Proc. R. Soc. London,* vol. 336, pp. 407–419, 1974.

[148] A. Block and B. B. Simms, “Desorption and exchange of adsorbed octadecylamine and stearic acid on steel and glass,” *J. Colloid Interface Sci.*, vol. 25, no. 4, pp. 514–518, 1967.

[149] J. J. Benítez, S. Kopta, D. F. Ogletree, and M. Salmeron, “Preparation and characterization of self-assembled monolayers of octadecylamine on mica using hydrophobic solvents,” *Langmuir*, vol. 18, no. 16, pp. 6096–6100, 2002.

[150] M. Doig and P. J. Camp, “The structures of hexadecylamine films adsorbed on iron-oxide surfaces in dodecane and hexadecane,” *Phys. Chem. Chem. Phys.*, vol. 17, no. 7, pp. 5248–5255, 2015.

[151] J. T. Woodward, I. Doudevski, H. D. Sikes, and D. K. Schwartz, “Kinetics of self-assembled monolayer growth explored via submonolayer coverage of incomplete films,” *J. Phys. Chem. B*, vol. 101, no. 38, pp. 7535–7541, 1997.

[152] J. J. Benítez, S. Kopta, I. Díez-Pérez, F. Sanz, D. F. Ogletree, and M. Salmeron, “Molecular packing changes of octadecylamine monolayers on mica induced by pressure and humidity,” *Langmuir*, vol. 19, no. 3, pp. 762–765, 2003.

[153] F. Moreno-Herrero, J. Colchero, J. Gómez-Herrero, and A. M. Baro, “Atomic force microscopy contact, tapping, and jumping modes for imaging biological samples in liquids,” *Phys. Rev. E - Stat. Nonlinear, Soft Matter Phys.*, vol. 69, no. 3 1, 2004.

[154] D. K. Schwartz, *Mechanisms and kinetics of self-assembled monolayer formation*, vol. 52. 2001.

[155] J. Dawczyk, N. Morgan, J. Russo, and H. Spikes, “Film Thickness and Friction of ZDDP Tribofilms,” *Tribol. Lett.*, vol. 67, no. 2, 2019.

[156] S. Kennedy and L. D. Moore, “Additive effects on lubricant fuel economy,” *SAE Tech. Pap.*, 1987.

[157] W. E. Waddey, H. Shaub, J. M. Pecoraro, and R. A. Carley, “IMPROVED FUEL ECONOMY VIA ENGINE OILS.,” *SAE Prepr*, no. 780599, 1978.

[158] C. Bovington, V. Anghel, and H. A. Spikes, “Predicting sequence VI and VIA fuel economy from laboratory bench tests,” *SAE Tech. Pap.*, 1996.

[159] L. Dobrenizki *et al.*, “Efficiency improvement in automobile bucket tappet/camshaft contacts by DLC coatings – Influence of engine oil, temperature and camshaft speed,” *Surf. Coatings Technol.*, vol. 308, pp. 360–373, 2016.

[160] F. Mao, C. Dong, and D. D. Macdonald, “Effect of octadecylamine on the corrosion behavior of Type 316SS in acetate buffer,” *Corros. Sci.*, vol. 98, pp. 192–200, 2015.

[161] N. Ochoa, F. Moran, and N. Pébère, “The synergistic effect between phosphonocarboxylic acid salts and fatty amines for the corrosion protection of a carbon steel,” *J. Appl. Electrochem.*, vol. 34, no. 5, pp. 487–493, 2004.

[162] F. G. Rounds, “Some Effects of Amines on Zinc Dialkyldithiophosphate Antiwear Performance as Measured in 4-Ball Wear Tests,” *A S L E Trans.*, vol. 24, no. 4, pp. 431–440, 1981.

[163] K. Eriksson, “Fatty amines as friction modifiers in engine oils: correlating adsorbed amount to friction and wear performance,” *Master’s thesis, Chalmers University of Technology, Gothenburg, Sweden*, 2014. .

[164] J. Zhang, E. Yamaguchi, and H. Spikes, “The Antagonism between Succinimide Dispersants and a Secondary Zinc Dialkyl Dithiophosphate,” *Tribol. Trans.*, vol. 57, no. 1, pp. 57–65, 2014.

[165] Z. Zhang *et al.*, “Interaction of ZDDP with Borated Dispersant Using XANES

and XPS," vol. 47:4, pp. 527–536, 2004.

[166] S. M. Lundgren, K. Eriksson, and B. Rossenaar, "Boosting the Friction Performance of Amine Friction Modifiers with MoDTC," *SAE Int. J. Fuels Lubr.*, vol. 8, no. 1, pp. 2015-01–0684, 2015.

[167] M. I. De Barros Bouchet *et al.*, "Booster effect of fatty amine on friction reduction performance of Mo-based additives," *Tribol. Int.*, vol. 119, no. November 2017, pp. 600–607, 2018.

[168] H. A. Spikes, "Additive-additive and additive-surface interactions in lubrication," *Lubr. Sci.*, vol. 2, no. 1, pp. 3–23, 1989.

[169] E. S. Yamaguchi, Z. Zhang, M. Kasrai, and G. M. Bancroft, "Study of the interaction of ZDDP and dispersants using X-ray absorption near edge structure spectroscopy — Part 2 : Tribochemical reactions," vol. 15, no. 4, pp. 385–394, 2003.

[170] H. Okubo, S. Watanabe, C. Tadokoro, and S. Sasaki, "Effects of concentration of zinc dialkyldithiophosphate on the tribological properties of tetrahedral amorphous carbon films in presence of organic friction modifiers," *Tribol. Int.*, vol. 94, pp. 446–457, 2016.

[171] S. Soltanahmadi, E. A. Esfahani, I. Nedelcu, A. Morina, M. C. P. van Eijk, and A. Neville, "Surface Reaction Films from Amine-Based Organic Friction Modifiers and Their Influence on Surface Fatigue and Friction," *Tribol. Lett.*, vol. 67, no. 3, 2019.

[172] T. P. H. Mansuy , P. Beccat Y. Huiban, "Investigation of interactions between antiwear and dispersent additives and their effect on surface activity of ZDDP," *Elsevier Sci. B.V.*, 1995.

[173] P. Taylor, N. E. Gallopoulos, and C. K. Murphy, "Interactions Between a Zinc Dialkylphosphorodithioate and Lubricating Oil Dispersants," vol. 8197, no. September 2013, pp. 37–41, 2008.

[174] J. M. Martin, C. Grossiord, T. Le Mogne, and J. Igarashi, "Role of nitrogen in tribochemical interaction between Zndtp and succinimide in boundary lubrication," *Tribol. Int.*, vol. 33, no. 7, pp. 453–459, 2000.

[175] Y. Wan, W. Liu, and T. Ren, "Effect of Amines on the Antiwear Propert ies of P-Containing Compounds as Oil Additives," vol. 6, no. April, pp. 283–290, 1994.

[176] H. Mansuy, P. Beccat, Y. Huiban, T. Palermo, and B. Desbat, "Investigation of

interactions between antiwear and dispersant additives and their effect on surface activity of zddp," *Tribol. Ser.*, vol. 30, no. C, pp. 423–432, 1995.

[177] P. G. Harrison, M. J. Begley, T. Kikabhai, and F. Killer, "Zinc(II) bis(O,O′-dialkyl dithiophosphates): Interaction with small nitrogen bases. The crystal and molecular structure of hexakis(μ-O,O′-diethyl dithiophosphato)-μ4-thio-tetrazinc, Zn4<[S2P(OEt)2]6S," *J. Chem. Soc. Dalt. Trans.*, no. 5, pp. 925–928, 1986.

[178] E. S. Yamaguchi, A. Onopchenko, M. M. Francisco, and C. Y. Chan, "The relative oxidation inhibition performance of some neutral and basic zinc dithiophosphate salts," *Tribol. Trans.*, vol. 42, no. 4, pp. 895–901, 1999.

[179] A. J. Burn, S. K. Dewan, I. Gosney, and P. S. G. Tan, "Inhibition of hydrolysis of 'normal' zinc(II) O,O′-di-isopropyl dithiophosphate by the 'basic' form," *J. Chem. Soc. Perkin Trans. 2*, no. 8, pp. 1311–1316, 1990.

[180] Z. Pawlak, B. E. Klamecki, T. Rauckyte, G. P. Shpenkov, and A. Kopkowski, "The tribochemical and micellar aspects of cutting fluids," *Tribol. Int.*, vol. 38, no. 1, pp. 1–4, 2005.

[181] L. Wu, Y. Zhang, G. Yang, S. Zhang, L. Yu, and P. Zhang, "Tribological properties of oleic acid-modified zinc oxide nanoparticles as the lubricant additive in poly-alpha olefin and diisooctyl sebacate base oils," *RSC Adv.*, vol. 6, no. 74, pp. 69836–69844, 2016.

[182] J. Guo, G. C. Barber, D. J. Schall, Q. Zou, and S. B. Jacob, "Tribological properties of ZnO and WS<inf>2</inf> nanofluids using different surfactants," *Wear*, vol. 382–383, pp. 8–14, 2017.

[183] X. Ran, X. Yu, and Q. Zou, "Effect of Particle Concentration on Tribological Properties of ZnO Nanofluids," *Tribol. Trans.*, vol. 60, no. 1, pp. 154–158, 2017.

[184] A. Elagouz, M. K. A. Ali, H. Xianjun, M. A. A. Abdelkareem, and M. A. Hassan, "Frictional performance evaluation of sliding surfaces lubricated by zinc-oxide nano-additives," *Surf. Eng.*, 2019.

[185] M. Shiomi and J. Mitsui, "Formulation Technology for Low Phosphorus Gasoline Engine Oils," *SAE Tech. Pap. Ser.*, no. 922301, 1992.

[186] M. Crobu, A. Rossi, and N. D. Spencer, "Effect of Chain-Length and Countersurface on the Tribochemistry of Bulk Zinc Polyphosphate Glasses," pp. 393–406, 2012.

[187] Z. Zhang, M. Kasrai, G. M. Bancroft, and E. S. Yamaguchi, “Study of the interaction of ZDDP and dispersants using X-ray absorption near edge structure spectroscopy — Part 1 : Thermal chemical reactions,” vol. 15, no. 4, pp. 377–384, 2003.

[188] “TE 77 High Frequency Machine.” [Online]. Available: http://www.phoenix-tribology.com/at2/leaflet/te77. [Accessed: 15-Jul-2018].

[189] S. Kosarieh, “Tribochemistry of Boundary Lubricated DLC/Steel Interfaces and Their Influence in Tribological Performance,” University of Leeds, 2013.

[190] Y. P. Delgado *et al.*, “Impact of wire-EDM on dry sliding friction and wear of WC-based and ZrO 2 -based composites,” *Wear*, vol. 271, no. 9–10, pp. 1951–1961, 2011.

[191] A. Morina, A. Neville, M. Priest, and J. H. Green, “ZDDP and MoDTC interactions and their effect on tribological performance - Tribofilm characteristics and its evolution,” *Tribol. Lett.*, vol. 24, no. 3, pp. 243–256, 2006.

[192] Astm, “ASTM G99: Standard Test Method for Wear Testing with a Pin-on-Disk Apparatus,” *ASTM Stand.*, vol. G99, no. Reapproved 2010, pp. 1–5, 2010.

[193] K. K. Mistry, a. Morina, a. Erdemir, and a. Neville, “Tribological Performance of EP Lubricants with Phosphorus-Based Additives,” *Tribol. Trans.*, vol. 56, no. 4, pp. 645–651, 2013.

[194] P. D. Stefan B. Kaemmer, “Application Note # 133 Introduction to Bruker ’ s ScanAsyst and PeakForce Tapping AFM Technology,” Santa Barbara, 2011.

[195] K. T. Miklozic, J. Graham, and H. Spikes, “Chemical and physical analysis of reaction films formed by molybdenum dialkyl-dithiocarbamate friction modifier additive using Raman and atomic force microscopy,” *Tribol. Lett.*, vol. 11, no. 2, pp. 71–81, 2001.

[196] B. Hafner, “Energy Dispersive Spectroscopy on the SEM: A Primer,” *Charact. Facil. Univ. Minnesota*, pp. 7–10, 2006.

[197] Noran, “Energy dispersive X-ray microanalysis: An Introduction,” *Noram Instruments*, p. 68, 1999.

[198] “LEMAS Leeds University.” [Online]. Available: https://www.engineering.leeds.ac.uk/imr/lemas/dualbeam-fib.shtml. [Accessed: 28-May-2015].

[199] W. F. Stickle, P. E. Sobol, and K. D. Bomben, *Handbook of X-ray*

Photoelectron Spectroscopy. Eden Prairie: Perkin-Elmer Corporation, 1992.

[200] D. Zemlyanov, “ELECTRON SPECTROSCOPY A new window opens,” no. October 2011, 2014.

[201] S. Hofmann, “Practical Surface Analysis : State of the Art and Recent Developments in AES , XPS , ISS and SIMS : I,” vol. 9, pp. 3–20, 1986.

[202] H. Liu and T. J. Webster, “Nanomedicine for implants: A review of studies and necessary experimental tools,” *Biomaterials*, vol. 28, no. 2, pp. 354–369, 2007.

[203] F. Mangolini, A. Rossi, N. D. Spencer, and I. Cagliari, “Tribochemistry of Triphenyl Phosphorothionate (TPPT) by In Situ Attenuated Total Reflection (ATR / FT-IR) Tribometry,” 2012.

[204] M. Crobu, A. Rossi, F. Mangolini, and N. D. Spencer, “Chain-length-identification strategy in zinc polyphosphate glasses by means of XPS and ToF-SIMS,” pp. 1415–1432, 2012.

[205] P. Petrov, D. B. Dimitrov, D. Papadimitriou, G. Beshkov, V. Krastev, and C. Georgiev, “Raman and X-ray photoelectron spectroscopy study of carbon nitride thin films,” *Appl. Surf. Sci.*, vol. 151, no. 3, pp. 233–238, 1999.

[206] I. Nedelcu, E. Piras, A. Rossi, and H. R. Pasaribu, “XPS analysis on the influence of water on the evolution of zinc dialkyldithiophosphate-derived reaction layer in lubricated rolling contacts,” *Surf. Interface Anal.*, vol. 44, no. 8, pp. 1219–1224, 2012.

[207] M. Descostes, F. Mercier, N. Thromat, C. Beaucaire, and M. Gautier-Soyer, “Use of XPS in the determination of chemical environment and oxidation state of iron and sulfur samples: Constitution of a data basis in binding energies for Fe and S reference compounds and applications to the evidence of surface species of an oxidized py,” *Appl. Surf. Sci.*, vol. 165, no. 4, pp. 288–302, 2000.

[208] E. C. Onyiriuka, “Zinc phosphate glass surfaces studied by XPS,” vol. 163, pp. 268–273, 1993.

[209] R. K. Brow, C. M. Arens, X. Yu, and E. Day, “An XPS study of iron phosphate glasses,” *Phys. Chem. Glas.*, vol. 35, no. 3, pp. 132–136.

[210] M. Karabulut, G. K. Marasinghe, C. S. Ray, D. E. Day, O. Ozturk, and G. D. Waddill, “X-ray photoelectron and Mossbauer spectroscopic studies of iron phosphate glasses containing U, Cs and Bi,” *J. Non. Cryst. Solids*, vol. 249, no. 2–3, pp. 106–116, 1999.

[211] “NIST X-ray Photoelectron Spectroscopy Database,” *NIST Standard*

Reference Database 20, Version 4.1, 2012. [Online]. Available: https://srdata.nist.gov/xps/Default.aspx. [Accessed: 20-Sep-2018].

[212] R. Heuberger, A. Rossi, and N. D. Spencer, “Reactivity of alkylated phosphorothionates with steel: A tribological and surface-analytical study,” *Lubr. Sci.*, vol. 20, no. 2, pp. 79–102, 2008.

[213] F. M. Piras, A. Rossi, and N. D. Spencer, “Combined in situ (ATR FT-IR) and ex situ (XPS) study of the ZnDTP-iron surface interaction,” *Tribol. Lett.*, vol. 15, no. 3, pp. 181–192, 2003.

[214] Z. Zhang, E. S. Yamaguchi, M. Kasrai, and G. M. Bancroft, “Tribofilms generated from ZDDP and DDP on steel surfaces: Part 1, growth, wear and morphology,” *Tribol. Lett.*, vol. 19, no. 3, pp. 211–220, 2005.

[215] M. Olla, G. Navarra, B. Elsener, and A. Rossi, “Nondestructive in-depth composition profile of oxy-hydroxide nanolayers on iron surfaces from ARXPS measurement,” *Surf. Interface Anal.*, vol. 38, no. 5, pp. 964–974, 2006.

[216] G. Bhargava, I. Gouzman, C. M. Chun, T. A. Ramanarayanan, and S. L. Bernasek, “Characterization of the ‘native’ surface thin film on pure polycrystalline iron: A high resolution XPS and TEM study,” *Appl. Surf. Sci.*, vol. 253, no. 9, pp. 4322–4329, 2007.

[217] M. Eglin, A. Rossi, and N. D. Spencer, “X-ray photoelectron spectroscopy analysis of tribostressed samples in the presence of ZnDTP: A combinatorial approach,” *Tribol. Lett.*, vol. 15, no. 3, pp. 199–209, 2003.

[218] M. L. Suominen Fuller, L. Rodriguez Fernandez, G. R. Massoumi, W. N. Lennar, M. Kasrai, and G. M. Bancroft, “The use of x-ray absorption spectroscopy for monitoring the thickness of antiwear films from ZDDP,” *Tribol. Lett.*, vol. 8, no. 4, pp. 187–192, 2000.

[219] M. I. De Barros-Bouchet *et al.*, “Tribochemistry of phosphorus additives: Experiments and first-principles calculations,” *RSC Adv.*, vol. 5, no. 61, pp. 49270–49279, 2015.

[220] H. FUJITA and H. A. SPIKES, “Study of Zinc Dialkyldithiophosphate Antiwear Film Formation and Removal Processes, Part II: Kinetic Model,” *Tribol. Trans.*, vol. 48, no. 4, pp. 567–575, 2005.

[221] H. Cen, A. Morina, A. Neville, R. Pasaribu, and I. Nedelcu, “Effect of water on ZDDP anti-wear performance and related tribochemistry in lubricated steel/steel pure sliding contacts,” *Tribol. Int.*, vol. 56, pp. 47–57, 2012.

[222] S. Soltanahmadi, A. Morina, M. C. P. Van Eijk, I. Nedelcu, and A. Neville, “Experimental observation of zinc dialkyl dithiophosphate (ZDDP) -induced iron sulphide formation,” *Appl. Surf. Sci.*, vol. 414, pp. 41–51, 2017.

[223] M. C. Righi, M. I. D. B. Bouchet, and J. M. Martin, “A comparative study on the functionality of S- and P-based lubricant additives by combined fi rst principles and experimental analysis,” pp. 47753–47760, 2016.

[224] P. A. Willermet, R. O. Carter III, and E. N. Boulos, “Lubricant-derived tribochemical films-An infra-red spectroscopic study,” *Tribol. Int.*, vol. 25, no. 6, pp. 371–380, 1992.

[225] D. Philippon, M.-I. de Barros-Bouchet, T. L. Mogne, E. Gresser, and J.-M. Martin, “Experimental simulation of phosphites additives tribochemical reactions by gas phase lubrication,” *Tribol. - Mater. Surfaces Interfaces*, vol. 1, no. 3, pp. 113–123, 2007.

[226] D. Philippon, M.-I. De Barros-Bouchet, T. Le Mogne, B. Vacher, O. Lerasle, and J.-M. Martin, “A multi-technique approach to the characterization of iron phosphide tribofilm,” *Thin Solid Films*, vol. 524, pp. 191–196, 2012.

[227] D. Philippon, M.-I. De Barros-Bouchet, T. Le Mogne, O. Lerasle, A. Bouffet, and J.-M. Martin, “Role of nascent metallic surfaces on the tribochemistry of phosphite lubricant additives,” *Tribol. Int.*, vol. 44, no. 6, pp. 684–691, 2011.

[228] M. C. Righi, S. Loehlé, M. I. De Barros Bouchet, D. Philippon, and J. M. Martin, “Trimethyl-phosphite dissociative adsorption on iron by combined first-principle calculations and XPS experiments,” *RSC Adv.*, vol. 5, no. 122, pp. 101162–101168, 2015.

[229] M. C. Righi, S. Loehlé, M. I. De Barros Bouchet, S. Mambingo-Doumbe, and J. M. Martin, “A comparative study on the functionality of S- and P-based lubricant additives by combined first principles and experimental analysis,” *RSC Adv.*, vol. 6, no. 53, pp. 47753–47760, 2016.

[230] H. S. Liu, T. S. Chin, and S. W. Yung, “FTIR and XPS studies of low-melting PbO-ZnO-P2O5 glasses,” *Mater. Chem. Phys.*, vol. 50, no. 1, pp. 1–10, 1997.

[231] O. J. Furlong, B. P. Miller, and W. T. Tysoe, “Shear-induced surface-to-bulk transport at room temperature in a sliding metal-metal interface,” *Tribol. Lett.*, vol. 41, no. 1, pp. 257–261, 2011.

[232] M. Salmeron, “Generation of defects in model lubricant monolayers and their contribution to energy dissipation in friction,” *Tribol. Lett.*, vol. 10, no. 1–2, pp.

69–79, 2001.

[233] N. Prathima *et al.*, “Thermal study of accumulation of conformational disorders in the self-assembled monolayers of C<inf>8</inf> and C<inf>18</inf> alkanethiols on the Au(111) surface,” *Langmuir*, vol. 21, no. 6, pp. 2364–2374, 2005.

[234] S. Jahanmir and M. Beltzer, “An adsorption model for friction in boundary lubrication,” *ASLE Trans.*, vol. 29, no. 3, pp. 423–430, 1986.

[235] M. Beltzer and S. Jahanmir, “Role of dispersion interactions between hydrocarbon chains in boundary lubrication,” *ASLE Trans.*, vol. 30, no. 1, pp. 47–54, 1987.

[236] Kirk-Othmer, *Encyclopedia of Chemistry Technology*, Volume 2. John Wiley & Sons.

[237] “Amine Ethoxylates.” [Online]. Available: https://www.oxiteno.us/products/amine-ethoxylates/. [Accessed: 29-Apr-2019].

[238] H. Zhao, A. Neville, A. Morina, R. Vickerman, and J. Durham, “Improved anti-shudder performance of ATFs-Influence of a new friction modifier and surface chemistry,” *Tribol. Int.*, vol. 46, no. 1, pp. 62–72, 2012.

[239] P. C. J. Beentjes, J. Van Den Brand, and J. H. W. De Wit, “Interaction of ester and acid groups containing organic compounds with iron oxide surfaces,” *J. Adhes. Sci. Technol.*, vol. 20, no. 1, pp. 1–18, 2006.

[240] B. F. Lewis, M. Mosesman, and W. H. Weinberg, “The chemisorption of H2O, HCOOH and CH3COOH on thin amorphous films of Al2O3,” *Surf. Sci.*, vol. 41, no. 1, pp. 142–164, 1974.

[241] J. T. Hall and P. K. Hansma, “Chemisorption of monocarboxylic acids on alumina: A tunneling spectroscopy study,” *Surf. Sci.*, vol. 77, no. 1, pp. 61–76, 1978.

[242] L. S. Hersh, E. C. Onyiriuka, and W. Hertl, “Amine-reactive surface chemistry of zinc phosphate glasses,” *J. Mater. Res.*, vol. 10, no. 8, pp. 2120–2127, 1995.

[243] P. G. Harrison and T. Kikabhai, “Proton and phosphorus-31 nuclear magnetic resonance study of zinc(II) O,O′-dialkyl dithiophosphates in solution,” *J. Chem. Soc. Dalt. Trans.*, no. 4, pp. 807–814, 1987.

[244] L. Bartha, G. Deak, and M. Kovacs, “Interaction of PIB-succinimides and other

Engine Oil Additives," no. February, pp. 173–180, 1997.

Appendix A: Lubricants screening friction data

Lubricant	Test 1	Test 2	Avg. COF	Std. Dev
BO + FM 1 + ZDDP	0.082	0.079	0.080	0.002
BO + FM 2 + ZDDP	0.067	0.064	0.066	0.002
BO + FM 3 + ZDDP	0.066	0.070	0.068	0.003
BO + FM 4 + ZDDP	0.064	0.069	0.066	0.003
BO + ZDDP	0.110	0.105	0.107	0.003
BO + FM 6 + ZDDP	0.073	0.077	0.075	0.003
BO + FM 7 + ZDDP	0.069	0.077	0.073	0.006
BO + FM 8 + ZDDP	0.076	0.076	0.076	0.000
BO + FM 9 + ZDDP	0.063	0.065	0.064	0.002
BO + FM 10 + ZDDP	0.049	0.050	0.049	0.001
BO + FM 11 + ZDDP	0.072	0.081	0.076	0.006
BO + FM 12 + ZDDP	0.062	0.069	0.066	0.005
BO + FM 13 + ZDDP	0.067	0.078	0.072	0.008
BO + FM 14 + ZDDP	0.088	0.093	0.090	0.004
BO + FM 15 + ZDDP	0.081	0.084	0.083	0.002
BO + FM 16 + ZDDP	0.077	0.081	0.079	0.003
BO + FM 17 + ZDDP	0.070	0.073	0.072	0.002
BO + FM 18 + ZDDP	0.077	0.078	0.078	0.001

Appendix B: Lubricants screening WF value ($x10^{-11}mm^3/Nmm$)

Lubricant	Test 1	Test 2	Avg. WF	Std. Dev
BO + FM 1 + ZDDP	2.10	2.56	2.33	0.325
BO + FM 2 + ZDDP	0.25	0.36	0.30	0.081
BO + FM 3 + ZDDP	0.37	0.37	0.37	0.001
BO + FM 4 + ZDDP	1.90	1.83	1.87	0.049
BO + ZDDP	1.40	1.12	1.26	0.198
BO + FM 6 + ZDDP	0.36	0.32	0.34	0.028
BO + FM 7 + ZDDP	0.33	0.30	0.31	0.021
BO + FM 8 + ZDDP	0.16	0.18	0.17	0.011
BO + FM 9 + ZDDP	0.67	0.34	0.50	0.236
BO + FM 10 + ZDDP	0.79	0.53	0.66	0.181
BO + FM 11 + ZDDP	0.28	0.30	0.29	0.011
BO + FM 12 + ZDDP	0.37	0.23	0.30	0.096
BO + FM 13 + ZDDP	0.50	0.42	0.46	0.055
BO + FM 14 + ZDDP	0.47	0.43	0.45	0.028
BO + FM 15 + ZDDP	0.55	0.53	0.54	0.018
BO + FM 16 + ZDDP	0.26	0.15	0.20	0.074
BO + FM 17 + ZDDP	0.31	0.31	0.31	0.004
BO + FM 18 + ZDDP	0.51	0.45	0.48	0.041

Appendix C: Friction and wear factor data of the lubricants having 0.5:1 and 1:1 molar ratio of FM to ZDDP

Friction data of the lubricants having 0.5:1 molar ratio of FM to ZDDP along with the lubricant blend of BO + ZDDP

Lubricant	Test 1	Test 2	Test 3	Avg. COF	Std. Dev.
BO + FM 1 + ZDDP	0.073	0.072	0.072	0.072	0.0004
BO + FM 4 + ZDDP	0.076	0.081	0.085	0.081	0.0046
BO + ZDDP	0.110	0.105	0.105	0.107	0.0028
BO + FM 8 + ZDDP	0.069	0.070	0.066	0.068	0.0022
BO + FM 10 + ZDDP	0.073	0.066	0.077	0.072	0.0058
BO + FM 14 + ZDDP	0.083	0.098	0.088	0.090	0.0075

Friction data of the lubricants having 1:1 molar ration of FM to ZDDP

Lubricant	Test 1	Test 2	Test 3	Avg. COF	Std. Dev.
BO + FM 1 + ZDDP	0.082	0.080	0.079	0.080	0.0017
BO + FM 4 + ZDDP	0.064	0.069	0.074	0.069	0.0048
BO + FM 8 + ZDDP	0.069	0.076	0.076	0.074	0.0039
BO + FM 10 + ZDDP	0.049	0.050	0.051	0.050	0.0012
BO + FM 14 + ZDDP	0.081	0.097	0.093	0.090	0.0085

Wear factor values (x 10^{-11}) of the lubricants having 0.5:1 molar ratio of FM to ZDDP along with the lubricant blend of BO + ZDDP

Lubricant	Test 1	Test 2	Test 3	Avg. WF	Std. Dev.
BO + FM 1 + ZDDP	2.84	3.13	3.43	3.13	0.298
BO + FM 4 + ZDDP	1.57	1.50	1.79	1.62	0.205
BO + ZDDP	1.4	1.12	1.38	1.30	0.156
BO + FM 8 + ZDDP	0.52	0.39	0.43	0.45	0.067
BO + FM 10 + ZDDP	0.80	0.40	0.60	0.60	0.2
BO + FM 14 + ZDDP	0.6	0.7	0.64	0.647	0.050

Wear factor values (x 10^{-11}) of the lubricants having 1:1 molar ratio of FM to ZDDP

Lubricant	Test 1	Test 2	Test 3	Avg. WF	Std. Dev.
BO + FM 1 + ZDDP	2.1	2.95	2.56	2.54	0.425
BO + FM 4 + ZDDP	1.9	1.8	1.9	1.87	0.058
BO + FM 8 + ZDDP	0.389	0.407	0.179	0.33	0.127
BO + FM 10 + ZDDP	0.79	0.53	0.38	0.57	0.207
BO + FM 14 + ZDDP	0.42	0.47	0.43	0.44	0.026

Appendix D: Sequential film formation tests

Friction behaviour of **ZDDP** in 30 minutes sequential film formation test (first half)

Lubricants	**Test 1**	**Test 2**	**Avg. COF**	**Std. Dev**
BO + ZDDP to BO + FM 1	0.098	0.102	0.100	0.003
BO + ZDDP to BO + FM 4	0.100	0.101	0.101	0.000
BO + ZDDP to BO + FM 8	0.101	0.104	0.102	0.002
BO + ZDDP to BO + FM 14	0.098	0.107	0.102	0.007

Friction behaviour of **ZDDP** in 60 minutes sequential film formation test (first half)

Lubricants	**Test 1**	**Test 2**	**Avg. COF**	**Std. Dev**
BO + ZDDP to BO + FM 1	0.103	0.106	0.104	0.002
BO + ZDDP to BO + FM 4	0.104	0.100	0.102	0.003
BO + ZDDP to BO + FM 8	0.104	0.101	0.102	0.002
BO + ZDDP to BO + FM 14	0.099	0.103	0.101	0.003

Friction behaviour of **ZDDP** in 120 minutes sequential film formation test (first half)

Lubricants	**Test 1**	**Test 2**	**Avg. COF**	**Std. Dev**
BO + ZDDP to BO + FM 1	0.105	0.104	0.104	0.001
BO + ZDDP to BO + FM 4	0.101	0.096	0.099	0.003
BO + ZDDP to BO + FM 8	0.106	0.098	0.102	0.005
BO + ZDDP to BO + FM 14	0.098	0.101	0.099	0.002

Friction behaviour of **FM 1 and ZDDP** in 30 minutes sequential film formation tests

Lubricants	**Test 1**	**Test 2**	**Avg. COF**	**Std. Dev**
BO + ZDDP to BO + FM 1	0.075	0.073	0.074	0.002
BO + FM 1 to BO + ZDDP	0.086	0.083	0.084	0.002
BO + FM 1 + ZDDP	0.096	0.093	0.095	0.002

Friction behaviour of **FM 1 and ZDDP** in 60 minutes sequential film formation tests

Lubricants	**Test 1**	**Test 2**	**Avg. COF**	**Std. Dev**
BO + ZDDP to BO + FM 1	0.078	0.077	0.078	0.001
BO + FM 1 to BO + ZDDP	0.091	0.089	0.089	0.001
BO + FM 1 + ZDDP	0.095	0.096	0.096	0.001

Friction behaviour of **FM 1 and ZDDP** in 120 minutes sequential film formation tests

Lubricants	**Test 1**	**Test 2**	**Avg. COF**	**Std. Dev**
BO + ZDDP to BO + FM 1	0.075	0.072	0.074	0.002
BO + FM 1 to BO + ZDDP	0.090	0.084	0.087	0.004
BO + FM 1 + ZDDP	0.082	0.080	0.081	0.002

Friction behaviour of **FM 4 and ZDDP** in 30 minutes sequential film formation tests

Lubricants	**Test 1**	**Test 2**	**Avg. COF**	**Std. Dev**
BO + ZDDP to BO + FM 4	0.082	0.083	0.083	0.001
BO + FM 4 to BO + ZDDP	0.09	0.09	0.09	0.000
BO + FM 4 + ZDDP	0.091	0.092	0.092	0.001

Friction behaviour of **FM 4 and ZDDP** in 60 minutes sequential film formation tests

Lubricants	**Test 1**	**Test 2**	**Avg. COF**	**Std. Dev**
BO + ZDDP to BO + FM 4	0.08	0.076	0.078	0.003
BO + FM 4 to BO + ZDDP	0.086	0.079	0.082	0.005
BO + FM 4 + ZDDP	0.091	0.093	0.092	0.001

Friction behaviour of **FM 4 and ZDDP** in 120 minutes sequential film formation tests

Lubricants	**Test 1**	**Test 2**	**Avg. COF**	**Std. Dev**
BO + ZDDP to BO + FM 4	0.082	0.078	0.08	0.003
BO + FM 4 to BO + ZDDP	0.085	0.086	0.086	0.000
BO + FM 4 + ZDDP	0.084	0.089	0.087	0.004

Friction behaviour of **FM 8 and ZDDP** in 30 minutes sequential film formation tests

Lubricants	**Test 1**	**Test 2**	**Avg. COF**	**Std. Dev**
BO + ZDDP to BO + FM 8	0.067	0.065	0.066	0.002
BO + FM 8 to BO + ZDDP	0.08	0.091	0.086	0.007
BO + FM 8 + ZDDP	0.077	0.078	0.077	0.001

Friction behaviour of **FM 8 and ZDDP** in 60 minutes sequential film formation tests

Lubricants	**Test 1**	**Test 2**	**Avg. COF**	**Std. Dev**
BO + ZDDP to BO + FM 8	0.065	0.074	0.069	0.006
BO + FM 8 to BO + ZDDP	0.085	0.087	0.086	0.001
BO + FM 8 + ZDDP	0.074	0.076	0.075	0.001

Friction behaviour of **FM 8 and ZDDP** in 120 minutes sequential film formation tests

Lubricants	**Test 1**	**Test 2**	**Avg. COF**	**Std. Dev**
BO + ZDDP to BO + FM 8	0.072	0.066	0.069	0.005
BO + FM 8 to BO + ZDDP	0.083	0.085	0.084	0.001
BO + FM 8 + ZDDP	0.068	0.076	0.072	0.006

Friction behaviour of **FM 14 and ZDDP** in 30 minutes sequential film formation tests

Lubricants	**Test 1**	**Test 2**	**Avg. COF**	**Std. Dev**
BO + ZDDP to BO + FM 14	0.075	0.088	0.082	0.009
BO + FM 14 to BO + ZDDP	0.082	0.088	0.085	0.004
BO + FM 14 + ZDDP	0.078	0.076	0.077	0.001

Friction behaviour of **FM 14 and ZDDP** in 60 minutes sequential film formation tests

Lubricants	**Test 1**	**Test 2**	**Avg. COF**	**Std. Dev**
BO + ZDDP to BO + FM 14	0.08	0.087	0.083	0.005
BO + FM 14 to BO + ZDDP	0.087	0.088	0.088	0.001
BO + FM 14 + ZDDP	0.092	0.082	0.087	0.007

Friction behaviour of **FM 14 and ZDDP** in 120 minutes sequential film formation tests

Lubricants	**Test 1**	**Test 2**	**Avg. COF**	**Std. Dev**
BO + ZDDP to BO + FM 14	0.088	0.086	0.087	0.001
BO + FM 14 to BO + ZDDP	0.088	0.083	0.085	0.003
BO + FM 14 + ZDDP	0.097	0.093	0.095	0.003